Structural and functional characterization of Testis-specific Y-encoded-like protein5: a novel member of NAP histone chaperone superfamily

Thesis submitted for the degree of

DOCTOR OF PHILOSOPHY (SCIENCE)

Of

JADAVPUR UNIVERSITY

SAMBIT DALUI

Division of Structural Biology and Bioinformatics

CSIR-Indian Institute of Chemical Biology

Jadavpur, Kolkata-700032

West Bengal, India

2022

Certificate from the Supervisor

This is to certify that the thesis entitled **'Structural and Functional Characterization of Testis-specific Y-encoded like protein 5: a novel member of NAP histone chaperone superfamily'** submitted by Mr. Sambit Dalui (Index No: 35/17/Life Sc./25) who got his name registered as SLSBT1203517 on 12.05.2017, for the award of Ph.D. (Science) degree of Jadavpur University, is absolutely based upon his own work. The work was carried out under the supervision of Dr Siddhartha Roy, and neither this thesis nor any part of it has been submitted for either any degree/diploma or any other academic award anywhere before.

28.06.2022

Signature of the supervisor

with date & official seal

SIDDHARTHA ROY
Principal Scientist
Structural Biology & Bioinformatics
CSIR-Indian Institute of Chemical Biology
4, Raja S C Mullick Road
Jadavpur, Kolkata-700 032

PREFACE

NAP histone chaperone superfamily is a growing group of histone chaperone proteins that show sequence similarity to NAP1 protein; but their expressions and functions are highly specific and is mainly dependent on the cell and/or tissue types. In this thesis entitled as **"Structural and Functional characterization of Testis-specific Y-encoded-like protein 5: a novel member of NAP histone chaperone superfamily",** we have described TSPYL5 as a novel member of the NAP histone chaperone family that binds specifically to histone H3/H4 and facilitates nucleosome assembly by depositing histone H3/H4 on naked DNA template *in vitro*.

I hereby declare that; this thesis contains literature review and original research work done by me as a part of my doctoral studies. This thesis work has been performed under the direct supervision of Dr Siddhartha Roy, Principal Scientist, Structural Biology and Bioinformatics Division, CSIR-Indian Institute of Chemical Biology, Kolkata. This thesis has been subdivided into 5 major chapters. **Chapter - I** contains the review of literature available on histone chaperones with main focus on NAP family histone chaperones and TSPYL5. **Chapter - II** illustrates the objectives of the work identified for this thesis. **Chapter - III** includes a detailed list of reagents and procedures used to perform the experiments and **Chapter - IV** contains results and experimental data obtained thereafter. Finally, in **Chapter - V**, I have discussed the results and significance of the findings of this thesis work.

All information of thesis has been obtained and prsented in accordance with existing academic rules and ethical conducts and all the references have been cited accordingly.

…………………………………………..

Sambit Dalui, Index No.: 35/17/Life Sc./25

Date:

Dedicated to

DADA & DADAI

(my late grandfathers) and

my beloved parent

Acknowledgement

*A very special mention to my senior turned teacher cum friend, **Dr. Rohit Kunar** from Cytogenetics Laboratory, BHU, who has been a friend, philosopher and guide in my journey of life and academics. Without his presence, I would not have been able to evolve and achieve anything. In this prefecture I extend my best regards with lots of love and ask him to always stay there with me.*

*I thank all my lab mates for their continuous help whenever I needed them. "Milk Tea" definitely helps me and **Dushyant da**, the hardworking, brilliant scientific mind, to blend well in lab. I thank him for his scientific inputs in my research. Thanks to **Anirban Da**, for all your efforts that helped me get along with the lab in my initial days and your sincere help in my research project. Our sweet and charming sister in lab, **Sinjini**, best wishes for her upcoming endeavours. **Avradeep**, new PhD student in our lab, I wish you all the success and happiness in life. I would also like to thank **Purbita**, a wonderful summer trainee I had in my PhD tenure and I wish her a lot of success in life. I would like to acknowledge the two lovely visiting summer students **Debjani** and **Sunil** for helping me in my work. A whole-hearted acknowledgement to the former national post-doctoral fellow of our lab, **Dr Senjuti Sen** for her help in several lab chores. Thank you all for being such lovely comrades of Lab 217 and for creating these golden memories that we have shared in the last few years.*

*I would also like to acknowledge my seniors, **Dr. Aritra Bej, Dr. Sourav Chowdhury, Dr. Somenath Roy Chowdhury, Dr. Arpita Bhoumik, Dr. Subhro Jyoti Saha, Dr. Anand Gupta, Dr. Asim Azhar Siddiqui, Dr. Somnath Mazumdar, Dr. Ayan Adhikary, Dr. Bartika Ghoshal, Dr. Avijit Goswami, Dr. Yogaditya Chakraborty, Dr. Dibyanti Mukherjee, Dr. Neerajana Datta, Dr. Veenita Khare, Dr. Nicky Didwania, Dr. Rudranil De, Dr. Kaushik Ghosh, Dr. Tridip Mahato, Dr. Ritobrita Chakraborty** for their support and guidance that helped me immensely over the years. I also thank **Dr. Chaitali Mukherjee** and her husband **Mr. Debarshi Mukherjee** for being there as a constant source of encouragement the entire time.*

*My course-work batchmates, **Sukanya, Shiladitya, Sonali, Kamran, Saroj, Priya, Saikat, Diptankar, Arijit, Subham, Dhreeren, Debojyoti, Samrat, Mayuri, Anoy, Krishanu, Snehasish, Jeet, Satadeepa,** and **Subarno** need special mention for their constant support in various matter in this journey. As we together shared our life struggles in the ultimate years of my PhD tenure, I would like to share my appreciation and regard towards **Akash** Saha for being my companion. I also take this opportunity to specially extend my regards and love to my beloved friends **Dr. Liberalis Debraj Boila** and **Dr. Sayantani Sinha**, from whom I have learnt a lot during my Ph.D. tenure. We have shared common interests both in academics and non-academics and even bonded over food and travel. I would also like to thank **Dr. Sounak Sahu**, my go-to buddy, **Dr. Aniket Bhattacharya** and **Dr. Aditya Ghoshal**, my counsellors in life, for chaperoning me in the field of research. I am grateful to **Dr. Krishna Kishore Sukla** and **Dr. Rachana Nagar**, my M.Sc dissertation mentors for introducing me to lab techniques, ethics work culture and guiding me ever since.*

*Last but not the least, I also thank my sincere juniors in IICB, **Syamantak, Sumit, Saikat, Debanjan, Vivek, Ishani, Shreya, Sujoy, Prathama, Avik, Kajal, Priyanka,** and **Pratiti**, for their constant support. This list is incomplete without the mention of **Mr. Sourav Hom Choudhury** and **Mr. Chayan Banerjee**, without whom I would never be able to complete my research manuscript. They have helped me innumerable times with an everlasting smile.*

……………………………………….

SAMBIT DALUI

"Dream, dream, dream.

Dreams transform into thoughts and thoughts result in

action."

A.P.J. Abdul Kalam

TABLE OF CONTENTS

TABLE OF CONTENTS

TABLE OF CONTENTS

Introduction

Chapter I: INTRODUCTION

1. Introduction

1.1. Eukaryotic Chromatin Architecture

The genetic material i.e., DNA in eukaryotic cell is organised inside a double membrane bound cell organelle referred to as the nucleus. The length of the DNA is much bigger than the nucleus in which it is contained. Hence, the DNA must be compacted in a manner that can help it easily fit inside the nucleus. To solve this problem, a special kind of protein, Histone, evolved in eukaryotes. Eukaryotic nucleus thus consists of a DNA-Histone protein complex referred to as the Chromosome, that helps in compaction of the DNA to simplify its storage inside the nuclear compartment. The general unit of Chromosome is Chromatin and the basic unit of Chromatin is referred to as the Nucleosome. The next level of DNA packaging is the 30 nm fiber (Thoma et al., 1979; Finch and Klug, 1976). This resembles a solenoid structure with each turn having 6 nucleosomes. H1 histone is required for stabilisation of this 30 nm structure. Experimental data shows that stripping H1 from chromatin maintains the nucleosomal 10 nm structure (bead on strings model), but not the 30 nm structure. This fibre probably folds by itself into the 300 nm fibrillar structure which houses a greater extent of DNA compaction. This 300 nm structure in turn becomes the fundamental functional unit of interphase chromatin. A 700 nm structure found in the metaphase chromosome finally characterises and sums up the final level of DNA packaging. This final form of condensed chromatin possesses a typical scaffolding structure which is well detected in metaphase stage chromosomes and seems to be the ultimate outcome of a vast array of folding patterns involved with the chromosomal DNA.
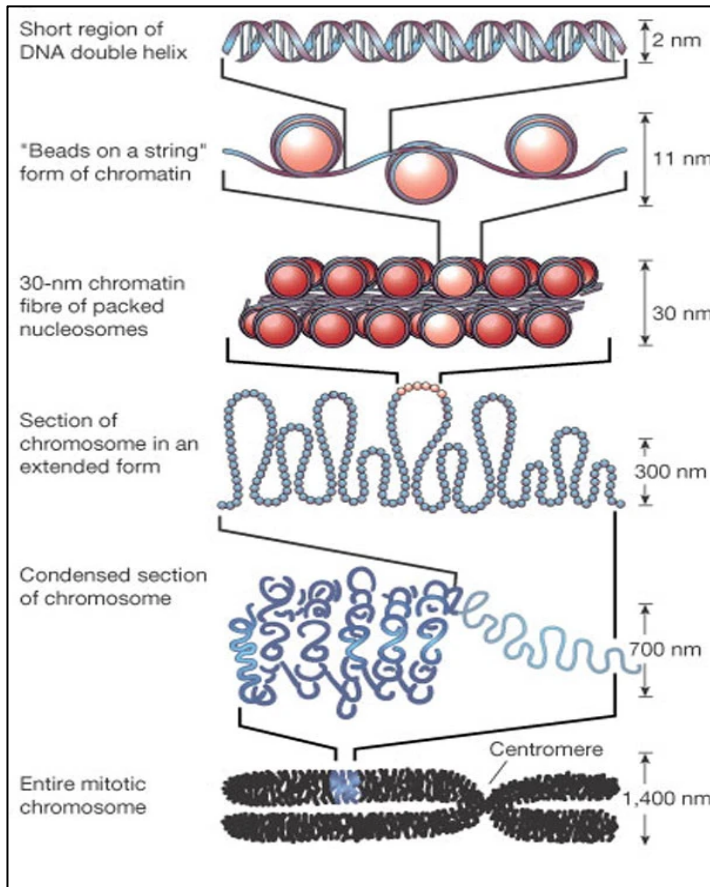
Figure 1.1. Organization of eukaryotic chromatin architecture. *The lowest level of organisation is the nucleosome, Nucleosomes are connected to each other by short stretches of linker DNA. At the next level of organisation, nucleosome is folded into ~30nm fiber and these fibers further fold into higher order structures. Condensations of chromatin fibers are mainly mediated through the inter-nucleosomal interactions, linker histones and non-histone proteins. (Figure adapted from Felsenfeld and Groudine, 2003).*

1.2. Nucleosome Structure: Histones and Histone Fold

In eukaryotes, nucleosome is the simplest packaging structure of chromatin comprised of a 146 bp DNA wrapped around an octameric configuration of histones. The octamer consists of two copies each of histone H2A, H2B, H3 and H4 that possess a strong affinity for DNA. Each of these histone proteins bears within it a histone fold domain containing three alpha-helices (α1, α2, α3) that are associated together by two short loops (L1 and L2) and allows for hetero-dimerisation of histones. Histone H2A with H2B and H3 with H4 forms the H2A/H2B and H3/H4 heterodimer via their α2–α3 helices to form four-helix bundles. Two histone H3/H4 dimers further oligomerise via H3-H3' four-helix bundles which act as the tetramerization interface for histone H3/H4. Nucleosome

assembly is initiated by deposition of tetrameric H3/H4 on DNA, thereby forming the 'tetrasome'. H3/H4 tetramer holds the central 'Dyad' position of the nucleosome. The rest of the DNA is then wrapped by two H2A/H2B dimers to complete the nucleosome assembly. Each of the H2A/H2B dimer individually contacts with the histone H3/H4 tetramer by way of a four-helix bundle formed between H4 α2–α3 and H2B α2–α3 helices. Canonical histones include some additional features more than traditional histone fold structure. Histone H2A consists of C-terminal stretch along with short amino-terminal
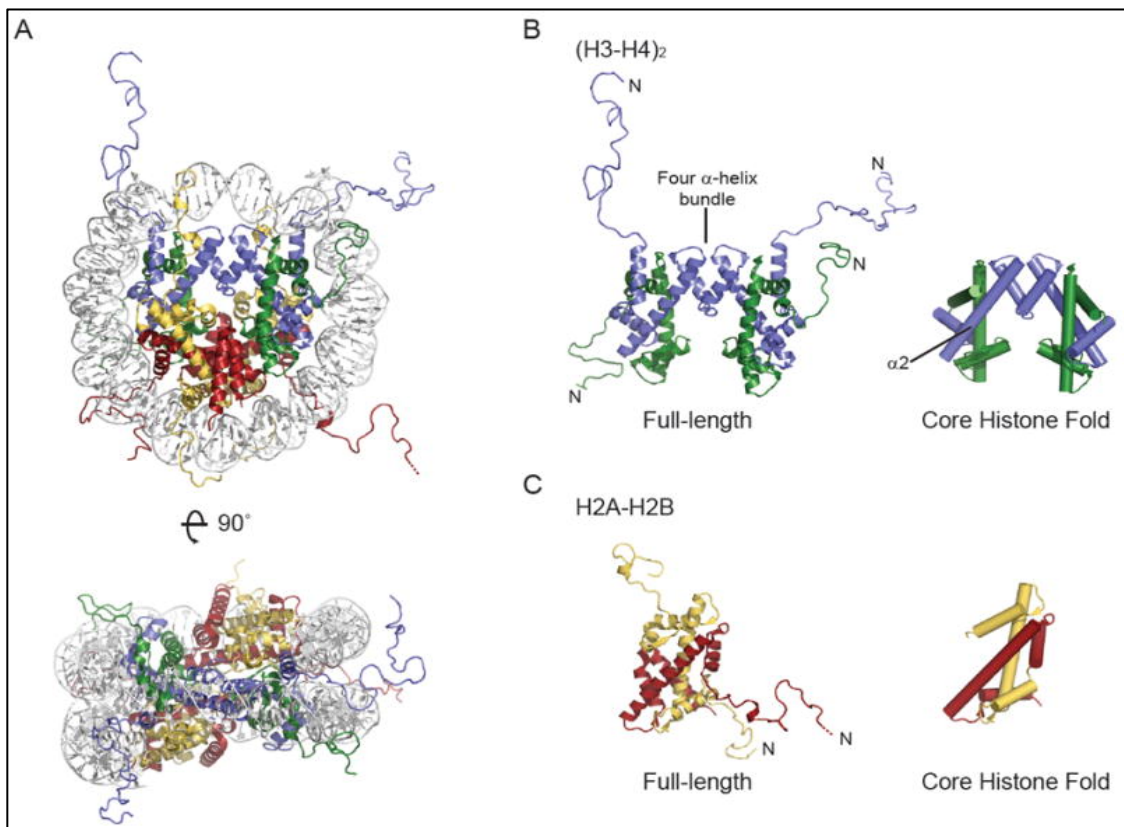
Figure 1.2. Components of Nucleosome. *Structure of the major-type nucleosome (A), H3 and H4 folds themselves to form a H3/H4 dimer. Two H3/H4 dimers form an (H3/H4)₂ hetero-tetramer (B), while. H2A and H2B fold among themselves to form H2A/H2B dimer (C). PDB ID: 1KX5. DNA is white, H2A is yellow and H2B is red, H3 is blue, and H4 is green respectively. The four α-helix bundle between two H3-H3' that mediates H3/H4 tetramer formation are indicated. Adopted from Elsässer and D'Arcy, 2012.*

helix (H2A αN) and two short alpha helices (the H2A docking domain). Histone H2B has a C-terminal α-helix (H2B αC) stretch while H3 comprises an N-terminal helix (H3 αN). C and N-terminal tails are found in all the canonical histones. All N-terminal histone tails undergo post-translational modifications, that influence the chromatin dynamicity.

Although, length of the DNA coupled with histone octamer differs across species, basic 146 bp length of DNA remains more or less constant. DNA between two histone octamers is termed 'linker DNA' that varies in length between 8 - 114 bp. This difference in the linker DNA length is species specific and depends either on the different developmental stages of the organism and/or specific regions of the genome of the organism.

1.3.   Histone variants: role in chromatin structure

Over the time scale of evolution, histone proteins have widely expanded starting from archaeal ancestors to higher eukaryotes. Further classification of histones into different types have resulted in chromatin differentiation in a manner that generates epigenetic consequences. Initial assumptions from literature presents that histone variants may recognisably change the nucleosome structure. However, nucleosome reconstitution experiments and other *in vitro* structural studies, has illustrated clearly that these histone variants neither dramatically alters the overall structure nor modifies the composition of the nucleosomes. In turn investigations show that histone variants establish a strong basis necessary for interpreting the need of chromatin participation in different cellular function and to build epigenetic memory.

CenH3, a well-studied histone H3 variant, induces a precise conformational alteration in nucleosome but is functionally preserved from yeast (Cse4) to humans (CENP-A). This centromeric variant plays a crucial role to define centromere in chromatid and guides the mitotic tubule assembly to kinetochore during mitosis. Other than CENP-A-H3, there are 3 other variants of histone H3 found in humans. While H3.1 and H3.2 are replication specific histone variants, H3.3 is strictly independent to replication process and also plays a vital role in maintaining heterochromatin structure. The histone H2A.X variant has a
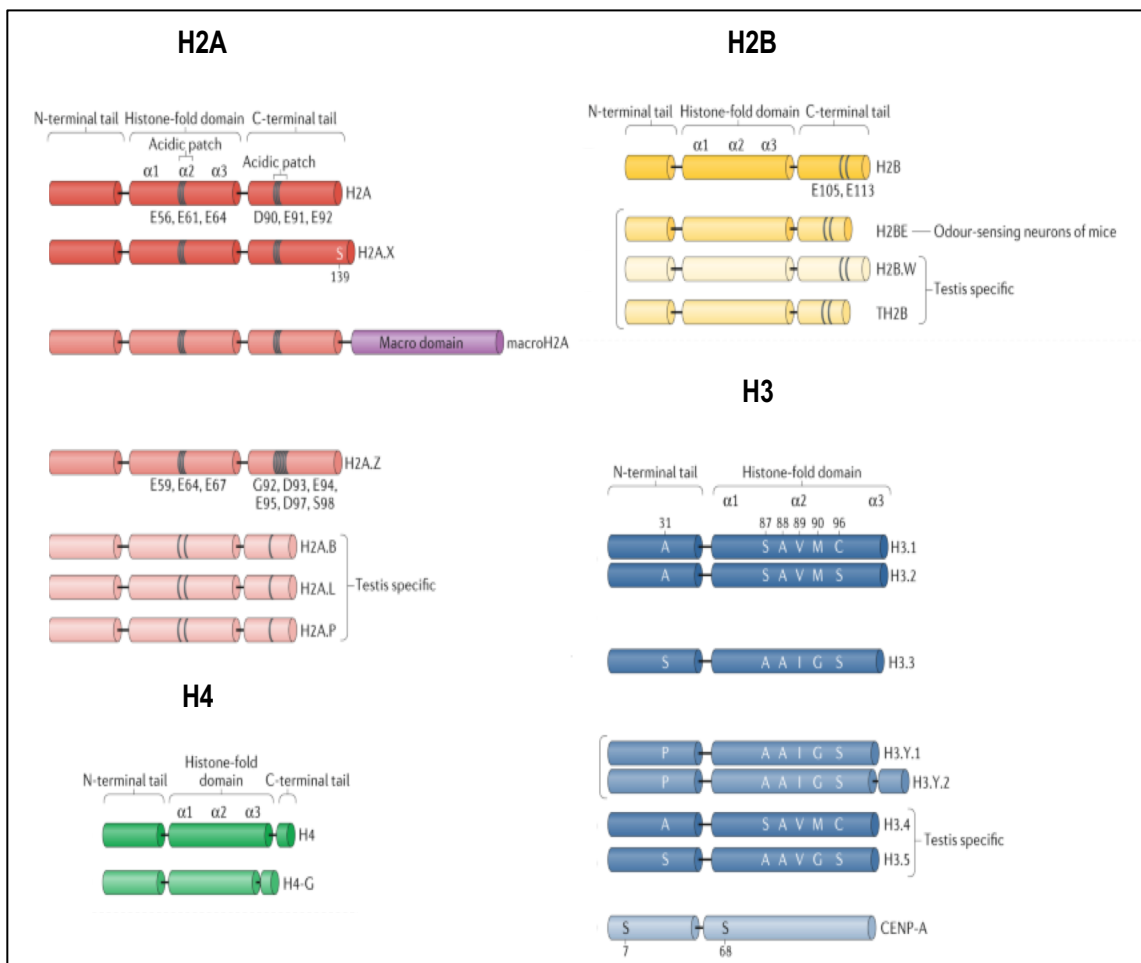
Figure 1.3. Pictorial description of Histone variants along with the canonical one. *Folds and domains of the histone H2A, HB, H3, and H4 and variants of histones H3 and H2A. Histone fold domain (HFD) is coloured as cyan. Figure adopted from Sara Martire & Laura A. Banaszynski, 2020.*

unique four amino-acid C-terminal stretch. At sites of DNA double-stranded breaks, H2A.X serine residue phosphorylation of that motif is one of the earlier events in the repair of double-strand break, which send signal and helps to accumulate repair machinery components. Phosphorylation of H2A.X identified during mammalian spermatogenesis, is an essential measure for XY chromosome pairing and condensation.

Structurally H2A.Z is divergent compared to other H2A variants. In yeast, H2A.Z is critical for neutralising heterochromatin formation and in demonstrating transcriptional capability of gene body. MacroH2A and H2A.B (also called H2A.Bbd), vertebrate specific histone H2A variants, have also been reported to display very different characteristics, where they hinder and facilitate transcription respectively. These variants localised on the epigenetically inactivated mammalian X chromosome

Some variants of H2B are reported recently but their functional significance is still unknown while H4 that doesn't have any variants is present as a canonical form in all eukaryotes. These studies highlight how a variant-containing nucleosome helps in differentiation of chromatin that in turn induces a specific downstream signal and exposes the histone surface which is then easily available for recognition by select nuclear proteins.

1.4. Chromatin assembly and disassembly

Chromatin is a dynamic cellular architecture that has varied structural configurations. Chromatin based on the nuclear staining patterns of haematoxylin dyes to visualise DNA is classified as either Euchromatic or Heterochromatic. Euchromatin refers to the relaxed

state of chromatin, which depicts its transcriptionally active or inactive state. Heterochromatin is defined as highly condensed and transcriptionally silenced chromatin. It exists as Constitutive heterochromatin, where genes are permanently silenced or as Facultative heterochromatin where genes are rarely expressed in any cell during a specific cell cycle or in the developmental stage of the organism. The structure of chromatin acts as a barrier to the cellular machinery before it can administrate to DNA for different DNA dependent cellular processes like DNA replication, transcription, and damage repair. These processes have encompassed dynamic changes in chromatin. When histones are locally
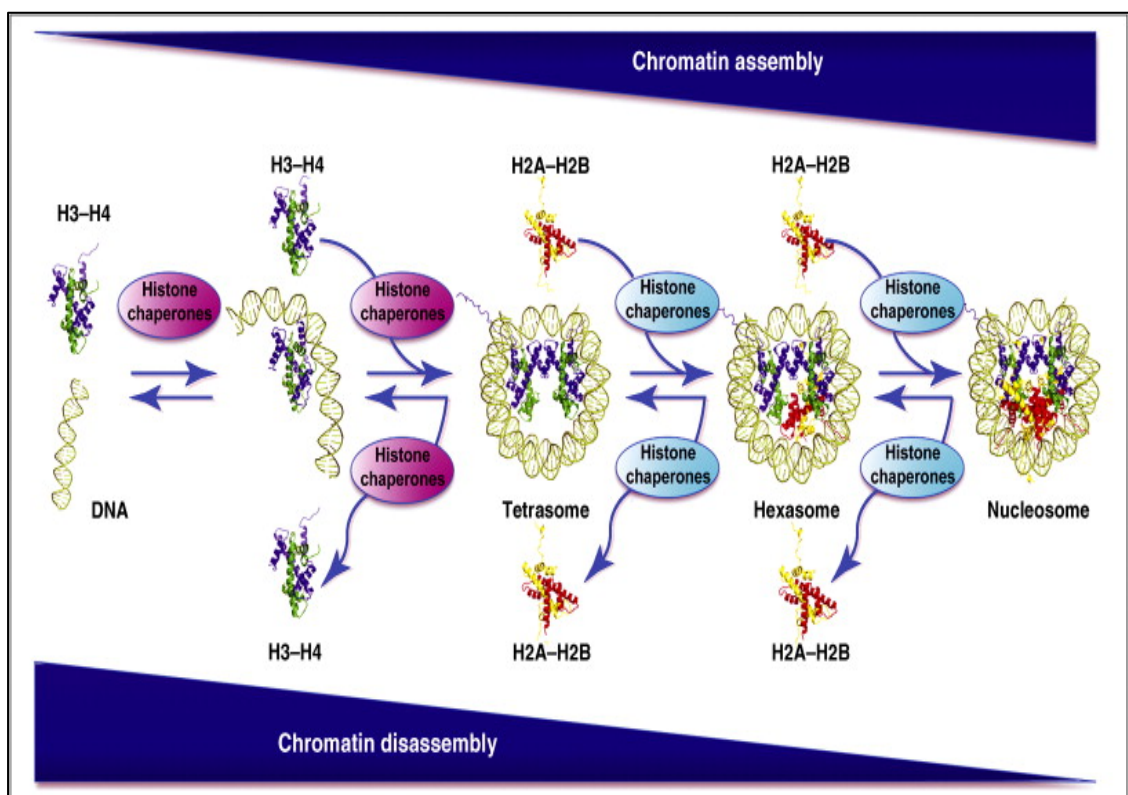
Figure 1.4. Stepwise assembly and disassembly of nucleosomes assisted by histone chaperones. *DNA is wrapped around two H3/H4 dimers and two H2A/H2B dimers to form the nucleosome core particle. Histone chaperones mediate each step of the chromatin assembly and disassembly process. Histone H2A is depicted in yellow, H2B in red, H3 in blue and H4 in green respectively. Figure adopted from Das et. al., 2010).*

removed in the vicinity of the DNA dependent processes – it is termed as "chromatin disassembly". Following the specific cellular activity, histones are again re-incorporated within the DNA, referred to as "chromatin assembly".

The chromatin assembly and disassembly processes were best understood during DNA replication and DNA repair where histones are removed from the parental strand of chromatin. Electron microscope analysis reveals presence of naked DNA behind the replication fork which confirms chromatin disassembly during the process of replication. (Luger et al., 2012; Alabert and Groth 2012).

Although chromatin architecture helps prevent DNA damage to some extent, intrinsic and extrinsic factors (UV light, mutagenic chemicals, free radicals, and gamma rays) are responsible for continuous DNA damage. This damage must be rapidly identified and efficiently repaired by the DNA repair machinery so that progress of mutations stops. The compactly packed chromatin retards the DNA repair machinery and the present DNA repair process on chromatin (Smerdon, 1991). It is of utmost importance to identify the DNA damage site. Once the site is recognised, the DNA repair machinery gains access to the site of damage. After repairing DNA lesion, chromatin rearrangement or assembly machinery then leads to that place and restores the chromatin structure (Ransom, 2010).

Chromatin assembly is not only closely associated with DNA replication or DNA repair process but is also associated with transcription processes. Transcriptional machinery and activators need to have access to their sequence-specific DNA binding sites within the upstream promoter and regulatory region and then the RNA polymerase

traverses through the template strand of the DNA. Following the end of transcription, DNA is reassembled with histones to form chromatin (Williams and Tyler, 2007).

The challenge of the chromatin assembly and disassembly machinery is to identify these diverse cellular processes and comply to *de novo* histone removal and refurbish chromatin by deposition of histone throughout the cell cycle in different chromosomal regions. Besides, they also must identify between old and newly synthesised canonical histones or variants across the genome. Failure to regulate this histone allocation system, can threaten regular harmony inside cells, such as maintenance of structural integrity of telomeres and centromeres, alteration of the barrier for cellular reprogramming and challenge genome integrity and DNA replication. So, to protect the epigenetic information and make sure the DNA dependent cellular functions are working properly, a special type of histone interacting proteins have evolved - Histone chaperones.

1.5.   Histone Chaperone

In general, a molecular chaperone is a group of proteins that interact with a target protein and prevent its misfolding, thereby avoiding production of inactive or aggregated proteins, e.g., Heat Shock Proteins (HSPs). Histone chaperones are proteins that equates well with histones to assist in their smooth interaction with other molecules. The pI of histone proteins is highly basic. The primary aim of histone chaperones is thus to guard these positively charged histones from the negatively charged DNA. Histone and DNA interact to form the nucleosome in an ordered manner. In the absence of histone chaperones, *in vitro* study in physiological ionic strength shows, histones and DNA swiftly

interact with each other and generate insoluble aggregates which is highly disordered in nature (Linger and Tyler, 2007). In a different study using Xenopus egg extracts, nucleosome assembly was achieved by mimicking physiological ionic strength (Laskey et al., 1977). Later Nucleoplasmin, nucleosome assembly factor, was isolated form Xenopus egg extracts which does not require cofactors, such as ATP to perform chromatin assembly in SV40 DNA. These studies regained widespread interest among the scientist community and new histone chaperones with different primary structures were subsequently isolated.

1.5.1. General mechanisms of chaperone-mediated histone escort

1.5.1.1. Structural features of Histone Chaperones

Structural studies on the histone chaperones give the mechanistic understanding about how these chaperones contribute to chromatin structure. Crystal structure of the histone chaperones and/or of histone chaperones-histone complex (Song et al., 2008; Ramos et al., 2010; Murzina et al., 2008; Hu et al., 2011; Zhou et al., 2011; Eitoku et al., 2008; Das et al., 2010) helps to emerge and advance the field of histone chaperones.

Histone chaperones belong to a diverse group of protein families which has less structural similarity but shares the common functional responsibility. Most chaperones have a globular core domain and an acidic region which sometimes play a crucial role for histone binding (Park and Luger, 2008). The acidic amino acid residues are also low in structural complexity. This flexible acidic stretch is hypothesized to have a pivotal role in shielding histone protein surfaces and promote histone transition from chaperone-bound form to nucleosomes (Park et al., 2005).

1.5.1.2. Histone Chaperones helps efficient nucleosome assembly

Histone chaperones follow two basic principles to interact with histones: through charge based (e.g., Nap1, VPS75) (Park et al, 2005, Bowman et al., 2011) or hydrophobic interfaces (e.g., Asf1, DAXX, HJURP, Scm3) (Hondele and Ladurner, 2011; Elsässer and D'Arcy, 2012). A histone-chaperone complex blocks all nonspecific interaction of histones and introduces them to their 'correct' orientation for nucleosome assembly. At times, histone chaperone binding to histones also contorts the histone dimer (Song et al., 2008; Murzina et al., 2008; Zhou et al., 2011).

1.5.1.3. Thermodynamics of Histone chaperones

Nucleosome assembly is a complex process and is eventually guided by affinities between its histone chaperones, DNA, and histone molecules (Andrews and Luger, 2011; Andrews et al., 2008; Koopmans et al., 2007). DNA is negatively charged while the histones are basic. So, their interactions are very strong and electrostatic in nature but unspecific. Thus, interaction of DNA and histones will give rise to irreversible aggregation through non-productive interactions (Figure 2.14.). Histone chaperones act as a shield between histone-histone and histone-DNA interactions by forming fewer stable histones and chaperone intermediates that allow histones to fold correctly to form the proper nucleosome structure, thus ensuring proper chromatin assembly and reducing formation of nonspecific histone-DNA aggregates (Elsässer and D'Arcy, 2012).

In Figure 1.5A, the free energy change is represented along the reaction coordinate, depicting the substrate as the product. Analogous to the thermodynamics principle,

substrates (DNA and histones) undergo a 'transition state' with highest free energy, which act as kinetic barrier before forming the product of low energy. In the absence of histone chaperones, nonspecific interactions of DNA with histones are greatly favoured forming
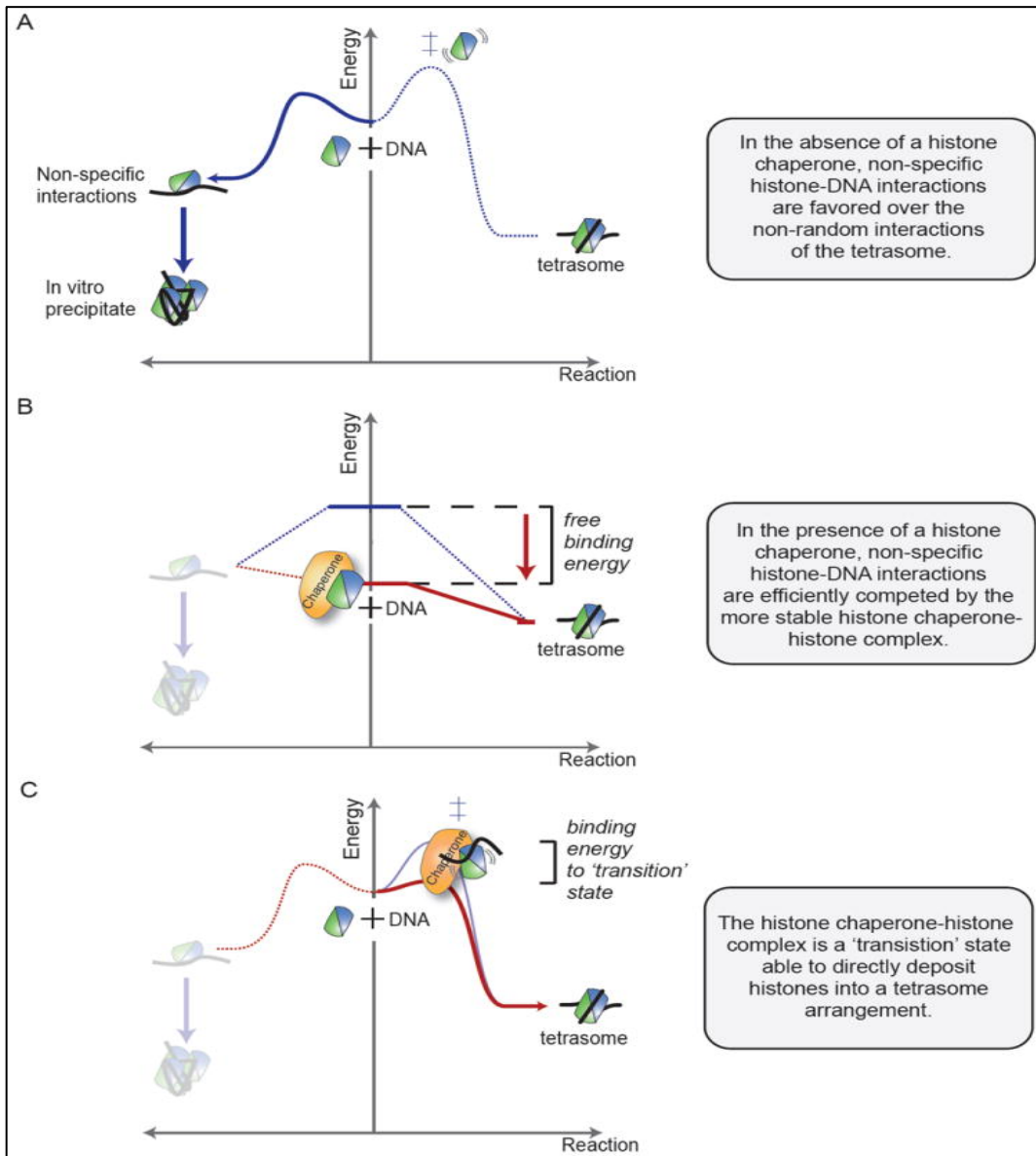
Figure 1.5. Schematic model of histone chaperone function illustrated as free-energy reaction. *Histone chaperones guide histones and DNA through thermodynamically unfavored intermediate states, to prevent non-specific aggregation and ultimately promote the assembly of a correctly folded nucleosome core particle. Diagram adopted from Elsässer and D'Arcy, 2012).*

aggregates (left) in contrast to the tetrasome formation (right) which require DNA and histones to orient systematically and form a conventional nucleosomal fold. Histone chaperones bind to histones with a free energy like that of final tetrasome because of which non-specific interaction with DNA (left) is thermodynamically more costly. This in turn favours tetrasome formation in presence of histone chaperones (Figure 1.5B). An alternative thermodynamic model of histone chaperone action depicted in Figure 1.5C, where a chaperone-histone-DNA trimeric complex formed as a 'transition state' is capable of direct deposition of histones onto DNA.

Nucleosome assembly is assumed to be sequential in nature and is initiated by the H3/H4 tetramers deposition on DNA, followed by H2A/H2B dimers. *In vitro* and *in vivo* experiments supported this hypothesis. Biophysically it was shown that H3/H4 associates with DNA at a greater affinity than H2A/H2B (Wilhelm et al., 1978). *In vivo* experiments, also supports that the yield for H2A/H2B is much more than for H3/H4 (Jamai et al., 2007).

Once the nucleosomes are fully assembled, nucleosome core particle transiently detaches itself from the surface of histone. This detachment occurs spontaneously as strength of DNA-octamer contacts increases that of chaperone-histone contacts (Koopmans et al., 2007). During disassembly of nucleosomes, ATP-dependent chromatin remodelers create a loop or torsion in the chromatin and propagates further (Figure 1.6B).

Such energy dependent process may provide temporary access to histone sites that are usually buried under the DNA. These events give rise to an opportunity for the histone chaperones to bind and disassemble the chromatin further. This destabilization of DNA-

histone interactions in chromatin also promotes progression of DNA or RNA polymerases (Kulaeva et al., 2009) and bring into action the histone free naked DNA template.
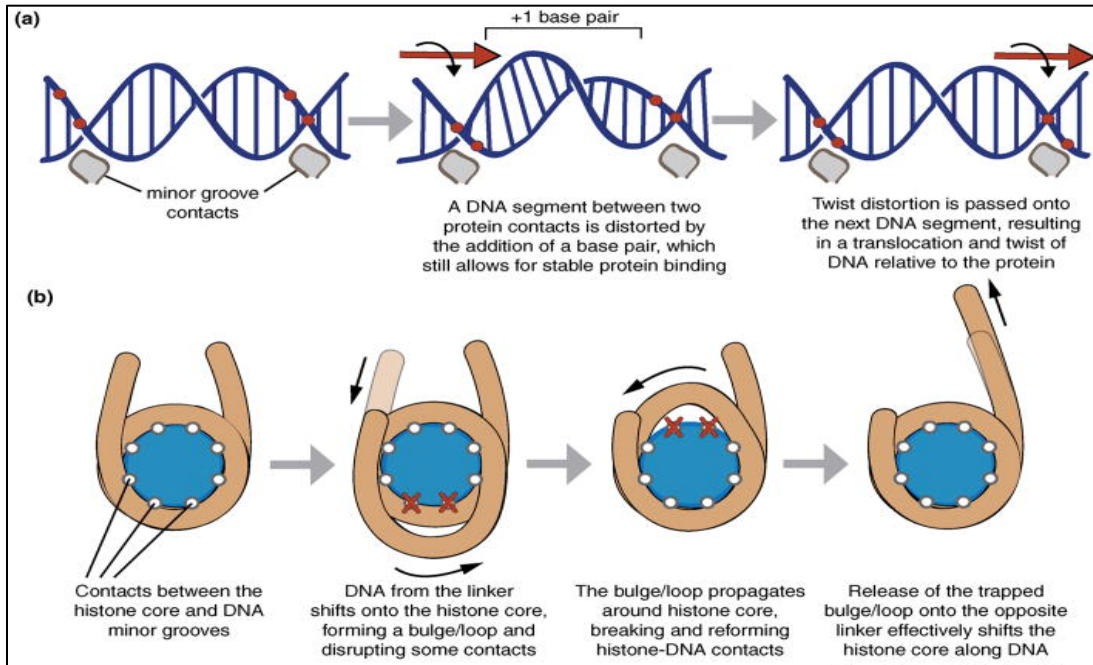
Figure 1.6. Schematic models of ATP-dependent chromatin remodeling action. *(a) Twist-diffusion model. (b) Loop-propagation model. (Adopted from Bowman, 2010).*

1.5.2. Recruitment of histone chaperones to chromatin

All interactions of histones, starting from synthesis in cytoplasm to successive incorporation into DNA to form nucleosomes in nucleus is regulated by histone chaperones. They are a diverse range of protein families, consisting of various protein folds but still bear common characteristics to bind and prevents unwanted connections during folding, transport, storage, assembly and disassembly of histones (Warren and Shechter, 2017). Histone chaperones have also been visualised to cooperate with chromatin modellers by acting as histone sinks or histone acceptors (Owen-Hughes, 1996; Swaminathan et al., 2005; Lorch et al., 2006). Although most histone chaperones prefer

binding either to histones H3/H4 or H2A/H2B individually, but a few recent studies show that some of the histone chaperones can interact both H3/H4 and H2A/H2B via different domains or subunits. Using different structural and functional studies, the histone chaperones can be classified into different groups according to their functions. It is essential that new histones are synthesized, processed, and transported to specific sites within the genome while old histones are required to be incorporated after disassembly. This total process is beautifully orchestrated by histone chaperones.

1.5.2.1. Role of histone chaperone in replication-dependent chromatin assembly and disassembly

Histone turnover is at the highest degree during replication to wrap the duplicated amount of genomic DNA that is synthesized in S-phase to form chromatin. Since chromatin hinders DNA polymerases from accessing the DNA template, histones are initially disassembled during replication. DNA helicase complex MCM2-7 along with the replication machinery evict the histones from the chromatin template. Histone chaperone Facilitates Chromatin Transcription (FACT), that associates with MCM4 (Gambus et al., 2006), pick up evicted histone H2A/H2B while histone H3/H4 is collected by ASF1. ASF1 with the helicase MCM2 forms a stable complex and then collects histones and leaves (Groth et al., 2007a, b; Tan et al., 2006). Nucleosomal conformation must be re-assembled with the pervious form after replication machinery goes through the DNA fork. This ensures genomic stability and preserves the epigenetic information. In re-assembled chromatin fibers, histones are sourced partially from recycled parental histones and the rest half is newly synthesized histones. In replication-coupled chromatin assembly process,

CAF-1 helps in deposition of histone H3.1 variant. Large subunit of CAF1, p150, physically interacts with PCNA in the replisome machinery and enhances chaperone activity (Rolef Ben-Shahar et al., 2009). ASF1 or MCM2 transfer H3/H4 dimers to the CAF-1 and promotes tetramer deposition. CAF-1 (p150 subunit) bears a dimerization domain pivotal for depositing H3/H4 tetramer onto DNA (Quivy et al., 2001; Tagami et al., 2004; Liu et al., 2012; Sauer et al, 2017). Asf1 and CAF-1, are decisive factors of DNA replication. Knock out of these chaperones lead to defects in chromosome segregation and proceeds to cell cycle arrest in S-phase (Nabatiyan and Krude, 2004; Hoek and Stillman, 2003; Groth et al., 2007a, b).

Newly synthetized histones remain secured by chaperones in the cytosol. The complex of histone-chaperone with the help of nuclear importing factors, Karyopherins is then imported into the nucleus. H2A/H2B dimer in yeast, is chaperoned by Nap1, that localizes in cytosol during G2 phase and then in S-phase goes inside the nucleus (Ito et al., 1996). H2A/H2B-yNAP1 complex is imported to the nucleus with the help of karyopherin Kap114 (Mosammaparast et al., 2002). Likewise, Asf1 chaperones histone H3/H4 and is brought into the nucleus by Kap123 (Glowczewski et al., 2004). Before incorporation into chromatin, newly synthesized non-nucleosomal histones were acetylated by histone acetyl transferases (HATs). Histone H3 is acetylated by Rtt109 at H3-K56 position when it is presented inside the nucleus as ASF1-H3/H4 complex. (Recht et al., 2006; Chen et al., 2008; Adkins et al., 2007; Driscoll et al., 2007).
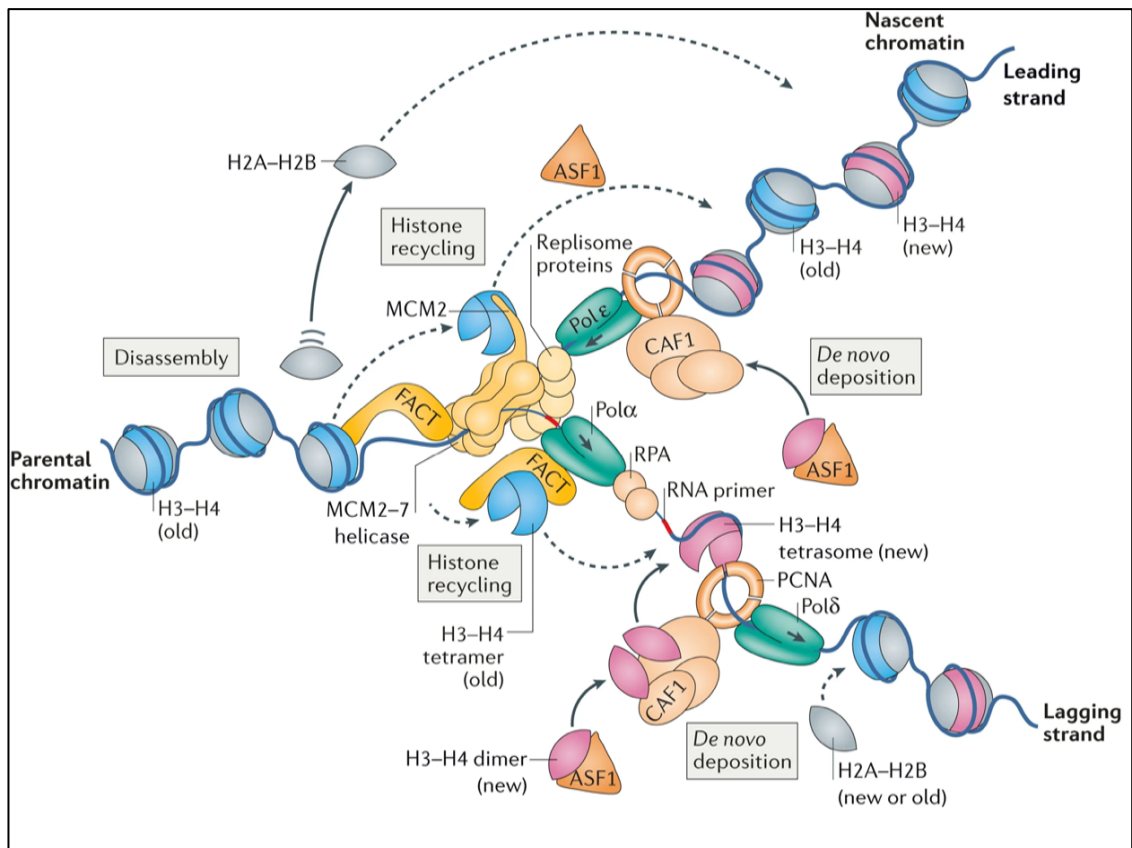
Figure 1.7. Schematic representation of histone chaperone role in replication-coupled nucleosome assembly. *Adopted from Hammond et al., 2017.*

After synthesis of H4, HAT1 complex acetylates its K5 and K12 position before being deposited on to the chromatin during chromatin assembly. (Fillingham et al., 2008; Barman et al., 2008). HAT activity of Rtt109 towards histone H3 is also stimulated by histone chaperone Vps75. In yeast, VPS75-H3/H4 complex advances the histone H3-K9 and H3-K27 acetylation by presenting the N-terminal histone H3 tail to Rtt109 (Abshiru et al., 2012; Fillingham et al., 2008; Su et al., 2011; Berndsen et al., 2008; Park et al., 2008). Nuclear Hif1, H3/H4 chaperone, also is reported to interact with the HAT complexes and helps modify histone H4-K91 before being chaperoned into DNA (Fillingham et al., 2008).

1.5.2.2.   Role of histone chaperone in replication-independent chromatin assembly and disassembly

Eukaryotic histone chaperones juggle histones H3/H4 in between two nucleosome assembly pathways: replication-coupled and replication-independent. Chromatin displays its dynamic nature strongly during transcription or DNA damage repair except for the replication process in S-phase. This replication-independent chromatin dynamics is generally maintained by histone chaperones ASF1, FACT, Spt6, Nap1, histone regulator (HIRA) and DAXX (Tagami et al., 2004; Campos and Reinberg, 2009).

1.5.2.2.1.   Transcription - coupled chromatin assembly and disassembly

Histone chaperones can regulate transcription initiation both positively and negatively. Histone chaperones Asf1, Spt6, FACT and HIRA were described to assist nucleosome disassembly and promote gene expression. On the other hand, Nap1, VPS75 and Chz1 have often been reported to be mediators of transcriptional repression (Kobor et al., 2004; Mizuguchi et al., 2004; Adkins 2006; Luk et al., 2007; Kaplan et al., 2008; Fillingham et al., 2009).

HIRA is a histone chaperone complex made up of three subunits of HIRA, two subunits of CABIN1 and an UBN1. HIRA functions as a histone H3.3 variant specific chaperone and is present in transcriptionally active segments of the genome (Tagami et al., 2004; Green et al., 2005; Ray-Gallet et al., 2002; Goldberg et al., 2010; Ray-Gallet et al., 2011; Schneiderman et al., 2012; Ray-Gallet et al., 2018), is tethered to the transcription machinery through RPA (Zhang et al., 2017) and encourages histone H3.3 deposition on

naked DNA (Ray-Gallet et al., 2011). ASF1 acts as the initial contributor for histone H3.3/H4 dimer to the HIRA complex.

HIRA-UBN1 subunit is analogous to CAF1-p48 subunit in replication coupled chromatin assembly and (Green et al., 2005; Tang et al., 2006) directly interacts with ASF1–H3.3/H4 (Daniel Ricketts et al., 2015, Verreault et al., 1998; Tie et al., 2001). FACT, in addition to being a replication machinery component, is also an essential histone chaperone that associates itself with transcription elongation on account of its association with RNA polymerases (RNA Pol-I, II and III) (Saunders et al., 2003; Birch et al.,
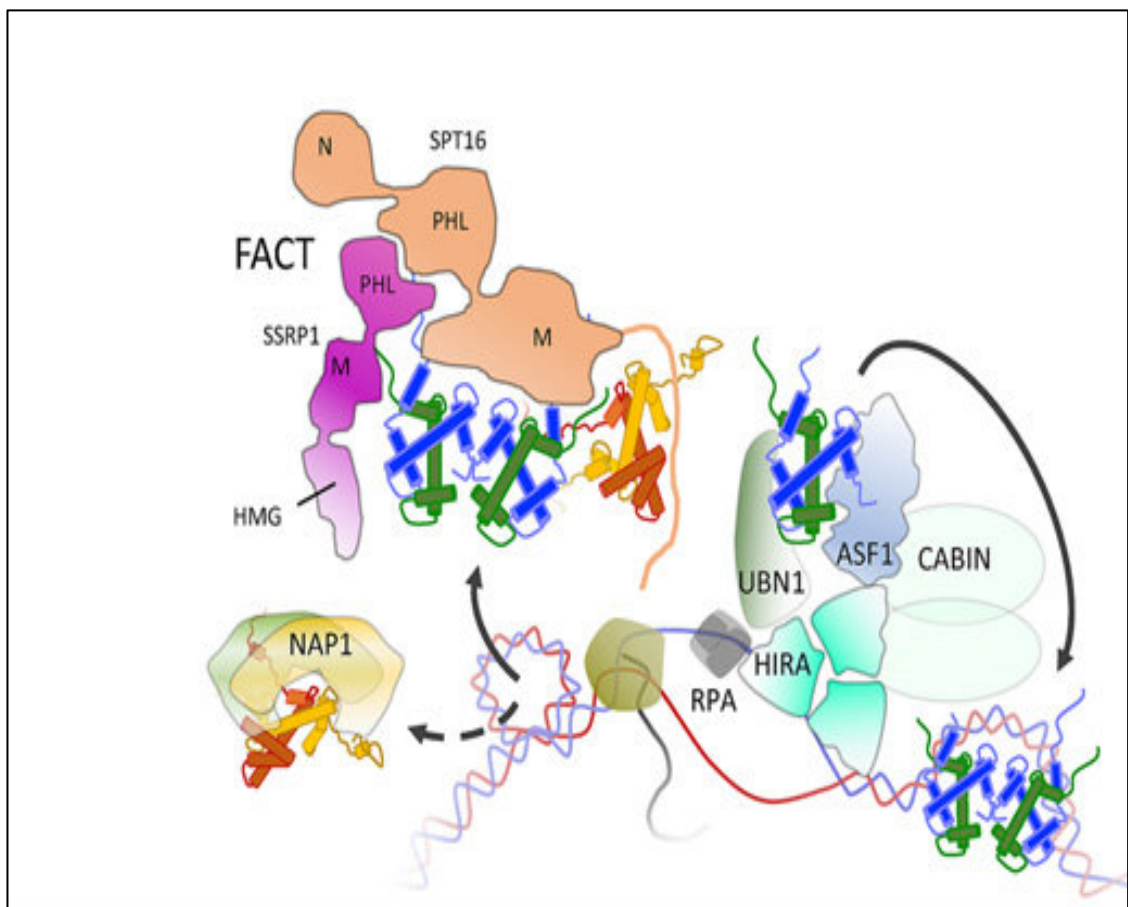
Figure 1.8. Role of histone chaperones in replication independent mechanisms. *Adopted from Pardal et al., 2019.*

2009; Orphanides et al., 1998; Mylonas and Tessarz, 2018). FACT is reported to assist RNA polymerase II processivity and ensure quick chromatin reassembly after transcription of active gene (Formosa, 2012).

ANP32E is a histone variant of H2A.Z specific histone chaperone which shows structural resemblance with FACT. ANP32E aids in H2A.Z–H2B dimers depletion from transcriptionally active genes and regulates enhancers and insulators (Obri et al., 2014). Nucleosome assembly protein 1 (Nap1) is another histone H2A/H2B specific chaperone that has also been reported to have role in transcription. H2A/H2B dimers are enveloped by Nap1 and prevents non-specific associations of H2A/H2B with DNA and promotes correct nucleosomal folds during chromatin assembly (Aguilar-Gurrieri et al., 2016; Andrews et al., 2010). In yeast, hexasomes are more abundant in ΔNap1 compared to WT, suggesting a preferential role of Nap1 in depositing H2A/H2B dimers (Aguilar-Gurrieri et al., 2016).

1.5.2.2.2. Role of histone chaperone in DNA Damage Repair

Histone chaperone CAF1 has been observed in double stranded break repair machinery. In the replisome, PCNA can also recruit CAF1 for repair, at damaged DNA sites (Moggs et al., 2000; Polo et al., 2006; Li, 2016; Brachet et al., 2015). In yeast, Rtt106 mediates replication coupled DNA repair and deposits histone H3/H4 (Huang et al., 2005). Recruitment of Rtt106 in damaged DNA site is less characterised which involve DNA (Liu et al., 2010), and associate histone chaperone interactions of Cac1 (CAF1 p150) (Huang et al., 2005) and FACT (Yang et al., 2016).

Interestingly, MCM2 and ASF1 in histones H3/H4 bound form can also engage TONSL (Saredi et al., 2016) as a histone chaperone. Ankyrin repeat domain (ARD) of TONSL recognizes the H4-K20 unmethylated (H4K20me0) form (Henikoff and Smith, 2015). Thus, TONSL exhibits dual function as a histone reader and (Saredi et al., 2016; Campos et al., 2015) histone chaperone. A large co-chaperone complex inclusive of MCM2, ASF1, TONSL and MMS22L promotes homologous recombination (Piwko et al., 2011). Role of TONSL in histone delivery or deposition remains unknown in damage repair system. TONSL, as it interacts with H4K20me0 (new histone mark), may utilize the
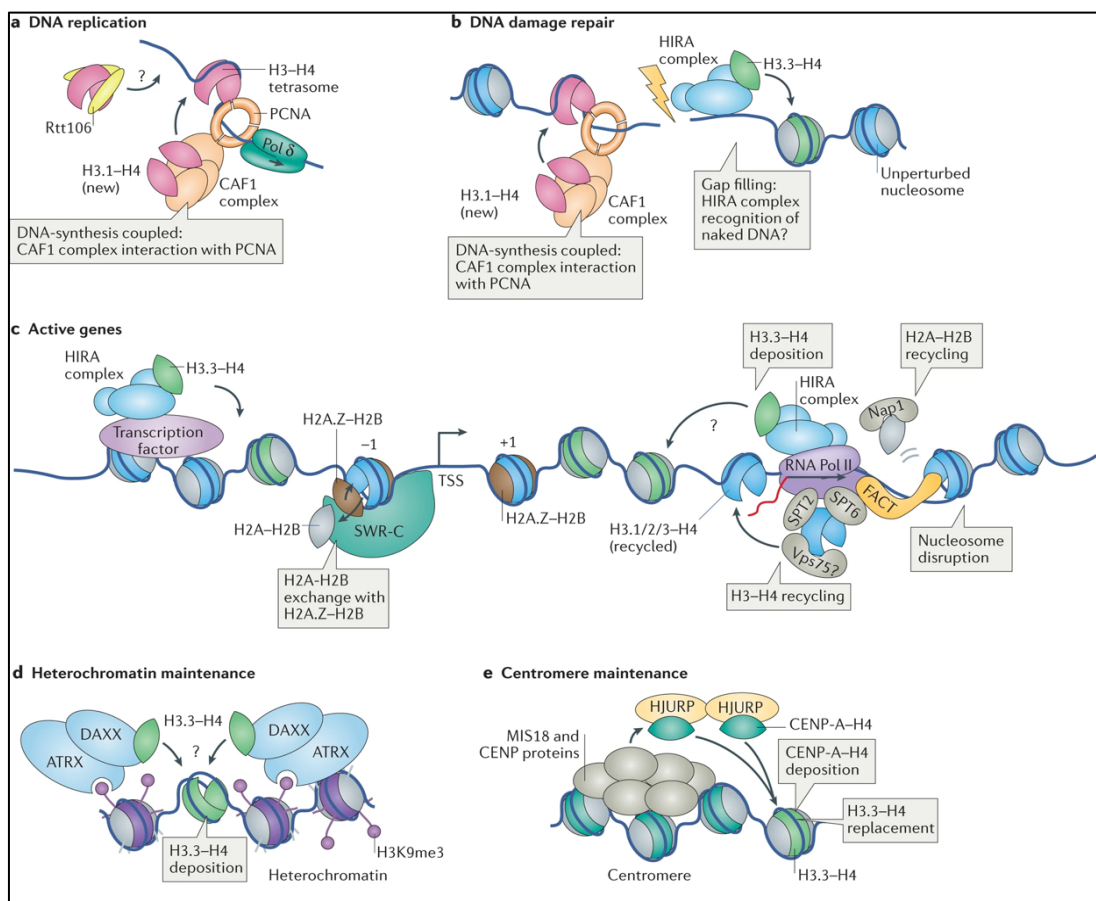
Figure 1.9. Employment of histone chaperones to chromatin. *Histone chaperones recognize canonical or histones variants and maintains the chromatin dynamics. Adopted from Hammond et al., 2017.*

new H3/H4 transport pathway, and thereby help histone H3/H4 deposition onto DNA after repair of DNA damage in the replication fork (Saredi et al., 2016).

1.5.2.2.3.   Role of histone chaperone in heterochromatin maintenance

H3.3 accumulate on actively transcribed genes and is found at silenced heterochromatin segments of the genome (e.g., telomeres, retrotransposons and pericentromeric regions) (Winkler et al., 2011). Dimeric complex of histone-binding protein, DAXX (Death Domain Associated Protein) and chromatin remodeler, α-thalassemia/mental retardation X-linked (ATRX) was identified as a histone chaperone. DAXX/ATRX complex is reported in histone H3.3 deposition and chromatin remodeling in heterochromatin region (Verreault et al., 1998; Kleinschmidt and Franke, 1982). DAXX wraps H3.3/H4 dimer in a way that it blocks the ASF1 towards histones. H3G90 of histone H3.3 is influential for DAXX interaction and any substitution mutation of histone H3.3 at G90 abolishes the DAXX-H3.3/H4 complex formation (Elsasser et al., 2012). ATRX sense heterochromatic marks H3K9me3 in genome and then recruits DAXX to heterochromatic mark enriched regions (Iwase et al., 2011) in the presence of heterochromatin protein 1 (HP1) (Lechner et al., 2005) or through long non-coding RNAs (Park et al., 2018). In turn, complex of ATRX/DAXX take part in propagating and maintaining this repressive state of chromatin (Voon et al., 2015; Dyer et al., 2017) and working as a positive feedback loop.

1.5.2.2.4.   Role of histone chaperone in centromeric chromatin maintenance

In budding yeast, Cse4/H4 (homologous to CENP-A) containing nucleosome was discovered at a centromeric region. After completing DNA replication in S-phase, it is

significant for centromere to divide and maintain the centromeric chromatin state. During this process histone chaperones help deposit CENP-A/H4 at centromere to complete true chromosome segregation (Muller et al., 2014). Scm3 chaperone helps in the centromeric chromatin dynamics where the old Cse4/H4 containing nucleosomes are removed during replication and new ones are replenished (Xiao et al., 2011; Stoler et al., 2007; Camahort et al., 2007; Shivaraju and Gerton 2011; Mizuguchi et al., 2007; Wisniewski et al., 2014).

However, incorporation of new CENP-A onto DNA is independent of replication, but it is deposited by histone chaperone HJURP before the next round of DNA replication (Jansen et al., 2007; Pidoux et al., 2009; Foltz et al., 2009; Dunleavy et al., 2009; Westhorpe et al., 2015). This HJURP dependent CENP-A deposition is cell cycle regulated (Muller et al., 2014; Foltz et al., 2009; Dunleavy et al., 2009) and needs various constitutive centromeric components like RBAP46/RBAP48 and MIS18 complex (Muller et al., 2014; Westhorpe et al., 2015; Foltz et al., 2006). Presence of CENP-A in chromatin defines the centromere and not the DNA sequence (Lando et al., 2012; Jansen et al., 2007) and it directs recruitment of other centromeric proteins and MIS18 (Westhorpe et al., 2015; Foltz et al., 2006). Thus, centromeric chromatin is maintained by a self-sustaining epigenetic mechanism that is governed by centromere specific histone chaperones.

1.6.   Categorisation of Histone Chaperones based on its Interacting Partner

Histone chaperones are also organised based on their histone cargo specificity. Table 1.1. depicts in detail the most studied H3/H4 and H2A/H2B specific histone chaperones, with their function, canonical or variant specificity and evolutionary conservation.

Table 1.1. Classification of histone chaperones according to their binding preference					
Categorisation of histone chaperones	Histone chaperones	Variant selectivity	Conservation	Main function(s)	References
H3-H4	ASF1 (*Drosophila melanogaster*)	H3.1-H4, H3.3-H4	Asf1 (*S. cerevisae, X. laevis*), Cia1 (*S. pombe*), Sga1, Sga2 (*Arabidopsis thaliana*), ASF1a, ASF1b (*M. musculus, H. sapiens*)	Histone donor for CAF-1 and HIRA	Tyler et al., 1999; Munakata et al., 2000; Umehara and Horikoshi, 2003
	CAF-1 complex (*Homo sapiens*)	**H3.1-H4**	-	Deposition factor coupled to DNA replication, synthesis, and repair	Smith and Stillman, 1989
	p150	**H3.1-H4**	Rif2/Cac1 (*S. cerevisae*), SPBC29A10.03C (*S. pombe*), Fas1 (*A. thaliana*), p180 (*D. melano-gaster*), p150 (*X. laevis, M. musculus*)		
	RbAp48	H3-H4	Msi1/Cac3 (*S. cerevisae*), Msi16 (*S. pombe*), Msi1 (*A. thaliana*), p55 (*D. melanogaster*), p48 (*X. laevis*), RbAp48 (*M. musculus*)		

	p60	**H3.1-H4**	Cac2 (*S. cerevisae*), SPAC26H5.03C (*S. pombe*), p150 (*D. melanogaster*), Fas2 (*A. thaliana*), p60 (*X. laevis, M. musculus*)		
	DAXX (with ATRX)	H3.3-H4	-	Deposition factor independent of DNA synthesis; telomere maintenance, ribosomal DNA, peri-centric hete-rochromatin	Goldberg et al., 2010; Drané et al., 2010
	Hif1(*Saccharo myces cerevisae*)	H3.3-H4	-	Assists HAT	Ai and Parthun, 2004
	HIRA	**H3.3-H4**	HIR1/HIR2 (*S. cerevisae*), HIRA (*D. melanogaster, A. thaliana, M. musculus, H. sapiens, X. laevis*), Sim2, Hip1 (*S. pombe*)	Deposition factor that is independent of DNA synthesis	Ray Gallet et al., 2002
	Cabin 1	**H3.3-H4**	Hip3 (*S. pombe*), Hir33 (*S. cerevisae*), AT4G32820 (*A. thaliana),* Cabin1 (*M. musculus*)	Deposition factor that is independent of DNA synthesis Centromere maintenance, deposition factor	Ray Gallet et al., 2002 Dunleavy et al., 2009; Foltz et al., 2009

	HIRA complex	**H3.3-H4**	-		
	UBN1 (ubinuclein 1)	**H3.3-H4**	-		
	HJURP (Holliday junction recognition protein) (*H. sapiens*)	CENP-A-H4	Sem3 (*S. cerevisae*), HJURP (*X. laevis, M. musculus*), CAL1 (*D. melanogaster*)		
	N1/N2 (*Xaenopus laevis*)	H3-H4	tNASP (testicular nuclear autoantigenic sperm protein), sNASP (somatic NASP) (*H. sapiens, M. musculus*)	NASP protects H3-H4 from degradation in human cells; H3-H4 storage in *X. laevis* oocytes	Kleinschmidt et al., 1985; Campos et al., 2010; Cook et al., 2011
	Rsf-1 (*H. sapiens*)	H3-H4	Rsf-1 (*M. musculus*)	Assists RC	Loyola et al., 2001
	SSRP1 (structure specific recognition protein) (FACT complex)	H3-H4	Pob3 (*S. pombe*), Pob3 (*S. cerevisae*), SSRP1 (*X. laevis, D. melanogaster, M. musculus*), SSRP (*A. thaliana*)	Assists in chromatin remodelling, transcription elongation	Belotserkovskaya et al., 2003
	Rtt106 (*S. cerevisae*)	H3-H4	SPAC6G9.03c (*S. pombe*)	Heterochromatin silencing	Huang et al., 2005
	Spt6 (*S. cerevisae*)	H3-H4	Spt6 (*D. melanogaster, S. pombe, M. musculus, X. laevis, H. sapiens*)	Transcription initiation and elongation	Bortvin and Winston, 1996

	Minichromosome maintenance protein 2 (MCM2) (*H. sapiens)*	CENP-A-, H3.1-, H3.2-, H3.3-H4	Mcm2 (*S. cerevisae*)	Part of MCM 2-7 complex of replication machinery consisting of HBD domain with which it helps in H3-H4 binding	Huang et al., 2015; Clement and Almouzni, 2015
	Tonsuku Like (TONSL) (*H. sapiens)*	H3-H4	-	Forms complex with MMS22 and facilitates histone chaperoning during DNA repair	Saredi et al., 2016
	Importin 4 (IPO4) (*H. sapiens)*	H3.1-, H3.2-, H3.3-H4, H1	-	Nuclear import receptor complex helps in importing H3-H4 from cytosol to nucleus	Groth et al., 2007a, b; Hammond et al., 2017
	Chz1 (*S. cerevisae*)	**H2A.Z-H2B**	HIRIP3? (*H. sapiens*)	Incorporation of H2A.Z by SWR1	Luk et al., 2007
H2A-H2B	Acidic-leucine-rich nuclear phosphoprotein 32E (ANP32E) (*H. sapiens*)	**H2A.Z-H2B**	-	Contains LRR, ZID domain and is a part of P400-TIP60 complex	Mao et al., 2014; Obri et al., 2014
	Protein YL1 (YL1) (*H. sapiens*)	**H2A.Z-H2B**	SWr complex 2 (Swc2) (*S. cerevisae*)	Contains ZID domain and is a part of SRCAP/SWR-C, P400-TIP60 complex	Liang et al., 2016; Latrick et al., 2016
	SET/TAF1b, CINAP (*M. musculus, H.*	H2A-H2B	Nap1 (*D. melanogaster, S. cerevisae,*	Cytosolic-nuclear transport,	Laskey et al., 1978; Rouguelle

	sapiens), Vps75 (*S. cerevisae)*, Nap1(*X. laevis*): Nap1-related protein; Nap1L2 (*Mus musculus*)		*H. sapiens M. musculus,)*, Nap1, Nap1.2 (*S. pombe*), NRP1, NRP2 (*A. thaliana*),	replication, transcription	and Avner, 1996; Okuwaki & Nagata, 1998; Selth and Svejstrup, 2007
	Nucleoplasmin (*X. laevis*), Nucleoplasmin 1 (NPM1) (*H. sapiens*)	H2A-H2B	NPM1, NPM2, NPM3 (*H. sapiens, M. musculus)*, Nip (*D. melanogaster*)	Cytosolic-nuclear transport, replication, transcription; Storage in *X. laevis* oocytes	Laskey et al., 1978; Okwuaki et al., 2001
	Nucleolin (*H. sapiens*)	**macroH2 A-H2B**	NSR1 (*S. cerevisae*), nucleolin (*X. laevis, A. thaliana, M. musculus*)	Assists in chromatin remodelling, transcription elongation	Angelov et al., 2006
	Spt16 (FACT complex)	H2A-H2B	Spt16 (*S. pombe, S. cerevisae, D. melanogaster, A. thaliana, M. musculus X. laevis*)	Assistance in chromatin remodelling, transcription elongation	Belotserko vskaya et al., 2003

1.7.   Classification of Histone chaperones based on Structure

Histone chaperones are not only involved in diverse DNA dependent processes but also show diverse structural properties (Eitoku et al., 2008; Gruss and Sogo, 1992). As a group, histone chaperones do not possess any sequence similarity between them but recent structural studies help researchers to categorise them in a few groups. In a way, histone chaperones are grouped according to their structural motifs.

1.7.1. Immunoglobulin-like folds

ASF1 is a well characterised histone chaperone which has a compact Ig-like β-sheet sandwich fold (Daganzo et al., 2003; Munakata et al., 2000; Tyler et al., 1999). This structural fold does not include the intrinsically disordered extended acidic tail but consists of the N-terminal core domain of ASF1. The core hydrophobic and acidic surface of ASF1 is conserved from yeasts to humans (Agez et al., 2007; Mousson et al., 2005; Daganzo et al., 2003; Umehara et al., 2002). The crystal structure of yeast ASF1-H3/H4 complex reveals that it blankets the C-terminal α-helix of histone H3, thereby occluding the tetramerization surface of H3/H4 (English et al., 2006). A single H3/H4 heterodimer and one molecule of ASF1 together constitute the Asf1–H3/H4 complex (Natsume et al., 2007; English et al., 2006, English et al., 2005; Tagami et al., 2004;). Yeast Yaf9, another histone chaperone takes part in acetylation of H2A.Z and its deposition in euchromatin regions precisely at active gene promoter site. The crystal structure of the conserved yeast domain of Yaf9 (Wang et al., 2009) also reveals an Ig like β-sandwich fold and shows strong structural similarity to yeast ASF1.

1.7.2. Nucleosome assembly protein 1-like fold

The NAP1 family of histone chaperones (Park et al., 2006) are involved in diverse roles like histone delivery from the cytoplasm (Ito et al., 1996; Mosammaparast et al., 2002), binding to histone H1 (Mazurkiewicz et al., 2006), as well as in assembling (Mazurkiewicz et al., 2006; Chang et al., 1997; Walter et al., 1995; Ishimi and Kikuchi,

1991) and disassembling nucleosomes (Sharma et al., 2008; Park et al., 2006; Lorch et al., 2006).
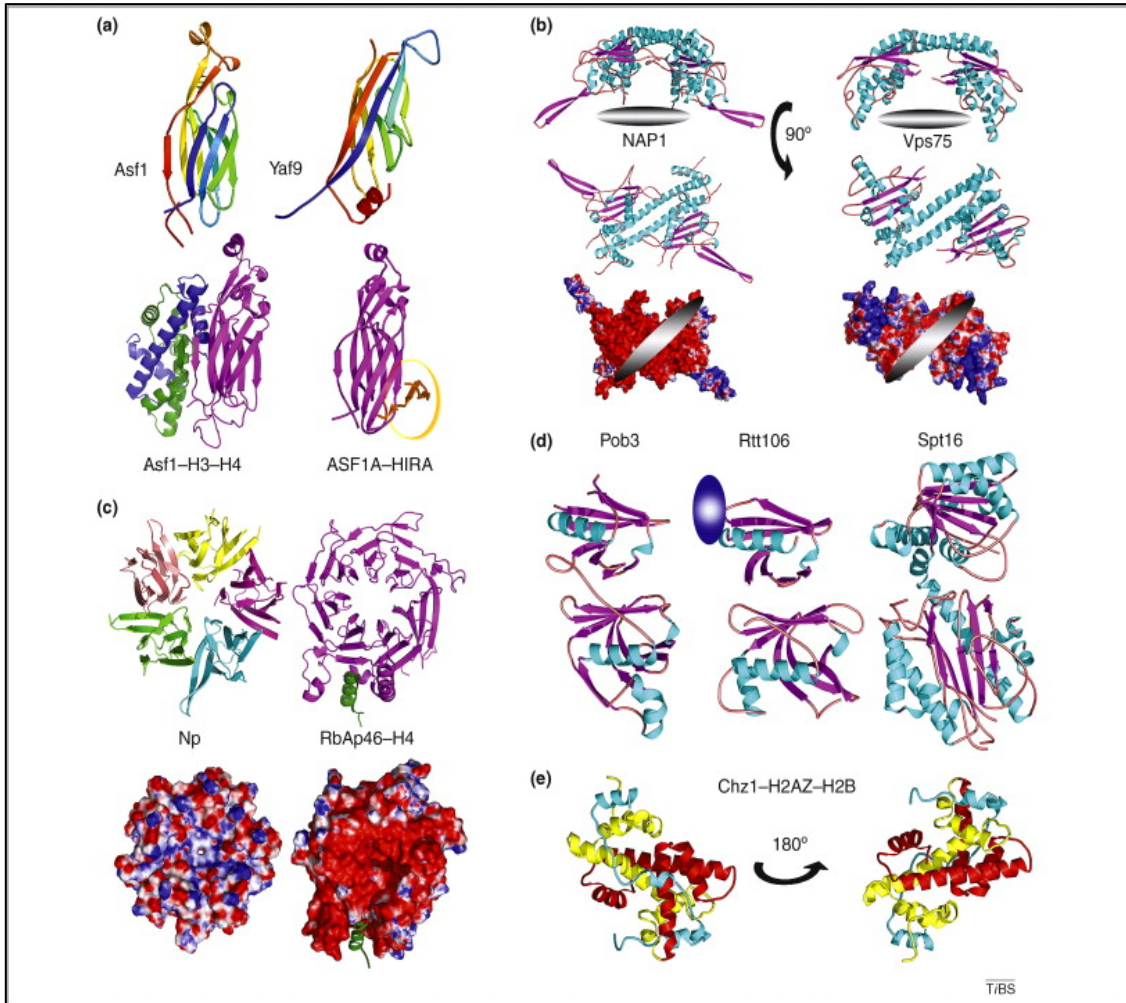
Figure 1.10. Structure based classification of histone chaperone. *3D structures from the RCSB Protein Data Bank are taken. (Image adopted from Das et al., 2010).*

The structure of yNap1 uncovered a unique α/β fold (Park et al., 2006; Park et al., 2008) that is deciphered to be conserved not only from *Plasmodium falciparum* to higher eukaryote NAP proteins (Gill et al., 2009) but also in extended NAP superfamily members, like SET/TAF-IB or inhibitor of acetyltransferases (INHAT) (Muto et al., 2007) and Vps75

(Park et al., 2008; Tang et al., 2008; Berndsen et al., 2008; Bowman et al., 2011; Bowman et al., 2014; Hammond et al., 2016).

Unlike other family of histone chaperones, these NAP fold containing chaperones are usually found as dimers. Long α-helix of two monomers form the α-α' dimerization interface. Surface charge distribution analysis and mutagenesis data revealed that histone binding generally involves the bottom surfaces of the α/β earmuff of NAP domains. (Park et al., 2006).

1.7.3. β-propeller fold or Nucleoplasmin fold

The N-terminal domain of Pob3 through interactions with the middle domain of Spt16 (Belotserkovskaya et al., 2004; O'Donnell et al., 2004) domain is thought to heterodimerize and together they are termed as FACT histone chaperone. The central domain of Pob3 resembles with Pleckstrin homology (PH) domain (VanDemark et al., 2006) which has a helix-capped β-barrel architecture. The N-terminal domain of Spt16 also acts as a histone chaperone fold that has been linked to pita-bread and aminopeptidase domains (Stuwe et al., 2008; VanDemark et al., 2008). Rtt106 has a preferential binding towards histones H3/H4 which is mediated by β-propeller fold or PH domain (Li et al., 2008), like Pob3.

1.7.4. Miscellaneous structural domains

In contrast to the above discussed histone chaperones with defined structures, many other histone chaperones are present across the species that does not possess any

recognizable sequence or structural motif. An NMR structure of Chz1-H2A.Z/H2B complex illustrates Chz1 with an irregular structure of α-helices which interact with the H2A.Z/H2B dimer in a conformation that covers only one surface of the histone dimer (Zhou et al., 2008). DNAJC9 histone binding domain (HBD) consists of two α-helices (αA and αB) and is connected by a loop Lb. Co-complex crystal structure shows that the αA helix of DNAJC9 HBD exhibits interaction efficacy with H3.3-L2 and H4-L1 loops. The αB helix of DNAJC9 on the other hand interacts with H3.3-α2 helix by forming an antiparallel coiled-coil like structure (Hammond et al., 2021).
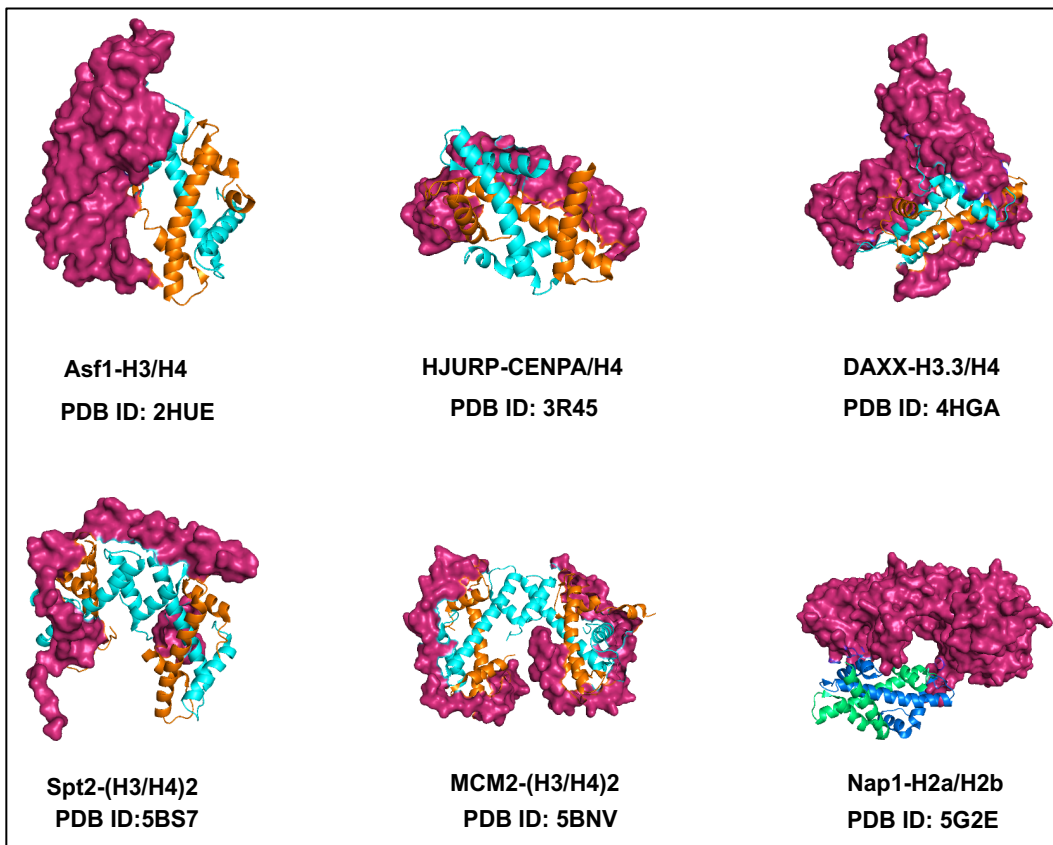
Figure 1.11. Structural depiction of histone chaperone-histone complexes. *3D crystal structures of different histone chaperone-histone complexes are adopted from different PDB ID, mentioned in the images. Histones are depicted as cartoon and histone chaperones are shown as surface representation.*

Crystal structure of MCM2-H3/H4 reveal that MCM2-HBDs wrap around the H3/H4 dimer along its lateral surface covering the tetramerization surface and holds its integrity as H3/H4 tetramer. MCM2-HBD mimics DNA and covers the DNA binding surfaces of the H3/H4 tetramer. The α2 helix of the MCM2-HBD interacts with the hydrophobic interface of H4 and blocks histones from forming nucleosomal connections. On the other hand, N-terminal loop and the α1 helix of MCM2-HBD interacts with the histone H4-α1 helix and L1-loop. MCM2-HBD L1 loop that in turn connects the α1 and α2 in the meantime stabilizes the complex by interacting with α1 and α2 helix of histone H3 (Huang et al., 2015).

1.8.   Co-chaperone complex

Histone chaperones are known to shield nucleosomal surfaces of histones without totally covering the histone fold. In recent times, combinatorial action of multiple histone chaperones is emerging as it has more potential to shield around the histones as a Co-chaperone complex. Crystal structure of MCM2–ASF1-H3/H4 complex reveals that MCM2 protects DNA and other nucleosomal surfaces of histone H3/H4 while ASF1 blocks the tetramerization surface of H3/H4 (Huang et al., 2015; Wang et al., 2015) and thereby promotes nucleosome assembly like that of MCM2-H3/H4 or ASF1–H3/H4 complex.

Recently, TONSL has also been crystallized with histones H3/H4 bound form of MCM2 and ASF1 (Saredi et al., 2016). ASF1, besides its key role in histone H3/H4 chaperoning, also forms multiple co-chaperone complexes with Vps75, UBN1, sNASP, RBAP46, RBAP48, MCM2 and TONSL (Hammond et al., 2016; Burgess and Zhang,

2013; Saredi et al., 2016; Campos et al., 2015; Jasencakova et al., 2010; Groth et al., 2005; Groth et al., 2007 a, b; Canpos et al., 2010; Haigney et al., 2015). Interestingly, RBAP46, sNASP, and ASF1 also engage histones H3/H4 in a single histone-chaperone complex (Jasencakova et al., 2010; Groth et al., 2007 a, b; Campos et al., 2010; Haigney et al., 2015). In addition, sNASP forms complex with HSP90 (Campos et al., 2010), and assemble H3/H4 dimer prior to its participation in other co-chaperone complexes.
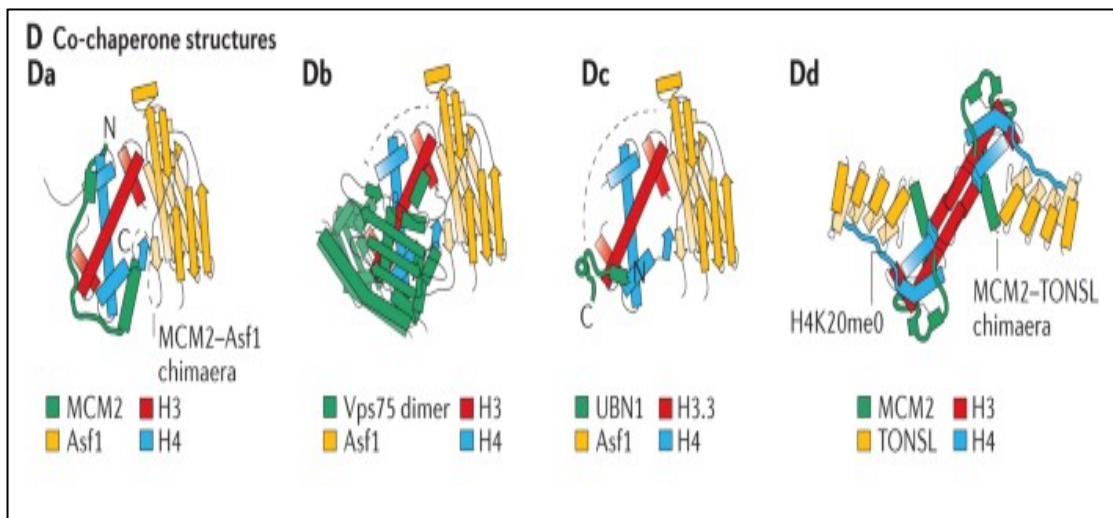
Figure 1.12. Structural folds and interacting regions of histone chaperone co-complexes. *Two-dimensional representations of 3D PDB structures of co-chaperone complex adopted from Hammond et al, 2017.*

The interactions of ASF1 with RBAP48 (Jasencakova et al., 2010), and UBN1 (Daniel Ricketts et al., 2015) are histone dependent in contrast, to other ASF1-CAF1 interaction which is pure chaperone-chaperone crosstalk (Daganzo et al., 2003; Malay et al., 2008; Tang et al., 2006). But it is still not clear how the reciprocity between histone dependent interaction and chaperone to chaperone crosstalk aid in the co-chaperone function and needs to be looked upon in further detail.

1.9.   NAP1 Family Histone Chaperone

In general chromatin interacting proteins such as ATP-dependent chromatin remodelling factors or histone reader, writer and eraser proteins contain specific recognizable catalytic domains. In contrast, histone chaperones do not possess singular uniform domain or a common sequence similarity. However, they are mostly conserved and show similar functions across the species. NAP1 is one of the most distinguished histone chaperones identified across varied diversity of species.

NAP1 was first purified and identified from *Xenopus laevis'* ovum as a transcription factor that facilitates *in vitro* nucleosome assembly (Laskey et al., 1978). Next, homologs of NAP1 have been critically recognised and then well characterized in various organisms across the species (Zlatanova et al., 2007). Interestingly, NAP1 histone chaperones though conserved across species, multiple NAP1 homologues were identified in higher eukaryotes. These proteins are collectively grouped and termed as NAP1 family proteins as they all harbour the NAP1 like α/β-protein fold (Park et al., 2006, Park et al., 2008). NAP1 family proteins grouped into NAP1, NAP1-like proteins family (NAP1L1–NAPL5), SE translocation (SET), CASK interacting nucleosome assembly protein (CINAP), Testis-specific protein Y-encoded family (TSPY) and testis-specific protein Y-encoded Like family (TSPYL) (Table 1.2.).

Table 1.2. All the NAP family members and their respective subfamilies				
Protein name		**Organism**	**Remarks**	**References**
NAP1	yNAP1	Yeast	Effect on expression of 10% of genome	Ohkuni et al., 2003
	xNAP1	*Xenopus*		Steer et al., 2003
	dNAP1	*Drosophila*		Lankenau et al., 2033
	mNAP1	Mouse		
VPS75		Yeast		
NAP1-Like proteins				
NAP1L1		Human	Human counterparts of yNAP1	Ishimi et al., 1987
NAP1L2		Mouse	Specifically expressed in brain tissue, embryonic lethality	Rogner et al., 2000
NAP1L3	MB20	Human	Expressed in brain tissue	Shen et al., 2001
NAP1L4	NAP2	Human	Candidate gene for Beckwith-Wiedemann syndrome	Rodriguez et al., 1997
NAP1L5		Human		Smith et al., 2003
SET				von Lindern et al., 1992
	TAF1B	Human	Stimulated the elongation of DNA replication	Matsumoto et al., 1993
	INHAT		Inhibits histone acetyl transferase	Seo et al., 2001
	PHAPII		Putative HLA-DR associated protein	Beresford et al., 2001
	StF-IT-1		transcription activator of P450c17, and initiates neurosteroidogenesis	Compagnone et al., 2000

	I2PP2A		Inhibits protein phosphatase 2A	Li et al., 1995
	IGAAD		Inhibits Granzyme-A-activated DNase	Fan et al., 2003
CINAP		Mouse	Broadly expressed in different tissues but few-fold higher expression in brain	Lin et al., 2006
TSPY proteins			Expressed in testis, encoded on the mammalian Y chromosome	Schnieders et al., 1996
TSPY1		Human	Regulates spermatogenesis, promotes cell proliferation upon action on CDK1	Shen et al., 2018
TSPY2		Human		Ratti et al., 2000
TSPY3		Human		Skaletsky et al., 2003
TSPY4		Human		
TSPY8		Human		
TSPY10		Human		
TSPY-Like proteins				
TSPYL1		Human	Mutation causes SIDDT syndrome Involved in the development of male reproductive system and the brain and brainstem	Vogel et al., 1998 Puffenberger et al., 2004
TSPYL2	CDA1, DENTT	Human	Part of the REST protein complex and acts as transcription repressor	Epping et al., 2015
TSPYL5		Human	Blocks USP7 activity towards p53, resulting in ubiquitination of p53	Epping et al., 2011
TSPYL6		Human	Associated with shorter telomere length and the risk of developing ischemic stroke	Liang et al., 2017

1.9.1. Structure of NAP domain

NAP family proteins are generally characterized by a central core highly conserved NAP domain and an extended N-terminal and C-terminal region of different lengths. The NAP domain is adequate for binding histones and for chaperone activity (Fujii Nakata et al., 1992) in case of NAP1. Crystal structure of yeast NAP1 (yNAP1) revealed (Park and Luger, 2006 a, b) that C- and N-terminal regions were mostly disorganised while core NAP domain consists of headphone shaped α/β-fold. yNAP1 core domain is a homodimer with
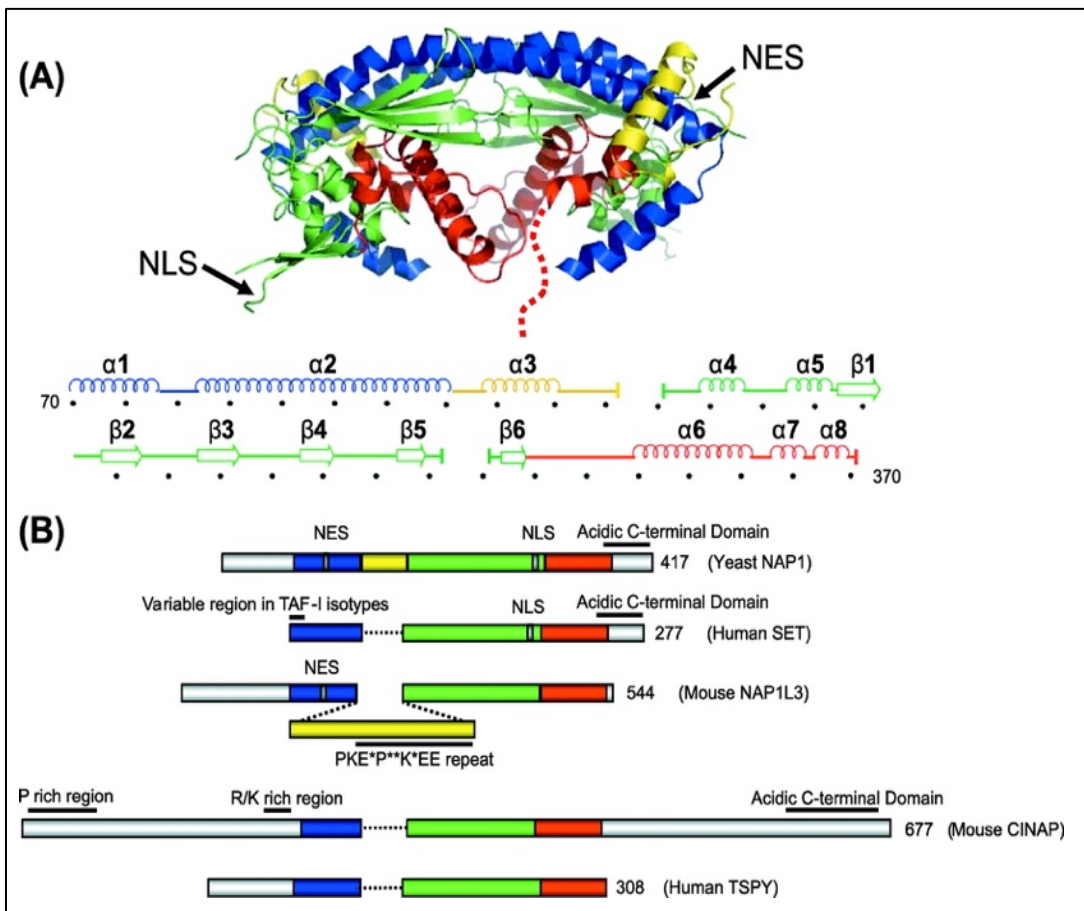
Fig. 1.13. Structural organization and domain of the NAP proteins. *(A) 3D crystal structure and secondary structure of yeast NAP1. (B) Alignments of different members of the NAP family depicting the position and length of the different domains of NAP proteins are. Adopted from Park et al., 2006.*

a long dimerization α-helix and an α/β domain found on every side of each monomer (Park et al., 2006, McBryant and Peersen, 2004).

The nuclear export sequence (NES), followed by an accessory domain is found at the end of the dimerization α-helix. A small antiparallel β-hairpin extending from the α/β fold of the core domain harbours the nuclear localization sequence (NLS). *In vitro* experiments suggest that the β-hairpin region and the C-terminal unstructured region act as a histone-binding region (Park and Luger, 2006 a, b).

In spite of having low amino acid sequence conservation across all members of the NAP family, core NAP domain shows significant structurally homology. The highest sequence and structural variability between members of NAP family is found in the accessory domain. Interestingly, accessory domain is completely absent in SET/TAF1B but it ranges up to 181 amino acids in case of NAP1L3 (Shen et al., 2001). Acidic C-terminal domain is a hallmark of the NAP family proteins which is mostly disordered, and highly flexible in nature (McBryant et al., 2003). The sequence of acidic region is conserved among NAP1 proteins but not in length. Though, SET/TAF1B possesses that acidic domain, in NAP1L5 it is very reduced in size. However, it is intriguing that the acidic region is long in CINAP but mostly absent in TSPY and NAPL3. But TSPYL family proteins interestingly have it in the N-terminal of their NAP domain (Park et al., 2006).

Though NAP protein is ubiquitously expressed but many of the orthologues of NAP1 is highly specific in their expression and remains conserved in certain tissues or cell types only. These NAP family members though were adopted in the group based on how strongly

they showed sequence homology with NAP1 protein but they often even showed diverse functions. In recent times, roles of NAP family proteins in cell cycle regulation, cell proliferation and gene expression are coming into limelight.

1.9.2. Expression patterns of NAP family genes

In human and mouse, homologue of NAP1-Like proteins has been part of the growing NAP family. NAP1L2, NAP1L3 and NAP1L5 are expressed specifically in neurons, whereas NAP1L1 and NAP1L4 are ubiquitously expressed (Attia et al., 2013). Loss of NAP1L2 in mouse has embryonic lethality and shows neural tube after mid-gestation period (Rogner et al., 2000).

Expression of histones are ramped up in the S phase to meet the requirement of histones for chromatin assembly after DNA replication in cell cycle. NAP1 expression both in transcript and protein levels are largely constant and highly synchronised with histone expression during cell cycle progression (Dong et al., 2003). Although, NAP1 is involved in nucleosome assembly during replication and transcription, all the NAP1 proteins are found to actively participate throughout the cellular proliferation. Gene expression of histone chaperone during the cell cycle needs further investigation which in turn will help us understand the regulatory mechanism for proper histone incorporation.

1.9.3. Functional diversity of NAP-Family proteins

NAP family members emerge as multifunctional proteins that are involved in nucleocytoplasmic shuttling, nucleosome sliding (nucleosome assembly and disassembly,

chromatin remodelling and altering gene expression, enzyme inhibition, transcription, replication, and apoptosis regulation (Matsumoto et al., 1993; Fujii Nakata et al., 1992; Kellogg and Murray, 1995; Walter et al., 1995; Mosammaparast et al., 2002; Cervoni et al., 2002; Fan et al., 2003; Mizuguchi et al., 2004; Levchenko and Jackson, 2004; Park et al., 2005; Okuwaki et al., 2005; Park and Luger, 2006 a, b).

1.9.3.1. Histone binding

Histone chaperones are known to assist histone assembly and disassembly function. Thus, to fulfil its function, histone chaperones first need to interact with histones. Reports show that yNAP1 can interact with both histone H2A/H2B and H3/H4 and successfully perform *in vitro* nucleosome assembly (Eitoku et al., 2008). Another NAP family protein in yeast, Vps75 binds with histone H3/H4 and maintains the integrity of the histone tetramer during cell cycles (Bowman et al., 2011, Bowman et al., 2014, Hammond et al., 2016). *In vivo* reports showed that *Drosophila* NAP1 and human NAP1L1 co-immuno precipitated with H2A/H2B (Ito et al., 1996, Chang et al., 1997). SET/TAF1B, which shows great sequence and structural similarity with yNAP1, has interestingly been found to interact with histone H3/H4 and is also able to exhibit histone chaperone function (Muto et al., 2007).

In biochemical assay, yNAP1 was shown to interact with all four core histones to facilitate nucleosome formation *in vitro* (Mazurkiewicz et al., 2006). This report rationally direct to the capability of yNAP1 to protect the histone surface during nucleosome assembly (D'Arcy et al., 2013) and safeguard non-nucleosomal interactions of histone-

DNA complex to prevent nonspecific aggregation (Andrews et al., 2010). The association of NAP1 with H3/H4 is considered essential for effective H2A/H2B incorporation, molecular mechanisms of which can be further identified.

1.9.3.2.   Chromatin assembly, disassembly, and remodelling

Although, molecular functions remain diverse between the different members of NAP family proteins, few reports implicate their role in chromatin assembly. yNAP1 is incorporated in *Xenopus* ovum to perform chromatin assembly *in vitro* (Wongwisansri and Laybourn, 2004; Ito et al., 1996). Biochemical studies *in vitro* using different domain deletion constructs also reported that the NAP domain is enough for chromatin assembly (Fujii Nakata et al., 1992). In contrast to the role of NAP1 in nucleosome assembly, yNAP1 was reported to disrupt the nucleosome and release the H2A/H2B dimer. The carboxy-terminal acidic region of yNAP1 has higher affinity towards H2A/H2B dimer and act as transitional substitute for DNA and removal of H2A/H2B dimers thus resulting in nucleosome sliding (Park et al., 2005).

SET/TAF1B has been reported to modulate viral chromatin structure and eventually stimulate replication and transcription. In contrast to yNAP1, the acidic carboxy-terminal stretch of SET/TAF1B though essential is not enough for alteration of chromatin (Miyaji-Yamaguchi et al., 1999; Matsumoto et al., 1999). yNAP1 is a part of the yeast SWR1 chromatin remodelling complex, which is known for H2A.Z-specific histone exchange (Mizuguchi et al., 2004). This result was also validated by *in vitro* studies where yNAP1 has exhibited role in exchange of histone variants H2A.Z/H2B into nucleosomes (Park et

al., 2005). It has also been reported that H2AB.bd/H2B dimers were efficiently disassembled from nucleosomes by human NAP1 (Okuwaki et al., 2005). VPS75 on the other hand is found to interact with H3/H4 tetramer and facilitate cooperative binding to other histone chaperone and transcription elongation factors like Rtt109, ASF1 (Xue et al., 2013; Selth et al., 2009). Thus, VPS75 has contribution in the histone H3/H4 recycling and histone acetylation during replication-independent chromatin remodelling (Hammond et al., 2016; Bowman et al., 2011; Bowman et al., 2014). NAP family proteins have histone binding activity but their role in chromatin dynamics gain specificity when they are part of a larger chromatin remodelling complex.

1.9.3.3. Transcription regulation

NAP1 has been reported to remove H2A/H2B dimers and in turn makes the chromatin more accessible to inspire the transcription factor binding to DNA (Walter et al., 1995). In human, SET/TAF1B promotes structural changes in chromatin around promoter regions and facilitates transcription (Okuwaki and Nagata, 1998; Kawase et al., 1996l; Telese et al., 2005; Compagnone et al., 2000). Expression of transcription factors like COUP-TF (chicken ovalbumin upstream promoter transcription factor), NGF-IB (nerve growth factor inducible protein B) and SF-1 (steroidogenic factor-1) are known to be regulated by SET/TAF1B (Compagnone et al., 2000). SET/TAF1B along with Fe65, regulates transcription of KA11 (Telese et al., 2005). NAP1 and SET/TAF1B also play a vital role in facilitating transcription elongation (Gamble et al. 2005). HumanNAP1 can also form a complex with E2 and p300 (Rehtanz et al., 2004) and is able to activate transcription of specific genes. *Xenopus* NAP1 is known to regulate expressions of many

genes in a tissue-specific manner (Steer et al., 2003). In mouse, CINAP shows role in binding CASK (calcium/calmodulin-dependent serine protein kinase) and forms a ternary complex with Tbr-1 (brain-specific T-box transcription factor-1) (Wang et al., 2004). CINAP modulates gene expression of Tbr-1 regulated genes. Altogether, these reports suggest the role of NAP family proteins in gene regulation and what they can perform as platforms for transcription factors.

1.9.3.4.   Nuclear shuttling

Drosophila NAP1 and human NAP1L4 has been found in the nucleus in S phase but is prominent during the G2 phase in the cytoplasm (Ito et al., 1996; Rodriguez et al., 1997). yNAP1 acts as a mediator protein for the nuclear import of histones H2A/H2B and as an adaptor between histone and karyopherin (Mosammaparast et al., 2002). A nuclear localization sequence (NLS) found embedded in the β-hairpin in NAP1 resembles the other nuclear proteins (Kalderon et al., 1984; Robbins et al., 1991). Along with NLS, NES also makes sure that after histone deposition, NAP1 is exported from the nucleus and thus histone shuttling continues (Yamaguchi et al., 2003). NES and NLS region of NAP1 lies in the accessory region which is highly variable in length and sequence among different NAP family proteins. So, the efficiency of nuclear import and export may differ among the NAP family proteins and needs to be explored further.

1.9.3.5.   Cell-cycle regulation

Few of the NAP family members are critical in regulating cell-cycle. Reports mention that *Xenopus* and yNAP1 along with SET/TAF1B interact with cyclin B (Kellogg and Murray,
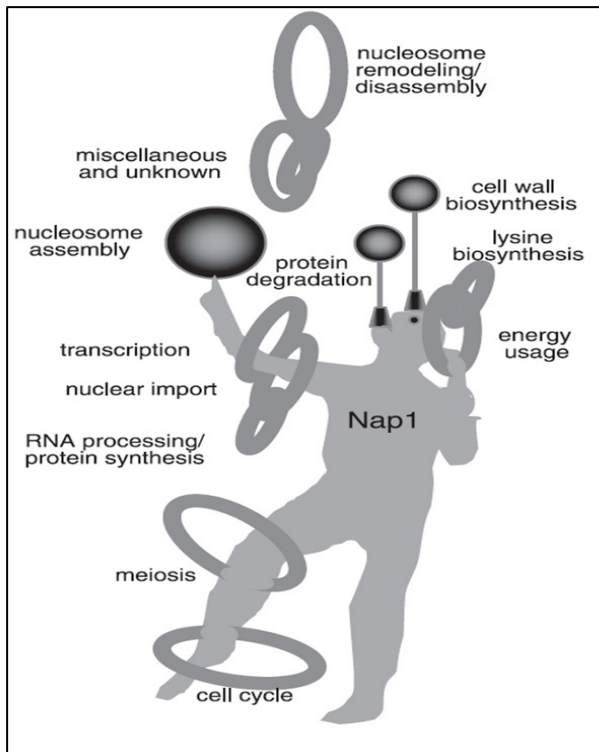
Fig. 1.14. NAP1 is an extraordinary juggler protein. *NAP1 capable to engage multiple proteins and doing multiple functions at same time. Adopted from Zaltanova et al., 2007.*

1995; Canela et al., 2003). *In vitro* analysis show cyclin B/cdc2 kinase complexes govern S/G2 transition, phosphorylates the NAP1 (Kellogg et al., 1995). The loss of function of NAP1 cause prolonged mitotic delays because NAP1 is crucial for Cyclin-B/Clb2 function (Kellogg and Murray, 1995; Kellogg et al., 1995). yNAP1 is also found to interact with several other mitosis regulatory factors like kinase Sda1, NAP1-binding protein 1 (NBP1), and Gin4 (Zimmerman and Kellogg, 2001; Shimizu et al., 2000; Altman and Kellogg, 1997). It is also reported that p21Cip1 interacts with SET/TAF1B and reverts inhibition of Cyclin-B/CDK2 complex but fails to act on Cyclin-A/CDK2 reactivation (Canela et al., 2003) and in turn regulates G2/M transition (Canela et al., 2003; Estanyol et al., 1999).

1.9.3.6. Apoptosis

It has been recently found that SET/TAF1B-containing apoptotic complex plays an important role in caspase-independent apoptosis (Fan et al., 2003). SET/TAF1B is a part of an apoptotic complex that consists of DNA binding protein HMG-2, a tumour suppressor

protein pp32, a base excision repair endonuclease APE-1 and a DNase enzyme called NM23-H1. The β5-β6 region of SET/TAF1B inhibits DNase activity of the complex (Russell and Ley, 2002; Fan et al., 2003).

1.10. Testis Specific Protein Y-encoded protein Family

Testis-specific protein Y-encoded (TSPY) protein is the product of a gene cluster located on the human Y chromosome and is specific to the locus Yp11.2. Testis-specific protein Y-encoded 1 (TSPY1) has been identified first and grouped initially as a NAP protein family member on the basis of its sequence similarity. The transcript level analysis of TSPY proteins confirmed their testis specificity and reported their role in spermatogonial proliferation (Schnieders et al., 1996). Just before the spermatogonia to spermatocyte transition, i.e. in the early spermatogenesis stage, TSPY-may get phosphorylated and its impairment thereafter leads to testicular tumorigenesis (Giachini et al., 2009; Shen et al., 2013). Although, specific function of TSPY proteins in other tissues and cells need to be characterized further, several testis-specific Y-like proteins (TSPYL1, TSPYL5, and TSPYL2/CDA1/DENTT) imply that TSPY family proteins exhibit both diverse as well as tissue-specific functions (Ozbun et al., 2001; Krick et al., 2003; Puffenberger et al., 2004).

1.11. Testis Specific Protein Y-encoded Like Subfamily

TSPYL proteins are structurally related to NAP family proteins and show diverse range of biological functions including cell cycle regulation, protein level regulation of p53, transcriptional repressor. TSPYL family of genes include 6 members out of which

four are coding genes (TSPYL1, TSPYL2, TSPYL4, TSPYL5) and one pseudogene (TSPYL3). TSPYL proteins are predicted to have the NAP domain but the nucleosome assembly activity yet needs to be characterised.

TSPYL2 (also reported as CDA1, DENTT) regulates SIRT1 and p300 function towards p53. In DNA damage system, TSPYL2 inhibits SIRT1 and thus SIRT1 mediated p53 deacetylation is disrupted. By facilitating SIRT1 inhibition it promotes p300 mediated p53 acetylation, p53-dependent transcriptional activation, and induction of p53-dependent apoptosis (Magni et al., 2015). TSPYL2 has also been reported as a component of the transcriptional repressor complex REST/NRSF. This complex plays a key role in regulation of the TGFβ pathway which promotes cell cycle arrest. On the other hand, TSPYL2/REST complex promotes TGFβ signalling by repressing expression of oncogene like tyrosine kinase receptor C (TrkC) and acts as a tumour suppressor in epithelial tissues (Epping et al., 2015).

1.12.   TSPYL5 as a member of TSPY Family

1.12.1. Nomenclature of TSPYL5

Testis Specific Protein, Y-encoded Like 5 (TSPYL5) is a novel NAP family protein (Vogel et al., 1998) located on chromosome 8 specifically at 8q22.1 locus (Qiu et al., 2016). TSPYL5 expression is not specific to either testis or any other tissue, rather it has been reported to be expressed ubiquitously in all cell types and tissues. TSPYL5 is thus named so on account of its sequence homology with TSPY specific sequence.

1.12.2. Expression Pattern of TSPYL5

The first clone of TSPYL5 generated from adult hippocampus cDNA library was initially designated as KIAA1750. The transcript contained 431 amino acids with a repetitive element at its 3' end. Low levels of TSPYL5 in all adult and foetal tissues was detected by RT-PCR and ELISA. TSPYL5 was also detected throughout different brain regions (Nagase et al., 2000).

5' end of TSPYL5 gene, including exon 1, contains CpG islands and its expression is regulated by aberrant DNA methylation. CpGs of TSPYL5 are hypermethylated in diverse types of cancer including glioma, glioblastoma, astrocytomas (Kim et al., 2006), gastric cancer (Jung et al., 2008), oesophageal squamous cell carcinomas (Oka et al., 2009), hepatocellular carcinoma (Qiu et al., 2016) and endometrial cancer (Witek et al., 2016). In some of these, hypermethylation at the CpG islands cause reduced TSPYL5 expression (Kim et al., 2006; Kim et al., 2010; Jung et al., 2008). It was also known to build resistance to γ-radiation in lung adenocarcinoma cells (Kim et al., 2010). Hypermethylation of TSPYL5 in multiple cancer invokes its role in cell cycle regulation, proliferation, and survival (Kim et al., 2006; Vachani et al., 2007; Jung et al., 2008; Kim et al., 2010). Compared to known maternal genes, TSPYL5 gene is actively expressed in early stage hESC and naïve hPSCs (Theunissen et al., 2014; Weissbein et al., 2017).

1.12.3. Putative Functions of TSPYL5

Caspase-1, caspase-3, Bax, ATF4, and CHOP proteins expression were reported to be upregulated on overexpression of TSPYL5. TSPYL5 thus acts as a tumour suppressor

that induces endoplasmic reticulum (ER) stress followed by initiation of apoptosis and repressed cell proliferation, migration, invasion of colorectal cancer cells (Huang et al., 2020). Significantly, TSPYL5 expression was found negligible or absent in most gastric cancer cell lines when compared to normal gastric tissue. CpG islands of the TSPYL5 promoter are very often found methylated in gastric cancers and thus loss of TSPYL5 expression may play an important role in human gastric cancer progression (Jung et al., 2008). Aberrant CpG island hypermethylation and histone deacetylation at TSPYL5 promoter region revealed that it has been a frequent target for epigenetic silencing in glioma and suppresses glioma cell growth in culture (Kim et al., 2006). Similar reports have also been found in hepatocellular carcinoma (HCC) cells where TSPYL5 promoter is hypermethylated and thus it acts as a potential biomarker for HCC (Qiu et al., 2016).

In contrast to these reports, TSPYL5 physically interacts with ubiquitin-specific protease 7 (USP7) and reduce USP7 interaction towards p53. USP7 protein can be subdivided into three distinct regions: N-terminal domain, C-terminal domain, and a central catalytic core domain in between the two. Immuno-pulldown assays show that TSPYL5 selectively binds to the N-terminal domain (residues 1 – 208 amino acids) of USP7 (Epping et al., 2011). This N-terminus region of USP7 was enough for the interaction with p53 also. Thus, it is plausible that TSPYL5 and p53 competes within themselves for binding to the same N-terminal region of USP7. It was observed that the interaction between p53 and USP7 is reduced when TSPYL5 is present, and it results in increased p53 ubiquitylation. This leads to inactivation of p53-target downstream genes and increases cell proliferation followed by oncogenic transformation (Epping et al., 2011). Like TSPYL5, viral Epstein-

Barr nuclear antigen 1 (EBNA1) binds to the N-terminus of USP7 and act as a viral oncogene (Hu et al., 2002; Holowaty et al., 2003; Saridakis et al., 2005). TSPYL5 thus phenocopies the effects of the EBNA1 and shows oncogene-like activity by suppressing p53 functions. Moreover, the binding of USP7 to TSPYL5 may influence various other proteins that are USP7 regulated. (Epping et al., 2011; Shen et al., 2018).

TSPYL5 mediated loss of p53 thus suppress the expression of p53 target genes (CDK1, p21, and BAX) which accelerate the G2/M phase transition in cell cycle. Overexpression of TSPYL5 therefore decreases cell apoptosis and accelerates cell proliferation (Shen et al., 2013; Shen et al., 2018). TSPYL1 is reported to act as a transcription factor and enhance the competitive binding of TSPYL5 towards USP7 in comparison with p53 that result in increased p53 ubiquitylation (Shen et al., 2018). TSPYL5 also show oncogenic function and expression and acts as a prognostic marker in
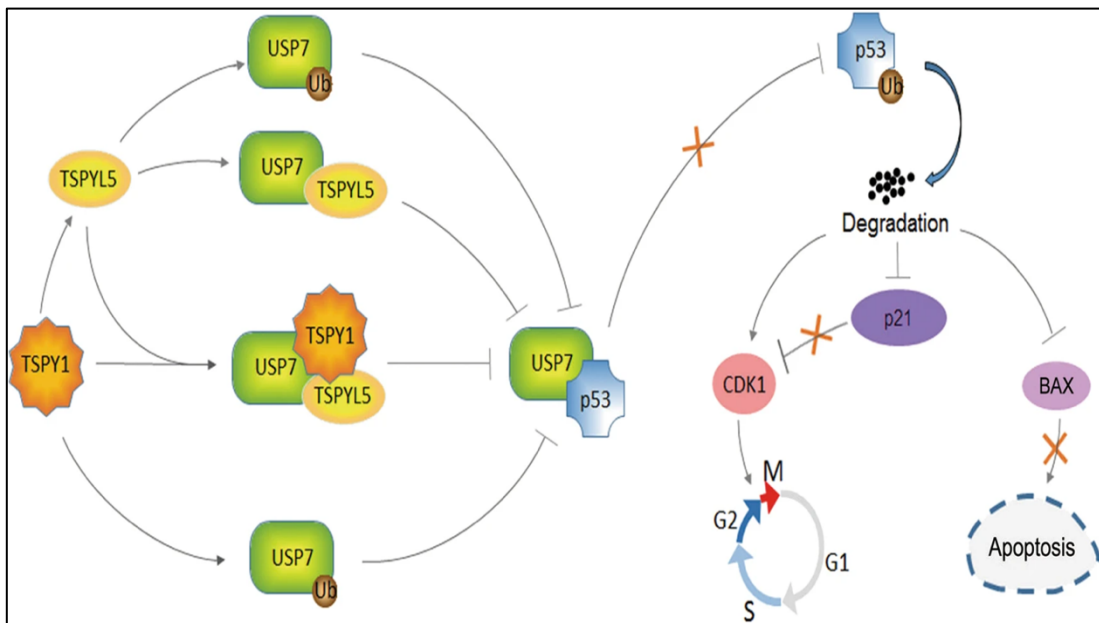
Figure 1.15. Flowchart for molecular action of TSPYL5 mediated p53 regulation *(adopted from Shen et al, 2018*

breast cancer (Shen et al., 2018; Epping et al., 2011). It was also shown to regulate the growth and proliferation of epithelial lung carcinoma cells by controlling p21(WAF1/Cip1) and PTEN/AKT pathways but not EGFR /AKT pathway. Knockdown of TSPYL5 elevated cellular levels of PTEN and p21 and inhibited AKT activation (Kim et al., 2010).

In a separate study it has been illustrated that TSPYL5, PML body component, prevents the polyubiquitination of POT1 and protects proteasomal degradation of POT1 exclusively in ALT+ cells (Episkopou et al., 2019). TSPYL5 has been identified as an uncharacterised PML body component and is also considered as a probable future therapeutic target. It co-localizes with ALT telomeres and maintains POT1 protein levels. TSPYL5 blocks USP7 and thus prevents the USP7-mediated poly-ubiquitination of POT1 and is followed by proteasomal degradation. So, TSPYL5 maintain POT1 levels in ALT+ cells and retains cell viability (Episkopou et al., 2019). It has been documented that, miR-380-5p has degraded TSPYL5 in mRNA level. microRNA mediated knockdown of TSPYL5 expression thus triggers p53 accumulation, which in turn may have effect on TEP1 function and results in inhibition of telomerase activity (Cimino-Reale et al., 2017). Interestingly, TSPYL5 was shown to bind gene promoters (Liu et al., 2013) and may thus affect gene expression (Liu et al., 2013; Park et al., 2006). Upon knockdown of TSPYL5 in hPSCs, RNA sequencing and following gene set enrichment analysis (GSEA) downregulation of differentiation involved genes and tumour suppressors has been observed; while the chromatin-related, pluripotency militance and growth factor genes were upregulated. Here human pluripotent stem cells (hPSCs) are principal candidates in disease modelling and regenerative medicine (Weissbein et al., 2017).

In conclusion, TSPYL5 can function as a tumour suppressor in glioma (Kim et al., 2006), ovarian cancer (Shao et al., 2017), gastric cancer (Jung et al., 2008) and colorectal cancers (Huang et al., 2020) but interestingly it also acts as an oncogene in lung cancers (Kim et al., 2010) and breast cancer (Lyu et al., 2015; Shen et al., 2018; Epping et al., 2011). Thus, TSPYL5 may be a promising contributor as a therapeutic target for cancer but biochemical functions of TSPYL5 specific to chromatin regulation yet needs to be explored.

Aim & Scope

Chapter II: AIM AND SCOPE

Genetic information is packaged into a compacted chromatin in eukaryotic organisms. All the DNA-mediated activities, like replication, transcription, recombination, and DNA repair put forward coordinated attempts of histone chaperones to facilitate the assembly and disassembly of chromatin by deposition or eviction of histones. The Nucleosome Assembly Protein (NAP) family of histone chaperones is conserved from yeasts to humans. NAP family proteins play an important part in histone shuttling from cytosol to nucleus, cell proliferation, cell-cycle regulation, and apoptosis. The testis specific Y-encoded-like proteins (TSPYLs) show remarkable similarity to the Testis specific Y-encoded protein (TSPY) and NAP proteins. There are six members in TSPYL family that includes TSPYL1 to TSPYL6. Genotype Tissue Expression (GTEx) datasets depict that most of the members of the TSPYL family are ubiquitously expressed in all the human tissues. TSPYL5, one of the members of the TSPYL family, harbours a NAP like domain which shows significant sequence homology with the nucleosome assembly protein domain (NAP) that functions in chromatin remodelling and transcription regulation.

The genetic polymorphisms, methylation status and mutations, for TSPYL5 is linked to various diseases. TSPYL5, a member of NAP superfamily, shows high frequency of DNA methylation-mediated silencing in both glioblastoma and gastric cancer. Interestingly, it also shows that increase in TSPYL5 expression reduces USP7 activity towards p53, resulting in increased ubiquitylation of p53 mediated degradation and causing oncogenesis. TSPYL5 silencing via promoter hypermethylation also downregulates tumour suppressor genes and upregulates genes contributing towards

oncogenic transformation. However, there is not much information available regarding its role in gene expression by regulating chromatin dynamics. The efficacy of TSPYL5 in chromatin context and its function as a histone chaperone during DNA mediated processes remains unclear.

Here we thus focus on elucidating the role of TSPYL5 in a chromatin context, which was previously not described, and try to characterize the structural and functional properties of TSPYL5. Tumour suppressor role of TSPYL5 was reported in several cancers like glioma (Kim et al, 2006), ovarian cancer (Shao et al, 2017), gastric cancer (Jung et al, 2008) and colorectal cancers (Huang et al, 2020). Interestingly, oncogenic properties of TSPYL5 are also cited in lung cancers (Kim et al, 2010), breast cancer (Lyu et al, 2015, Shen et al, 2018, Epping et al, 2011). So, our studies will help in better understanding of TSPYL5 expression and function in human and may provide new insight into the epigenetic basis of cell cycle regulation and cancer progression.

Objectives of our study:

- Localisation of TSPYL5 in cell.

- Confirming the membership of TSPYL5 in NAP protein family.

- Sequence and structural characterisation of NAP Like domain of TSPYL5.

- Identifying the histone binding partner specificity of TSPYL5.

- Characterisation of the histone binding of TSPYL5.

- Decipher the TSPYL5 interacting region of its histone partner.

- Validate the Nucleosome assembly and histone deposition function of TSPYL5.

- Characterise the role of TSPYL5 in gene regulation and chromatin assembly/disassembly processes.

Even today we have very limited knowledge regarding the molecular mechanism of TSPYL5 in context of whether it reorganizes histones or not, and which part of the TSPYL5 is vital to this chaperone function. Therefore, we also decide to study the TSPYL5 using a structure based biophysical-biochemical approach. We hope that we will be able to gain better understanding of histone recycling process and get a better picture of the role of TSPYL5 in chromatin alteration through nucleosome rearrangement.

Materials & Methods

Chapter III: MATERIALS AND METHODS

2.1. Materials

Table 2.1. Reagents

Sl. No.	Item	Catalog No.
1.	BL21(DE3) pLysS Cells	Thermo, C606010
2.	Rosetta™(DE3) pLysS cells	Novagen, 70956
3.	pGEX-6p1 Plasmid-AmpR	GE Healthcare GE28-9546-48
4.	pETite N-His SUMO Plasmid-KanR	Lucigen 49003-2
5.	pETite N-His plasmid-KanR	Lucigen 49003-1
6.	Expresso® T7 HIS-SUMO Expression System	Lucigen
7.	Quick Change Site directed mutagenesis kit	Stratagene #200524
8.	Kanamycin	Gold Bio K-120-5
9.	Ampicillin	Gold Bio A-301-5
10.	Chloramphenicol	Gold Bio C-105-5
11.	IPTG	Gold Bio I2481C100
12.	Para-formaldehyde	Sigma P6148
13.	PVDF membrane	Merck
14.	Ni-NTA beads	Bio-Rad
15.	Glutathione Sepharose 4B beads (GST) beads	GE Healthcare, 17-0756-01
16.	r-Protein A Sepharose Fast Flow beads	GE Healthcare, 17-1279-01
17.	Streptavidin Sepharose High Performance beads	GE Healthcare, 17-5113-01
18.	Amicon Ultra centrifuge filter units (100 kDa cut-off)	Millipore ACS510012
19.	DSS Crosslinker	Thermo Scientific 21655
20.	Topoisomerase-I	ThermoScientific 38042024
22.	ProteoSilver staining kit	Sigma ROTSIL2-1KT

23.	Dynabeads™M-280 Streptavidin	Thermo 60210
24.	Ni-NTA Sensor for BLI	(Forte´ Bio NTA, 18-5102)
25.	Streptavidin Sensor for BLI	(Forte´ Bio SA, 18-5019)
26.	Tri Chloro Acetic acid (TCA)	Sigma
27.	Mini and Midi Prep Spin Kit	Qiagen
28.	BamHI	NEB
29.	Hind III	NEB
30.	XhoI	NEB
31.	NdeI	NEB
32.	Platinum Pfx polymerase	Thermo
33.	DpnI	NEB
34.	PreScission protease	GE Healthcare
35.	SEC Superdex 200 GL 10/300 Increase.	GE Healthcare
36.	ENrich SEC 70-10/300	Bio-Rad
37.	Amicon centrifuge filter (100 kDa cut-off)	Millipore
38.	Pre casted gradient SDS PAGE 4 - 12% Bis-Tris	Thermo
39.	DAPI containing mounting media.	Thermo
40.	MNase Enzyme	Sigma
41.	Phenol-Chloroform-Isoamyl alcohol (PCI)	Hi-Media
42.	Dulbecco's Modified Eagle's Medium (DMEM)	Gibco
43.	Heat inactivated Foetal bovine serum (FBS)	Gibco
44.	Penicillin/Streptomycin Mix	Gibco
45.	Anti-Anti (Anti-fungal and anti-microbial)	Gibco
46.	Lipofectamine 2000	Invitrogen
47.	GelGreen DNA staining dye	GoldBio

Table 2.2. Antibodies

Antibody	Company	Catalog No.
Anti-GST-HRP	GE HealthCare	RPN1236
Anti-Flag-HRP	Sigma	A8592
Anti-Flag Monoclonal	Sigma	F1804
Anti-tubulin	Thermo	A11126
Anti-GAPDH	Abcam	ab9485
Anti-Histone H3	Abcam	ab10799
Anti-Histone H4	Abcam	ab10158
Anti-Histone H2A	Abcam	Ab18255
Anti-Histone H2B	Abcam	Ab52985
Anti-Rabbit IgG-HRP	Sigma	A1949
Anti-Mouse IgG-HRP	Promega	W402B
Anti-Rabbit Alexa Fluor 594	Invitrogen	A11029
Anti-Mouse Alexa Fluor 488	Invitrogen	A11032

Table 2.3. Primers

Primer Name	Sequence (5' to 3')
TSPYL5 cloning primers:	
S268AE270A-F	GTAGCTCAGTACCTCTTTCGCTTGGGCATTCAGAAAGGATGCTAGC
S268AE270A-R	GCTAGCATCCTTTCTGAATGCCCAAGCGAAAGAGGTACTGAGCTAC
S340AN343AE345A-F	AAAGAAACTACGGTTGTTTGCTGGGGCTCCCTGGGCTAGGGACTGGAGATCATGC
S340AN343AE345A-R	GCATGATCTCCAGTCCCTAGCCCAGGGAGCCCCAGCAAACAACCGTAGTTTCTTT
TSPYL5E187STOP-F	GGGAGGAAAAGAAGTGAGAGAGGGATGCAGG
TSPYL5E187STOP-R	CCTGCATCCCTCTCTCACTTCTTTTCCTCCC
TSPYL5petit-176-385-F	CTGGAAGTTCTGTTCCAGGGGCCCAATACCTCGGTGTCAGCTGG
TSPYL5petit-176-385-R	GTGGCGGCCGCTCTATTATTCACTCAAAAGGTAGAACT

Histone Tail-Deletion primers:	
H3-Hu-1-His-petite-F	CATCATCACCACCATCACGCGCGTACCAAGCAGACC
H3-Hu-114-His-petite-R	GTGGCGGCCGCTCTATTACGCGTGGATCGCGCACAG
H3-Hu-60-His-petite-F	CATCATCACCACCATCACCTGCTGATTCGTAAACTGCCG
H3-Hu-136-His-petite-R	GTGGCGGCCGCTCTATTACGCACGTTCGCCACGAATA
H4-Hu-21-His-petite-F	CATCATCACCACCATCACGTGCTGCGTGACAACATCC
H4-Hu-102-His-petite-R	GTGGCGGCCGCTCTATTAGCCACCAAAGCCATACAGG
H4-Hu-1-His-petite-F	CATCATCACCACCATCACAGCGGTCGTGGCAAGGGT
H4-Hu-92-His-petite-R	GTGGCGGCCGCTCTATTAACGCTTCAGCGCGTAAACCA
H3L126R-F	CGAATACGACGCGCCCGTTGAATATCTTTCGGCA
H3L126R-R	TGCCGAAAGATATTCAACGGGCGCGTCGTATTCG
H3I130R-F	ACGTTCGCCACGCCTACGACGCGCCAGTTGAATATC
H3I130R-R	GATATTCAACTGGCGCGTCGTAGGCGTGGCGAACGT
Biotin601-146-F	CGGGATCCTAATGACCAAGG
Biotin601-146-R	GGGAGCTCGGAACACTATCC

Table 2.4. Plasmid constructs

Plasmid	**Insert**	**Antibiotic**
pGEX6p1-TSPYL5-NLD	Having 198 - 388 aa	Ampicillin
pGEX6p1-TSPYL5-HBM1	S268A/E270A	Ampicillin
pGEX6p1-TSPYL5-HBM2	S340A/N343A/E345A	Ampicillin
pGEX6p1-TSPYL5 HBM (1+2)	S268A/E270AS340A/N343A/E345A	Ampicillin
pGEX6p1-TSPYL5-ΔNLD	Having 1 - 203 aa	Ampicillin
pGEX6p1-TSPYL5-FL	WT having 1 - 417 Full length	Ampicillin
pCR3-FLAG-TSPYL5-FL	WT having 1 - 417 Full length	Ampicillin
pETiteN-His-SUMO-TSPYL5-NLD	Having 198 - 388 aa	Kanamycin
pETite N-His H3ΔC	Having 1 - 114 aa	Kanamycin
pETite N-His H3ΔN	Having 60 - 136 aa	Kanamycin
pETduet-1 Histone H3/H4	WT	Ampicillin
pETduet-1 Histone H3M/H4	C110E/L126R/I130E	Ampicillin
pET28a H2A	WT	Kanamycin
pET28a H2B	WT	Kanamycin

pET28a H3	WT	Kanamycin
pET28a H4	WT	Kanamycin

Table 2.5. Peptides

Peptides	**Sequence**	**Company**
Biotinylated-H3 (1-21)	MARTKQTARKSTGGKAPRKQL	GL-Biochem
Biotinylated-H3 (21-44)	LATKAARKSAPATGGVKKPHRYRP	GL-Biochem
Biotinylated-H3 (44-69)	PGTVALREIRRYQKSTELLIRKLPFQ	GL-Biochem
Biotinylated-H3 (69-89)	QRLVREIAQDFKTDLRFQSSA	GL-Biochem
Biotinylated-H3 (90-120)	YLVGLFEDTNLCAIHAKRVTI	GL-Biochem
Biotinylated-H3 (120-135)	IMPKDIQLARRIRGERA	GL-Biochem

Table 2.6. Instruments

Instrument	**Company**
GE-Acta Pure FPLC System	GE Healthcare
ImageJ (Version 1.80-172)	NIH, USA
Malvern Nano ZS	Malvern, UK
FLUOVIEW FV1000	OLYMPUS
Octet-RED BLI system	Forte´ Bio
NanoDrop	Thermo
Ultracentrifuge (SW60Ti rotor)	Beckman
Prism7	GraphPad
Optilab T-rEX Refractive Index Detector	Wyatt
Dawn Heleos II Multi-Angle Light Scattering (MALS)	Wyatt
CD Spectro-polarimeter	JASCO-J715

2.2. Methods

2.2.1. Chemically competent cell preparation

To transform *E. coli* cells and incorporate DNA into them, cells can be treated in two ways. One, electrically, where competent cells are prepared using HEPES buffer and given pulse shock for easy DNA uptake. Another way is to treat cells with high concentration of divalent cations (Ca^{2+} and Mg^{2+}) that makes them permeable for DNA uptake. In our study we used chemically competent *E. coli* cells, DH5α, BL21DE3, BL21DE3 (pLysS), Rosetta-pLysS strains. To prepare primary culture, 50 µL of old competent cells was inoculated in 15 mL Luria Broth (LB) media overnight at 37°C at 200 rpm shaking. 1 mL of overnight culture was inoculated in 200 mL LB media the following day (For the BL21-DE3-pLysS and Rosetta-pLysS host strain, culture must contain chloramphenicol at a desired concentration of 37 µg/mL in addition to maintaining the expression plasmid pACYC-T7 lysozyme), and further grown at 37°C with 200 rpm shaking, till $O.D_{600nm}$ reached 0.4. Successive steps were performed on ice to maintain 4°C. Culture cells were pulled by centrifugation for 15 min at 6000 rpm, followed by resuspension of pellet in 65 mL of 100 mM $MgCl_2$ (ice cold) and incubated at 4°C for 15 min. Cells were again pelleted at same speed, resuspended in 80 mL of pre-chilled $CaCl_2$ and incubated for 30 min on ice. This suspension was spin down and re-dissolved in ice cold mix of 1.8 mL 100 mM $CaCl_2$ and 1.2 mL 50% glycerol. Competent cell suspension was aliquoted (50 µL), snap freeze in liquid nitrogen and kept at -80°C. Cells were streaked on ampicillin or kanamycin LB agar plates to check for contamination.

2.2.2. Transformation

Transformation of chemically competent *E.coli* cells was performed using plasmid DNA. Briefly, 100 ng plasmid DNA was added to the competent cell suspension, following incubation for 30 min on ice. This step helps the DNA to be homogeneously attached to the cell surface of the bacterial cells with the help of divalent ions. After incubation, heat shock for 60 s at 42°C was given followed by cold shock on ice for next 5 min. The *E. coli* cells were revived by adding 1 mL of LB media and let it grow for 1 hr with constant shaking at 200 rpm at 37°C. Cells were then pelleted at 2500 rpm at RT for 5 min. The pellet was further resuspended in minimum volume (100 - 200 µL), plated on required antibiotic (specific to the plasmid selection) containing LB agar plates and kept overnight at 37°C. Visible colonies were observed next day.

2.2.3. Plasmid DNA isolation

The plasmid DNA for transforming in chemically competent cells, needs to be isolated from cultured media. The Qiagen Mini-Prep Spin Kit was used for isolation of plasmid DNA from smaller culture volume (10-15 mL), whereas Qiagen Maxi-Prep Kit was used for isolation from larger culture volume (100-200 mL), according to manufacturer's protocol. In brief, the overnight transformed *E. coli* culture was pelleted at 6000 rpm for 15 min at 4°C. The pellet was again resuspended, followed by lysis with lysis buffer. Lysed cells were then mixed with recommended solutions of the kit and centrifuged at high speed. The supernatant containing the plasmid DNA was loaded on to the purification column. Captured plasmids were then eluted in TE buffer following an

adequate wash. DNA concentration was estimated in a nanodrop spectrophotometer and analysed on agarose gel. After analysis the plasmids were stored at -20°C.

2.2.4. Cloning and site directed mutagenesis

2.2.4.1. Conventional Cloning

TSPYL5 Wild type Full length (TSPYL5 WT FL), NLD (NAP Like domain 198-388 aa) and ΔNLD (1-205 aa) domains were cloned in pGEX-6p1vector with N-Terminal GST PreScission protease cleavable tag for bacterial expression. The primers designed with restriction enzyme sites as adapters at the end were used for generating the insert of TSPYL5 clones while inserts of TSPYL5 clones prepared previously by PCR using TSPYL5-PCR3-Flag FL construct used as template and PCR product then checked and purified. WT pGEX-6p1 vector and the inserts as PCR products of the TSPYL5 clones were digested with BamHI and XhoI restriction sites respectively as per manufacturer's protocol and cleaned using Qiagen PCR purification kit. The purified double digested inserts and vector were ligated with T4 DNA ligase as recommended by the manufacturer. NLD and ΔNLD of TSPYL5 were also subcloned from TSPYL5-PCR3-FLAG-Full length plasmid in pCMV-FLAG mammalian expression vector (Biobharati) using the BamHI and XhoI restriction enzymes. The PCR product was then transformed in chemically competent DH5α *E. coli* cells. Next day colonies were picked and cultured in same antibiotic positive LB media. Plasmids were isolated from overnight grown cultures and screened for positive clone by PCR. All positive clones were confirmed using Sanger DNA sequencing.

Histones H3 and H4 was PCR-amplified from cDNA isolated from HEK293T cells and cloned sequentially using both the multiple cloning site (MCS) of pETduet-1 vector.

First Histone H3 was cloned in MCS-I using BamHI and HindIII restriction endonucleases. After sequencing confirmation, H4 was cloned in MCS-II using NdeI and XhoI. Fully ligated pETduet-1-H3/H4 clone was also confirmed by sequencing. Histone H3 has a N-terminal His-tag, H4 was untagged. Similarly, histone H2A and H2B were cloned in RSF-duet-1 vector using both MCS-I and II.

2.2.4.2. Single shot Expresso® T7 Cloning

2.2.4.2.1. Expresso T7 SUMO Cloning

TSPYL5 C-terminal region was also cloned in pETite N-His SUMO Kan[R] (Lucigen) expression vector using the Expresso T7 SUMO Cloning and Expression System which encompasses an inducible T7 expression system (Steinmetz et al., 2011). The pETite™ N-His SUMO Vector is provided in a pre-processed, linearized format to allow instant enzyme-free cloning. After amplification of the desired target gene with appropriate primers, the PCR product was then incubated with the pETite N-His SUMO vector

Figure 2.1. **pETite N-His SUMO Kan expression vector**. *RBS, ribosome binding site; ATG, translation start site; Stop, translation end site; Kan, kanamycin resistance gene; Ori, origin of replication. T7-transcription terminators (T) prevent transcription into or out of the insert. The 6xHis affinity tag is fused to the amino terminus of the SUMO-tagged protein.*

and directly transformed into chemically competent HI-Control 10G Cells (supplied with the vector). Recombination machinery within the host cells helped to join the vector with the insert (Figure 2.1. and 2.2.).

Step 1: Amplify the target gene, using primers that contains 18bp overlap with the vector ends

Step 2: Mix the PCR product and linear pEtite vector in a mictofuge tube

① Vector and Insert assembly ② Transformed vector ③ Bacterial transformation

Step 3: Mixed solution transformed into HiControl 10G cell and selcet the colony by Kanamycin plate

Step 4: Verify the recombinant clones by sequencing

Step 5: Transform into HiControl BL21(DE3) Cells for expression of the target genes

Figure 2.2. **Expresso cloning**. *Target gene amplified with primers and then mixed with the pre-processed pETite vector and transformed into HI-Control 10G cells.*

Using user-supplied primers having 18 nucleotides (nt) of overlap with the ends of the vector, the insert of interest is amplified (Figure 2.3.). The sequence in the forward primer corresponds to the carboxyl terminus of the SUMO fusion partner and that in the reverse primer is inclusive of vector sequences and a stop codon. Recombination between the insert and the vector and takes place inside the host strain *E. coli* where fusion of the

gene of interest PCR to vector occurs. No restriction digestion, ligation, or enzymatic treatment is mandatory for successful recombination.
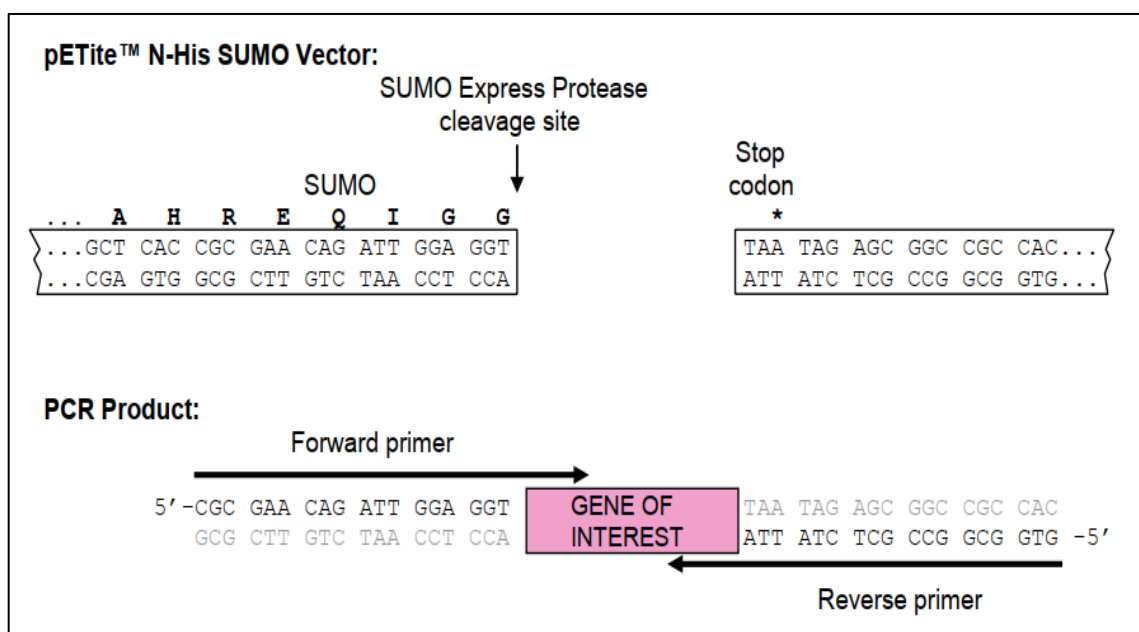
Figure 2.3 Gene insertion into the MCS site of pETite N-His SUMO Vector for protein expression. *Primers have the flanking sequences matching to the vector sequence contiguous to the insertion site. Recombination within the host cell fuses the blunt PCR product to the vector.*

SUMO Forward and pETite™ Reverse primers sequences are:

SUMO Forward: 5'–ATTCAAGCTGATCAGACCCCTGAA–3'

pETite Reverse: 5'–CTCAAGACCCGTTTAGAGGC–3'

HI-Control™ 10G Cells are recA and endA deficient to provide high quality plasmid DNA during cloning. SUMO Forward and pETite Reverse Sequencing Primers are present inside the Kit and used in sequencing to confirm for the clone.

2.2.4.2.2. Expresso T7 N-His Cloning

H3 tail deleted constructs, both H3ΔC-term (having 1-114 amino acids) and H3ΔN-term (having 60-136 amino acids) was also prepared in pETite N-His vector using Expresso

T7-His cloning system (Lucigen) like Expresso T7 SUMO cloning. All the clones were confirmed by sequencing. H4 tail deleted constructs both H4ΔC-term (having 1-92 amino acids) and H4ΔN-term (having 1-102 amino acids) was also prepared similarly.

2.2.4.3. Site directed mutagenesis

TSPYL5 histone binding deficient mutants (HBM), namely HBM1 (S268A/E270A), HBM2 (S340A/N343A/E345A) and HBM (1+2) (S268A/E270AS340A/N343A/E345A) was generated as per the standard protocol using the Quick-change Site-directed mutagenesis kit (Stratagene). Briefly using the template, the sequence specific primers and Platinum Pfx polymerase (Thermo Scientific) PCR was performed. The PCR products were digested with DpnI, the digested product transformed in DH5α *E. coli* cells and colonies were then screened for positive clones. All positive clones were confirmed using Sanger DNA sequencing. Histone H3/H4 tetramer disruptive mutant (H3M), having point mutations at three amino acids (C110E/L126R/I130E), was also generated in the WT-H3-H4 pETduet-1 vector using site directed mutagenesis as per previously described methods.

2.2.5. Cell culture, Over expression and siRNA transfection

HeLa, HEK293T & SH-SY5Y, SK-N-SH cells were cultured and harvested in Dulbecco's Modified Eagle's Medium (DMEM), supplemented with 10% heat inactivated Foetal bovine serum (FBS) and Penicillin/Streptomycin; 10 µL/mL of medium at 37°C in 5% (v/v) CO_2. Every alternate day media was changed for the SK-N-SH and SH-SY5Y cells to maintain healthy growth. All cell lines were acquired from ATCC are were first tested negative to avoid all possible chances of mycoplasma contamination.

HEK293T cells were transiently transfected with FLAG-TSPYL5 WT for fractionation assay and HeLa cells were then transfected with FLAG-TSPYL5 (for immunofluorescence) using Lipofectamine 2000 as per manufacturer's protocol.

2.2.6. *In-Vitro* Protein expression and purification

2.2.6.1. GST Tagged Protein Purification

In order to prepare different wild type and mutant recombinant TSPYL5 proteins, chemically competent BL21(DE3)-pLysS and Rosetta™(DE3) pLysS cells (Novagen) were transformed with different pGEX-6p1 constructs following regular protocols. Briefly, transformed colony were taken and inoculated in 100 mL LB media with ampicillin (100 µg/mL) for primary culture and grown in 37°C shaker overnight. From the primary culture, 5% of secondary LB media volume was used to inoculate and let it grow at 37 °C in shaker incubator till OD_{600nm} reached 0.6 - 0.8 and then induced using 1 mM IPTG at 18°C for 16 hr. Induced cells were pelleted and resuspended in lysis buffer (20 mM Tris pH 8.0, 200 mM NaCl, 0.05% NP40, 1 mM PMSF, 1 mM DTT). After incubation for half hour on ice, viscus cell lysate obtained was further lysed with sonication until it became watery. The lysate was then centrifuged twice at 13000 rpm for 30 min at 4°C to remove un-lysed cells and debris. The supernatant was subjected to Glutathione Sepharose beads binding for 2 hr in rotator mixer at 4°C. The beads were subsequently washed with wash buffer (20 mM Tris pH 8.0, 500 mM NaCl, 1 mM DTT, 1 mM PMSF) for four times using 10 mL of the wash buffer each time after pelleting cells each time by centrifugation at 1000 rpm, 4°C, 5 min and then stored at 4°C. The proteins were eluted from bead using reduced glutathione,

by incubating the protein bound beads twice with elution buffer (20 mM Tris, 200 mM NaCl, 5% Glycerol, 1 mM DTT, 100 mM reduced glutathione, 1 mM PMSF with final pH maintained at 9.0) at 4°C for 1 hr each time.

Eluted proteins were purified to homogeneity using gel filtration size exclusion chromatography column Superdex 200 Increase 10/300 GL in Acta Pure FPLC system. The fractions corresponding to protein of interest were collected and concentrated using centricon. The purification profile of each domain is shown below. For biophysical assays bead bound GST proteins were cleaved by PreScission protease. After cleavage, beads were spun at 1000 rpm for 5 min at 4°C and the supernatant was then subjected to gel filtration chromatography as described earlier.

2.2.6.1. His Tagged Protein Purification

2.2.6.1.1. His-SUMO Tagged TSPYL5 Protein Purification

His-Sumo TSPYL5-NLD was prepared by transforming BL21(DE3) pLysS cells with pETite N-His-Sumo TSPYL5-NLD construct and transformed cells were grown in 37°C shaker overnight. Secondary culture inoculum taken from overnight grown primary culture was grown till OD_{600nm} reached 0.6-0.8 and then induced using 1 mM IPTG (GoldBio) at 18°C for 16 hr. Induced cells were pelleted down, resuspended in lysis buffer (20 mM Tris pH 8.0, 500 mM NaCl, 0.05% NP40, 1 mM PMSF, 1 mM TECEP, 20 mM Imidazole) and further lysed with sonication. Lysate was then centrifuged at 13000 rpm for 30 min at 4°C and supernatant was subjected to Ni-NTA bead (Bio-Rad) for 2 hr in rotator mixer at 4°C. The beads were then washed with wash buffer (20 mM Tris pH 8.0, 500 mM

NaCl, 1 mM TECEP, 1 mM PMSF, 50 mM Imidazole) for four times at 4°C. The bead bound proteins were then eluted twice using His elution buffer (20 mM Tris pH 8.0, 500 mM NaCl, 5% Glycerol, 1 mM TECEP, 500 mM Imidazole, 1 mM) for 1 hr at 4°C.

2.2.6.1.2. His Tagged Histone purification

Recombinant human histones H2A, H2B, H3 and H4 cloned in pET28a vector were a kind gift from Dr. Shin-ichi Tate (Hiroshima University). His tagged histone constructs were expressed in BL21(DE3)-pLysS cells followed by purification and refolding according to standard procedures (Luger et al., 1999 a, b). In brief, histones transformed in BL21 colonies were flushed into a 100 mL LB media with kanamycin (50 μg/mL) and grown for 1-2 hr. This primary culture was used for inoculating secondary culture and let grown till OD_{600nm} reached 1.0 and then induced using 1mM IPTG (GoldBio) at 37°C for 4 hr. Cells were then pelleted down and resuspended in lysis buffer (20 mM Tris pH 8.0, 200 mM NaCl, 0.05% NP40, 1 mM PMSF, 1 mM TECEP, 20 mM Imidazole), sonicated and then centrifuged at 13000 rpm for 30 min at 4°C. The supernatant was then discarded, and the pellet was further treated for histone purification.

Histones need to be resuspended in Urea resuspension buffer (50 mM Tris pH 8.0, 6 M Urea, 2 M NaCl, 1 mM PMSF, 5 mM β-Mercaptoethanol) to be solubilised from insoluble pellet fraction. Urea makes the histone unfolded and soluble. Solutions were then spun on 10000 rpm at RT for 30 min to remove the insoluble cell debris. Unfolded histones were then incubated with preincubated Ni-NTA (Bio-Rad) beads overnight for binding. The following day beads were separated and washed with Urea wash buffer (50 mM Tris

pH 8.0, 6 M Urea, 2 M NaCl, 1 mM PMSF, 5 mM β-Mercaptoethanol, 20 mM Imidazole) thrice. Histones were then eluted from the obtained washed beads using Urea elution buffer (50 mM Tris pH 8.0, 6 M Urea, 2 M NaCl, 1 mM PMSF, 1 mM TECEP, 500 mM Imidazole).

Purity of eluted histones were verified by SDS PAGE and concentration measured. Equimolar amounts of unfolded histone H3 and H4 were mixed in Histone Unfolding buffer (20 mM TRIS pH 7.5, 6 M Urea, 5 mM β-mercaptoethanol, 2 M NaCl, 1 mM EDTA, 1 mM PMSF). The resultant H3-H4 mixture was incubated for an hour and then dialysed for 16-18 hr at 4°C against Histone Refolding buffer (10 mM TRIS, pH 7.5, 2 M NaCl, 10% Glycerol, 1 mM EDTA, 5 mM β-mercaptoethanol,1mM PMSF) with 3-4 buffer changes. Refolded histone H3-H4 was run in Histone Size exclusion buffer (20 mM HEPES pH 7.5, 2 M NaCl, 1 mM EDTA, 2 mM β-mercaptoethanol, 1 mM PMSF) on a pre-equilibrated ENrich SEC-70 10/300 mm column (Bio-Rad) and fractions were
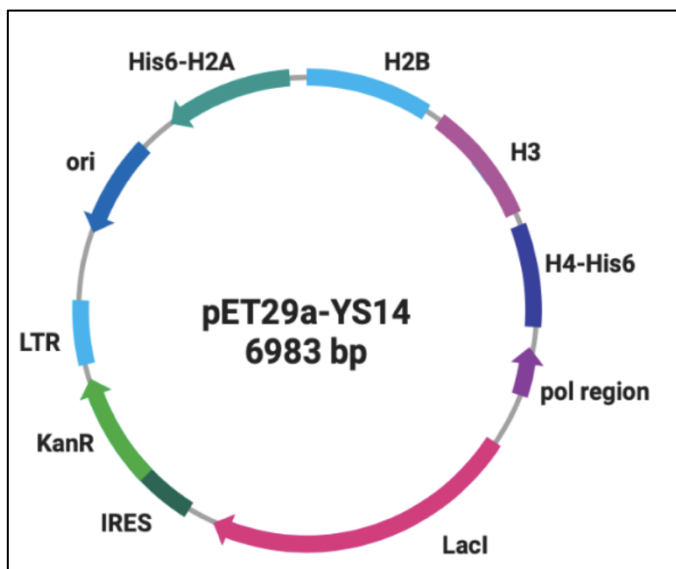
Figure 2.4. **Polycistronic arrangements of histones in the pET29a-YS15 construct.** *Xenopus laevis histones H2A only have His6-Thrombin tagged in the N-terminal. H2B, H3 and H4 followed by H2A. H4 also contain Thrombin tag at the C-terminal tail.*

collected and concentrated in the same buffer using a centricon. Aliquots of purified H3-H4 were stored in 50% glycerol at −80°C until further use.

Refolding and purification of histone H2A-H2B was also performed similarly and stored in 50% glycerol in aliquots at −80°C until further use. For preparing core histones we used pET29a-YS14 constructs where *Xenopus laevis* histones (H2A, H2B, H3 and H4) are polycistronic and show co-expression (Figure 2.4.). BL21 was transformed with pET29a-YS14 cultured in kanamycin (50 ug/mL) and let grown till OD_{600nm} reached 0.8 and then induced using 1mM IPTG (GoldBio) at 37°C for 4 hr. Cells were then pelleted down and resuspended in Core histone lysis buffer (20 mM Tris pH 8.0, 2 M NaCl, 0.05% NP40, 1 mM PMSF, 1 mM TECEP, 20 mM Imidazole) and core histone proteins purification were performed by using standard His- tagged protein purification procedure. Bead bound proteins were then eluted with Core histone elution buffer (20 mM Tris pH 8.0, 2 M NaCl, 0.05% NP40, 1 mM PMSF, 1 mM TECEP, 500 mM Imidazole) and dialysed against Core histone storage buffer (20 mM Tris pH 8.0, 2 M NaCl, 0.05% NP40, 1 mM PMSF, 1 mM TECEP, 20% Glycerol) to remove the imidazole. Dialysed core histones were then concentrated to desirable concentration of 1 mg/mL and stored at -80°C.

WT Histone H3/H4 and tetramer disruptive mutant H3M/H4 was also expressed in ampicillin antibiotic LB media using the same methods and buffer used for polycistronic core histone expression and purification. In brief, WT-H3/H4 or H3M/H4 pETduet-1 clones were transformed in Rosetta-pLysS and expressed, purified, and stored in -80°C for future use with 40% Glycerol, used as a cryo-protectant.

2.2.7. Reconstitution of Tetrasome and Nucleosome

Standard protocols (Dyer et al., 2004) was followed for reconstitution of Tetrasome and/or Nucleosome. Briefly, WT H3/H4 tetramers were mixed with 147 bp DNA (derived from the canonical Widom sequence) in Reconstitution buffer (20 mM TRIS, pH 8.0, 2 M NaCl, 1 mM EDTA, 1 mM DTT, 5% Glycerol) and dialysed against 1.5 M NaCl Reconstitution buffer for 2–3 hr at 4°C. The dialysed samples then transferred into lower (first 1 M, 0.5 M and then 0.25 M) NaCl concentration reconstitution buffer for 2-3 hr each with the penultimate dialysis being an overnight step using Nucleosome storage buffer (20 mM TRIS, pH 8.0, 150 mM NaCl, 1 mM EDTA, 1 mM DTT). Reconstituted Tetrasome or Nucleosome was checked in 6.0% native PAGE run in 1X TAE buffer. Concentration of the core histone were checked and then stored in 4°C for future use.

2.2.8. TSPYL5-H3-H4 complex formation and Analytical gel filtration

To prepare TSPYL5-H3H4 complex, we co-transformed and co-expressed pETite-His-SUMO TSPYL5-NLD and pETduet-1-H3/H4 constructs in BL21-pLysS cell and purified it using standard His-protein purification protocol with some alternation. In brief, co-transformed TSPYL5-H3/H4 were grown in 37°C shaker overnight. Secondary culture inoculum taken from overnight grown primary culture was grown till OD_{600nm} reached 0.6 and then induced using 0.8 mM IPTG (GoldBio) at 27°C for 8 hr. Induced cells were pelleted down, resuspended in H3/H4 lysis buffer (20 mM Tris pH 8.0, 2 M NaCl, 0.05% NP40, 1 mM PMSF, 1 mM TECEP, 20 mM Imidazole) and sonicated. Sonicated lysate was then centrifuged at 13000 rpm for 30 min at 4°C and supernatant was subjected to Ni-NTA bead binding for 2 hr. Beads were then washed with wash buffer (20 mM Tris pH

8.0, 2 M NaCl, 1 mM TECEP, 1 mM PMSF, 50 mM Imidazole) and proteins were eluted twice using H3/H4 elution buffer (20 mM Tris pH 8.0, 2 M NaCl, 5% Glycerol, 1 mM TECEP, 500 mM Imidazole, 1 mM) for 1 hr at 4°C. Eluted proteins were confirmed in SDS PAGE. The eluted solution containing both TSPYL5 and H3/H4 was loaded on a ENrich SEC 70-10/300 column in H3/H4-SEC buffer (20 mM HEPES pH 7.5, 2 M NaCl, 2 mM TECEP) and fractions were run on SDS PAGE to check the size exclusion profiles. Fractions containing the complex was pooled and concentrated using Amicon centrifuge filter units (100 kDa cut-off) (Millipore) in H3/H4 storage buffer (20 mM HEPES pH 7.5, 2 M NaCl, 2 mM TECEP, 5% Glycerol). Concentrated TSPYL5-H3/H4 complex was flash frozen in liquid nitrogen and stored at −80°C for longer storage.

2.2.9. SEC-MALS of protein complexes

Molecular weight in solution is important for biomolecular research not only to check the protein quality but also homogeneity and oligomeric properties of a protein. Size-exclusion chromatography separates and determines MW of proteins and other macro-molecules. However we need to perform a separate experiment to confirm their basic biophysical properties in solution. Multi-angle laser light scattering combined with UV and RI detectors coupled with SEC skips the usefulness of that extra experiment and makes SEC-MALS an essential in every lab to help characterize proteins or other macromolecules. Oligomeric state and polydispersity of macromolecular samples can also be determined by SEC-MALS.
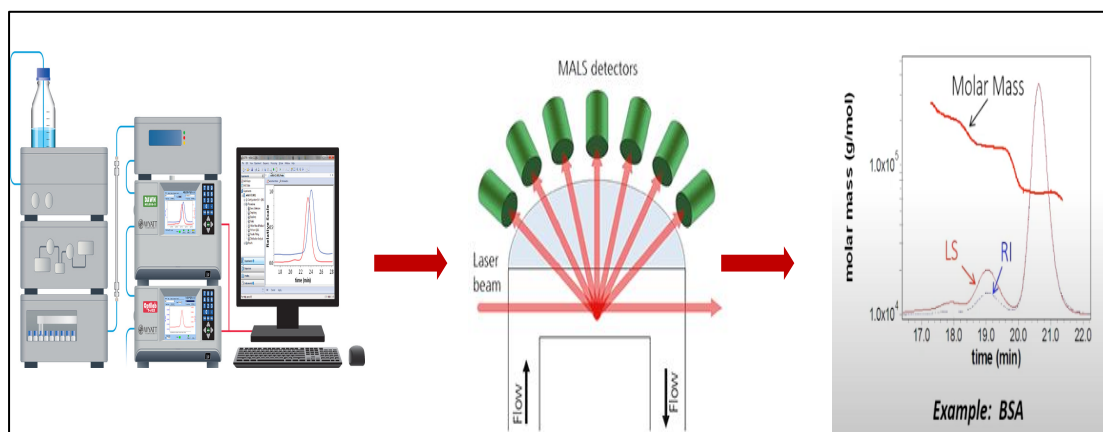
Figure 2.5. *Pictorial representation of the workflow of SEC-MALS system.*

The SEC-MALS system in our institute provides light scattering detectors (LS) and refractive index (RI) detector from Wyatt and FPLC system with UV detector from GE. SEC-MALS system instrument requirements include:

- Wyatt Dawn Heleos II Multi-Angle Light Scattering (MALS) detector 8 angle.

- Wyatt Optilab T-rEX Refractive Index Detector

- GE-Acta Pure Fast Performance Liquid Chromatography(FPLC) System

- Variable wavelength UV detector

- Analytical SEC Column: SEC Superdex 200 GL 10/300 Increase.

Buffers need to be thoroughly degassed and filtered through 0.1 μm filters (recommended) for noise free data collection. All columns and the system are equilibrated with the HBS (20 mM HEPES pH 7-7.5, 2 M NaCl, 1 mM TECEP).

Refractive index (RI) and light scattering (LS) values need to stabilized (up to 4 digit after the decimal) before data collection. It is recommended to do a size-exclusion chromatography purification prior to analytical SEC-MALS to allow for efficient buffer

exchange and for clearing all debris and aggregates in solution. BSA (67 KDa) at 2 mg/mL is used for system calibration before each set of run. Typical range of 500-800 µg/injection of samples always give a good light scattering signal.

The amount of light scattered at 0° is directly proportional to the molar mass and the concentration.

$$I_{scattered} \propto M \cdot c \cdot \left(\frac{dn}{dc}\right)^2 \qquad \text{.......Equation. 1}$$

$$M = \frac{R(0)}{Kc\left(\frac{dn}{dc}\right)^2} \qquad \text{.......Equation. 2}$$

SEC-MALS determines MW simultaneously during the elution time using Equation 1, where '**M**' denotes the molecular weight of analyte, '**c**' is the weight concentration determined by the UV or dRI detector, '**R(0)**' is the reduced Rayleigh ratio (i.e., it estimates amount of light relative to the laser intensity that is scattered by the analyte) determined by MALS detector, **dn/dc** is the refractive index increment of analyte (essentially the difference between refractive index of analyte and buffer), **K** a system constant.

MALS measures the light scattered by the analyte into several angles relative to the laser beam. SEC-MALS is considered an 'absolute' method because all the in-line instruments are independently calibrated irrespective of the columns used and do not rely on any reference standards. dRI is a universal concentration detector and does not depend on aromatic amino acids or UV chromophores. So there lies no further need to guess or

calculate from sequence the UV extinction coefficient of proteins, and concentrations response **dn/dc** of almost all pure proteins in aqueous buffer has the same value (0.185 mL/g). Purified TSPYL5-H3/H4 complexes were analysed using SEC-MALS. The average molecular mass of the sample peaks in the elution fractions was measured from the cumulative data obtained from both detectors. ASTRA software Version 7.3.2 (Wyatt Technology) was used with Wyatt's MALS for data acquisition, processing and analysis. Biophysical characterization including size, molar mass, distributions and percentage aggregate, conjugate analysis, percentage recovery, conformational analysis can also be performed using this software. ASTRA graphically represents multiple sample SEC-MALS results in a unique 3 axis chromatogram (where absolute MW versus elution volume and relative Rayleigh ratio is plotted against each other for side-by-side comparison. EASI Graph and corresponding data have been consolidated into respective EASI tables.

2.2.10. EMSA and Tetrasome assembly assay

To determine the DNA-binding ability of TSPYL5, we used Electrophoretic Mobility Shift Assay where it has been observed that the electrophoretic mobility of a protein–DNA complex is typically less than free DNA.

Materials:

- EMSA buffer: 10 mM HEPES pH 7.5, 5 mM EDTA, 1 M KCl, 1 mM TECEP, 5% v/v glycerol, 0.10 mg/mL BSA.

- Electrophoresis buffer: 10X Tris–Acetate–EDTA (TAE). Working stock 1X.

- 5% (w/v) Native PAGE for EMSA composition:

10X Tris–acetate–EDTA electrophoresis buffer	2 mL
40% (59:1) w/v acrylamide–bisacrylamide stock solution	2.5 mL
dH$_2$O	15.5 mL
10% Ammonium persulfate	200 μL
TEMED (N,N,N',N'-tetra-methyl ethylenediamine)	35 μL

- 10X EMSA Loading Dye: 10 mM Tris, 1 mM EDTA, 50% v/v glycerol, 0.001% w/v bromophenol blue.

Prepared EMSA PAGE gel was placed into a SDS free Running PAGE apparatus of Bio-Rad, reservoirs filled with 1X TAE running buffer and the gel was set for pre-run equilibration for 30 - 45 min. Samples for EMSA were prepared during this equilibration process. DNA (different lengths) with increasing concentration of TSPYL5 were incubated in microfuge tube for 30 min at 20°C. Loading dye was added to the samples and electrophoresis performed at 30 V.

2.2.10.1. DNA binding EMSA

Different lengths of DNA (20, 40, 80 and 146 bp) were incubated with increasing concentrations of TSPYL5-NLD in EMSA buffer. The samples were maintained on ice for 30 min and then heat shifted at 25°C for 20 min prior to analysis. The binding reactions were analysed on a 5% gel run on a native PAGE system using 1x TAE running buffer. The gel was stained with GelGreen™ to visualise DNA-bound complexes. Once images were developed for DNA representing bands the same gels were then stained with Coomassie Blue for protein staining. Band intensities of DNA bound proteins in the

corresponding DNA gel pictures were quantified by ImageJ (Version 1.80-172). Data was analysed in Prism (Version 7) and plotted using Hill equation binding model.

2.2.10.2. Tetrasome assembly assay using EMSA

Normally a chaperone-histone ratio between 0.5 - 4 fold is used for tetrasome assembly assay. Increasing concentrations of TSPYL5-NLD or TSPYL5-HBM (1+2) were mixed with histone H3/H4 (100 nM tetramer concentration used in each microfuge tube) and incubated at 4°C for 10 - 15 min in EMSA buffer. 80 bp dsDNA Widom 601 sequence was added to the pre-mix TSPYL5-H3/H4 complex at 100 nM concentration. The final mix was then shifted to 25°C and incubated for 20 min prior to EMSA analysis. The binding reactions were analysed on 5% native 1x TAE running buffer. The gel was stained with GelGreen to visualise DNA-bound complexes. Histone tetrasome was prepared by salt dialysis methods. H3/H4 tetramers was mixed with 80 bp canonical Widom sequence in high salt assembly buffer (20 mM TRIS, pH 8.0, 2 M NaCl, 1 mM EDTA, 1 mM DTT) and dialyzed in the same buffer for 2 - 3 hr at 4°C. The dialyzed DNA-Histone H3/H4 mix was then gradually transferred to lower (from 1 M to 0.25 M NaCl gradually) salt concentration buffer for 2 hr in each step and finally dialyzed overnight in 250 mM NaCl assembly buffer. Samples were taken out from dialysis buffer, newly formed tetrasomes were run in native PAGE and used as input samples in tetrasome assembly assay.

2.2.11. Plasmid supercoiling assay

Topoisomerase-I are ATP-independent enzymes that play an essential role in nuclear functions like DNA replication, transcription, chromosome segregation and recombination.

Topoisomerase-I reaction relaxes negatively supercoiled DNA. Supercoiled DNA has a different electrophoretic mobility compared to that of completely relaxed DNA. Isolated plasmid DNA from *E. coli* are mostly negatively supercoiled. Supercoiled plasmid can be treated by Topoisomerase-I to help it relax. Histone chaperones are well known to deposit histones in relaxed plasmid DNA and make it supercoiled. So, Topoisomerase-I are employed to cut relaxed plasmid DNA used as a template to check histone deposition activity of histone chaperones.

Materials:

- 10× Supercoiling assay buffer (100 mM HEPES pH 7.5, 150 mM NaCl, 50% glycerol and 50 mg/mL BSA)

- Substrate: Supercoiled pBlueScript plasmid DNA(pBS)

- Enzyme: Topoisomerase I

- 5× loading dye

- 0.8% agarose gel

- Histone Chaperone: TSPYL5-NLD and TSPYL5-HBM (1+2)

- Histone H3/H4

In this assay, pBS plasmid is relaxed by Topoisomerase-I. 2 μl of 10× Supercoiling assay buffer is added to 200 ng plasmid DNA in each reaction tube kept on ice. All volumes were adjusted with distilled water to reach a final reaction volume of 20 μL in each tube. Varied amounts of Topoisomerase-I were then added and samples were then incubated for 30 min at 37°C. 5 μL of 5× loading dye was added to each tube and all samples were run

on a 0.8% agarose gel for 2-3 hr at 10 V. Gels were stained similarly as mentioned before with GelGreen that stained for DNA bands and the destained with water prior to analysing in an UV transilluminator. The amount of Topoisomerase-I needed to completely relax a supercoiled pBS plasmid under this condition was subsequently determined from this experiment.

Histones H3-H4 were incubated with increasing concentrations of TSPYL5-NLD or TSPYL5-HBM (1+2) in 15 µL supercoiling assay buffer at 37°C for 30 min in a separate series of microfuge tubes. pBS supercoiled plasmid DNA were treated with previously determined unit of Topoisomerase-I for 30 min at 37°C separately to relax it completely. Followed by Topoisomerase-I treatment relaxed plasmid DNA were added to TSPYL5-H3H4 mix and incubated for 60 min at 25°C. Reactions were terminated with equal volume of Stop buffer (25% Glycerol, 60 mM Tris-HCl, pH 8.0, 30 mM EDTA, 2.0% SDS) and incubated for another 20 min. Samples were resolved by electrophoresis in 0.8% agarose gel followed by staining and then checked in an UV transilluminator.

2.2.12. Dynamic Light Scattering (DLS)

Dynamic Light Scattering (DLS) is a non-invasive technique that quantitatively estimates the size distribution of different molecules in a solution without affecting their state of equilibrium (Bohidar, 1989; Yarmush et al., 1987). Measurements are taken at 25°C using a back-scatter apparatus having a constant 90˚ scattering angle. 1 mg/mL of TSPYL5-NLD and TSPYL5-H3/H4 complex were used for analysing their size distribution in this study.

2.2.13. DSS cross-linking experiments

TSPYL5-NLD, H3/H4 and TSPYL5-H3/H4 complex were buffer exchanged to Cross-linking buffer because crosslinking experiments could not be performed in Tris Buffer. Buffer exchanged TSPYL5-NLD, H3/H4 and TSPYL5-H3/H4 complex were incubated with DSS crosslinker for 30 min at 25°C. Reactions were quenched by addition of Stop Buffer for 15 min at 25°C and samples were TCA precipitated. After TCA precipitation, samples were analysed in SDS-PAGE and transferred to PVDF membranes by western blot.

Materials:

- DSS Crosslinker or Disuccinimidyl suberate

  Chemical Formula: $C_{16}H_{20}N_2O_8$

  Molecular Weight: 368.34 Da

  Spacer Arm Length: 11.4 Å

  Storage: Store at -20°C and protect

  from moisture, light, and

  humidity.
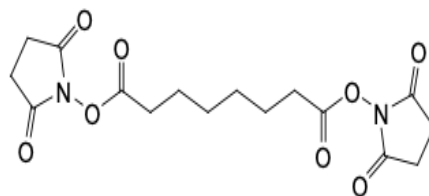
- 10× Crosslinking buffer (20 mM HEPES pH 7.5, 200 mM NaCl, 1mM TECEP)

- TSPYL5-NLD , Histone H3/H4 and TSPYL5-H3/H4 complex (Buffer exchanged)

- Stop Buffer (1.5 M Tris-HCl pH 8.0)

- 100% TCA (w/v): 50 g Trichloroacetic acid (TCA) dissolved into dH_2O and volume made up to 50 mL, stored at RT.

- Ice cold 100% Acetone

- 5X SDS-Loading Dye

- pre-4-12% Bis-Tris gradient SDS-PAGE (Thermo casted gel)

- 20X MOPS-Running Buffer (1 M MOPS, 1 M Tris Base. 2% SDS, 20 mM EDTA pH 7.7, Stored at 4°C.) 1X working stock prepared prior to run.

- 20X Bis-Tris Transfer Buffer (500 mM Bicine, 500 mM Bis-Tris Base, 2% SDS, 20 mM EDTA pH 7.7, Stored at 4°C). 1X working stock solution was prepared prior to run by freshly adding 20% Methanol.

DSS crosslinker is also prepared immediately before use by dissolving it in 100% DMSO or DMF. Calculation of the preparations are as follows:

Weigh 2mg of crosslinker into a microcentrifuge tube.

Solvent volume to add to 2mg DSS	Buffer volume to add to 2mg BS^3	Crosslinker Concentration
432µL*	277µL*	12.5mM
216µL	140µL	25mM
108µL	70µL	50mM
54µL	35µL	100mM

*The maximum volume that can be added to the No-Weigh vial is 800µL.

The crosslinker is then added to the protein sample. For samples < 5mg/mL in concentration, a 20-50 fold molar excess of the crosslinker is used to a final crosslinker concentration of 1-5 mM for each reaction. The reaction mixture is incubated for 30 min at room temperature and then quenched by addition of Stop Buffer to achieve a final concentration of 50 mM Tris buffer, pH 8.0. After incubating the quenching reaction at room temperature for 15 min the samples undergo TCA precipitation. The protocol followed is as:

- To 4 volumes of crosslinked protein sample, 1 volume of 100% TCA were added and incubated for 10 min at ice.

- Samples centrifuged at 13,000 rpm for 10 min at 4°C.

- Supernatant was removed and protein pellet washed with 200 μL ice cold acetone.

- Microfuge tubes further centrifuged at 13,000 rpm for 10 min at 4°C.

- Acetone wash repeated again twice.

- Dry protein pellet I kept on 95°C heat block for 5-10 min to get rid of the acetone.

- 30 μL 1x Running buffer added to the pellet along with 4X SDS loading buffer, heated in the heat block before loading onto 4-12% Bis-Tris gradient polyacrylamide gel.

Bis-Tris SDS PAGE Running procedure:

Samples loaded into Bis-Tris SDS PAGE gel were run in 1X MOPS running buffer for 200 V for 50-60 min for complete separation. Presence of MOPS in the running buffer and Bis-Tris in the running buffer helps the proteins separate distinctly. After separation the gels are transferred using 1x Bis-Tris Transfer Buffer at 30 V for 60 min. Transferred membrane is then blocked with 5% BSA-TSB-T (Tris-Buffer Saline with 0.1% Tween-20) buffer and probed with specific antibodies like H3, H4, TSPYL5.

2.2.14. Western blot analysis of mammalian cell lysate

For preparing whole cell lysates, cells were re-suspended in LaemmLi Buffer (4% SDS, 20% Glycerol and 120 mM Tris-HCl pH 6.8) (LaemmLi, 1970) and sonicated before analysing it by Western blot. Samples were run on 11% or 15% SDS-PAGE, transferred

onto a PVDF membrane followed by blocking in 5% BSA in 1x TBS-T and probed for specific antibodies. Primary and Secondary antibodies used are enlisted in Table 2.

2.2.15. Immuno-precipitation (IP)

Cells were harvested from the cultured plate and cross-linked with 4% para-formaldehyde in PBS at room temperature for 15 min. All types of cross-linked cells were then lysed with RIPA IP buffer (50 mM HEPES pH7.5, 150 mM NaCl, 1.5 mM MgCl$_2$, 1mM EDTA, 1% Triton X-100, 5% Glycerol, 1 mM DTT, 2 mM Protease inhibitor cocktail) and incubated on ice for one hour followed by centrifugation at 13000 rpm for 10 min at 4°C. After pre-clearing approximately 500 µg-1500 µg lysates were incubated with required antibodies overnight. Next day previously equilibrated Protein-A bead were added to the antibody incubated cell lysates for immuno-precipitation for 1 hr at 4°C. IP samples were then centrifuged, supernatant discarded and beads washed thoroughly thrice using the RIPA IP buffer. Washed IP beads were then analysed by western blotting.

2.2.16. Peptide pull down assay

Peptide pull down assays were done following standard protocol (Wysocka, 2006). Briefly, Biotinylated Histone H3 Peptides were purchased from GL-Biochem: H3 (1 - 21), H3 (21-44), H3 (44-69), H3 (69-89), H3 (105-120), H3 (120-135). In a fresh PVDF membrane soaked with 1x transfer buffer all the biotinylated peptides were dot blotted to check the concentration and the amount needed to use for IP was subsequently determined. Histone H3 peptides were incubated overnight with GST tagged TSPYL5-NLD in IP buffer (50 mM HEPES pH7.5, 150 mM NaCl, 1.5 mM MgCl$_2$, 1mM EDTA, 1% Triton X-100,

5% Glycerol, 1 mM DTT, 2 mM Protease inhibitor cocktail) at 4°C. The reactions were subjected for 2 hr at 4°C to pre-equilibrated Streptavidin beads for trapping the biotinylated peptides. Samples were then centrifuged at 1000 rpm for 10 min at 4°C and the supernatant was discarded. Beads were washed thrice with IP Buffer and the IP samples were analysed by western blotting using GST antibody to check pulled GST-TSPYL5.

2.2.17. *In-vitro* Protein-Protein interaction studies

The recombinant Histones, Core Histone, Tetrasome and Nucleosome interactions with GST and GST-TSPYL5 proteins were performed as per standard protocol. Briefly, proteins were incubated with histones in equal molar ratio in Binding buffer (50 mM HEPES pH 7.5, 200 mM NaCl, 0.05% NP40, 1 mM DTT, 5% Glycerol, 1 mM PMSF) for 2-4 hr. Glutathione Sepharose (GST) beads were blocked with 5% BSA+Binding buffer. Pre-blocked GST beads were added to the mixed samples, incubated for 1 hr and GST proteins then pulled down. Supernatant was discarded following centrifugation and protein bound beads were washed thrice with binding buffer. Bound beads were then loaded on SDS PAGE and analysed by western blotting.

2.2.18. Cell Fractionation

Chromatin fractionation was done following the protocol from Li and Stern, 2005 with some modifications. In brief, untransfected and FLAG-TSPYL5 transfected HEK293T cells were harvested from almost 90% confluent 60 mm dish, resuspended in Hypotonic Buffer (10 mM HEPES, pH 7.4, 10 mM NaCl, 6 mM $MgCl_2$, 2mM DTT, 0.05% NP40, 2 mM PMSF, 1X PIC), and then homogenised with a Dounce glass homogeniser on

ice and kept for 5 min. The mix was then centrifuged at 3000 rpm for 5 min at 4ºC. The supernatant was collected as Cytosolic fraction. The pellet was resuspended in Nuclear extraction buffer (20 mM HEPES pH 7.4, 420 mM NaCl, 1.5 mM MgCl$_2$, 0.2 mM EDTA, 1 mM DTT, 20% Glycerol, 0.5% NP40) and treated with DNase I at 37°C for 30 min. After the incubation, the mixture was further centrifuged at 13000 rpm for 10 min at 4°C. The supernatant fraction was again collected as Nuclear fraction and the pellet was discarded. Fractions were analysed by western blot using β-Tubulin as cytosolic marker and Histone H2B as Nuclear marker along with anti-TSPYL5 and anti-FLAG used to detect the localization of TSPYL5.

2.2.19. Co-immunofluorescence and confocal microscopy

Co-immunofluorescence staining was performed as per standard protocol (Das et al., 2010). Untransfected and FLAG-TSPYL5 transfected HEK293T cells and SH-SY5Y cells were cultured in poly-l-lysine coated coverslip till they reached 50-60% confluency. Cells were then fixed in 4% Para-formaldehyde (PFA) and crosslinking was quenched by adding fresh FBS media. Fixed cells were permeabilised in permeabilization buffer (1% Triton X-100 diluted in 1x PBS) for 10-20 min and washed thoroughly with 1x PBS. Permeabilised cells were then blocked in 3% BSA, dissolved in 1xP BS for 30 min at room temperature. This was followed by incubating the cells with anti-FLAG (rabbit raised) and anti-H3 (mouse raised) primary antibodies overnight for 1 hr at 4ºC. The next day, cells were thoroughly washed with 1x PBS-T and incubated with Alexa fluor 488 and Alexa fluor 594 conjugated mouse and rabbit secondary antibodies respectively for 1 hr at room temperature. Cells were then washed with 1x PBS-T and mounted on a pre-washed slide

having DAPI containing mounting media. All imaging was done on confocal scanning microscope.

2.2.20. Bio-layer Interferometry (BLI) study for kinetic assays

An analogous technique of surface plasmon resonance (SPR) is Bio-layer Interferometry (BLI). A standard protocol was used to do the association and dissociation kinetics study (Abdiche et al., 2008) using Octet-RED BLI system of Forte′ Bio utilising Ni-NTA or Streptavidin coated sensors with some modification. In brief, all steps were done at 20°C, and all sensors were stirred in 200 µL of samples at 1000 rpm speed and measurements recorded over 2 hr. For protein-protein binding assay, recombinant His tagged histone H3-H4 or H2A/H2B were immobilised on Ni-NTA biosensors in Binding buffer (50 mM HEPES pH 7.5, 150 mM NaCl, 0.05% NP40, 1 mM DTT, 5% Glycerol, 0.5 mg/mL BSA). TSPYL5 (WT, deletion mutant and point mutants) were kept in different concentrations on the 96-well plate and titrated against it. To score the peptide-protein interaction biotinylated Histone H3 (44 - 69), H3 (105 - 120), H3 (120 – 135) were immobilised on streptavidin biosensors in binding buffer and TSPYL5-NLD were titrated against them.

A reference sensor with immobilised Histone but without TSPYL5 was used as a negative control and to confirm that added ligands in buffer did not alter the BLI signal. All data were collected in triplicates. After data collection and reference subtraction each data was corrected with Savitsky-Golay filtering. All these processes and curve fitting (to determine the kinetic rates association & dissociation) was analysed using Forte′ Bio's

software (version 11x). Graphs were plotted as response versus time. Minimal loading (0.2 – 0.4 nm per sensor) of histones was found to be favourable for kinetic responses.

2.2.21. MNase Assay

Chromatin was isolated from transfected and un-transfected HeLa/ HEK 293T cells as per standard protocol (Das et al., 2006). Nuclear pellet was isolated from cells by previously described cell fractionation procedure. Isolated nuclei were digested in Nuclei digestion buffer (10 mM Tris-HCl pH 8.0, 3 mM $CaCl_2$, 150 mM NaCl, 10% glycerol, 0.2 mM PMSF) with MNase (Sigma, 0.2 Units/μL) for 2-5min at 37°C. After MNase digestion, reaction was quenched by adding an equal volume of Stop buffer (20 mM Tris pH 7.5, 200 mM NaCl, 10 mM EDTA, 2% SDS, 0.2 mg/mL Proteinase K) and incubating for 30min at 37°C. DNA was purified from the samples using phenol-chloroform-isoamyl alcohol (PCI) extraction and followed by ethanol precipitation method. DNA pellet was dissolved in 1x TE buffer and concentration of the samples were determined using NanoDrop spectrometer. Samples were loaded in 2% Agarose gel and followed by GelGreen™ staining. Gel images were then analysed in ImageJ software.

2.22. Sucrose gradient fractionation of chromatin fragments

Nuclear pellet was digested with MNase using standard protocol (Das et al., 2006) as previously described. Digested chromatin was extracted from the nuclei pellet by incubating with 1x TE buffer for 2 hr for two times at 4°C. Supernatant of each incubation step were pulled and loaded on a linear sucrose gradient of 10-40% in NTE buffer (10 mM Tris-HCl pH 7.5, 10 mM NaCl, 1 mM EDTA). Sucrose loaded samples were then

fractionated by centrifugation in Beckman ultracentrifuge (SW60Ti rotor) at 30,000 rpm for 14-15 hr. Fractions were taken out from the centrifuge tube. Fractions of each gradient was dialysed against 1x TE buffer to remove excess sucrose in solution. Dialysed fractions were analysed in 2% Agarose gel and followed by staining to identify the chromatin fraction with mono-, di-, tri- or higher order nucleosomal repeat.

2.23. Circular dichroism (CD) spectroscopy

The circular dichroism (CD) spectroscopy experiments were done by standard protocol (Das et al., 2006, 2010). In brief, purified higher order chromatin, H1-stripped chromatin, protein stripped genomic DNA were purified using previously described MNase digestion and sucrose gradient fractionation. All the different chromatin samples were incubated in CD buffer (10 mM HEPES pH-7.5, 25 mM NaCl) with increasing concentration of recombinant TSPYL5-NLD at 20°C for 90 min. The circular dichroism (CD) spectra of each sample were recorded at room temperature in a JASCO model J715 Spectro-polarimeter at settings from 250-300 nm. All the data were processed, smoothed and plotted using GraphPad Prism7 software.

2.24. Quantification And Statistical Analysis

Statistical analysis has been calculated in GraphPad Prism7 software (GraphPad) and significance determined by the value of $p < 0.05$.

Results

3. Results

3.1. Sequence Analysis of TSPYL5

The open reading frame of human TSPYL5 gene is 4441 bp and translated polypeptide of 417 amino acids codes for 45 kDa protein. Antibodies recognized FLAG-tagged and endogenous TSPYL5 at approximately 47 kDa in western blot SDS-PAGE (Epping et al., 2011; Episkopou et al., 2019). Unlike other SET/TAF1B protein or NAP1 proteins where acidic region is C-terminal, Uniprot sequence analysis reveals the acidic domain comprising of aspartic acid and glutamic acid at the N-terminal of the NAP domain (Uniport ID: Q86VY4).

```
                          NLS
  1   MSGRSRGRKSSRAKNRGKGRAKARVRPAPDDAPRDPDPSQYQSLGEDTQAAQVQAGAGW   59

 60   GGLEAAASAQLLRLGEEAACRLPLDCGLALRARAAGDHGQAAARPGPGKAASLSERLAA  118

119   DTVFVGTAGTVGRPKNAPRVGNRRGPAGKKAPETCSTAGRGPQVIAGGRQKKGAAGENT  177

                 ACIDIC REGION
178   SVSAGEEKKEERDAGSGPPATEGSMDTLENVQLKLENMNAQADRAYLRLSRKFGQLRLQ  236

237   HLERRNHLIQNIPGFWGQAFQNHPQLASFLNSQEKEVLSYLNSLEVEELGLARLGYKIK  295

                     NAP DOMAIN
296   FYFDRNPYFQNKVLIKEYGCGPSGQVVSRSTPIQWLPGHDLQSLSQGNPENNRSFFGWF  354

355   SNHSSIESDKIVEIINEELWPNPLQFYLLSEGARVEKGKEKEGRQGPGKQPMETTQPGV  413

414   SQSN
```

Figure 3.1. Amino acid composition of full length human TSPYL5 illustrating the various domains. *The sequence and distribution of nuclear localization signals (NLS), acidic region and NAP domain of human TSPYL5 are colored as pink, yellow and gray respectively.*

TSPYL5 has a putative NLS [Software: cNLS mapper (https://nls-mapper.iab.keio.ac.jp/cgi-bin/NLS_Mapper_form.cgi)] which suggests that localisation may be in both the nucleus and the cytoplasm.
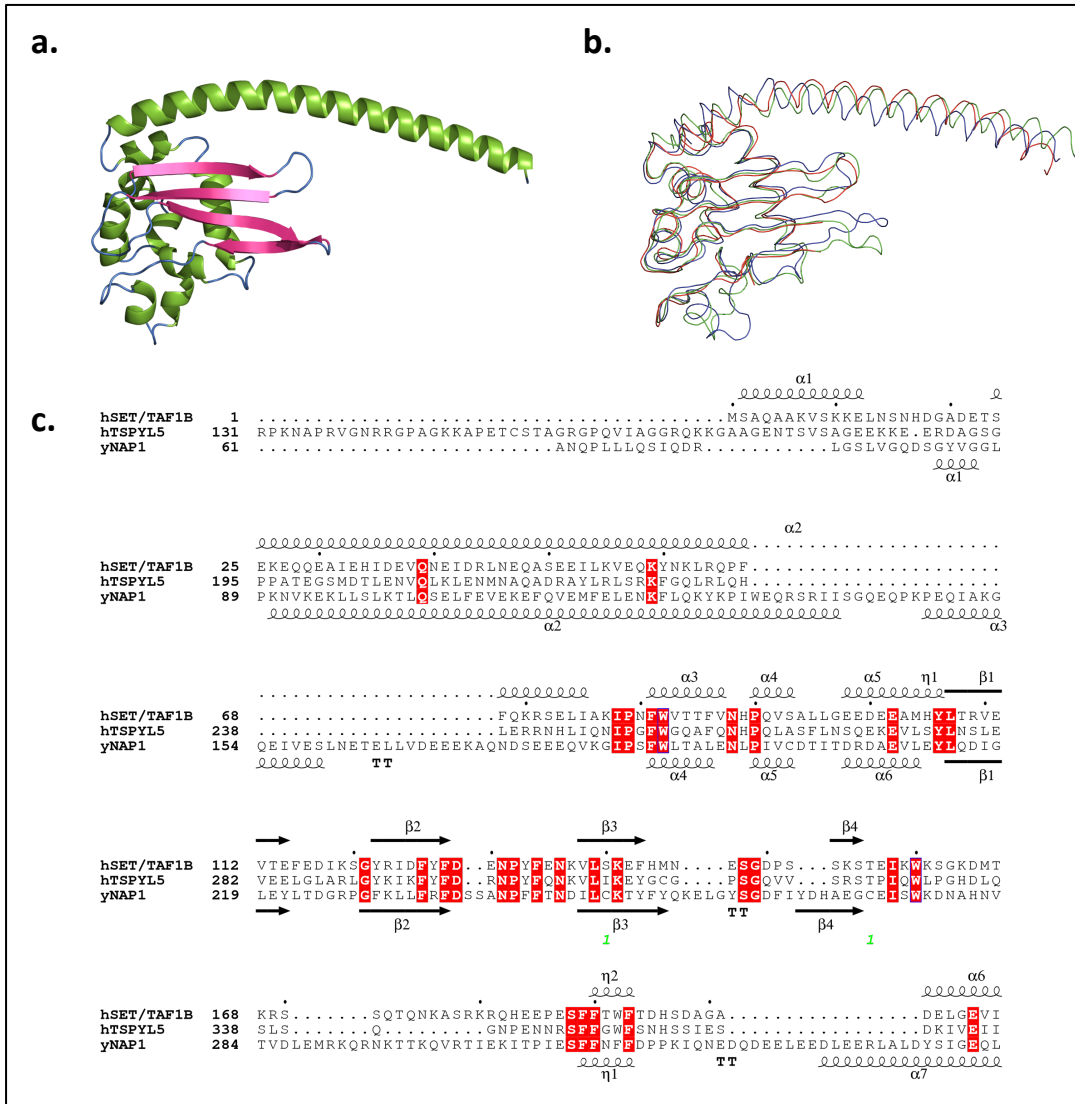

Figure 3.2. Sequence based structure prediction of human TSPYL5 and comparison with other NAP domain. *(a) Molecular model of TSPYL5 (198-398) in cartoon representation using Alpha Fold. Secondary structure is represented in colour codes- Helix (green), Beta sheet (pink), Loop (blue). (b)Superimposition of the C-alpha trace of earmuff domains of TSPYL5 from Alpha Fold (green), RoseTTAFold (blue) and SET/TAF-1B (red). (c) Multiple Sequence alignment of human TSPYL5 (Q86VY4) with ScNAP1 (P25293) and HsSET/TAF1B (Q01105) (Uniprot accession ids within parenthesis) where identical residues are labelled in red.*

3.2. TSPYL5 shows homology with NAP histone chaperones

Nucleosome assembly proteins (NAP), that are characterized by the conserved α/β-earmuff motif across different species facilitate *in vitro* assembly of nucleosomes. To find out possible proteins with sequence and structural similarity with TSPYL5, we employed multiple sequence alignment of NAP proteins across different species. The alignment result suggests that TSPYL5 is a homologue of NAP family proteins that remains conserved among eukaryotes (Figure 3.4.). Identical residues across different proteins have been highlighted in red with the NAP1 accessory region being marked in blue.
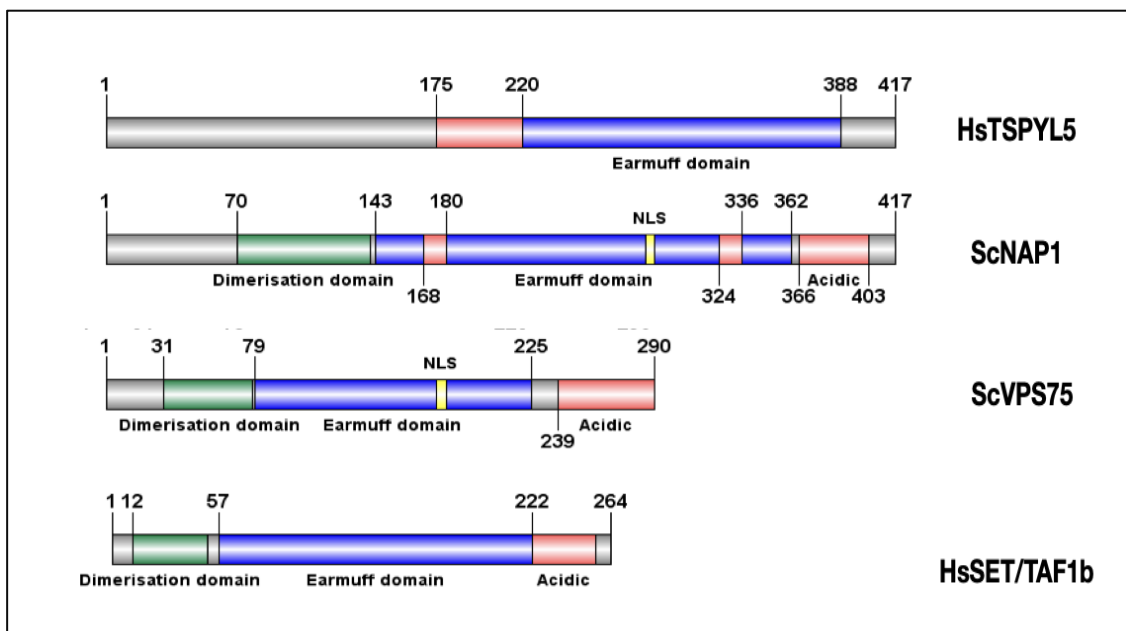
Figure 3.3. Domain architecture of human TSPYL5 (Q86VY4) along with other members of NAP protein family across different species. *Domain analysis with amino acid residues numbers of different NAP1 proteins along with TSPYL5 are represented in a cartoon representation.*
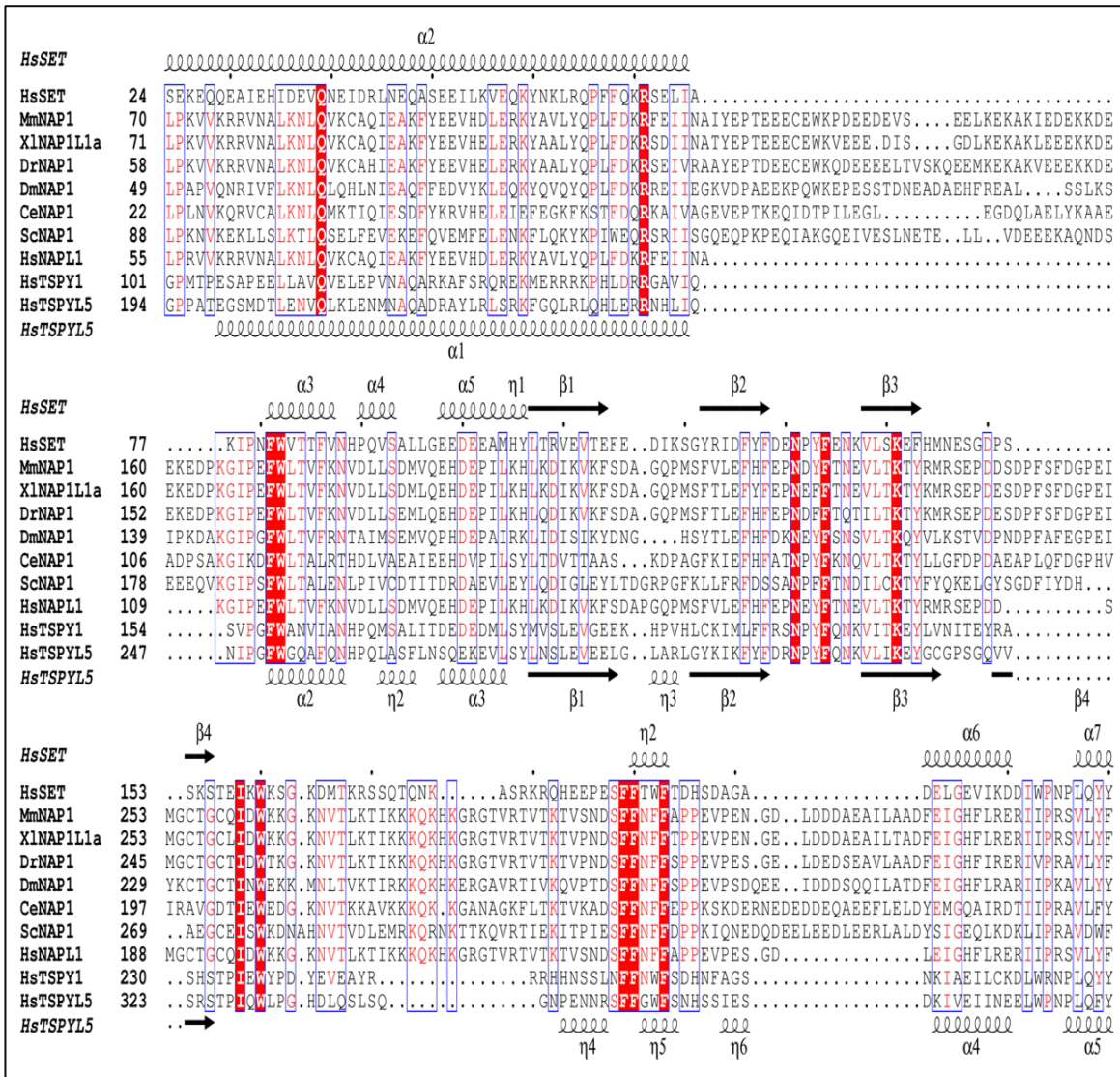
Figure 3.4. Multiple Sequence alignment of human TSPYL5 (Q86VY4) with members of NAP protein family across different species. *The different NAP family members (Uniprot accession ids within parenthesis) included in the analysis were, ScNAP1 (P25293), CeNAP1 (Q19007), DmNAP1 (Q9W1G7), DrNAP1 (Q803X7), XlNAP1 (Q4U0Y4), MmNAP1 (P28656), HsNAP1L1 (P55209), HsTSPY1 (Q01534), HsSET/TAF1B (Q01105). Identical residues are labelled in red. NAP1 accessory region is highlighted in blue. Secondary structure prediction of SET/TAF1B (PDB ID: 2E50) is shown above the multiple sequence alignment where alpha helix and beta-strand are indicated.*

3.3. TSPYL5, bonafide member of diverse NAP family proteins in human

Interestingly, compared to other eukaryotes, the NAP proteins in human genome exists as multiple diverse sub-families. To understand the similarity between the different NAP family proteins in human, we generated a phylogenetic tree using a maximum likelihood approach. Tree data shows divergence of human NAP proteins into three distinguished sub-families: NAP1-Like proteins (NAP1L) (shown in red), TSPY proteins (shown in yellow) and TSPY-Like proteins (shown in blue), while human SET/TAF1b diverged and remained distinct from the above sub-families (Figure 3.4.).
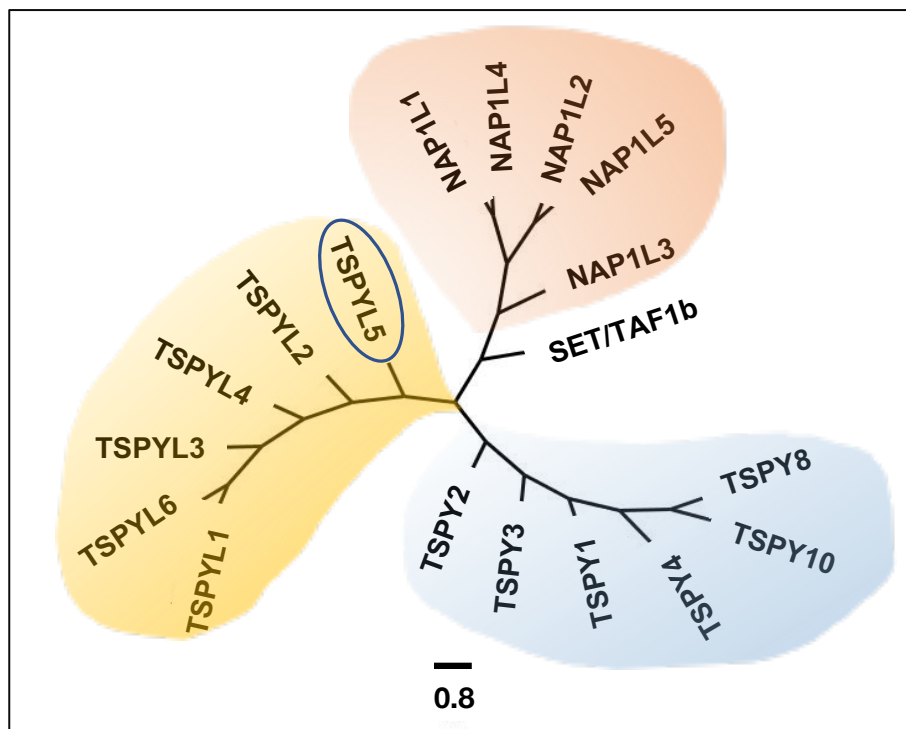

Figure 3.4. Phylogenetic tree depicting different NAP like proteins in human. *MEGA-X and Figtree Software packages were used for the analysis. Scale bar is indicated in figure.*

3.4. TSPYL5 expresses ubiquitously in all tissues

Multiple sequence analysis shows that TSPYL5 is a new member of NAP histone chaperone family in human. NAP1 is a bona fide histone chaperone that is present in all eukaryotes. So, presence of TSPYL5 along with NAP1 in humans is interesting and may contribute in diverse function than NAP1. To find out the expression of human TSPYL5 in different tissues, we checked the GTEx portal for transcript analysis. GTEx analysis suggests that TSPYL5 is a ubiquitously expressed protein in human with relatively higher expression in reproductive organs and brain tissues compared to very low expression in blood and liver cells (Figure 3.5.).
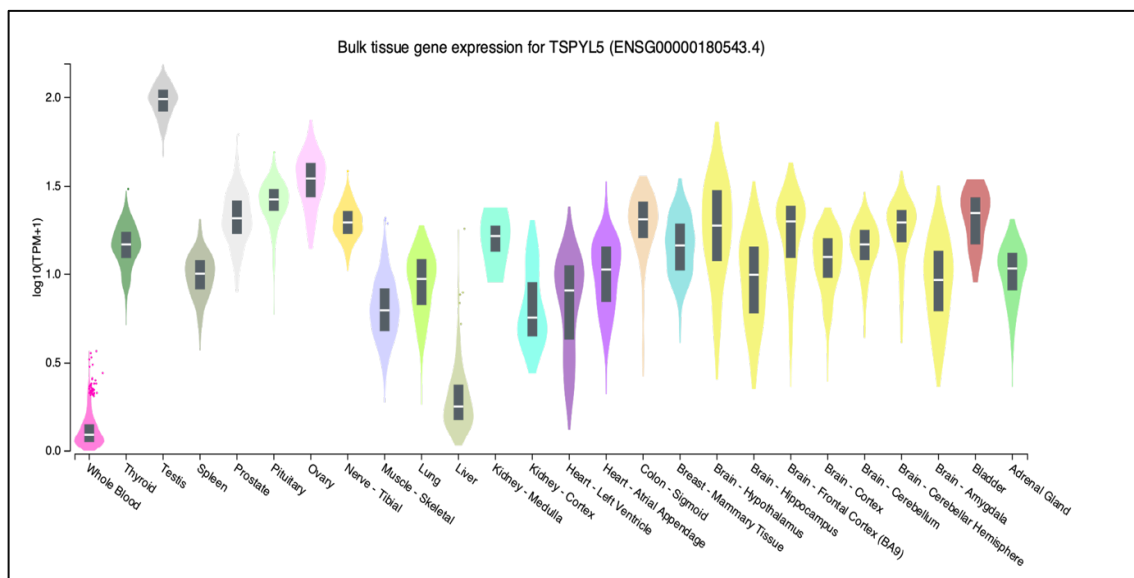
Figure 3.5. GTEx Analysis of TSPYL5 transcript. Adapted from GTEx Release V8 (dbGaP Accession phs000424.v8.p2). *Expression values are shown in TPM (Transcripts Per Million), calculated from a gene model with isoforms collapsed to a single gene. No other normalization steps have been applied. Box plots have been depicted as median and 25th and 75th percentiles; points are displayed as outliers if they are above or below 1.5 times the interquartile range.*

3.5. TSPYL5 expression profile in different cell lines

Following TSPYL5 expression profile analysis using GTEx, we sought out to check the transcript profile of TSPYL5 in various cell lines to have a clear idea of TSPYL5 expression in them. Protein and RNA expression profile shows that it has a significantly high level expression in SH-SY5Y (shown in yellow) and SCLC-21H (shown in olive green) cells compared to other cell lines taken from varied organs (Figure 3.6.).
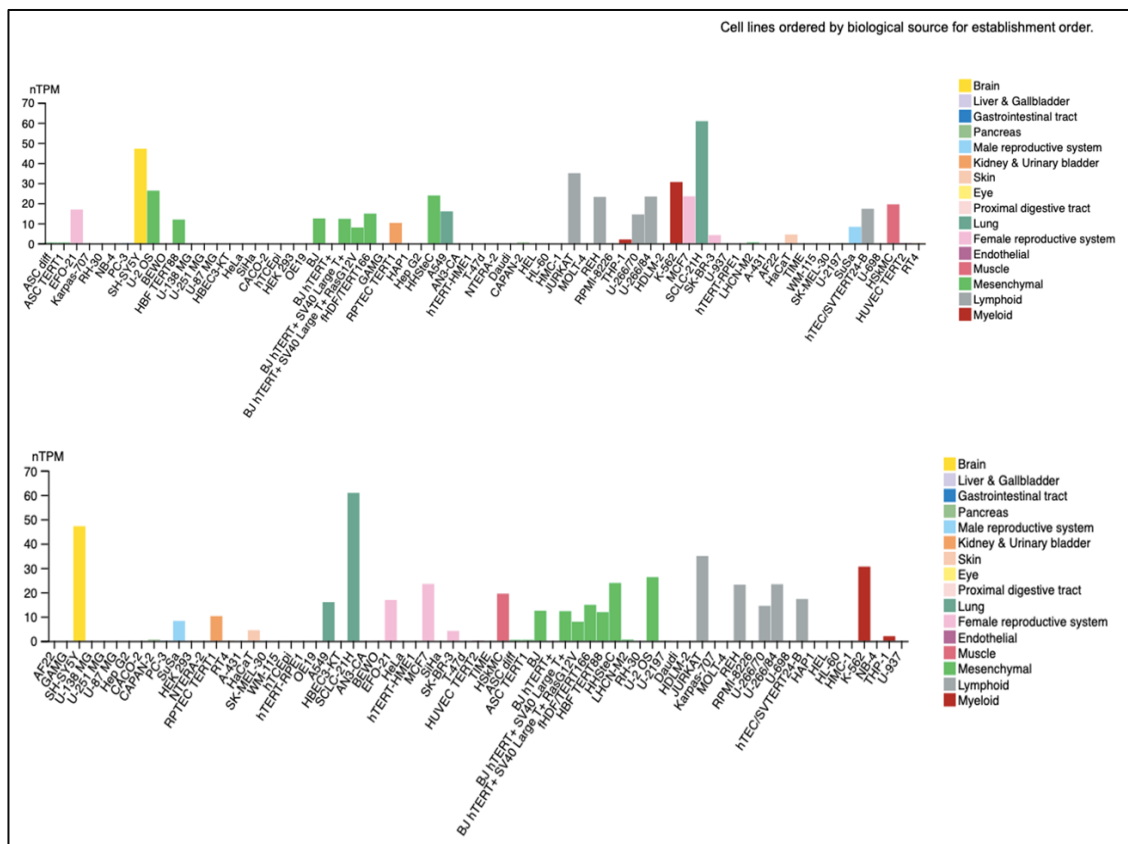

Figure 3.6. Protein and mRNA expression Analysis of TSPYL5, adapted from Human Protein Atlas. *Expression values are shown in nTPM. Values of all samples from 2 different data set (HPA & GTEx) were normalized separately using Trimmed mean of M values (TMM). The resulting normalized transcript expression values, denoted by nTPM, were calculated for each gene in every sample.*

3.6. TSPYL5 localizes in both nucleus and cytoplasm

NAP family member proteins have been reported to be involved in multiple pathways including nucleocytoplasmic shuttling, chromatin assembly and remodelling, replication, transcription, gene silencing and apoptosis which requires cytoplasmic or nuclear
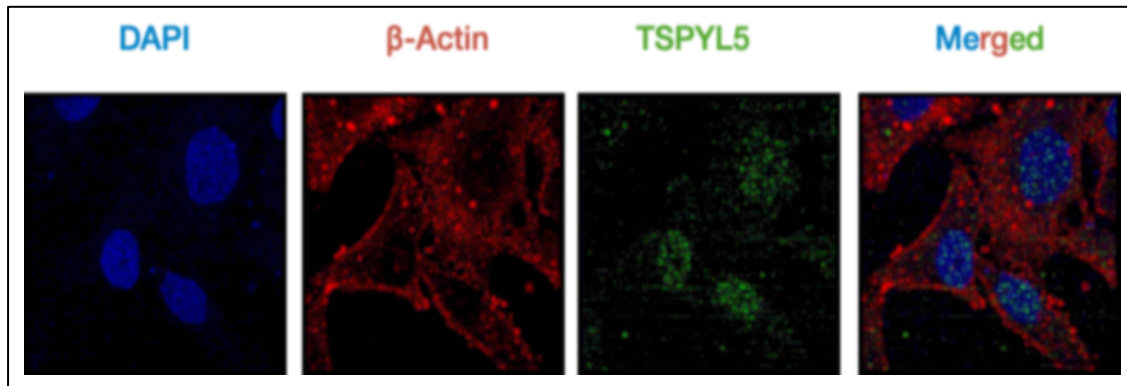
Figure 3.7.1. Co-localisation analysis of TSPYL5. *Immunofluorescence showing localization of TSPYL5 (Green-Alexa 488) in SHSY5Y cells. Nucleus was stained with DAPI (Blue). Scale bar 100 μm.*

localization or both. To look into the localization of TSPYL5, we next performed an Immuno-fluorescence assay in SH-SY5Y neuroblastoma cells which previously showed high endogenous expression during our expression profile analysis in different cell lines. The cells depicted significant localisation as observed under confocal microscope when stained with Alexa Fluor 594 (red): Actin, Alexa Fluor 488 (green): TSPYL5, in contrast to DAPI stained nuclei (Blue) (Figure 3.7.1.).
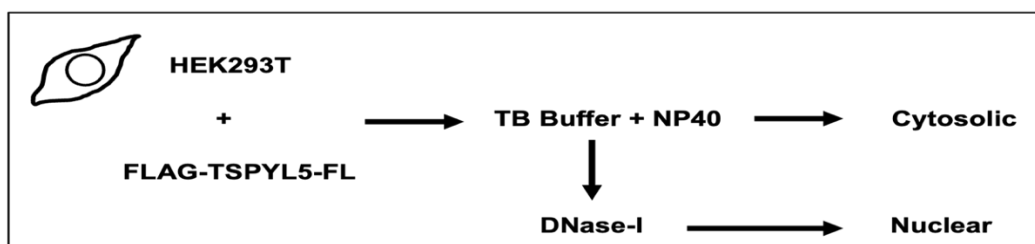
To re-validate the immunofluorescence results obtained, when FLAG-TSPYL5 was transfected in HEK293T cell line and similar cell fractionation assay was performed in both cytosolic and nuclear fractions, TSPYL5 was found to be present in both nuclear as well as cytosolic fractions when detected by western blot where tubulin and H3 were used as cytosolic and nuclear markers respectively (Figure 3.7.2.).
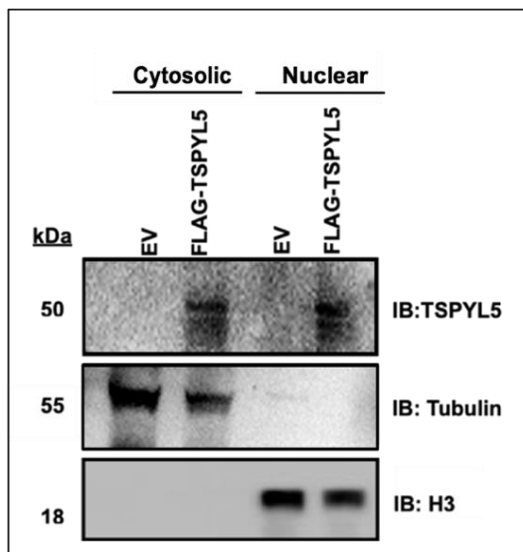
Figure 3.7.2. *HEK293T cells were transfected with empty vector (EV; as a negative control) and FLAG–TSPYL5. The localization of TSYPL5 was detected using western blotting of the fractionated sample fractions. Tubulin and H3 were used as cytosolic and nuclear markers respectively.*

3.7. TSPYL5 interacts with Histone H3/H4 *ex-vivo*

Nuclear localization of TSPYL5 however raises the possibility of it having a role in chromatin context, which has not yet been studied. Previously, NAP family histone chaperones have been widely reported to interact with both histones H2A/H2B and H3/H4. To identify histone interacting partners of TSPYL5, we performed FLAG-
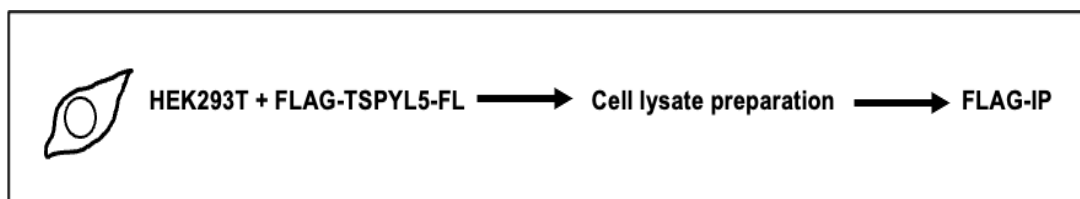
Immunopulldown (FLAG-IP) assay using overexpressed FLAG-TSPYL5 in HEK293T cells followed by immunoblotting with anti-FLAG and different anti-histone antibodies. These experiments have led to the findings that TSPYL5 specifically interacts with histones H3 and H4 but not with histone H2A and H2B (Figure 3.8.).
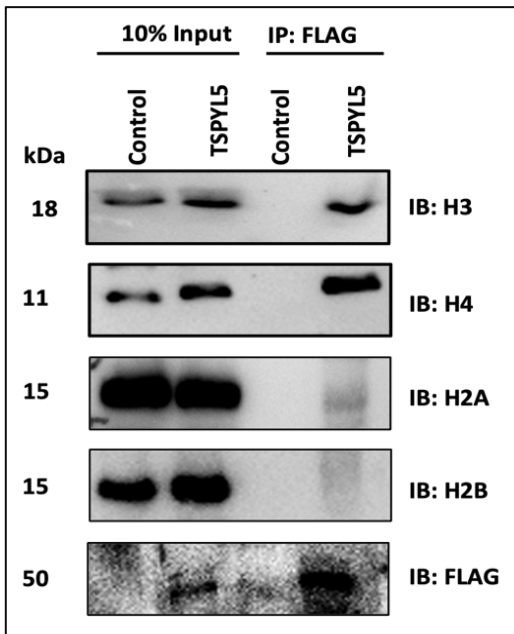
Figure 3.8. Immuno-pulldown analysis of TSPYL5. *Western blot showing FLAG-immuno-pulldown (FLAG-IP) assay results with HEK293T cell lysates of over-expressed FLAG-TSPYL5 or empty vector (EV) followed by immunoblot using anti-H2A, anti-H2B, anti-H3, anti-H4 and anti-FLAG antibodies.*

3.8. Endogenous TSPYL5 interacts with Histone H3/H4

Next, we wanted to look into the histone interaction pattern of endogenous TSPYL5. Since endogenous expression of TSPYL5 is significantly higher in SH-SY5Y cell line compared to HEK293T, we performed immuno-pulldown assay involving endogenous TSPYL5 in SH-SY5Y cells. Pulled samples using anti-TSPYL5 antibody were immuno-blotted with different histone antibodies, whereby TSPYL5 was found to interact specifically with both histones H3 and H4 (Figure 3.9.). These results were significantly
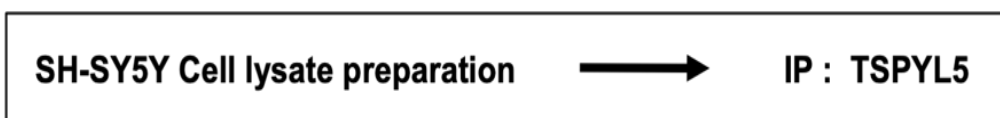
similar to interaction patterns of TSPYL5 in HEK293T cells where FLAG-TSPYL5 was overexpressed previously (Figure 3.8.).
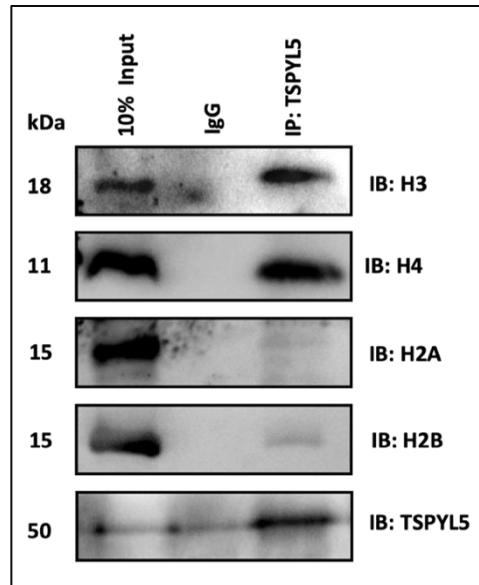
Figure 3.9. Endogenous immuno-pulldown (IP) assay of TSPYL5 *from SH-SY5Y cells with immunoglobulin G (IgG) and anti-TSPYL5 antibody followed by immunoblot with anti-H2A, anti-H2B, anti-H3, anti-H4 and anti-TSPYL5 antibodies.*

3.9. Endogenous Histone H3 interacts with TSPYL5

SH-SY5Y Cell lysate preparation ⟶ IP : H3

We further confirmed the interaction of TSPYL5 in SH-SY5Y cells with histones H3 and H4 by performing a reverse IP with anti-H3 antibody. The presence of histone H4
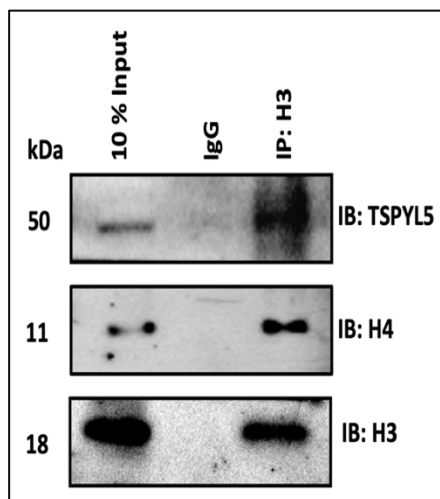
Figure 3.8. Endogenous IP of Histone H3 from SH-SY5Y cells *with IgG and anti-H3 antibody followed by immunoblot with anti-H3, anti-H4 and anti-TSPYL5 antibodies.*

105

in IP-H3 results confirmed the relevance of the experiment and the observed presence of TSPYL5 in pulldown fractions confirm the probable physical interactions between TSPYL5 and histone H3 (Figure 3.10.)

3.10. Recombinant TSPYL5 also interacts with histone H3/H4 *in vitro*

To check if TSPYL5 directly interacts with recombinant histones, we further performed a GST pulldown assay *in vitro* using purified recombinant GST-tagged TSPYL5-FL and histones H2A/H2B dimer and H3/H4 tetramer. Here we found robust interaction of TSPYL5-FL with histones H3/H4 but not with histones H2A/H2B on probing the blots with anti-GST and anti-histone antibodies (Figure 3.11.).
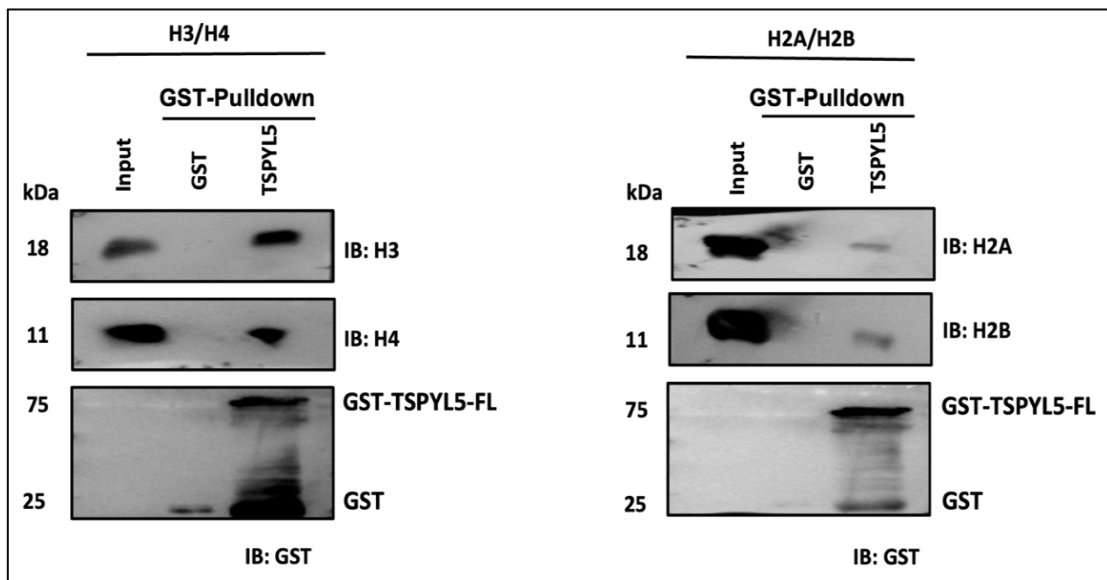
Figure 3.11. In-vitro GST pull-down assay *of the GST tagged TSPYL5 Full length (GST-TSPYL5-FL) with recombinant histone H2A/H2B dimer and H3/H4 tetramer. Blots were probed using anti-H2A, anti-H2B, anti-H3, anti-H4 and anti-GST antibodies.*

3.11. Recombinant histone H3 is the primary interacting partner of TSPYL5

To particularly designate which histone within the H3/H4 tetramer complex is the key interacting partner of TSPYL5, we subsequently performed *in vitro* pulldown assays of purified GST-tagged TSPYL5-NLD with recombinant single histones H2A, H2B, H3 and H4. Western blot analysis of this assay elucidated a strong interaction of GST tagged TSPYL5-NLD with histone H3 in particular but not with other histones H2A, H2B and H4 (Figure 3.12.). Recombinant histones were used as input samples while only GST was loaded as control for IP samples. The blots were once again probed similarly as before with anti-GST and anti-histone antibodies.

Figure 3.12. In-vitro GST pull-down assay *of the GST tagged TSPYL5 NLD with single recombinant histone H2A, H2B, H3 and H4. Blots were probed using anti-H2A, anti-H2B, anti-H3, anti-H4 and anti-GST antibodies.*

3.12. Domain architecture of TSPYL5 and their role in histone interaction

Subsequent analyses involved identifying the specific region of TSPYL5 that was participated in H3/H4 interaction. For proceeding with this we expressed and purified
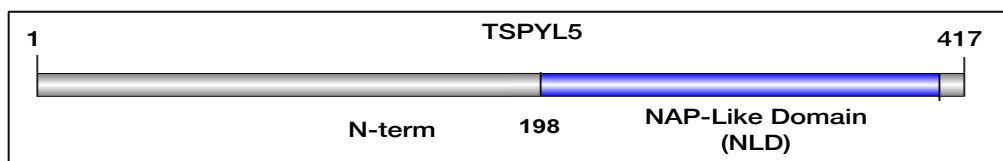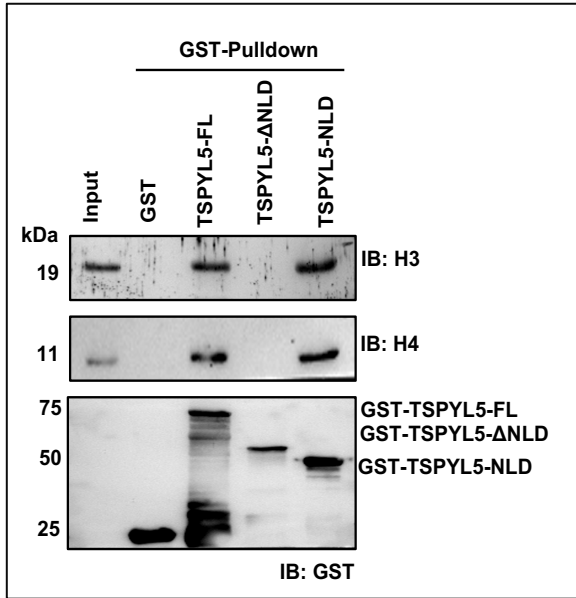
Figure 3.13.1. In-vitro GST pull-down assay *of the GST tagged TSPYL5-FL, N-term & NAP Like Domain (NLD) proteins with recombinant H3/H4. GST was used as control. Blots were probed with anti-H3, anti-H4 and anti-GST antibodies.*

different deletion constructs of TSPYL5 alongside TSPYL5-FL. GST-Immuno-pulldown assay involving FL, NLD and ΔNLD constructs of TSPYL5 has been used for studying their H3/H4 binding ability. It was observed from these blots that the TSPYL5-FL and NLD constructs showed binding with histones H3 and H4 almost to an equal extent, while TSPYL5-ΔNLD fails to interact with histones (Figure 3.13.1).

We have also cloned TSPYL5-FL and ΔNLD construct in mammalian expression vector pCR3-FLAG. FLAG constructs of TSPYL5 were then checked for their H3/H4 binding ability through a FLAG-pulldown assay. IP results here in coherence with the GST pulldown assay showed that TSPYL5-ΔNLD fails to bind histone H3/H4 in contrast to TSPYL5-FL (Figure 3.13.2). Thus, domain deletion IP

Figure 3.13.2. FLAG pull-down assay *of the FLAG tagged TSPYL5 FL, ΔNLD proteins with histone H3. Blots were probed with anti-H3, and anti-FLAG antibodies. IgG used a control.*

experiments here suggested that TSPYL5-NLD is essential for interaction with histone H3/H4 both *in vitro* and *ex vivo*.

In support of our IP results we next wanted to quantify the affinity of TSPYL5 contacts with histone H3/H4 biophysically. We employed Bio-Layer Interferometry (BLI) assay for this and used Ni-NTA biosensors to load His-tagged histone H3/H4 protein and used the different constructs of TSPYL5 in varying concentrations to quantify the binding affinity. Our biophysical assay results were also in sync with the in vitro and ex vivo
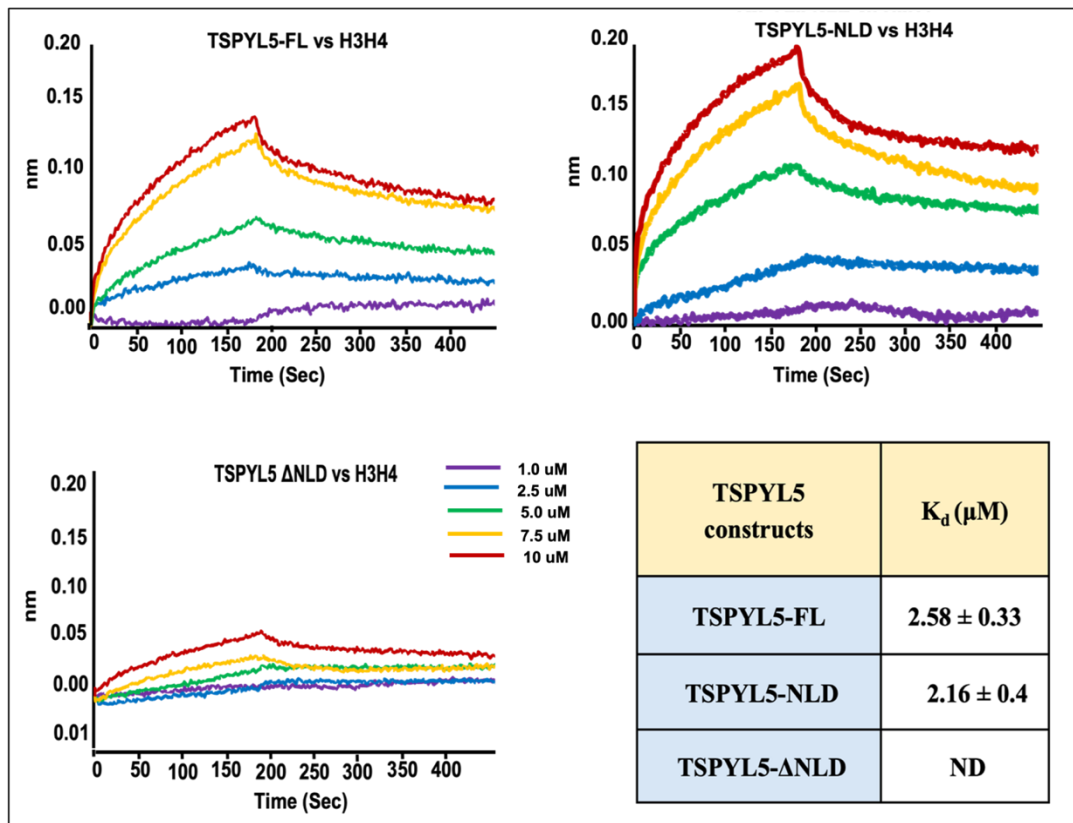
Figure 3.13.3. Binding kinetics of GST-TSPYL5-FL, GST-TSPYL5-NLD and GST-TSPYL5-ΔNLD proteins with recombinant His tagged H3/H4 histone using Bio-layer Interferometry (BLI). *His-tagged histones H3/H4 were immobilized on Ni-NTA biosensor. TSPYL5 was used as analyte at varied concentrations which has been denoted in different colors. K_d values of the binding kinetics has been calculated from the spectral data obtained.*

pulldown assays and thereby confirmed the binding affinity of TSPYL5 towards histone H3/H4. The Kd values for each type of construct was also calculated thereafter (Figure 3.13.3).

3.13. Mapping of TSPYL5 interacting surface with histone H3

We next fine-mapped the regions involved in histone H3-TSPYL5 interaction. In our attempt, to identify the TSPYL5 binding surface of histone H3, we have generated different biotin tagged H3 peptide fragments incorporating full length histone H3. This was followed by an *in vitro* peptide-pulldown assay to score the interaction between biotinylated H3 peptides and TSPYL5-NLD and the results revealed that histone peptides involving C-terminal H3 tail, encompassing both 105 - 120 and 120 - 136 region had significant interaction affinity with TSPYL5-NLD (Figure 3.14.1.). We quantified the affinity of TSPYL5-NLD towards histone H3 C-terminal region biophysically, using BLI. We used streptavidin biosensors to load biotinylated peptides and different concentrations of TSPYL5-NLD in the wells to run the experiments for the quantification assay. This
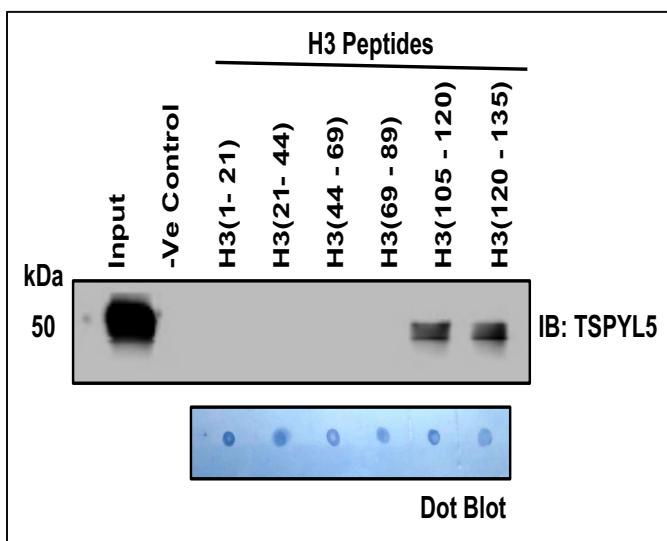
Figure 3.14.1. In-vitro peptide pull-down assay of the GST-TSPYL5 NLD proteins *(GST as control) with biotinylated histone H3 peptides. Blots were probed with anti-TSPYL5 antibody. Equal loading of peptides was detected with Amido black stain.*

helped us confirm that TSPYL5-NLD binds to histone H3 C-terminal tail (120-136) with significantly higher affinity (K_d = 4.19 ± 2.78 μM) compared to other histone H3 peptides (Figure 3.14.2).
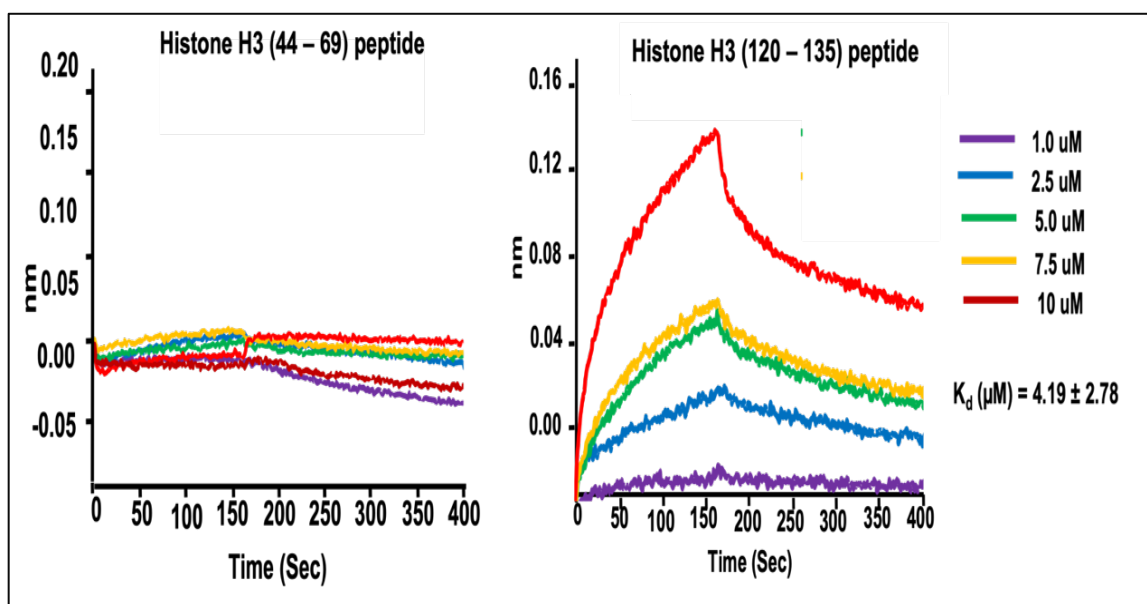
Figure 3.14.2. Binding kinetics of TSPYL5 NLD with biotinylated histone H3 peptides using Bio-layer Interferometry (BLI). *Biotin-tagged histones H3 were immobilized on streptavidin biosensor. Different concentration of TSPYL5-NLD (as shown in different colors) were used as analytes. K_d values of the binding kinetics of biotinylated histone H3 peptides with TSPYL5 NLD protein were denoted.*

To further investigate, if C-terminal tail of H3 alone was sufficient for TSPYL5 interaction, we generated and purified histone H3 C-terminal tail deleted protein (H3ΔC) which lacks the last 21 residues. We have performed CD spectroscopy with histone H3-WT and H3ΔC-term mutants to check weather H3 C-terminal tail deletion had any effect on its structural conformation. CD spectral analysis was in parity with BLI results and re-
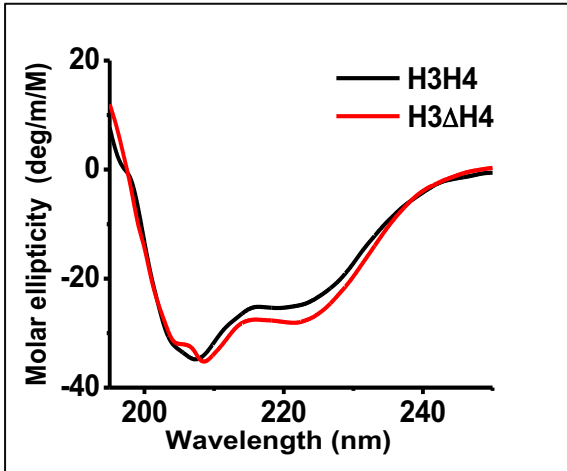
Figure 3.14.3. CD Spectroscopic analysis. *Far-UV CD spectra of Histone His-H3/H4 or His-H3ΔC-term/H4 constructs.*

assured the observation that there was no significant structural change upon deletion that would affect the interaction (Figure 3.14.3.).

We followed up our analyses with an *in vitro* GST pulldown assay using histone H3-WT and H3ΔC with GST-TSPYL5-NLD and subsequently blotted with anti-His (as both Histone H3 and H3M constructs were His tagged) and anti-GST antibodies. The assay pointed out significant loss of interaction of histone H3ΔC with TSPYL5 compared to H3-WT (Figure 3.14.4.).
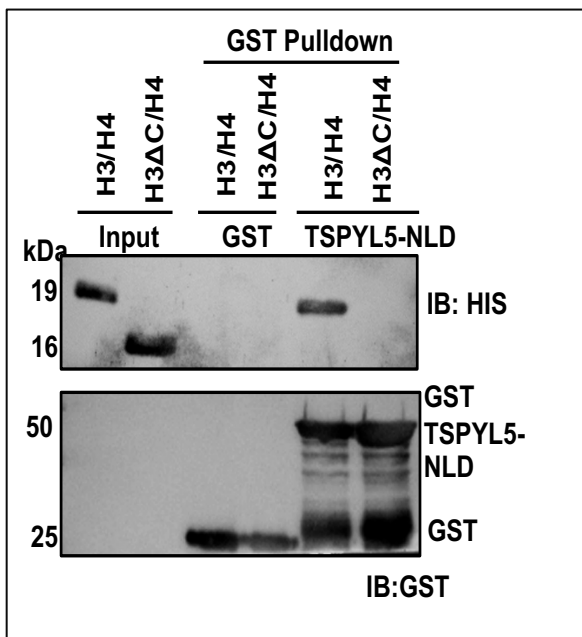
Figure 3.14.4. In vitro GST pull-down assay *of the GST-TSPYL5 NLD with recombinant His tagged H3-H4 or H3ΔCterm-H4 and subsequently blotted with anti-His and anti-GST antibodies.*

3.14. Mapping of histone H3 interacting surface of TSPYL5

To map the residues of TSPYL5 that are involved in histone H3/H4 binding, we aligned yeast NAP1 (yNAP1)and human SET/TAF1B alongside TSPYL5. We identified the loop regions of TSPYL5 which is possibly responsible for histone interaction just like yNAP1 and SET/TAF1B.
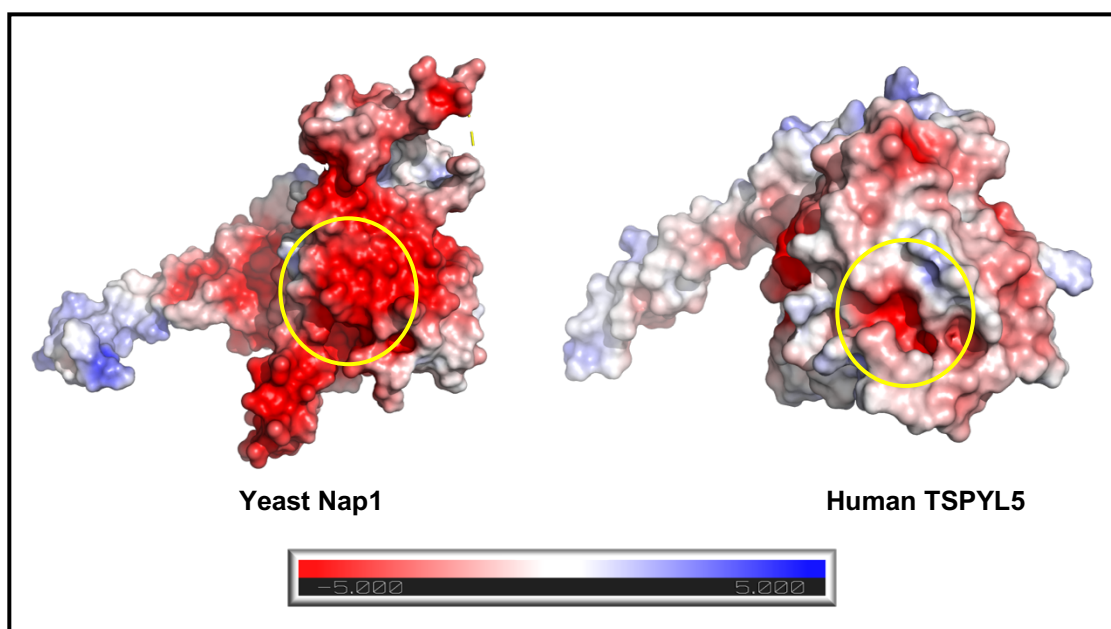
Figure 3.15.1. Comparison of histone binding region of yNAP1 and human TSPYL5. *Electrostatic surface potential generated using APBS (Baker et. al., 2001) programme in Pymol of crystal structure of yNAP1 with that of human TSPYL5 model structure. As shown in the figure, blue, red, and grey indicates positive, negative & hydrophobic surface potentials respectively. The histone binding regions of both proteins are denoted with yellow circles.*

We have prepared multiple point mutations where specific amino acid residues were converted into alanine residues at different regions of TSPYL5-NLD and we named them as Histone binding deficient mutants (HBM). Among those mutants, HBM1 (S268A/E270A), HBM2 (S340A/N343A/E345A) and HBM (1 + 2)
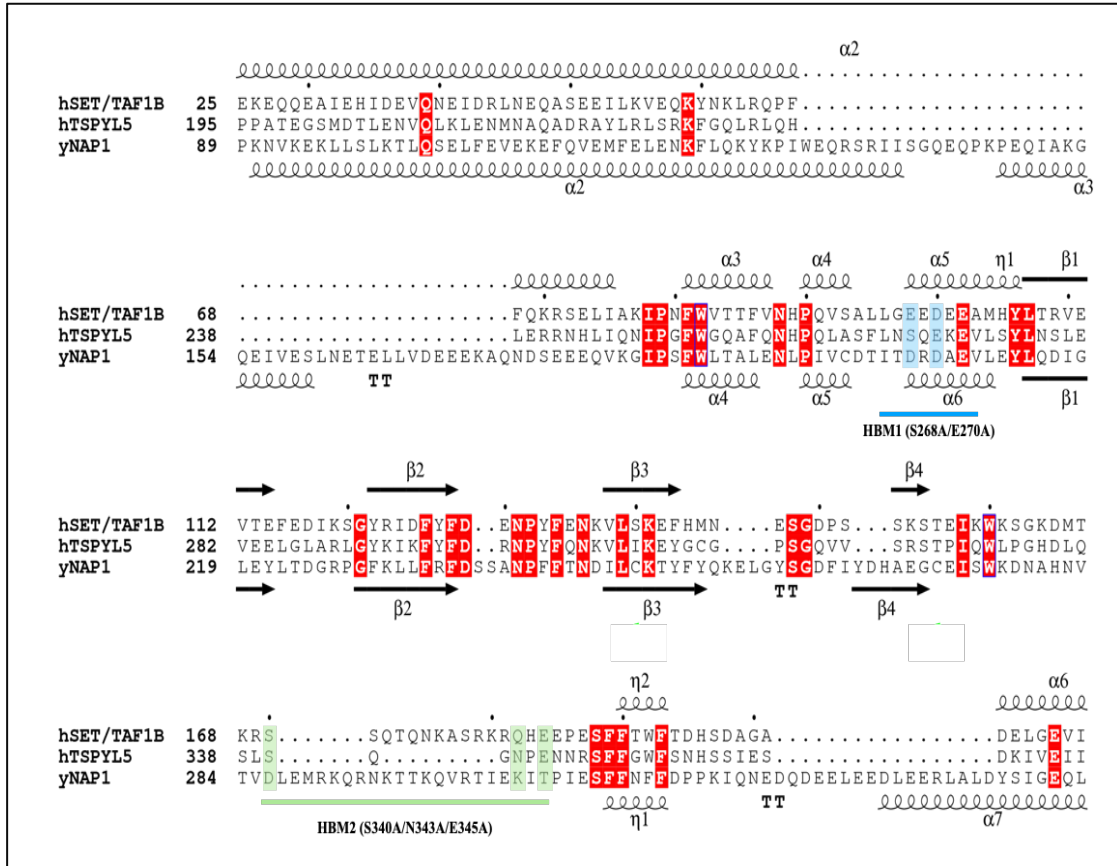
Figure 3.15.2. ClustalW sequence alignment. *Structure based multiple sequence alignment of yNAP1 (PDB: 5G2E) and human SET/TAF1B (PDB: 2E50) with TSPYL5 using ESPrit3 software.*

(S268A/E270A/S340A/N343A/E345A) mutations have been highlighted in the structure based multiple sequence alignment (Figure 3.15.2.) and also in the TSPYL5-NLD model
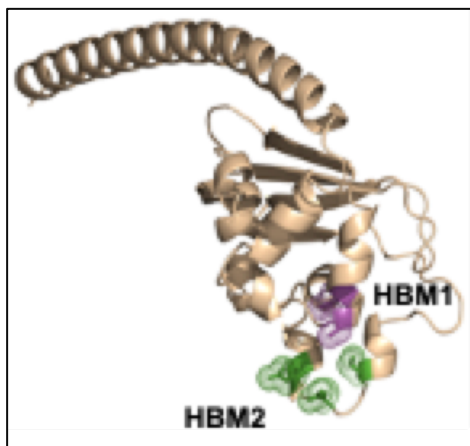
cartoon representation located at the bottom of the earmuff domain (Figure 3.15.3.).

Figure 3.15.3. Molecular modelling *of TSPYL5 NLD (198-388) done using AlphaFold software and histone binding residues are highlighted.*
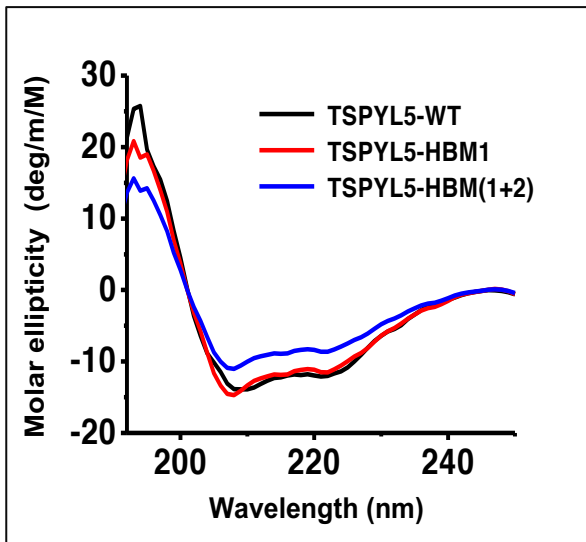
Figure 3.15.4. Far-UV CD spectral *comparative analysis of WT-TSPYL5-NLD and Histone Binding Mutant (HBM) constructs.*

We have further expressed, purified and solubilized all the Histone Binding Mutant (HBM) proteins likewise as WT proteins. In order to confirm that the structural conformation of TSPYL5 remained unaltered upon mutations, we performed CD spectroscopy analysis of TSPYL5-NLD and HBM mutants. Using CD spectroscopy analysis, we have found that the mutations didn't hamper the structural conformational of the WT-TSPYL5-NLD protein (Figure 3.15.4.).

Next, we performed GST pulldown assay using GST-TSPYL5-NLD, HBM1, HBM2 and HBM (1+2) with histones H3/H4 and blotted it with anti-GST, anti-H3 and anti-H4 antibodies. The IP results revealed that when both HBM 1 and 2 mutations were combined, i.e. HBM (1+2) it had marked loss of interaction ability with histone H3/H4 compared to WT-TSPYL5-NLD. Interaction patterns
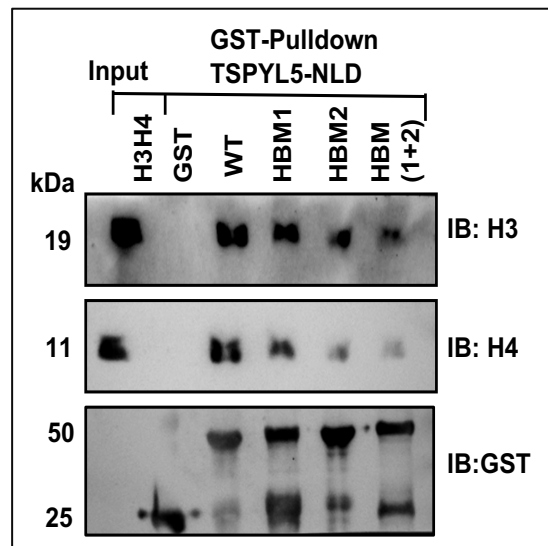
Figure 3.15.5. In vitro GST pull-down assay *of the GST-TSPYL5-NLD wild-type (WT) and different histone binding mutants HBM1, HBM2 and HBM (1+2) with recombinant H3/H4 and subsequently blotted with anti-H3, anti-H4 and anti-GST antibodies.*

were also seen with HBM1 alone and to a certain extent with HBM2 alone in contrast to that of HBM (1+2) (Figure 3.15.5.).

We further revalidated our GST-IP results by characterizing the histone interaction of TSPYL5 using BLI. As mentioned earlier we used Ni-NTA biosensors to load His-tagged histone H3/H4 protein and used different TSPYL5-HBM constructs in varied
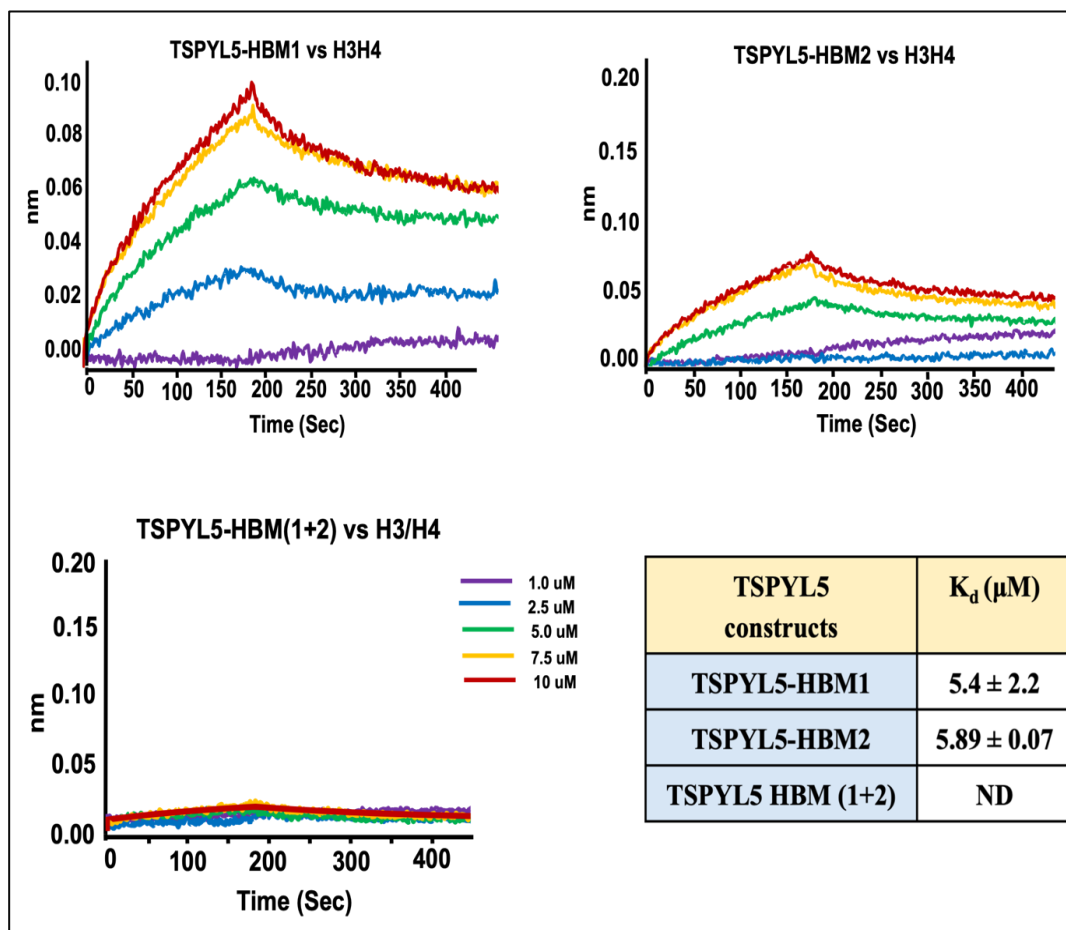
Figure 3.15.6. Binding kinetics of GST-TSPYL5-HBM1, GST-TSPYL5-HBM2 and GST-TSPYL5-HBM3 proteins with recombinant histone His tagged H3/H4 using Bio-layer Interferometry (BLI). *His-tagged histones H3/H4 were immobilized on Ni-NTA biosensor. Different constructs of GST-TSPYL5 were used as analytes at different concentrations which is denoted using different colors. Table also denotes the Kd values for different constructs of GST-TSPYL5 and their H3/H4 interaction.*

concentrations to quantify the binding affinity. Dissociation constant (Kd) values obtained previously from kinetics study illustrated a stronger interaction of H3/H4 with TSPYL5-NLD-WT compared to the HBM (1+2) which showed no detectable binding affinity to H3/H4. Interaction of different HBM constructs of TSPYL5 (HBM1, HBM2) with histone H3/H4 has also been substantiated with the corresponding K_d values in the associated table showing values, that were inferred from spectral data of the BLI study (Figure 3.15.6.).

3.14. Characterisation of TSPYL5 and H3/H4 complex

To reconstitute the complex of TSPYL5-NLD-H3/H4, we used His-SUMO-TSPYL5-NLD and His-H3/H4 constructs and co-expressed them in *E.coli*-BL21 cells.
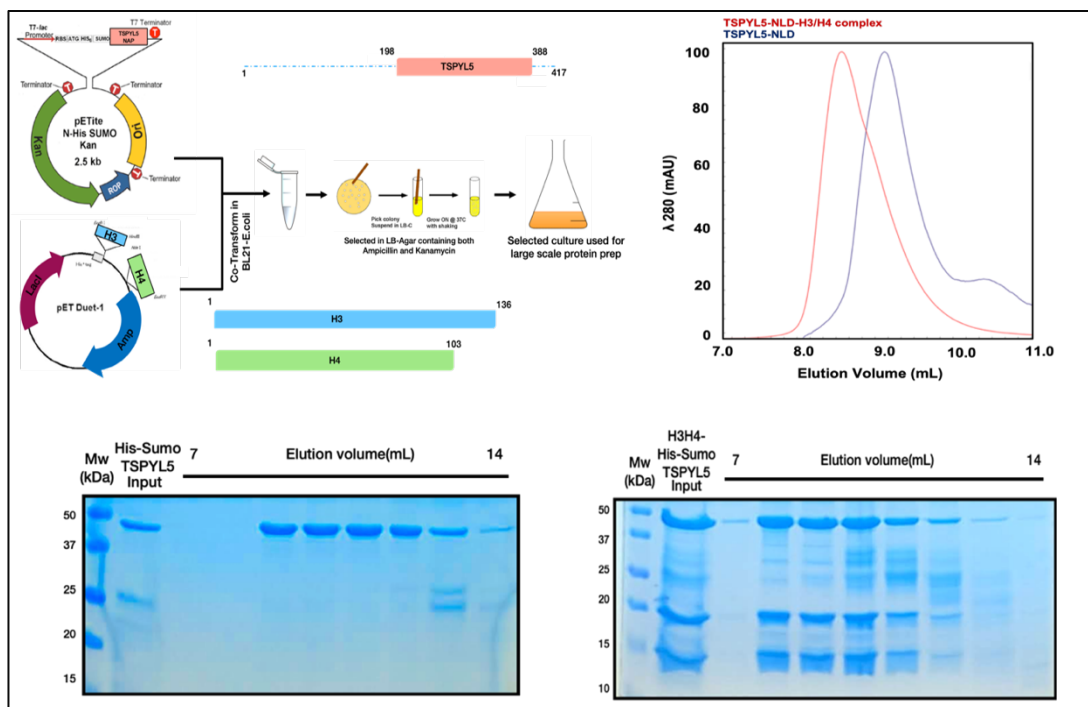
Figure 3.16.1. Schematic diagram depicts the workflow of expression and purification of TSPYL5-H3/H4 complex *in vitro. Size exclusion profile of His-SUMO_TSPYL5-NLD and His-SUMO_TSPYL5-NLD-H3/H4 complex in Size Exclusion buffer (20 mM HEPES pH-7.5, 1 mM TECEP, 2 M NaCl). Eluted samples from the size exclusion chromatography run in SDS PAGE to analyze the fractions.*

TSPYL5-H3/H4 complex was co-purified using Ni-NTA affinity chromatography column and the purified protein was further purified using size-exclusion chromatography. Fractions that showed presence of the complex (determined from mass values of chromatographic spectral data) were collected separately, concentrated and stored at -80°C for long term use. They were also analysed for accuracy in SDS-PAGE (Figure 3.16.1.).

Molecular stoichiometry data of the TSPYL5-NLD, H3/H4 and TSPYL5-NLD-H3/H4 complex in solution was further corroborated using size-exclusion chromatography coupled with multiple-angle light scattering (SEC-MALS) to also measure the molecular mass of the complex. His-SUMO-TSPYL5-NLD shows molecular weight of 74.15 kDa (error 3%, expected dimer mass was 72 kDa) in SEC-MALS when run in lower salt buffer
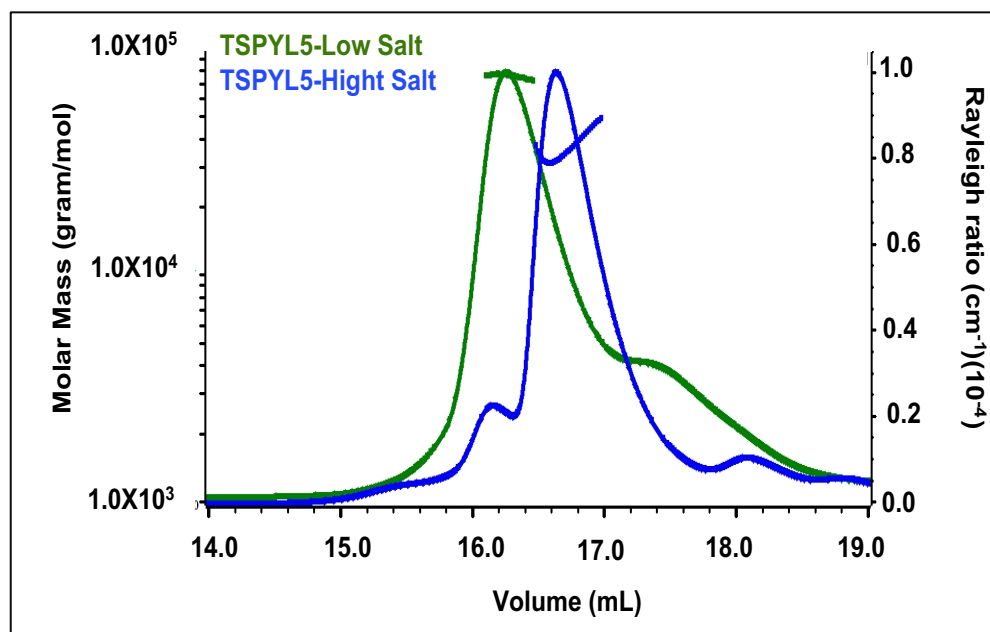
Figure 3.16.2. SEC-MALS analysis *showing normalized Refractive Index (RI) trace of His-SUMO TSPYL5 NLD in low salt-200 mM NaCl buffer (green) & in high salt-2 M NaCl buffer. The calculated Molar mass is shown as a dashed line in the respective peak colour plotted against the elution volume (mL). Buffer condition: 20 mM HEPES pH-7.5, 1 mM TECEP, 200 mM (low) or 2 M NaCl (high).*

(200 mM NaCl). But, surprisingly, when His-SUMO-TSPYL5-NLD was run in high salt buffer (2 M NaCl) it measured as 34.39 kDa (error 4%, expected monomer mass was 36kDa) (Figure 3.16.2.). The corresponding values for molar mass as obtained from SEC-MALS in both low and high salt buffer, their error scale and expected mass has been depicted in Table 3.1.

Complex	Molecular Ratio 1	Expected Mass 1 (kDa)	Molecular Ratio 2	Expected Mass 2 (kDa)	Molecular Ratio 3	Expected Mass 3 (kDa)	Measured Mass (kDa)	Error
TSPYL5-NLD Low Salt	1	36	**2**	**72**	-	-	74.15	3.0%
TSPYL5-NLD High Salt	**1**	**36**	2	72	-	-	34.39	4.0%

Table 3.1. Table showing of Molar mass measurements by SEC-MALS. *Calculated stoichiometric ratio and molecular mass of each sample that correspond to the experimental measured mass are indicated in red.*

As histone H3/H4 data only availed under high-salt (2 M NaCl) condition, we performed subsequent SEC-MALS analysis using SEC buffer in 2 M NaCl. The molecular mass of His-H3/H4 was measured at 54.83 kDa (error 2%, expected histone H3/H4 tetramer mass was 56 kDa). The His-SUMO-TSPYL5 NLD-H3/H4 complex was measured at 129.31 kDa (error 1%,) where we hypothesized that possibly two TSPYL5 bind to histone H3/H4 as two dimer of H3/H4 or one tetramer to form a complex having a

molar mass of 128 kDa. The values have again been depicted in a similar table form in Table 3.2. and the spectral data curve has been illustrated in Figure 3.16.3.
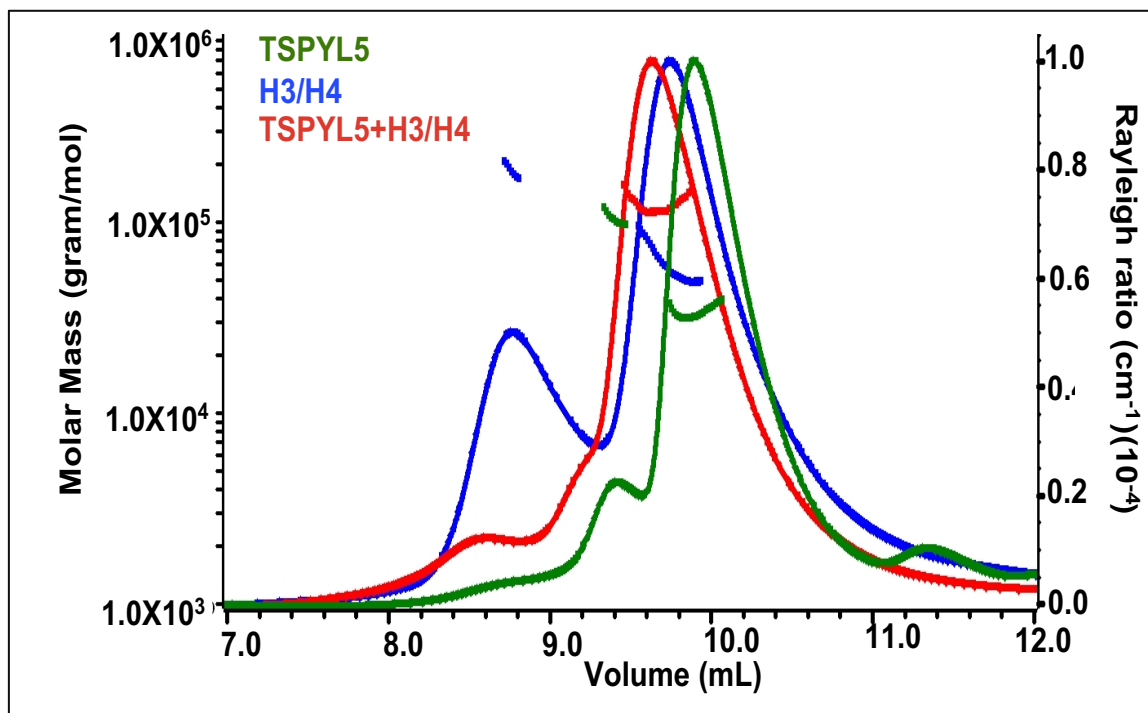
Figuree 3.16.3. SEC-MALS analysis *showing normalized Refractive Index (RI) trace of Histone His-H3/H4 (blue), His-SUMO TSPYL5 NLD (green) & His-SUMO TSPYL5 NLD-H3/H4 complex (red). The calculated Molar mass is shown as a dashed line in the respective peak colour plotted against the elution volume (mL). Buffer condition: 20 mM HEPES pH-7.5, 1 mM TECEP, 2 M NaCl).*

Complex	Molecular Ratio 1	Expected Mass 1 (kDa)	Molecular Ratio 2	Expected Mass 2 (kDa)	Molecular Ratio 3	Expected Mass 3 (kDa)	Measured Mass (kDa)	Error
H3/H4	1:1	28	2:2	56	-	-	54.83	2.0%
TSPYL5-NLD	1	36	2	72	-	-	34.39	4.0%
TSPYL5-NLD+H3/H4	1:1:1	64	1:2:2	92	2:2:2	128	128.31	1.0%

Table 3.2. Molar mass measurements by SEC-MALS. *Calculated stoichiometric ratio and molecular mass of each sample corresponding to the measured mass are indicated in red.*

Fractions collected during the experiment from all three sample sets (TSPYL5, H3/H4 and TSPYL5+H3H4 complex) were run separately on SDS-PAGE to re-confirm their molecular weight and also check the purity of the sample. Results were in parity with molar mass results obtained from SEC-MALS. While TSPYL5 and H3/H4 samples run separately showed a distinct single band corresponding to their respective molecular weights, gel run with samples from the TSPYL5+H3/H4 complex showed bands for both TSPYL5, H3/H4 and the combined mass of the two (Figure 3.16.4.).

Figure 3.16.4. SDS PAGE profile of eluted samples from SEC-MALS experiments. *Color of the box also indicated the samples according to the SEC-MALS profile. Fraction numbers corresponding to elution volume (mL) are indicated on top of each gel.*

Histones H3/H4 persists as dimer or tetramer in solution, depending on the salt concentration. To understand whether TSPYL5 interacts to two H3/H4 dimers or one H3/H4 tetramer, we performed protein cross-linking experiments. To do this, we incubated

His-SUMO-TSPYL5-NLD and H3/H4 either alone (as control) or with DSS crosslinker and resolved crosslinked complexes by SDSPAGE followed by western blot. Immunoblotting with anti-H3, anti-TSPYL5 antibodies revealed the presence of higher molecular weight species in the crosslinking sample of the TSPYL5-H3/H4 mix. New band appearing in the western blot resided between molecular weight of 150 and 100 kDa marker which was absent when His-SUMO-TSPYL5-NLD and H3/H4 were crosslinked separately. Results indicated that TSPYL5 can bind to both two H3/H4 dimers or one H3/H4 tetramer (Figure 3.16.5.).
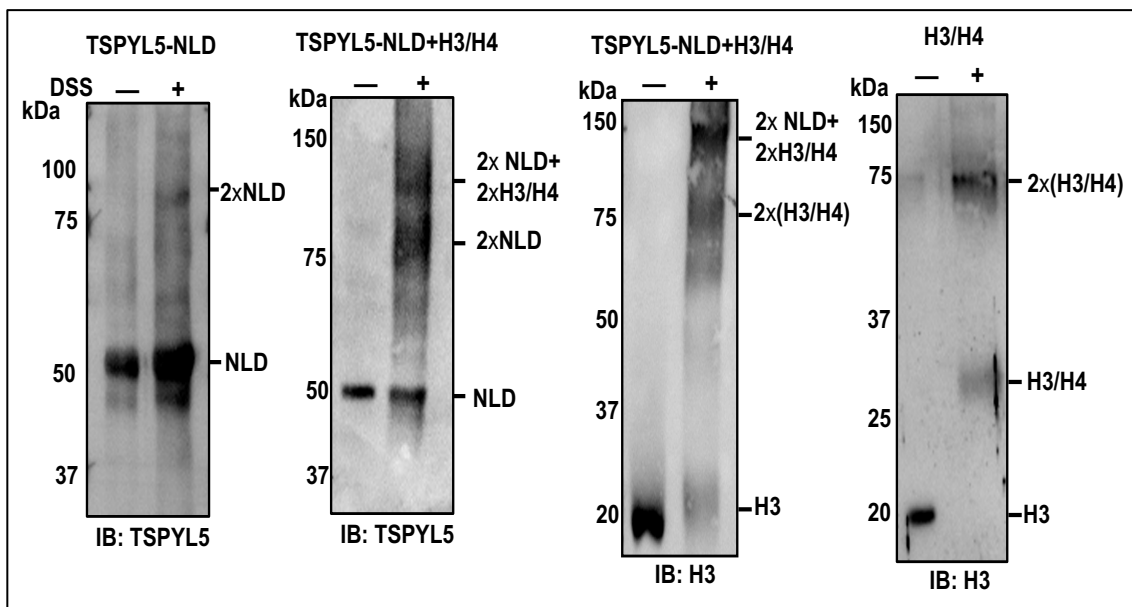
Figure 3.16.5. DSS cross-linking experiments performed on TSPYL5-NLD, TSPYL5-NLD H3/H4 complex and H3/H4. *Western blot analysis of DSS mediated cross-linking of His-SUMO TSPYL5-NLD, H3/H4 His-SUMO TSPYL5-NLD complex and His-H3/H4. In each case Lane 1 shows control without DSS; lane 2 shows sample incubated with 2.5 mM DSS. Species appearing in the cross-linking H3H4 His-SUMO-TSPYL5-NLD complex are indicated.*

SEC-MALS and solution crosslinking studies highlighted that TSPYL5 dimer forms a complex with H3/H4 under both conditions: two H3/H4 dimer or one tetramer.

Previously using peptide IP and GST-IP along with biophysical experiments we analysed that the C-terminal stretch of histone H3 is responsible for interacting with TSPYL5. This C-terminal region of histone H3, spanning 105-136 amino acids, harbors the α2–α3 helices which is also responsible for 2 histone H3/H4 dimer to H3/H4 tetramer formation. H3-H3' dimerization that leads to H3/H4 tetramer formation is possible by few important residues. We hence mutated those residues and prepared tetramerization disruptive mutant histone H3M (C110E/L126R/I130E) constructs and were able to purify H3M/H4 which is also constitutively a dimer. WT Histone H3/H4 and mutated histone H3M/H4 were taken to perform GST pulldown assay with GST-TSPYL5-NLD and followed by immunoblotting with respective antibodies. After analysis of the IP results, it was found that TSPYL5-NLD binds equally with H3/H4 dimer (involving H3M/H4) and H3/H4 tetramer. Results thus indicated that TSPYL5 does not discriminate between histone H3/H4 dimer and tetramer. Collectively, these results suggested that one TSPYL5 dimer can bind with two histones H3/H4 dimers or a single H3/H4 tetramer and form a stable complex (Figure 3.16.6.).

Figure 3.16.6. In vitro GST pull-down assay *of the GST-TSPYL5 NLD with recombinant His tagged H3/H4 or tetramerization disruptive mutant H3M/H4, subsequently blotted with anti-H3, H4 and GST antibodies. H3M mutation residues are shown in the sequence alignment.*
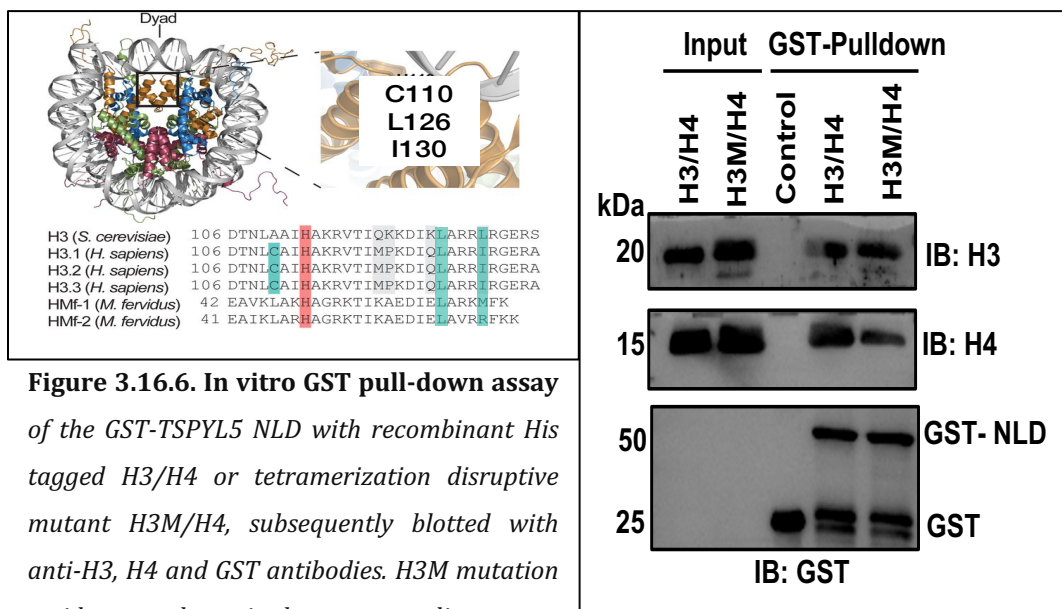
3.16. TSPYL5 has unique size dependent DNA binding properties

Histone chaperones, apart from their ability to interact with histones, have also been reported to bind DNA in order to regulate DNA mediated processes. To check if TSPYL5 has DNA binding ability, we used electrophoretic mobility shift assay (EMSA) using different DNA fragments ranging from 10 - 330 base pair (bp) as a substrate against TSPYL5-NLD used in increasing concentrations (0 – 8.0 µM). In EMSA results it was found that TSPYL5-NLD binds to DNA above 80 bp (i.e., 100 and 330 bp used here) length but interestingly it showed no binding with the shorter fragments of DNA (Figure 3.17.1.).
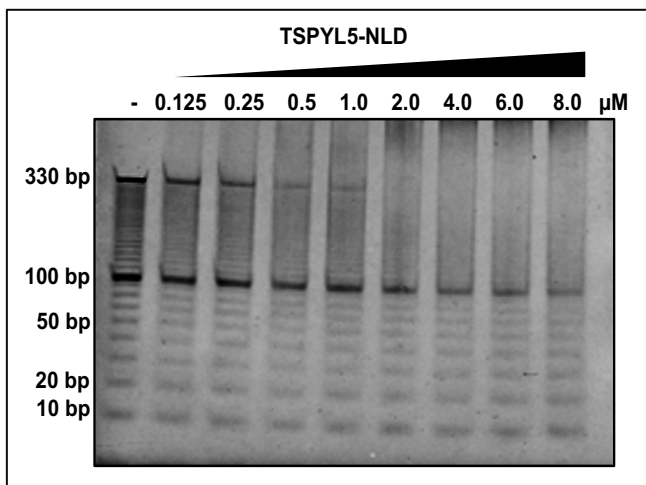
Figure 3.17.1. *EMSA showing TSPYL5-NLD binding to DNA fragments of varying lengths (10 - 330 bp).*

To further confirm the DNA binding specificity of TSPYL5, we have performed EMSA with 20, 40, 80 and 146 bp dsDNA substrates individually. Increasing concentrations of TSPYL5-NLD was incubated with each type of DNA fragments to further investigate if the specific length of DNA was a necessity for TSPYL5 binding. EMSA results were analysed and we have found that TSPYL5 shows markedly high affinity towards 80 bp and 146 bp DNA. On the other hand, TSPYL5 doesn't show any significant binding towards 20 bp and 40 bp DNA (Figure 3.17.2.).
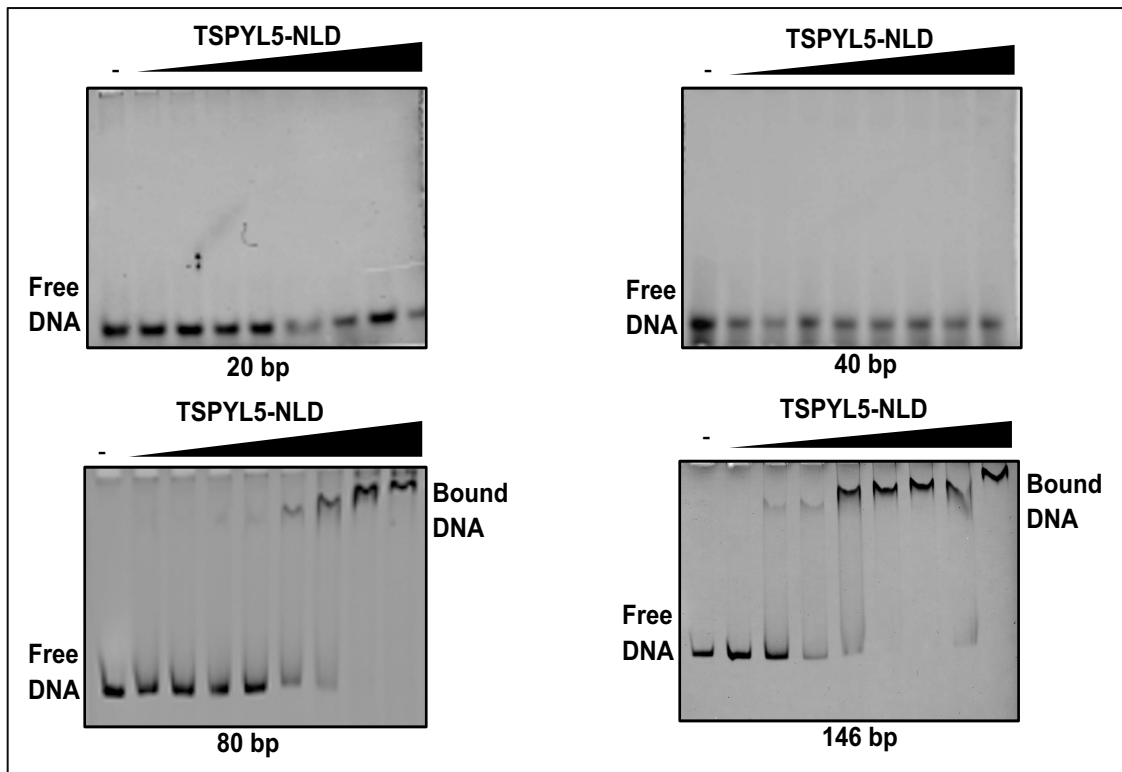
Figure 3.17.2. EMSA showing binding of TSPYL5-NLD using 20, 40, 80 and 146 bp DNA respectively. *Increasing amounts of TSPYL5 (0.06, 0.125, 0.25, 0.5, 1, 2, 4, 8, 16 or 32 μM) were mixed with 1 μM DNA.*

Interestingly, it is well documented that minimum 80 bp DNA is a prerequisite to dock H3/H4 tetramer while 146 bp DNA is a minimal essential length of DNA to assemble a complete nucleosome. Thus, TSPYL5 binding to these longer DNA fragments suggests that it may have a role in DNA mediated histone deposition process. To quantify the DNA binding affinity of TSPYL5, we measured the substrate DNA depletion upon TSPYL5 binding in EMSA assays. The binding curve was plotted against increasing concentrations of TSPYL5-NLD. TSPYL5-NLD shows strong binding towards 80 and 146 bp of DNA with a K_d value 0.51 and 0.38 µM respectively (Figure 3.17.3.).
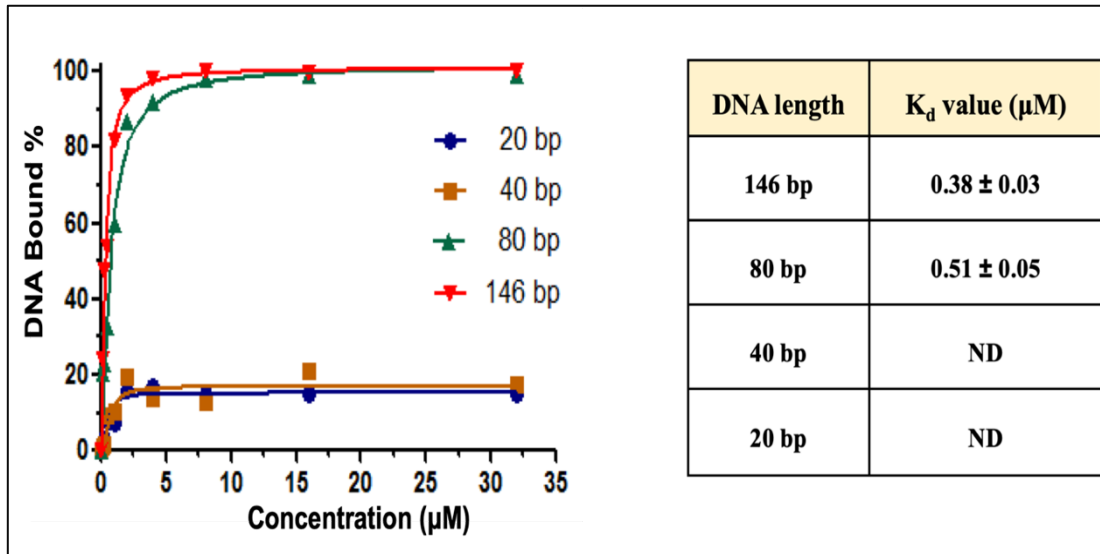
Figure 3.17.3. Corresponding binding curves of TSPYL5-NLD to 20 bp, 40 bp, 80 bp and 146 bp DNA interaction. *The binding intensity is quantified by DNA depletion upon interaction with TSPYL5-NLD and dissociation constant (K_d) is calculated using Hill plot.*

Next, to find out if the NLD domain is sufficient for DNA binding of TSPYL5, we used TSPYL5-ΔNLD in increasing concentration with 146 bp DNA as substrate and performed EMSA. EMSA results shows no detectable DNA binding of TSPYL5-ΔNLD. This indicated that NLD is essential and a primary requirement for DNA binding activity of TSPYL5. To explore further, if the histone binding residues of TSPYL5 were also involved in its DNA binding, we performed EMSA using histone binding deficient mutant TSPYL5-HBM (1+2) in increasing concentrations with 146 bp DNA substrate. Here we did not observe any significant DNA binding affinity of TSPYL5-HBM (1+2). EMSA results here thus recommended that the DNA binding surface of TSPYL5 may overlap with its histone binding surface, which possibly leads to loss of DNA binding function of TSPYL5 when histone binding surfaces were mutated (Figure 3.17.4.).
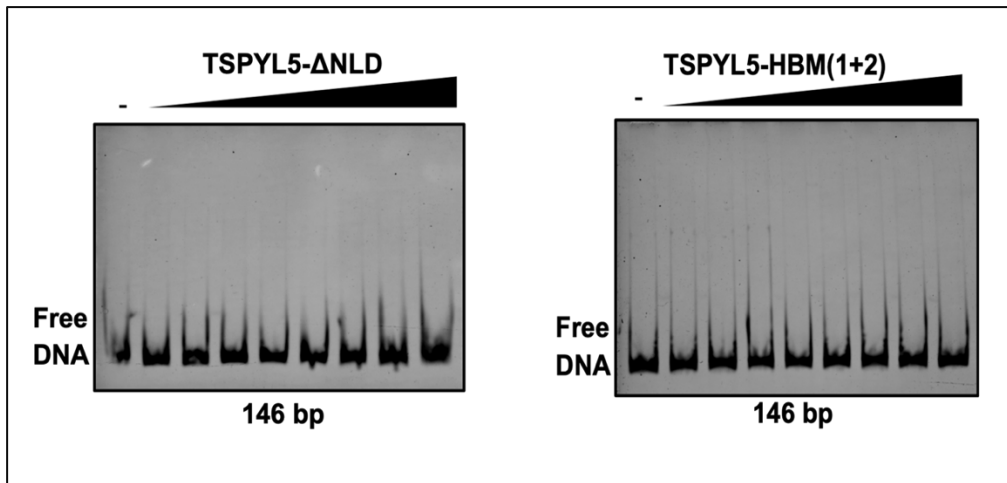
Figure 3.17.4. *EMSA showing binding of 146 bp DNA to increasing concentration of TSPYL5- ΔNLD and HBM (1+2). Free DNA and TSPYL5-bound DNA are indicated.*

3.15. TSPYL5 promotes tetrasome formation & plasmid supercoiling *in vitro*

To determine if TSPYL5 acts as a bonafide histone H3/H4 chaperone, we performed an *in vitro* histone deposition assay. But we first wished to nullify the chances of self-deposition of histone H3/H4 on DNA. So we used 146bp DNA as a substrate and incubated

it with increasing concentrations of histone H3/H4. Upon incubation, we were able to narrow down the optimal concentration which will not show self-deposition on DNA (Figure 3.18.1.). Using the optimal concentration i.e.
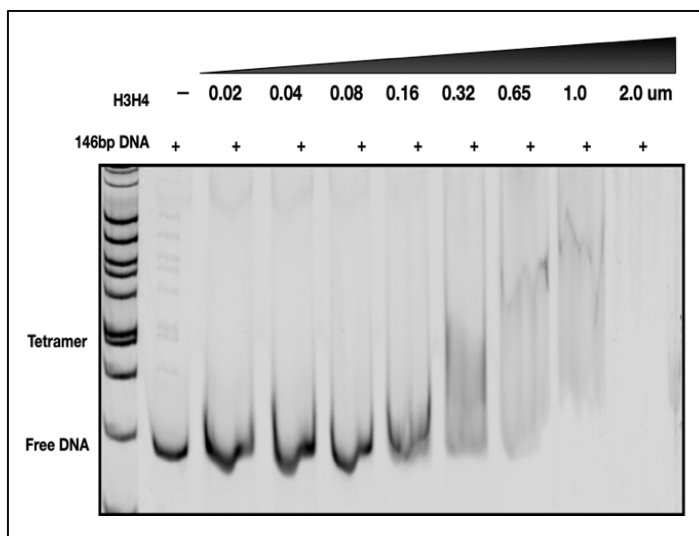
Figure 3.18.1. *EMSA showing 146bp linear DNA (Widom 601 sequence) and its interaction with increasing concentration of histone H3/H4.*

0.15 μM of H3/H4 on to linear DNA substrate we next performed histone deposition assay.

The TSPYL5-NLD-H3/H4 mix were previously prepared using 0.15 μM of histone H3/H4 and increasing concentration of TSPYL5-NLD. Then 146bp DNA were incubated with pre-incubated histone H3/H4-TSPYL5-NLD mix and resolved in native-PAGE. TSPYL5-NLD in increasing concentrations was able to deposit H3/H4 on to linear 146 bp DNA substrate. In contrast, histone binding deficient mutant TSPYL5-HBM (1+2),
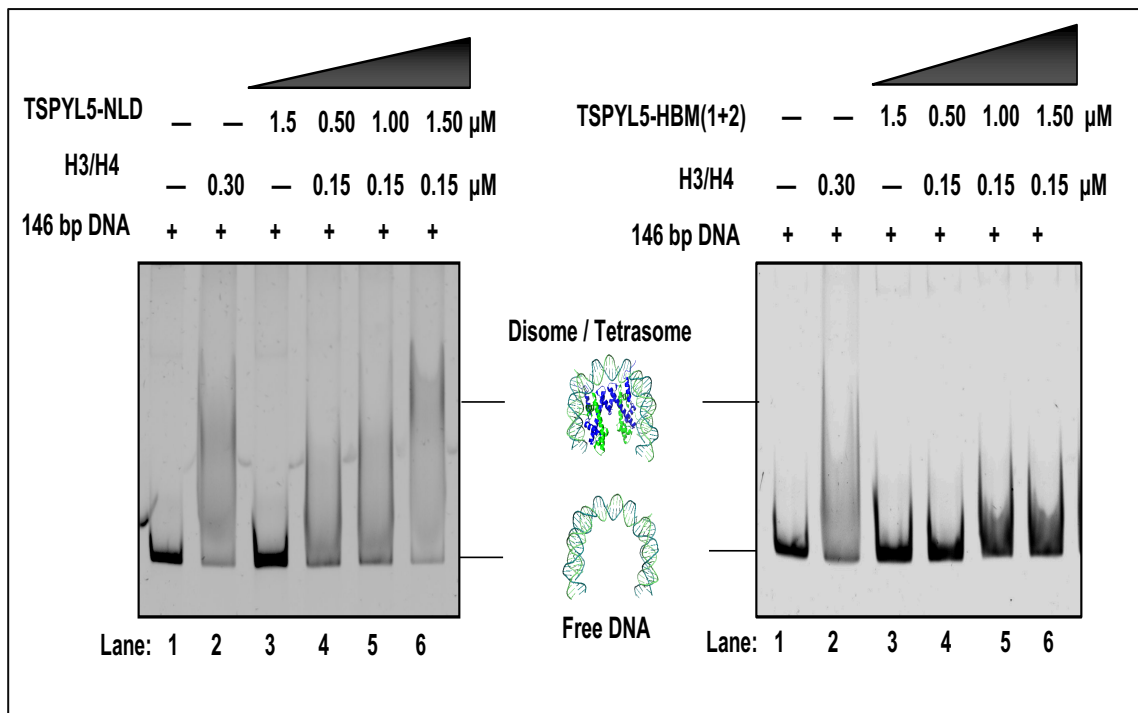
Figure 3.18.2. Tetrasome assembly assay performed with 146bp linear DNA (Widom 601 sequence), H3H4 and TSPYL5. *Samples run in 7% native PAGE and stained with Gel green. Lane 1 and Lane 2 shows free DNA input and tetrasome input (preassembled by salt dilution method) respectively; Lane 3 shows GST TSPYL5 NLD-WT with free DNA. Lanes 4-8 shows free DNA incubated with H3-H4 with increasing concentrations of GST TSPYL5 NLD-WT as indicated in the figure. Free DNA and Tetrasome are indicated. Tetrasome assembly assay performed similarly as NLD experiments using increasing concentration of GST TSPYL5 NLD-HBM3.*

which shows impaired histone H3/H4 association *in vitro*, was unable to deposit histones (Figure 3.18.2.).
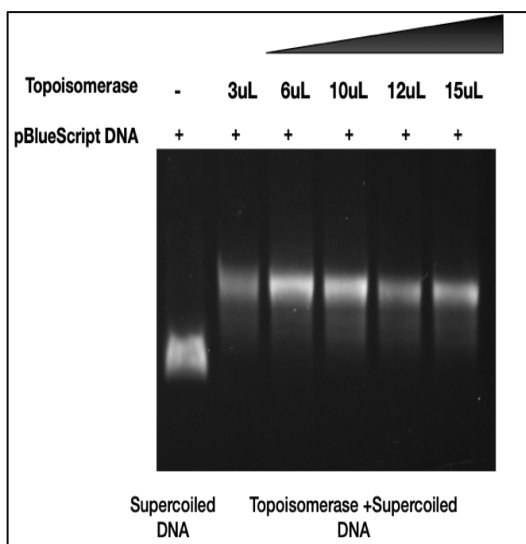
Figure 3.18.3. pBS DNA resolved with native agarose gel electrophoresis. *Lane 1 shows supercoiled pBS DNA input; Lane 2-6 shows PBS DNA relaxed by increasing concentration of Topoisomerase-I (different dilution of Topoisomerase-I from stock used to measure the enzyme activity).*

pBlue Script (pBS) plasmid is mainly supercoiled in nature. Upon Topoisomerase-I treatment the plasmid DNA relaxed in to a linear form. It was thus essential for us to optimize the Topoisomerase-I concentration for further use of the relaxed plasmid during the plasmid supercoiling assay. Topoisomerase-I stocks were diluted in Supercoiling assay buffer and used in increasing concentrations to reach an optimized enzyme concentration for digestion (Figure 3.18.3.).

It was also required that we optimised the Histone H3/H4 concentration in order to avoid all probability that histones would self-deposit onto relaxed pBS DNA. So upon optimisation of the Topoisomerase-I concentration, we next optimised histone H3/H4 concentration that was required for supercoiling assay. We thus used increasing concentrations of histone H3/H4 and incubated it with Topoisomerase-I treated previously with relaxed pBS DNA (Figure 3.18.4.).
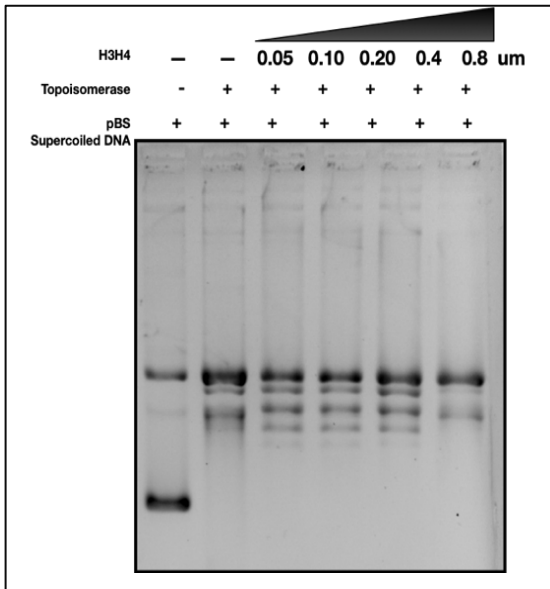
Figure 3.18.4. Topoisomerase-I treated relaxed pBS DNA incubated with histone H3/H4 *and resolved with native agarose gel electrophoresis to check the optimal experimental concentration of H3/H4. Lane 1 shows supercoiled pBS DNA input; Lane 2: Topoisomerase-I relaxed pBS DNA, Lane 3-6 shows Topoisomerase-I relaxed pBS DNA incubated with increasing concentrations of histone H3/H4.*

As we see TSPYL5 have DNA binding properties, so it was vital to also understand the TSPYL5 optimal concentration needed to avoid false positive data from the supercoiling assay. We used increasing concentrations of TSPYL5-NLD and incubates it with Topoisomerase-I treated previously relaxed pBS DNA. Upon resolving it in agarose gel, optimal TSPYL5-NLD concentrations were denoted which were used for further supercoiling assay (Figure 3.18.5.).

Finally, to investigate if TSPYL5 could facilitate DNA supercoiling upon histone deposition, we performed a plasmid supercoiling assay using Topoisomerase-I treated relaxed pBS plasmid DNA. Increasing concentrations of TSPYL5-NLD were pre-mixed with histone H3/H4 and upon incubation with relaxed plasmid DNA it resulted in efficient supercoiling of pBS plasmid DNA as observed in agarose gels. The results propose that TSPYL5 may have a role in promoting DNA supercoiling upon histone deposition. However, the TSPYL5-HBM (1+2) which have mutated histone binding sites, failed to facilitate plasmid supercoiling *in vitro*. Together, these results put forward am
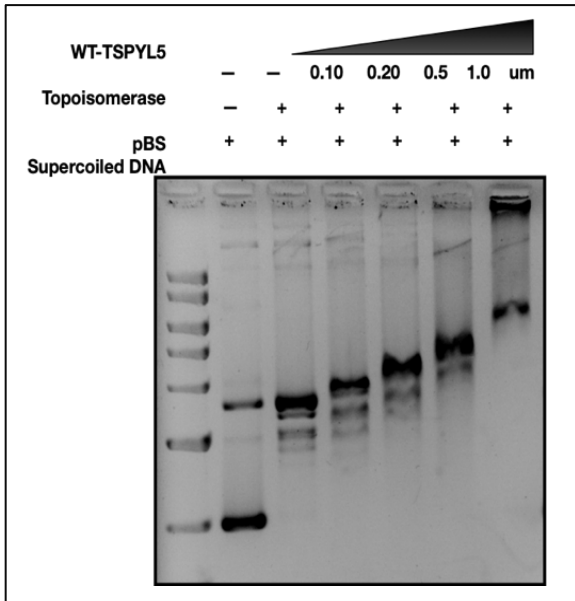
Figure 3.18.5. Topoisomerase-I treated relaxed pBS DNA incubated with TSPYL5-NLD and resolved with native agarose gel electrophoresis *to check the optimal experimental concentration TSPYL5. Lane 1 shows supercoiled pBS DNA input; Lane 2: Topoisomerase-I relaxed pBS DNA, Lane 3-6 shows Topoisomerase-I relaxed pBS DNA incubated with increasing concentration TSPYL5-NLD-WT.*

idea that the histone binding residues of TSPYL5 are critical for both its histone deposition

and plasmid supercoiling activity (Figure 3.18.6.).
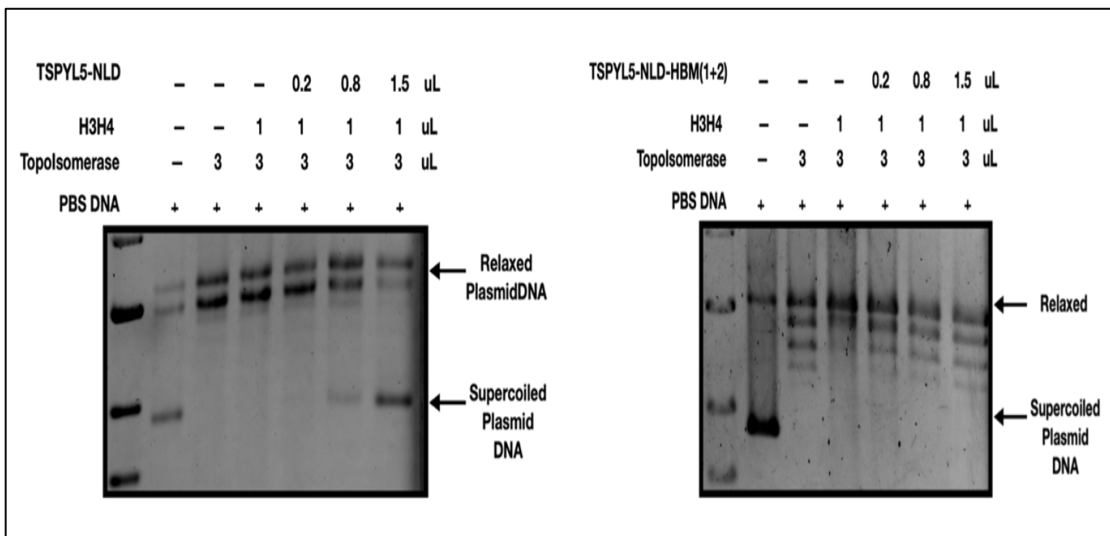
Figure 3.18.6. Plasmid supercoiling assay performed with p-Blue Script (PBS) DNA and Topoisomerase-I, histone H3-H4 and GST TSPYL5 NLD-WT. *Samples were resolved with native agarose gel electrophoresis. Lane 1 shows supercoiled PBS DNA input; Lane 2 shows PBS DNA relaxed by Topoisomerase-I; and Lanes 3–6 show pre-relaxed PBS DNA with Topoisomerase-I, incubated with histone H3-H4 and increasing concentrations of GST TSPYL5 NLD-WT. Relaxed, and Supercoiled plasmid is indicated. Plasmid supercoiling assay was also performed similarly using increasing concentrations of GST TSPYL5-NLD-HBM3.*

3.18. *In vitro* CD analysis reveals chromatin compaction ability of TSPYL5

Circular dichroism (CD) spectroscopy analysis can be used as an effective *in vitro* technique to score chromatin compaction biophysically. Chromatin is made of DNA which in turn is wrapped with proteins (mainly histones and histone interacting proteins). DNA shows a significant peak in the wavelength range of 250 – 290 nm. Upon chromatin compaction, the accessible region of DNA of chromatin was decreased and thereby illustrated a loss of absorbance value in CD spectra near this wavelength range. Using this experimental principle, we used higher order chromatin form HeLa cells and incubated them with varied increasing concentrations of TSPYL5-NLD *in vitro* and checked their CD spectral absorbance. Chromatin of HeLa cells compacted upon incubation with increasing concentrations of TSPYL5 (Figure 3.19.1.). The bar graphs show mean residual ellipticity value at a particular wavelength of 270 nm plotted against the increasing concentrations of TSPYL5 (colour coded to the signal curve and in shades of grey in the bar graph).
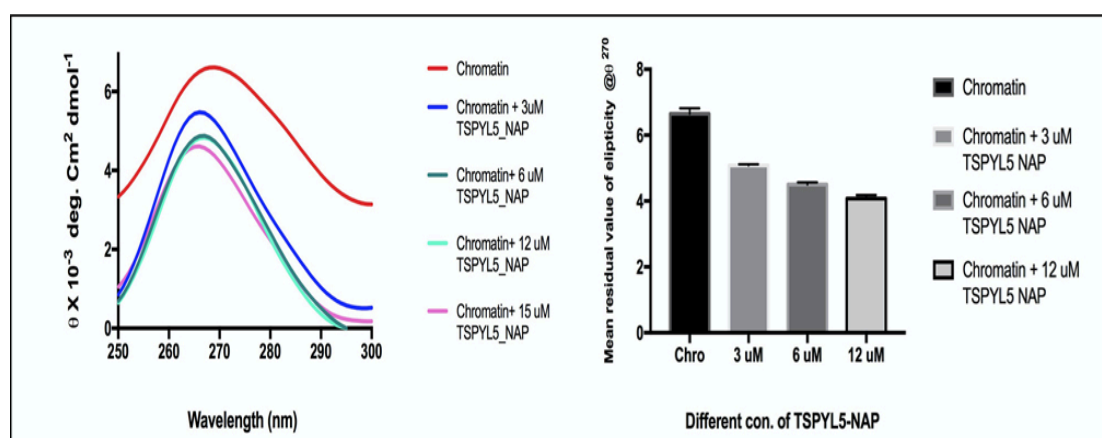
Figure 3.19.1. Far-UV CD spectral analysis *of TSPYL5-NLD treated with Higher Order chromatin. Mean residual ellipticity value (θ) at 270 nM were plotted against TSPYL5 concentration. Each data was taken 3 times and statistical analysis were also used.*

Next we have stripped histone H1 in particular from the isolated chromatin pool and performed the same CD experiments using increasing concentrations of TSPYL5. Surprisingly H1 stripped chromatin doesn't compact as efficiently as WT chromatin (Figure 3.19.2.), which propounds that TSPYL5 may have a crucial role in histone H1 mediated higher order chromatin compaction.
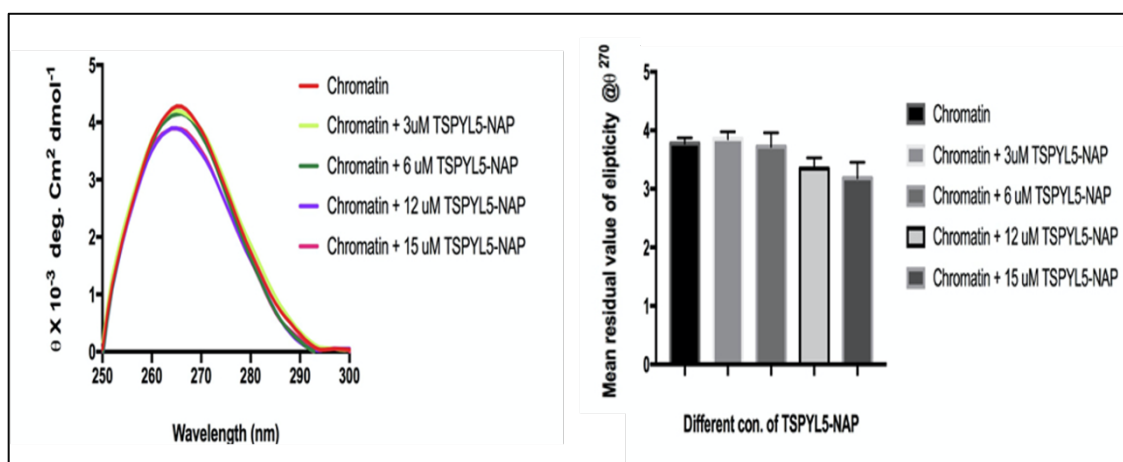
Figure 3.19.2. Far-UV CD spectral analysis *of TSPYL5-NLD treated with Histone H1 stripped chromatin. Each data was taken 3 times and statistical analysis were also used.*

It is known that post-translational modification of histones play a key role in chromatin compaction. Acetylated chromatin tends to open more in nature when compared to methylated chromatin. Thus, to further quantify the role of TSPYL5 in chromatin compaction, we have used histone de-acetylation complex (HDAC) inhibitor in cell culture so that all the HDACs in cells were inhibited and thus the chromatin becomes more de-acetylated in nature. De-acetylated chromatin in general were more open in nature, so TSPYL5 was unable to compact HDAC inhibitor treated chromatin as swiftly as WT HeLa cells (Figure 3.19.3.).
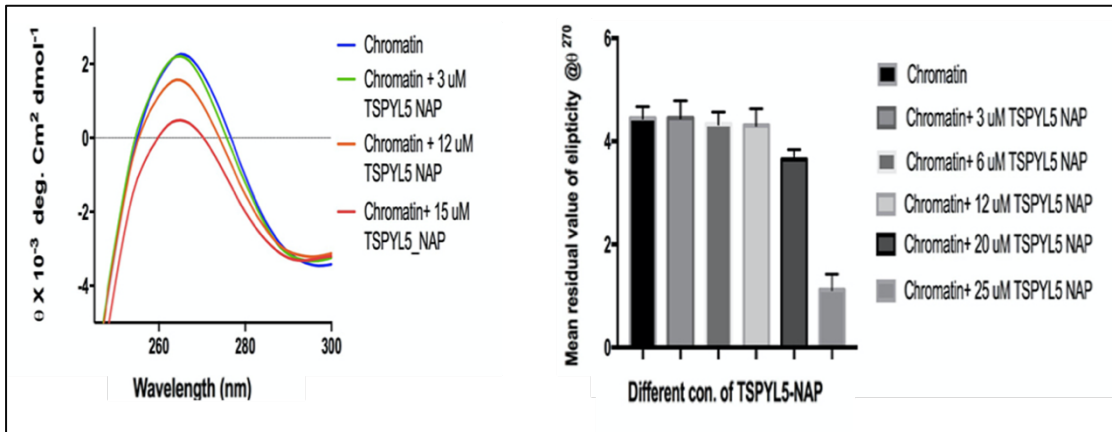
Figure 3.19.3. Far-UV CD spectral analysis *of TSPYL5-NLD treated chromatin isolated from HDAC inhibitor treated cells. Each data was taken 3 times and statistical analysis were also used.*

On the other hand, when chromatin was isolated form histone acetyl transferase (HAT) inhibitor treated HeLa cells and similar CD experiments were performed using increasing concentrations of TSPYL5, it not only depicted significant chromatin compaction but it was even better than that was observe earlier with WT chromatin. This brought us to the conclusion that since HAT inhibitor treated chromatin lacks HATs in cells so chromatin is more compacted in nature. This result suggests that less acetylated
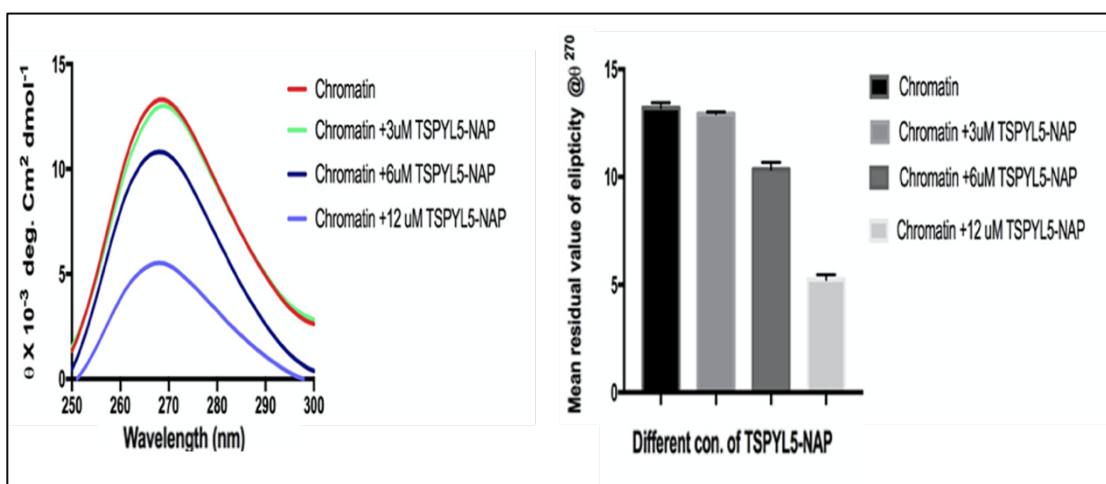
Figure 3.19.4. Far-UV CD spectral analysis *of TSPYL5-NLD treated chromatin isolated from HAT inhibitor treated cells. Each data was taken 3 times and statistical analysis were also used.*

chromatin which is more compacted in nature can assist TSPYL5 in mediating more efficient chromatin compaction (Figure 3.19.4.).

To nullify the role of TSPYL5 in DNA mediated compaction, we next stripped all the histones from chromatin followed by genomic DNA isolation. Isolated genomic DNA was next used to perform TSPYL5 interaction study using similar set of CD experiments. CD spectral results again did hint towards any significant role of TSPYL5 in compacting DNA, which thereby strengthened the observation and the hypothesis regarding the role of TSPYL5 in chromatin compaction in a histone dependent manner.

Discussion

Chapter V: DISCUSSION

4. Discussion

Chromatin assembly and disassembly processes involve nucleosome opening and reformation which works in a sequential manner. In chromatin assembly, two histone H3/H4 dimers is deposited initially forming the tetramer and is then followed by incorporation of histones H2A/H2B. All these processes are accompanied by various histone chaperones that govern and catalyse each step (Smith and Stillman, 1991; Das et al., 2010).

NAP1, a distinct family of histone chaperones found in yeast, contains multiple NAP1 homologues in higher eukaryotes. NAP family histone chaperones are generally described as H2A and H2B specific (Mosammaparast et al., 2001; Mosammaparast et al., 2002; Park and Luger, 2006; Andrews et al., 2010), although a few other *in vitro* studies have reported that H3/H4 tetramers binds yNAP1 (McBryant et al., 2003; Tóth et al., 2005; Andrews et al., 2010; Newman et al., 2012). *In vitro* studies also show that, histone H3/H4 tetramer can be bound by yNAP1 and transferred to a supercoiled plasmid to form a tetrasome where as yNAP1 helps in transfer of H2A-H2B dimer to this tetrasome (Ito et al., 1996; Nakagawa et al., 2001). While yeast Vps75 (having signature NAP like fold) shows preferential binding for histone H3/H4 over H2A/H2B (Selth and Svejstrup, 2007; Bowman et al., 2014; Hammond et al., 2016), SET/TAF-1B also shows specific interaction towards histone H3/H4 (Muto et al., 2007).

SET/TAF-1B (Muto et al., 2007), ClNAP, NAP1-like proteins (NAP1L1–5) (Qiao et al., 2018), Testis-specific protein Y-encoded (TSPY1-10) (Shen et al., 2018) and TSPY-like (1 - 6) are also part of the growing NAP family where all of them show sequence

similarity to NAP1 and their expressions are highly specific depending upon cell types and tissues. Here, we identified and characterized a NAP family histone chaperone in human, TSPYL5, that harbors the signature NAP-like fold. AlphaFold model structure confirm that the C-terminal region of TSPYL5 forms the signature NAP like headphone structure consisting of a globular earmuff domain and a long helical head. Unlike other members of NAP family proteins which have acidic amino acid stretch towards the C-terminal, TSPYL5 have the Acidic stretch towards the N-terminal region between 175 - 200 amino acids.

The genetic polymorphisms, mutations, and DNA hypermethylation status for TSPYL5 gene can alter gene expression, which is often correlated with several human diseases, mostly cancers. TSPYL5 exhibited a high frequency of DNA methylation-mediated silencing in both glioblastoma and gastric cancer (Jung et al., 2008). But the role for TSPYL5 in specific chromatin-related processes is still unclear. Insights from the sequence based phylogenetic analysis and structural architecture of TSPYL5 indicate its potential role in gene regulation via interaction with histone proteins, but no studies have so far been conducted.

To avoid artifacts due to transfection mediated overexpression of TSPYL5, we have checked the expression profile of TSPYL5 across the cell lines and were able to identify and choose cells having high TSPYL5 expression for our study. We have demonstrated the localization of endogenous and overexpressed TSPYL5 in SH-SY5Y and HEK293T cells respectively. Immunofluorescence for endogenous TSPYL5 should have been performed using reliable antibodies, which were not yet available. So, we purified the TSPYL5 protein

in vitro and raised anti-TSPYL5 antibodies and used it for immunofluorescence and cell fractionation experiments. Localization of TSPYL5 in nucleus implicated the role of its gene regulation in chromatin context.

NAP1, which predominantly binds H2A/H2B have been reported to associate with amino terminal tails of histone H3/H4. *In vivo*, only histones H2A/H2B have been outlied in complex with yNAP1 (Ito et al., 1996; Chang et al., 1997; Gavin et al., 2002) whereas *in vitro* yNAP1 binds H3/H4. It is important that a technique exists in the living cells that would help preclude the binding of histones H3 and H4 to yNAP1, but it remains to be an uncovered mystery. One probable reason for this could be the presence of other H3/H4 binding histone chaperones, for example CAF1, MCM2, HIRA, FACT, that may block the sites on (H3-H4)$_2$ that are indispensable for the interaction of NAP1. Biophysical analysis of yNAP1-histones complexes is well characterized (Newman et al., 2012) but only the 3D structure of yNAP1-H2A/H2B complex were solved using cryo-EM (Aguilar-Gurrieri et al., 2016) while the yNAP1-H3/H4 complex structure is yet to be resolved. Interestingly, SET/TAF1B/INHAT, which also consists of dimeric headphones like NAP1 like fold, is reported to interact with the histone H3/H4 (Muto et al., 2007). Relative character of the earmuff domains significantly differed between these NAP proteins which may be the cause for some differences in the structures of these proteins. Structural differences thus can relate to their functions. VPS75, another NAP family protein in yeast demonstrates preferential binding for (H3-H4)$_2$ tetramers over (H2A-H2B) dimers (Selth and Svejstrup, 2007). These reports reveal that NAP family proteins have a diverse role in cells and

currently many experiments are being conducted worldwide to elucidate the histone preferences and function of NAP family proteins.

In our study, using *in vitro* and *ex vivo* immune-pulldown assay, we illustrated that TSPYL5 shows a preferential interaction for H3/H4 over that of H2A/H2B. Immuno-pulldown results depict that TSPYL5 is linked to the H3/H4 specific histone chaperones. Reverse immune-pulldown experiment also signifies that the histone-TSPYL5 interaction is not only direct but also one-to-one specific. Similar reports have been found in studies for NAP1 and SET/TAF1B and VPS75 where histone H3/H4 interaction is profoundly characterized *in vitro*. Subsequently, it was important to characterize the histone interaction surface of TSPYL5.

We first mapped the histone H3/H4 interacting regions of TSPYL5, using different domains of TSPYL5 construct. It was observed that the TSPYL5-NLD, which predominantly consists of NAP like domain and lacks the acidic stretch, specifically interacts with histone H3/H4. TSPYL5-ΔNLD, N-terminal unstructured region of TSPYL5, were unable to show any interaction with histone H3/H4. This result correlates with the SET/TAF1B/INHAT histone binding properties where N-terminal, NAP like fold, is sufficient for the histone H3/H4 binding. The C-terminal acidic stretch of SET/TAF1B/INHAT is only a prerequisite for H2A/H2B specific interaction (Muto et al., 2007). VPS75, also shows that it is not the C-terminal acidic stretch but the NAP-like domain of VPS75 that is essential for histone H3 binding (Tang et al., 2008; Danilenko et al., 2019). This proposes that like other NAP family histone chaperones yNAP1, SET/TAF1B and VPS75, the NAP like fold is sufficient for histone interaction in TSPYL5.

In our succeeding approach to identify the region of H3 participating in the interaction with TSPYL5 we found that H3 C-terminal tail (105 - 136 amino acids) display stout interaction with TSPYL5 on utilizing biotinylated peptide pulldown assay involving different stretches of histone H3 peptides. Biochemical and biophysical analysis also confirmed that TSPYL5-NLD shows significant specificity towards H3 (105 – 136 amino acids) when compared to all other peptides.

Multiple NAP family members have been reported to interact with histones, but their binding surfaces have not been well characterized. It was exciting that our peptide pull-down results explored the specific C-terminal tail region of histone H3 that is involved in the binding of TSPYL5, and it was further confirmed using an immune-pulldown assay involving TSPYL5-NLD and H3 C-terminal tail deletion construct. Immuno-pulldown results unclothe that TSPYL5 interaction is abolished with H3ΔC/H4 but is retained with WT H3/H4. In contrast, yNAP1 was reported to interact *in vitro* with the histone H3 N-terminal tail (McBryant et al., 2003). This recommends that the binding fashions of different NAP family proteins to histones may involve different binding regions of histones and in turn signifies the diverse role of different NAP proteins in varied cellular contexts.

On the other hand, it was unveiled that NAP family proteins utilize the loops, connecting the helices located at the globular NAP-like domain, for its histone binding. The involved loops were always found to be present on the surface of the earmuff domain. So, to characterize the critical amino acid stretches of TSPYL5 responsible for histone association, we use different point mutated constructs of TSPYL5-NLD in the loop region. From the biochemical and biophysical experiments, we have found that amino acids

encompassing the HBM1 and HBM2 region together play a critical role in histone interaction. In the case of yNAP1, similar results were observed when both HBR regions were mutated and thereby exhibited reduced H2A–H2B binding (Aguilar–Gurrieri et al., 2016). We have also investigated the surface charges of that region and it doesn't exhibit acidic properties but is rather mixed with neutral and charged amino acids. We have compared the charged surfaces of different NAP proteins. Histone binding region of TSPYL5 shows significant difference in charge and structure compared to the other NAP proteins. These findings confirm that amino acids in the loop region of HBM 1 and 2 together may create a crucial pocket for histone H3/H4 interaction. So, when HBM 1 and 2 together were mutated, it showed loss of histone interaction.

Previously, experiments have indicated that one dimer of yeast NAP1 associates with one dimer of histone H2A/H2B or of H3/H4 and forms a complex (McBryant et al., 2003; Newman, 2012; Aguilar-Gurrieri, 2016). Initial low-resolution hydrogen deuterium exchange (HDX) experiments recommended that a yNap1 dimer brings together in a tetrameric conformation two copies of H2A/H2B where each NAP1 copy interacts with one H2A/H2B heterodimer (D'Arcy et al., 2013). Instead, the group of Aguilar-Gurrieri reported that only a single H2A/H2B dimer fits inside the binding pocket of one Nap1 dimer (Aguilar-Gurrieri, 2016). Under physiological buffer conditions in an *in vitro* system, higher order complexes also formed between NAP1 and histones (Tóth, 2005; Newman, 2012; Aguilar-Gurrieri, 2016). Six copies of this yNap1–H2A/H2B complex that form the asymmetric unit found in crystallographic spaces group, can also provide explanation on the oligomerization of NAP proteins in presence of interacting histones.

The concave surface of the headphone shaped yNap1 homodimer interacts with H2A/H2B dimer via H2A exclusively (Aguilar-Gurrieri, 2016). However, the histone H3/H4 binding and the complex formation of NAP1-H3/H4 is still not characterized.

NAP forms stoichiometric complexes with histone counterpart at a stoichiometric ratio of one NAP dimer to one histone heterodimer and is estimated to be (NAP2-H2A/H2B)$_4$ and (NAP2-H3/H4)$_4$. In physiological salt conditions, one dimer of NAP associates with one dimer of histones (H2A/H2B or H3/H4), forming complex of higher order assemblies. Higher order assemblies were characterized by both AUC experiments and SEC-MALS study (Tóth et al., 2005; Newman et al., 2012) and they characterized NAP-histone complexes for the first time.

Unlike yNAP1, yeast Vps75 can interact with both H3/H4 dimer or tetramer (Hammond, 2016). The pattern in which H3/H4 dimers bind Vps75 dimers agrees with the tetramerization pattern of histone H3/H4. Thus, Vps75 dimer can act as a platform either to assemble H3/H4 tetramers from two cognate histone H3/H4 dimers or to catch evicted histone H3/H4 tetramers from chromatin during histone disassembly. There is a chance that other NAP family histone chaperones can also tag along with histones H3/H4 like Vps75 and help in histone H3/H4 recycling (Selth and Svejstrup, 2007; Xu et al., 2010; Bowman et al., 2011; Hammond, 2016).

DSS crosslinking results showed that TSPYL5 was able to bind H3/H4 and form stable complexes in-between 100 and 150 kDa molecular markers. Molecular mass of the new species appearing in the DSS crosslinking assay is only possible if the complex formed between them was (TSPYL5-H3/H4)$_2$ in this manner. Our next aim was to elucidate the

molecular stoichiometry of the TSPYL5-H3/H4 complex. We can co-purify TSPYL5 and histone H3/H4 complex using recombinant protein purification process. TSPYL5-H3/H4 complex was then incorporated in SEC-MALS study. We have found that TSPYL5 and histone H3/H4 form co-complexes at a stoichiometric ratio of 2:2:2. The molecular mass can only be achieved if one TSPYL5 dimer interacts with two histone H3/H4 dimer or one histone H3/H4 tetramer. Parental histone H3/H4 recycling during chromatin disassembly is still under consideration. The main question was whether histone H3/H4 recycles as a tetramer or dimer during the DNA replication-independent and replication-dependent chromatin rearrangements (Margueron and Reinberg, 2010; Probst et al., 2009; Annunziato, 2005; Tagami et al., 2004; Song et al., 2007; Groth, 2009; Xu et al., 2010). So, to further confirm TSPYL5-H3/H4 interaction, we performed immuno-pulldown assay involving histone H3/H4 and H3M/H4 with TSPYL5. Immuno-pulldown results further characterized the interaction of TSPYL5 with both histone H3/H4 tetramers or dimer H3M/H4 (histone dimer consists of tetramerization disruptive mutant H3M) and confirms that TSPYL5 didn't differentiate between them. Thus, stable TSPYL5-H3/H4 complex of 128 kDa was formed during crosslinking and confirmed in SEC-MALS, can either consist of two TSPYL5 dimer with one histone H3/H4 tetramer or two TSPYL5 dimer with two histone H3/H4 dimer.

Thus, crosslinking assays, in-solution SEC-MALS and IP results emphasized on the molecular understanding of histone transfer mechanism of TSPYL5 and suggested that TSPYL5 can act as a podium to assemble two H3/H4 dimers to form a tetramer and/or it can even fetch evicted histone H3/H4 tetramer during chromatin disassembly of

replication-independent and replication-dependent processes. These observations were coherent with and strongly supported literature studies of NAP family histone chaperones like yNAP1 and yVPS75 (Bowman et al., 2011, 2014; Hammond et al., 2016).
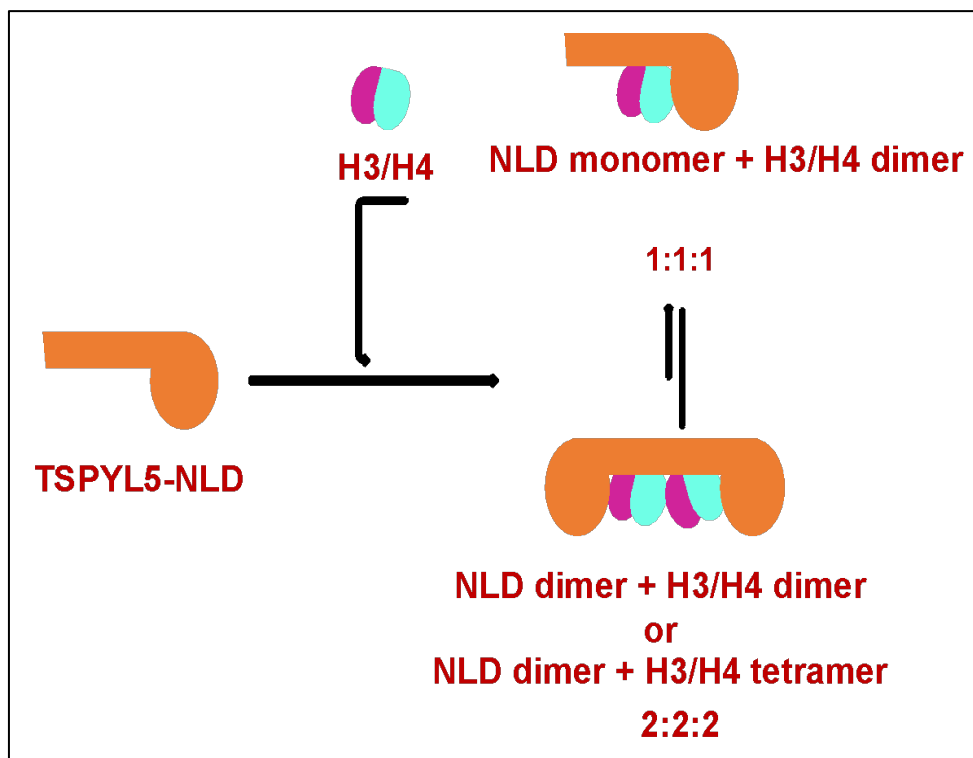
Figure 4.1. Schematic representation of the binding mode for TSPYL5-NLD and HS/H4 complex. *Figure illustrates possibility of binding in either conditions of H3/H4 dimer or H3/H4 tetrameric form.*

Histone chaperones, assist chromatin assembly and disassembly process in each step. Histone chaperones which are directly involved in DNA mediated histone deposition process also exhibit DNA binding property alongside their histone interacting ability. Yeast CAF1, which is involved in nucleosome assembly during replication shows DNA binding property through the coiled coil and WHD regions of the Cac1 sub-unit (Mattiroli et al., 2017; Sauer et al., 2017). Rtt106 and HIRA, which were involved in direct deposition of

different histone H3 variants, binds to DNA directly (Pchelintsev et al., 2013; Ray-Gallet et al., 2011; Liu et al., 2010). Our findings denote that TSPYL5 has similar DNA binding properties with specific affinity towards 80 bp or higher length DNA fragments, but not with its shorter DNA counterparts. It is noteworthy that yCAF1 also shows similar mode of DNA binding (Sauer et al., 2017). This advocates that TSPYL5 may have a direct role in DNA mediated nucleosome assembly processes which can be further characterized.

Our biochemical and biophysical analyses demonstrated that the bottom of the earmuff domain of TSPYL5 interacts with histone H3/H4 and is also important for nucleosome assembly. TSPYL5-H3/H4 complex facilitates nucleosome assembly *in vitro* and confirms the histone chaperone activity of TSPYL5. TSPYL5 mediated histone H3/H4 deposition on DNA shows that it does not protect the entire region of the DNA binding surface of the histone H3/H4. The percentage of accessibility of the strong DNA binding sites of TSPYL5 bound histones H3/H4, provide a means by which TSPYL5 facilitate histone tetramer deposition directly onto DNA. Our EMSA results confirm the availability of the DNA binding sites around the same site of histone binding region of TSPYL5. These results also can explain that TSPYL5 associated histone H3/H4 complexes can facilitate histone deposition where TSPYL5-DNA complexes provide the proper cleft for H3/H4-DNA complex formation. Histone deposition activity of TSPYL5 can endorse the role of TSPYL5 in chromatin context and could possibly remove the chance of it to be a soluble histone chaperone like Nucleoplasmin or NASP.

In several cancers like glioma (Kim et al., 2006), ovarian cancer (Shao et al., 2017), gastric cancer (Jung et al., 2008) and colorectal cancers (Huang et al., 2020) TSPYL5 is

reported to act as a tumour suppressor. In contrast to these reports, TSPYL5 have also been described as an oncogene in lung cancers (Kim et al., 2010) and breast cancer (Lyu et al., 2015, Shen et al., 2018, Epping et al., 2011).

USP7 is an enigmatic factor that also forms a stable complex with maintenance methyltransferases, DNMT1 and E3 ligase, UHRF-1 (Cheng et al., 2015; Zhang et al., 2015). UHRF1 mediated histone H3 Lysine (K) 23 ubiquitination facilitates DNMT1 recruitment to sites of DNA methylation during DNA replication (Nishiyama et al., 2013). Histone H3 ubiquitination influence the dynamic action of DNMT1 in S-phase of cell cycle but interestingly ubiquitination mark on histone H3K23 was removed after the replication (Yamaguchi et al., 2017). USP7 deubiquitinate histone H3K23 and suppresses DNMT1 loading on hemi-methylated DNA and in turn regulates genome wide DNA methylation (Li et al., 2020). In our study we have shown that C-terminal NLD domain of TSPYL5 has histone H3 binding and histone H3/H4 chaperoning activity. Along with its histone chaperone function, TSPYL5 may also act as an anchorage where histone H3 and USP7 docks together in a context dependent manner and influence the USP7 functions that negatively regulates UHRF1 mediated histone H3 ubiquitination.

Both histone chaperone function of TSPYL5 also need to correlate within the light of cancer proliferation and progression. The idea that TSPYL5 directly regulates gene expression due to its histone chaperonin function and thus regulate oncogenesis is itself potentially exciting and gives us licence for further investigation. It is thus important to employ biochemical and genetic high-throughput analysis together to get into an in-depth knowledge and detailed understanding of the function of TSPYL5.

In conclusion, we pronounce documentation of TSPYL5 as a novel member of the NAP histone chaperone family which may assist chromatin assembly using its NAP like domain. This information should offer useful information to resolve the intricacies of the histone recycling process that is associated with all the DNA mediated processes like replication, transcription, and DNA repair.

Summary
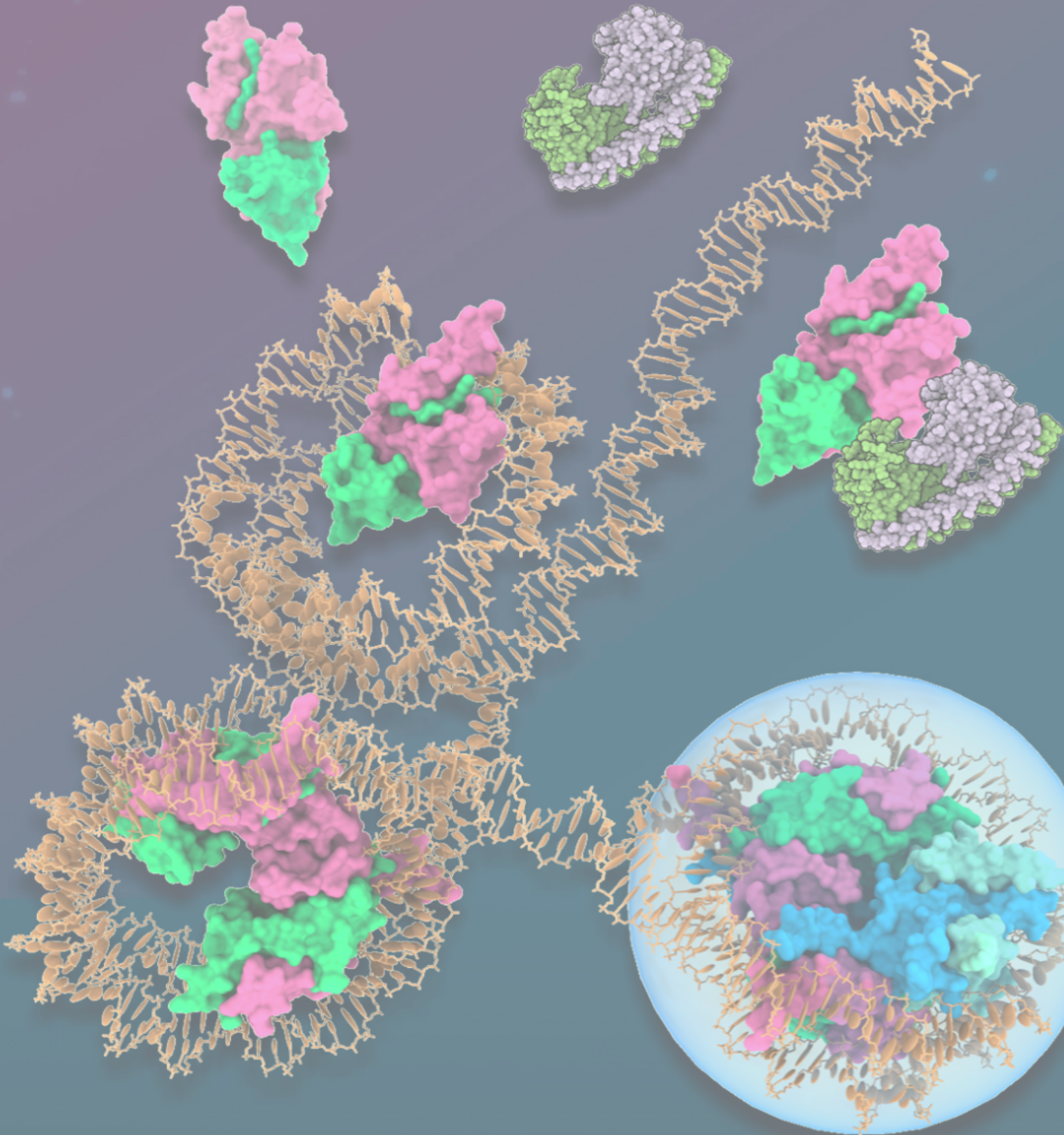
5. Summary

The ladder starts by the initial deposition of tetramer on chromatin free genomic DNA and then two dimers come together and form the nucleosome. Chromatin opens first and again reassembles after different cellular events like DNA replication, transcription, and damage repair processes have taken place. This chromatin assembly and disassembly is governed by different histone chaperones (Smith and Stillman, 1991; Das et al., 2010).

NAP histone chaperone superfamily is a growing group of histone chaperone proteins that shows sequence similarity to NAP1 protein, but their expressions are highly specific, and is mainly dependent upon the cell and/or tissue types. In this report, we have identified and characterized a NAP family member histone chaperone in human, TSPYL5.

TSPYL5 harbors the signature NAP Like fold at the C-terminal region which was revealed by a sequence homology analysis of TSPYL5 with SET/TAF1B and other NAP family proteins. AlphaFold structural analysis reports that, TSPYL5 has a typical NAP like fold at the C-terminal region which bears a α- helical ''head'' and a globular ''earmuff'' segment of the headphone. The globular earmuff domain contains a 4 stranded β-sheet (β1 – β4) with 5 α - helices (α2 - α5) arranged below the α1 helical head. NAP family histone chaperones are in general described as H2A/H2B specific (Mosammaparast et al., 2001; Mosammaparast et al., 2002; Park 2006; Andrews et al., 2010) but few studies also reported that yNAP1 has preferential binding for H3/H4

tetramers *in vitro* (McBryant et al., 2003; Tóth et al., 2005; Andrews et al., 2010; Newman et al., 2012). Specific interaction towards histone H3/H4 were shown by Yeast Vps75 (Selth and Svejstrup, 2007; Bowman et al., 2014; Hammond et al., 2016) and SET/TAF-IB (Muto et al., 2007). Although tumour suppressor function of TSPYL5 were reported in several cancers like glioma (Kim et al., 2006), ovarian cancer (Shao et al., 2017), gastric cancer (Jung et al., 2008) and colorectal cancers (Huang et al, 2020) it has also been reported to act as an oncogene in lung cancers (Kim et al, 2010) and breast cancer (Lyu et al., 2015; Shen et al., 2018; Epping et al., 2011). Thus, TSPYL5 may act as a promising therapeutic target for cancer. In contrast to its role in cancer, TSPYL5, as it harbors NAP domain may also participate in specific chromatin-related processes but it still requires extensive investigation.

In vitro and *ex vivo* immuno pull-down assays revealed that TSPYL5 prefers H3/H4 over H2A/H2B. In our study, using Immuno pulldown, results suggest that TSPYL5 belongs to the H3/H4 family of histone chaperones. Using different domain deletion constructs we mapped the histone H3/H4 interacting regions of TSPYL5 and observed that TSPYL5-NLD (NAP like domain) specifically interacts with histone H3/H4 but TSPYL5-ΔNLD failed to do so. Aiming to find out which part of histone H3 is involved in TSPYL5 interaction, we performed biotinylated peptide pulldown assay using different stretch of histone H3 peptides. We were enlightened from the peptide-IP results that the C-terminal tail region of histone H3 (ranging from 105 - 136 amino acids) is responsible for TSPYL5 interaction. We further created different point mutated constructs of TSPYL5-NLD and used them to characterize the critical amino acid

residues of TSPYL5 that are responsible for histone association. Biochemical and biophysical study revealed that amino acids comprising S268A/E270AS340A/N343A/E345A of TSPYL5 plays a critical role in histone H3/H4 interaction. Previously, experiments have suggested that one dimer of yNAP1 associates with one dimer of histone H2A/H2B or H3/H4 and formed a complex (Newman et al., 2012; Aguilar-Gurrieri et al., 2016). Under physiological buffer conditions *in vitro* system higher order complexes also form between NAP1 and histones (Tóth et al., 2005; Newman et al., 2012; Aguilar-Gurrieri et al., 2016). Vps75 in contrast can interact with both histone H3/H4 dimer or tetramer (Hammond et al., 2016). We co-purified TSPYL5 and histone H3/H4 complex and using DSS crosslinking assay showed that TSPYL5 can bind to histone H3/H4 and form a stable complex. Incorporating the TSPYL5-H3/H4 complex in SEC-MALS study, we have found that TSPYL5 and histone H3/H4 forms complexes at a stoichiometric ratio of 2:2:2, where one TSPYL5 dimer interacts with two histone H3/H4 dimer or one H3/H4 tetramer. Mutating the tetramer forming residues of histone H3-H3', we have also shown that histone H3/H4 in both dimeric and tetrameric conformation were able to interact with TSPYL5. Our biochemical and biophysical analyses demonstrated that the bottom of the earmuff domain of TSPYL5 interacts with histone H3/H4, and it is important for nucleosome assembly *in vitro*. TSPYL5-H3/H4 complex facilitates nucleosome assembly *in vitro* which confirmed the activity of TSPYL5 as a histone chaperone. Histone deposition activity of TSPYL5 validated the role of TSPYL5 in chromatin context. TSPYL5 can act as a docking platform for histone H3/H4 dimer to form tetramer before depositing to DNA, can grab histone H3/H4

tetramer during chromatin assembly/disassembly processes and enable tetramer disposition.

In conclusion, we described TSPYL5 as a novel member of the NAP histone chaperone family that binds specifically to histone H3/H4 and facilitates nucleosome assembly by depositing histone H3/H4 to naked DNA template *in vitro*. Our work may provide useful idea to generate some important information to resolve the enigma of histone re-cycling process that are associated with DNA mediated processes.

Abdiche, Y., Malashock, D., Pinkerton, A., and Pons, J. (2008). Determining kinetics and affinities of protein interactions using a parallel real-time label-free biosensor, the Octet. Anal Biochem *377*, 209–217. https://doi.org/10.1016/j.ab.2008.03.035.

Abshiru, N., Ippersiel, K., Tang, Y., Yuan, H., Marmorstein, R., Verreault, A., and Thibault, P. (2013). Chaperone-mediated acetylation of histones by Rtt109 identified by quantitative proteomics. J Proteomics *81*, 80–90. https://doi.org/10.1016/j.jprot.2012.09.026.

Adkins, M.W., and Tyler, J.K. (2006). Transcriptional activators are dispensable for transcription in the absence of Spt6-mediated chromatin reassembly of promoter regions. Mol Cell *21*, 405–416. https://doi.org/10.1016/j.molcel.2005.12.010.

Adkins, M.W., Carson, J.J., English, C.M., Ramey, C.J., and Tyler, J.K. (2007). The histone chaperone anti-silencing function 1 stimulates the acetylation of newly synthesized histone H3 in S-phase. J Biol Chem *282*, 1334–1340. https://doi.org/10.1074/jbc.M608025200.

Agez, M., Chen, J., Guerois, R., van Heijenoort, C., Thuret, J.-Y., Mann, C., and Ochsenbein, F. (2007). Structure of the histone chaperone ASF1 bound to the histone H3 C-terminal helix and functional insights. Structure *15*, 191–199. https://doi.org/10.1016/j.str.2007.01.002.

Aguilar-Gurrieri, C., Larabi, A., Vinayachandran, V., Patel, N.A., Yen, K., Reja, R., Ebong, I., Schoehn, G., Robinson, C.V., Pugh, B.F., et al. (2016). Structural evidence for Nap1-dependent H2A–H2B deposition and nucleosome assembly. EMBO J *35*, 1465–1482. https://doi.org/10.15252/embj.201694105.

Ai, X., and Parthun, M.R. (2004). The nuclear Hat1p/Hat2p complex: a molecular link between type B histone acetyltransferases and chromatin assembly. Mol Cell *14*, 195–205. https://doi.org/10.1016/s1097-2765(04)00184-4.

Alabert, C., and Groth, A. (2012). Chromatin replication and epigenome maintenance. Nat Rev Mol Cell Biol *13*, 153–167. https://doi.org/10.1038/nrm3288.

Altman, R., and Kellogg, D. (1997). Control of mitotic events by Nap1 and the Gin4 kinase. J Cell Biol *138*, 119–130. https://doi.org/10.1083/jcb.138.1.119.

Andrews, A.J., and Luger, K. (2011). Nucleosome structure(s) and stability: variations on a theme. Annu Rev Biophys *40*, 99–117. https://doi.org/10.1146/annurev-biophys-042910-155329.

Andrews, A.J., Downing, G., Brown, K., Park, Y.-J., and Luger, K. (2008). A thermodynamic model for Nap1-histone interactions. J Biol Chem *283*, 32412–32418. https://doi.org/10.1074/jbc.M805918200.

Andrews, A.J., Chen, X., Zevin, A., Stargell, L.A., and Luger, K. (2010). The histone chaperone Nap1 promotes nucleosome assembly by eliminating non-nucleosomal histone DNA interactions. Mol Cell *37*, 834–842. https://doi.org/10.1016/j.molcel.2010.01.037.

Angelov, D., Bondarenko, V.A., Almagro, S., Menoni, H., Mongélard, F., Hans, F., Mietton, F., Studitsky, V.M., Hamiche, A., Dimitrov, S., et al. (2006). Nucleolin is a histone chaperone with FACT-like activity and assists remodeling of nucleosomes. EMBO J *25*, 1669–1679. https://doi.org/10.1038/sj.emboj.7601046.

Annunziato, A.T. (2005). Split decision: what happens to nucleosomes during DNA replication? J Biol Chem *280*, 12065–12068. https://doi.org/10.1074/jbc.R400039200.

Attia, M., Rachez, C., Avner, P., and Rogner, U.C. (2013). Nucleosome assembly proteins and their interacting proteins in neuronal differentiation. Arch Biochem Biophys *534*, 20–26. https://doi.org/10.1016/j.abb.2012.09.011.

Baer, B.W., and Rhodes, D. (1983). Eukaryotic RNA polymerase II binds to nucleosome cores from transcribed genes. Nature *301*, 482–488. https://doi.org/10.1038/301482a0.

Barman, H.K., Takami, Y., Nishijima, H., Shibahara, K., Sanematsu, F., and Nakayama, T. (2008). Histone acetyltransferase-1 regulates integrity of cytosolic histone H3-H4 containing complex. Biochem Biophys Res Commun *373*, 624–630. https://doi.org/10.1016/j.bbrc.2008.06.100.

Belotserkovskaya, R., Oh, S., Bondarenko, V.A., Orphanides, G., Studitsky, V.M., and Reinberg, D. (2003). FACT facilitates transcription-dependent nucleosome alteration. Science *301*, 1090–1093. https://doi.org/10.1126/science.1085703.

Belotserkovskaya, R., Saunders, A., Lis, J.T., and Reinberg, D. (2004). Transcription through chromatin: understanding a complex FACT. Biochimica et Biophysica Acta (BBA) - Gene Structure and Expression *1677*, 87–99. https://doi.org/10.1016/j.bbaexp.2003.09.017.

Ben-Shahar, T.R., Castillo, A.G., Osborne, M.J., Borden, K.L.B., Kornblatt, J., and Verreault, A. (2009). Two Fundamentally Distinct PCNA Interaction Peptides Contribute to Chromatin Assembly Factor 1 Function. Mol Cell Biol *29*, 6353–6365. https://doi.org/10.1128/MCB.01051-09.

Beresford, P.J., Zhang, D., Oh, D.Y., Fan, Z., Greer, E.L., Russo, M.L., Jaju, M., and Lieberman, J. (2001). Granzyme A activates an endoplasmic reticulum-associated caspase-independent nuclease to induce single-stranded DNA nicks. J Biol Chem *276*, 43285–43293. https://doi.org/10.1074/jbc.M108137200.

Berndsen, C.E., Tsubota, T., Lindner, S.E., Lee, S., Holton, J.M., Kaufman, P.D., Keck, J.L., and Denu, J.M. (2008). Molecular functions of the histone acetyltransferase chaperone complex Rtt109-Vps75. Nat Struct Mol Biol *15*, 948–956. https://doi.org/10.1038/nsmb.1459.

Birch, J.L., Tan, B.C.-M., Panov, K.I., Panova, T.B., Andersen, J.S., Owen-Hughes, T.A., Russell, J., Lee, S.-C., and Zomerdijk, J.C.B.M. (2009). FACT facilitates chromatin transcription by RNA polymerases I and III. EMBO J *28*, 854–865. https://doi.org/10.1038/emboj.2009.33.

Bohidar, H.B. (1989). Light scattering study of solution properties of bovine serum albumin, insulin, and polystyrene under moderate pressure. Colloid & Polymer Sci *267*, 292–300. https://doi.org/10.1007/BF01413622.

Bortvin, A., and Winston, F. (1996). Evidence that Spt6p controls chromatin structure by a direct interaction with histones. Science *272*, 1473–1476. https://doi.org/10.1126/science.272.5267.1473.

Bowman, G.D. (2010). Mechanisms of ATP-Dependent Nucleosome Sliding. Curr Opin Struct Biol *20*, 73–81. https://doi.org/10.1016/j.sbi.2009.12.002.

Bowman, A., Ward, R., Wiechens, N., Singh, V., El-Mkami, H., Norman, D.G., and Owen-Hughes, T. (2011). The Histone Chaperones Nap1 and Vps75 Bind Histones H3 and H4 in a Tetrameric Conformation. Mol Cell *41*, 398–408. https://doi.org/10.1016/j.molcel.2011.01.025.

Bowman, A., Hammond, C.M., Stirling, A., Ward, R., Shang, W., El-Mkami, H., Robinson, D.A., Svergun, D.I., Norman, D.G., and Owen-Hughes, T. (2014). The histone chaperones Vps75 and Nap1 form ring-like, tetrameric structures in solution. Nucleic Acids Res *42*, 6038–6051. https://doi.org/10.1093/nar/gku232.

Brachet, E., Béneut, C., Serrentino, M.-E., and Borde, V. (2015). The CAF-1 and Hir Histone Chaperones Associate with Sites of Meiotic Double-Strand Breaks in Budding Yeast. PLoS One *10*, e0125965. https://doi.org/10.1371/journal.pone.0125965.

Burgess, R.J., and Zhang, Z. (2013). Histone chaperones in nucleosome assembly and human disease. Nat Struct Mol Biol *20*, 14–22. https://doi.org/10.1038/nsmb.2461.

Calvert, M.E.K., Keck, K.M., Ptak, C., Shabanowitz, J., Hunt, D.F., and Pemberton, L.F. (2008). Phosphorylation by casein kinase 2 regulates Nap1 localization and function. Mol Cell Biol *28*, 1313–1325. https://doi.org/10.1128/MCB.01035-07.

Camahort, R., Li, B., Florens, L., Swanson, S.K., Washburn, M.P., and Gerton, J.L. (2007). Scm3 is essential to recruit the histone h3 variant cse4 to centromeres and to maintain a functional kinetochore. Mol Cell *26*, 853–865. https://doi.org/10.1016/j.molcel.2007.05.013.

Campos, E.I., and Reinberg, D. (2009). Histones: annotating chromatin. Annu Rev Genet *43*, 559–599. https://doi.org/10.1146/annurev.genet.032608.103928.

Campos, E.I., Fillingham, J., Li, G., Zheng, H., Voigt, P., Kuo, W.-H.W., Seepany, H., Gao, Z., Day, L.A., Greenblatt, J.F., et al. (2010). The program for processing newly synthesized histones H3.1 and H4. Nat Struct Mol Biol *17*, 1343–1351. https://doi.org/10.1038/nsmb.1911.

Campos, E.I., Smits, A.H., Kang, Y.-H., Landry, S., Escobar, T.M., Nayak, S., Ueberheide, B.M., Durocher, D., Vermeulen, M., Hurwitz, J., et al. (2015). Analysis of the Histone H3.1 Interactome: A Suitable Chaperone for the Right Event. Mol Cell *60*, 697–709. https://doi.org/10.1016/j.molcel.2015.08.005.

Canela, N., Rodriguez-Vilarrupla, A., Estanyol, J.M., Diaz, C., Pujol, M.J., Agell, N., and Bachs, O. (2003). The SET protein regulates G2/M transition by modulating cyclin B-cyclin-dependent kinase 1 activity. J Biol Chem *278*, 1158–1164. https://doi.org/10.1074/jbc.M207497200.

Cervoni, N., Detich, N., Seo, S.-B., Chakravarti, D., and Szyf, M. (2002). The oncoprotein Set/TAF-1beta, an inhibitor of histone acetyltransferase, inhibits active demethylation of DNA, integrating DNA methylation and transcriptional silencing. J Biol Chem *277*, 25026–25031. https://doi.org/10.1074/jbc.M202256200.

Chang, L., Loranger, S.S., Mizzen, C., Ernst, S.G., Allis, C.D., and Annunziato, A.T. (1997). Histones in transit: cytosolic histone complexes and diacetylation of H4 during nucleosome assembly in human cells. Biochemistry *36*, 469–480. https://doi.org/10.1021/bi962069i.

Chen, C.-C., Carson, J.J., Feser, J., Tamburini, B., Zabaronick, S., Linger, J., and Tyler, J.K. (2008). Acetylated lysine 56 on histone H3 drives chromatin assembly after repair and signals for the completion of repair. Cell *134*, 231–243. https://doi.org/10.1016/j.cell.2008.06.035.

Cheng, J., Yang, H., Fang, J., Ma, L., Gong, R., Wang, P., Li, Z., and Xu, Y. (2015). Molecular mechanism for USP7-mediated DNMT1 stabilization by acetylation. Nat Commun *6*, 7023. https://doi.org/10.1038/ncomms8023.

Cimino-Reale, G., Gandellini, P., Santambrogio, F., Recagni, M., Zaffaroni, N., and Folini, M. (2017). miR-380-5p-mediated repression of TEP1 and TSPYL5 interferes with telomerase activity and favours the emergence of an "ALT-like" phenotype in diffuse malignant peritoneal mesothelioma cells. J Hematol Oncol *10*, 140. https://doi.org/10.1186/s13045-017-0510-3.

Clément, C., and Almouzni, G. (2015). MCM2 binding to histones H3-H4 and ASF1 supports a tetramer-to-dimer model for histone inheritance at the replication fork. Nat Struct Mol Biol *22*, 587–589. https://doi.org/10.1038/nsmb.3067.

Compagnone, N.A., Zhang, P., Vigne, J.L., and Mellon, S.H. (2000). Novel role for the nuclear phosphoprotein SET in transcriptional activation of P450c17 and initiation of neurosteroidogenesis. Mol Endocrinol *14*, 875–888. https://doi.org/10.1210/mend.14.6.0469.

Cook, A.J.L., Gurard-Levin, Z.A., Vassias, I., and Almouzni, G. (2011). A specific function for the histone chaperone NASP to fine-tune a reservoir of soluble H3-H4 in the histone supply chain. Mol Cell *44*, 918–927. https://doi.org/10.1016/j.molcel.2011.11.021.

Daganzo, S.M., Erzberger, J.P., Lam, W.M., Skordalakes, E., Zhang, R., Franco, A.A., Brill, S.J., Adams, P.D., Berger, J.M., and Kaufman, P.D. (2003). Structure and function of the conserved core of histone deposition protein Asf1. Curr Biol *13*, 2148–2158. https://doi.org/10.1016/j.cub.2003.11.027.

Daniel Ricketts, M., Frederick, B., Hoff, H., Tang, Y., Schultz, D.C., Singh Rai, T., Grazia Vizioli, M., Adams, P.D., and Marmorstein, R. (2015). Ubinuclein-1 confers histone H3.3-specific-binding by the HIRA histone chaperone complex. Nat Commun *6*, 7711. https://doi.org/10.1038/ncomms8711.

Danilenko, N., Lercher, L., Kirkpatrick, J., Gabel, F., Codutti, L., and Carlomagno, T. (2019). Histone chaperone exploits intrinsic disorder to switch acetylation specificity. Nat Commun *10*, 3435. https://doi.org/10.1038/s41467-019-11410-7.

D'Arcy, S., Martin, K.W., Panchenko, T., Chen, X., Bergeron, S., Stargell, L.A., Black, B.E., and Luger, K. (2013). Chaperone Nap1 shields histone surfaces used in a nucleosome and can put H2A-H2B in an unconventional tetrameric form. Mol Cell *51*, 10.1016/j.molcel.2013.07.015. https://doi.org/10.1016/j.molcel.2013.07.015.

Das, C., Hizume, K., Batta, K., Kumar, B.R.P., Gadad, S.S., Ganguly, S., Lorain, S., Verreault, A., Sadhale, P.P., Takeyasu, K., et al. (2006). Transcriptional coactivator PC4, a chromatin-associated protein, induces chromatin condensation. Mol Cell Biol *26*, 8303–8315. https://doi.org/10.1128/MCB.00887-06.

Das, C., Tyler, J.K., and Churchill, M.E.A. (2010). The histone shuffle: histone chaperones in an energetic dance. Trends Biochem Sci *35*, 476–489. https://doi.org/10.1016/j.tibs.2010.04.001.

Dong, A., Zhu, Y., Yu, Y., Cao, K., Sun, C., and Shen, W.-H. (2003). Regulation of biosynthesis and intracellular localization of rice and tobacco homologues of nucleosome assembly protein 1. Planta *216*, 561–570. https://doi.org/10.1007/s00425-002-0910-6.

Dong, A., Liu, Z., Zhu, Y., Yu, F., Li, Z., Cao, K., and Shen, W.-H. (2005). Interacting Proteins and Differences in Nuclear Transport Reveal Specific Functions for the NAP1 Family Proteins in Plants. Plant Physiol *138*, 1446–1456. https://doi.org/10.1104/pp.105.060509.

Drané, P., Ouararhni, K., Depaux, A., Shuaib, M., and Hamiche, A. (2010). The death-associated protein DAXX is a novel histone chaperone involved in the replication-independent deposition of H3.3. Genes Dev *24*, 1253–1265. https://doi.org/10.1101/gad.566910.

Duc, C., Benoit, M., Le Goff, S., Simon, L., Poulet, A., Cotterell, S., Tatout, C., and Probst, A.V. (2015). The histone chaperone complex HIR maintains nucleosome occupancy and counterbalances impaired histone deposition in CAF-1 complex mutants. Plant J *81*, 707–722. https://doi.org/10.1111/tpj.12758.

Dunleavy, E.M., Roche, D., Tagami, H., Lacoste, N., Ray-Gallet, D., Nakamura, Y., Daigo, Y., Nakatani, Y., and Almouzni-Pettinotti, G. (2009). HJURP is a cell-cycle-dependent maintenance and deposition factor of CENP-A at centromeres. Cell *137*, 485–497. https://doi.org/10.1016/j.cell.2009.02.040.

Dyer, P.N., Edayathumangalam, R.S., White, C.L., Bao, Y., Chakravarthy, S., Muthurajan, U.M., and Luger, K. (2004). Reconstitution of nucleosome core particles from recombinant histones and DNA. Methods Enzymol *375*, 23–44. https://doi.org/10.1016/s0076-6879(03)75002-2.

Dyer, J.O., Dutta, A., Gogol, M., Weake, V.M., Dialynas, G., Wu, X., Seidel, C., Zhang, Y., Florens, L., Washburn, M.P., et al. (2017). Myeloid Leukemia Factor Acts in a

Chaperone Complex to Regulate Transcription Factor Stability and Gene Expression. J Mol Biol *429*, 2093–2107. https://doi.org/10.1016/j.jmb.2016.10.026.

Eitoku, M., Sato, L., Senda, T., and Horikoshi, M. (2008). Histone chaperones: 30 years from isolation to elucidation of the mechanisms of nucleosome assembly and disassembly. Cell Mol Life Sci *65*, 414–444. https://doi.org/10.1007/s00018-007-7305-6.

Elsässer, S.J., and D'Arcy, S. (2012). Towards a mechanism for histone chaperones. Biochimica et Biophysica Acta (BBA) - Gene Regulatory Mechanisms *1819*, 211–221. https://doi.org/10.1016/j.bbagrm.2011.07.007.

Elsässer, S.J., Huang, H., Lewis, P.W., Chin, J.W., Allis, C.D., and Patel, D.J. (2012). DAXX envelops a histone H3.3-H4 dimer for H3.3-specific recognition. Nature *491*, 560–565. https://doi.org/10.1038/nature11608.

English, C.M., Maluf, N.K., Tripet, B., Churchill, M.E.A., and Tyler, J.K. (2005). ASF1 binds to a heterodimer of histones H3 and H4: a two-step mechanism for the assembly of the H3-H4 heterotetramer on DNA. Biochemistry *44*, 13673–13682. https://doi.org/10.1021/bi051333h.

English, C.M., Adkins, M.W., Carson, J.J., Churchill, M.E.A., and Tyler, J.K. (2006). Structural Basis for the Histone Chaperone Activity of Asf1. Cell *127*, 495–508. https://doi.org/10.1016/j.cell.2006.08.047.

Episkopou, H., Diman, A., Claude, E., Viceconte, N., and Decottignies, A. (2019). TSPYL5 Depletion Induces Specific Death of ALT Cells through USP7-Dependent Proteasomal Degradation of POT1. Mol Cell *75*, 469-482.e6. https://doi.org/10.1016/j.molcel.2019.05.027.

Epping, M.T., Meijer, L.A.T., Krijgsman, O., Bos, J.L., Pandolfi, P.P., and Bernards, R. (2011). TSPYL5 suppresses p53 levels and function by physical interaction with USP7. Nat Cell Biol *13*, 102–108. https://doi.org/10.1038/ncb2142.

Epping, J., van Deenen, N., Niephaus, E., Stolze, A., Fricke, J., Huber, C., Eisenreich, W., Twyman, R.M., Prüfer, D., and Schulze Gronover, C. (2015). A rubber transferase activator is necessary for natural rubber biosynthesis in dandelion. Nature Plants *1*, 1–9. https://doi.org/10.1038/nplants.2015.48.

Epping, M., Kampermann, H., macchiavello, C., and Bruß, D. (2017). Multi-partite entanglement can speed up quantum key distribution in networks. New J. Phys. *19*, 093012. https://doi.org/10.1088/1367-2630/aa8487.

Estanyol, J.M., Jaumot, M., Casanovas, O., Rodriguez-Vilarrupla, A., Agell, N., and Bachs, O. (1999). The Protein SET Regulates the Inhibitory Effect of p21Cip1 on Cyclin E-Cyclin-dependent Kinase 2 Activity*. Journal of Biological Chemistry *274*, 33161–33165. https://doi.org/10.1074/jbc.274.46.33161.

Fan, Z., Beresford, P.J., Oh, D.Y., Zhang, D., and Lieberman, J. (2003). Tumor suppressor NM23-H1 is a granzyme A-activated DNase during CTL-mediated apoptosis, and the nucleosome assembly protein SET is its inhibitor. Cell *112*, 659–672. https://doi.org/10.1016/s0092-8674(03)00150-8.

Felsenfeld, G., and Groudine, M. (2003). Controlling the double helix. Nature *421*, 448–453. https://doi.org/10.1038/nature01411.

Fillingham, J., Recht, J., Silva, A.C., Suter, B., Emili, A., Stagljar, I., Krogan, N.J., Allis, C.D., Keogh, M.-C., and Greenblatt, J.F. (2008). Chaperone Control of the Activity and Specificity of the Histone H3 Acetyltransferase Rtt109. Mol Cell Biol *28*, 4342–4353. https://doi.org/10.1128/MCB.00182-08.

Fillingham, J., Kainth, P., Lambert, J.-P., van Bakel, H., Tsui, K., Peña-Castillo, L., Nislow, C., Figeys, D., Hughes, T.R., Greenblatt, J., et al. (2009). Two-color cell array screen reveals interdependent roles for histone chaperones and a chromatin boundary regulator in histone gene repression. Mol Cell *35*, 340–351. https://doi.org/10.1016/j.molcel.2009.06.023.

Finch, J.T., and Klug, A. (1976). Solenoidal model for superstructure in chromatin. Proc Natl Acad Sci U S A *73*, 1897–1901. https://doi.org/10.1073/pnas.73.6.1897.

Foltz, D.R., Jansen, L.E.T., Black, B.E., Bailey, A.O., Yates, J.R., and Cleveland, D.W. (2006). The human CENP-A centromeric nucleosome-associated complex. Nat Cell Biol *8*, 458–469. https://doi.org/10.1038/ncb1397.

Foltz, D.R., Jansen, L.E.T., Bailey, A.O., Yates, J.R., Bassett, E.A., Wood, S., Black, B.E., and Cleveland, D.W. (2009). Centromere-Specific Assembly of CENP-A Nucleosomes Is Mediated by HJURP. Cell *137*, 472–484. https://doi.org/10.1016/j.cell.2009.02.039.

Formosa, T. (2012). The role of FACT in making and breaking nucleosomes. Biochim Biophys Acta *1819*, 247–255. https://doi.org/10.1016/j.bbagrm.2011.07.009.

Fujii-Nakata, T., Ishimi, Y., Okuda, A., and Kikuchi, A. (1992). Functional analysis of nucleosome assembly protein, NAP-1. The negatively charged COOH-terminal region is not necessary for the intrinsic assembly activity. J Biol Chem *267*, 20980–20986. .

Galichet, A., and Gruissem, W. (2006). Developmentally controlled farnesylation modulates AtNAP1;1 function in cell proliferation and cell expansion during Arabidopsis leaf development. Plant Physiol *142*, 1412–1426. https://doi.org/10.1104/pp.106.088344.

Gambus, A., Jones, R.C., Sanchez-Diaz, A., Kanemaki, M., van Deursen, F., Edmondson, R.D., and Labib, K. (2006). GINS maintains association of Cdc45 with MCM in replisome progression complexes at eukaryotic DNA replication forks. Nat Cell Biol *8*, 358–366. https://doi.org/10.1038/ncb1382.

Gavin, A.-C., Bösche, M., Krause, R., Grandi, P., Marzioch, M., Bauer, A., Schultz, J., Rick, J.M., Michon, A.-M., Cruciat, C.-M., et al. (2002). Functional organization of the yeast proteome by systematic analysis of protein complexes. Nature *415*, 141–147. https://doi.org/10.1038/415141a.

Giachini, C., Nuti, F., Turner, D.J., Laface, I., Xue, Y., Daguin, F., Forti, G., Tyler-Smith, C., and Krausz, C. (2009). TSPY1 copy number variation influences spermatogenesis and shows differences among Y lineages. J Clin Endocrinol Metab *94*, 4016–4022. https://doi.org/10.1210/jc.2009-1029.

Gill, J., Yogavel, M., Kumar, A., Belrhali, H., Jain, S.K., Rug, M., Brown, M., Maier, A.G., and Sharma, A. (2009). Crystal Structure of Malaria Parasite Nucleosome Assembly Protein. Journal of Biological Chemistry *284*, 10076–10087. https://doi.org/10.1074/jbc.M808633200.

Glowczewski, L., Waterborg, J.H., and Berman, J.G. (2004). Yeast Chromatin Assembly Complex 1 Protein Excludes Nonacetylatable Forms of Histone H4 from Chromatin and the Nucleus. Mol Cell Biol *24*, 10180–10192. https://doi.org/10.1128/MCB.24.23.10180-10192.2004.

Goldberg, A.D., Banaszynski, L.A., Noh, K.-M., Lewis, P.W., Elsaesser, S.J., Stadler, S., Dewell, S., Law, M., Guo, X., Li, X., et al. (2010). Distinct factors control histone variant H3.3 localization at specific genomic regions. Cell *140*, 678–691. https://doi.org/10.1016/j.cell.2010.01.003.

Green, E.M., Antczak, A.J., Bailey, A.O., Franco, A.A., Wu, K.J., Yates, J.R., and Kaufman, P.D. (2005). Replication-independent histone deposition by the HIR complex and Asf1. Curr Biol *15*, 2044–2049. https://doi.org/10.1016/j.cub.2005.10.053.

Groth, A. (2009). Replicating chromatin: a tale of histones. Biochem Cell Biol *87*, 51–63. https://doi.org/10.1139/O08-102.

Groth, A., Ray-Gallet, D., Quivy, J.-P., Lukas, J., Bartek, J., and Almouzni, G. (2005). Human Asf1 regulates the flow of S phase histones during replicational stress. Mol Cell *17*, 301–311. https://doi.org/10.1016/j.molcel.2004.12.018.

Groth, A., Corpet, A., Cook, A.J.L., Roche, D., Bartek, J., Lukas, J., and Almouzni, G. (2007a). Regulation of replication fork progression through histone supply and demand. Science *318*, 1928–1931. https://doi.org/10.1126/science.1148992.

Groth, A., Rocha, W., Verreault, A., and Almouzni, G. (2007b). Chromatin challenges during DNA replication and repair. Cell *128*, 721–733. https://doi.org/10.1016/j.cell.2007.01.030.

Gruss, C., and Sogo, Josém. (1992). Chromatin replication. BioEssays *14*, 1–8. https://doi.org/10.1002/bies.950140102.

Haigney, A., Ricketts, M.D., and Marmorstein, R. (2015). Dissecting the Molecular Roles of Histone Chaperones in Histone Acetylation by Type B Histone Acetyltransferases (HAT-B). J Biol Chem *290*, 30648–30657. https://doi.org/10.1074/jbc.M115.688523.

Hammond, C.M., Sundaramoorthy, R., Larance, M., Lamond, A., Stevens, M.A., El-Mkami, H., Norman, D.G., and Owen-Hughes, T. (2016). The histone chaperone Vps75 forms multiple oligomeric assemblies capable of mediating exchange between histone H3-H4 tetramers and Asf1-H3-H4 complexes. Nucleic Acids Res *44*, 6157–6172. https://doi.org/10.1093/nar/gkw209.

Hammond, C.M., Strømme, C.B., Huang, H., Patel, D.J., and Groth, A. (2017). Histone chaperone networks shaping chromatin function. Nat Rev Mol Cell Biol *18*, 141–158. https://doi.org/10.1038/nrm.2016.159.

Hammond, C.M., Bao, H., Hendriks, I.A., Carraro, M., García-Nieto, A., Liu, Y., Reverón-Gómez, N., Spanos, C., Chen, L., Rappsilber, J., et al. (2021). DNAJC9 integrates heat shock molecular chaperones into the histone chaperone network. Mol Cell *81*, 2533-2548.e9. https://doi.org/10.1016/j.molcel.2021.03.041.

Harata, M., Oma, Y., Mizuno, S., Jiang, Y.W., Stillman, D.J., and Wintersberger, U. (1999). The Nuclear Actin-related Protein of Saccharomyces cerevisiae, Act3p/Arp4, Interacts with Core Histones. Mol Biol Cell *10*, 2595–2605. .

Henikoff, S., and Smith, M.M. (2015). Histone variants and epigenetics. Cold Spring Harb Perspect Biol *7*, a019364. https://doi.org/10.1101/cshperspect.a019364.

Hevner, R.F., Shi, L., Justice, N., Hsueh, Y., Sheng, M., Smiga, S., Bulfone, A., Goffinet, A.M., Campagnoni, A.T., and Rubenstein, J.L. (2001). Tbr1 regulates differentiation of the preplate and layer 6. Neuron *29*, 353–366. https://doi.org/10.1016/s0896-6273(01)00211-2.

Hoek, M., and Stillman, B. (2003). Chromatin assembly factor 1 is essential and couples chromatin assembly to DNA replication in vivo. Proc Natl Acad Sci U S A *100*, 12183–12188. https://doi.org/10.1073/pnas.1635158100.

Holowaty, M.N., Zeghouf, M., Wu, H., Tellam, J., Athanasopoulos, V., Greenblatt, J., and Frappier, L. (2003). Protein profiling with Epstein-Barr nuclear antigen-1 reveals an interaction with the herpesvirus-associated ubiquitin-specific protease HAUSP/USP7. J Biol Chem *278*, 29987–29994. https://doi.org/10.1074/jbc.M303977200.

Hondele, M., and Ladurner, A.G. (2011). The chaperone-histone partnership: for the greater good of histone traffic and chromatin plasticity. Curr Opin Struct Biol *21*, 698–708. https://doi.org/10.1016/j.sbi.2011.10.003.

Hu, M., Li, P., Li, M., Li, W., Yao, T., Wu, J.-W., Gu, W., Cohen, R.E., and Shi, Y. (2002). Crystal Structure of a UBP-Family Deubiquitinating Enzyme in Isolation and in Complex with Ubiquitin Aldehyde. Cell *111*, 1041–1054. https://doi.org/10.1016/S0092-8674(02)01199-6.

Hu, H., Liu, Y., Wang, M., Fang, J., Huang, H., Yang, N., Li, Y., Wang, J., Yao, X., Shi, Y., et al. (2011). Structure of a CENP-A-histone H4 heterodimer in complex with chaperone HJURP. Genes Dev *25*, 901–906. https://doi.org/10.1101/gad.2045111.

Huang, S., Zhou, H., Katzmann, D., Hochstrasser, M., Atanasova, E., and Zhang, Z. (2005). Rtt106p is a histone chaperone involved in heterochromatin-mediated silencing. Proc Natl Acad Sci U S A *102*, 13410–13415. https://doi.org/10.1073/pnas.0506176102.

Huang, H., Strømme, C.B., Saredi, G., Hödl, M., Strandsby, A., González-Aguilera, C., Chen, S., Groth, A., and Patel, D.J. (2015). A unique binding mode enables MCM2 to chaperone histones H3-H4 at replication forks. Nat Struct Mol Biol *22*, 618–626. https://doi.org/10.1038/nsmb.3055.

Huang, C., He, C., Ruan, P., and Zhou, R. (2020). TSPYL5 activates endoplasmic reticulum stress to inhibit cell proliferation, migration and invasion in colorectal cancer. Oncol Rep *44*, 449–456. https://doi.org/10.3892/or.2020.7639.

Iglesias, J., Trigueros, M., Rojas-Triana, M., Fernández, M., Albar, J.P., Bustos, R., Paz-Ares, J., and Rubio, V. (2013). Proteomics identifies ubiquitin-proteasome targets and new roles for chromatin-remodeling in the Arabidopsis response to phosphate starvation. J Proteomics *94*, 1–22. https://doi.org/10.1016/j.jprot.2013.08.015.

Ishimi, Y., and Kikuchi, A. (1991). Identification and molecular cloning of yeast homolog of nucleosome assembly protein I which facilitates nucleosome assembly in vitro. J Biol Chem *266*, 7025–7029. .

Ishimi, Y., Kojima, M., Yamada, M., and Hanaoka, F. (1987). Binding mode of nucleosome-assembly protein (AP-I) and histones. Eur J Biochem *162*, 19–24. https://doi.org/10.1111/j.1432-1033.1987.tb10535.x.

Ito, T., Bulger, M., Kobayashi, R., and Kadonaga, J.T. (1996). Drosophila NAP-1 is a core histone chaperone that functions in ATP-facilitated assembly of regularly spaced nucleosomal arrays. Mol Cell Biol *16*, 3112–3124. https://doi.org/10.1128/MCB.16.6.3112.

Ito, T., Bulger, M., Pazin, M.J., Kobayashi, R., and Kadonaga, J.T. (1997). ACF, an ISWI-containing and ATP-utilizing chromatin assembly and remodeling factor. Cell *90*, 145–155. https://doi.org/10.1016/s0092-8674(00)80321-9.

Iwase, S., Xiang, B., Ghosh, S., Ren, T., Lewis, P.W., Cochrane, J.C., Allis, C.D., Picketts, D.J., Patel, D.J., Li, H., et al. (2011). ATRX ADD domain links an atypical histone methylation recognition mechanism to human mental-retardation syndrome. Nat Struct Mol Biol *18*, 769–776. https://doi.org/10.1038/nsmb.2062.

Jamai, A., Imoberdorf, R.M., and Strubin, M. (2007). Continuous histone H2B and transcription-dependent histone H3 exchange in yeast cells outside of replication. Mol Cell *25*, 345–355. https://doi.org/10.1016/j.molcel.2007.01.019.

Jansen, L.E.T., Black, B.E., Foltz, D.R., and Cleveland, D.W. (2007). Propagation of centromeric chromatin requires exit from mitosis. J Cell Biol *176*, 795–805. https://doi.org/10.1083/jcb.200701066.

Jasencakova, Z., Scharf, A.N.D., Ask, K., Corpet, A., Imhof, A., Almouzni, G., and Groth, A. (2010). Replication stress interferes with histone recycling and predeposition marking of new histones. Mol Cell *37*, 736–743. https://doi.org/10.1016/j.molcel.2010.01.033.

Jung, Y., Park, J., Bang, Y.-J., and Kim, T.-Y. (2008). Gene silencing of TSPYL5 mediated by aberrant promoter methylation in gastric cancers. Lab Invest *88*, 153–160. https://doi.org/10.1038/labinvest.3700706.

Kalderon, D., Roberts, B.L., Richardson, W.D., and Smith, A.E. (1984). A short amino acid sequence able to specify nuclear location. Cell *39*, 499–509. https://doi.org/10.1016/0092-8674(84)90457-4.

Kaplan, T., Liu, C.L., Erkmann, J.A., Holik, J., Grunstein, M., Kaufman, P.D., Friedman, N., and Rando, O.J. (2008). Cell Cycle– and Chaperone-Mediated Regulation of H3K56ac Incorporation in Yeast. PLoS Genet *4*, e1000270. https://doi.org/10.1371/journal.pgen.1000270.

Kawase, H., Okuwaki, M., Miyaji, M., Ohba, R., Handa, H., Ishimi, Y., Fujii-Nakata, T., Kikuchi, A., and Nagata, K. (1996). NAP-I is a functional homologue of TAF-I that is required for replication and transcription of the adenovirus genome in a chromatin-like structure. Genes Cells *1*, 1045–1056. https://doi.org/10.1046/j.1365-2443.1996.d01-223.x.

Kaya, H., Shibahara, K.I., Taoka, K.I., Iwabuchi, M., Stillman, B., and Araki, T. (2001). FASCIATA genes for chromatin assembly factor-1 in arabidopsis maintain the cellular organization of apical meristems. Cell *104*, 131–142. https://doi.org/10.1016/s0092-8674(01)00197-0.

Keck, K.M., and Pemberton, L.F. (2013). Histone chaperones link histone nuclear import and chromatin assembly. Biochim Biophys Acta *1819*, 277–289. .

Kellogg, D.R., and Murray, A.W. (1995). NAP1 acts with Clb1 to perform mitotic functions and to suppress polar bud growth in budding yeast. J Cell Biol *130*, 675–685. https://doi.org/10.1083/jcb.130.3.675.

Kellogg, D.R., Kikuchi, A., Fujii-Nakata, T., Turck, C.W., and Murray, A.W. (1995). Members of the NAP/SET family of proteins interact specifically with B-type cyclins. J Cell Biol *130*, 661–673. https://doi.org/10.1083/jcb.130.3.661.

Kepert, J.F., Mazurkiewicz, J., Heuvelman, G.L., Tóth, K.F., and Rippe, K. (2005). NAP1 Modulates Binding of Linker Histone H1 to Chromatin and Induces an Extended Chromatin Fiber Conformation. Journal of Biological Chemistry *280*, 34063–34072. https://doi.org/10.1074/jbc.M507322200.

Kim, T.-Y., Zhong, S., Fields, C.R., Kim, J.H., and Robertson, K.D. (2006a). Epigenomic profiling reveals novel and frequent targets of aberrant DNA methylation-mediated

silencing in malignant glioma. Cancer Res *66*, 7490–7501. https://doi.org/10.1158/0008-5472.CAN-05-4552.

Kim, T.-Y., Zhong, S., Fields, C.R., Kim, J.H., and Robertson, K.D. (2006b). Epigenomic profiling reveals novel and frequent targets of aberrant DNA methylation-mediated silencing in malignant glioma. Cancer Res *66*, 7490–7501. https://doi.org/10.1158/0008-5472.CAN-05-4552.

Kim, E.J., Lee, S.Y., Kim, T.R., Choi, S.I., Cho, E.W., Kim, K.C., and Kim, I.G. (2010). TSPYL5 is involved in cell growth and the resistance to radiation in A549 cells via the regulation of p21(WAF1/Cip1) and PTEN/AKT pathway. Biochem Biophys Res Commun *392*, 448–453. https://doi.org/10.1016/j.bbrc.2010.01.045.

Kleinschmidt, J.A., and Franke, W.W. (1982). Soluble acidic complexes containing histones H3 and H4 in nuclei of Xenopus laevis oocytes. Cell *29*, 799–809. https://doi.org/10.1016/0092-8674(82)90442-1.

Kleinschmidt, J.A., Fortkamp, E., Krohne, G., Zentgraf, H., and Franke, W.W. (1985). Co-existence of two different types of soluble histone complexes in nuclei of Xenopus laevis oocytes. J Biol Chem *260*, 1166–1176. .

Kobor, Michael.S., Venkatasubrahmanyam, S., Meneghini, M.D., Gin, J.W., Jennings, J.L., Link, A.J., Madhani, H.D., and Rine, J. (2004). A Protein Complex Containing the Conserved Swi2/Snf2-Related ATPase Swr1p Deposits Histone Variant H2A.Z into Euchromatin. PLoS Biol *2*, e131. https://doi.org/10.1371/journal.pbio.0020131.

Koopmans, W.J.A., Brehm, A., Logie, C., Schmidt, T., and van Noort, J. (2007). Single-pair FRET microscopy reveals mononucleosome dynamics. J Fluoresc *17*, 785–795. https://doi.org/10.1007/s10895-007-0218-9.

Krick, R., Jakubiczka, S., and Arnemann, J. (2003). Expression, alternative splicing and haplotype analysis of transcribed testis specific protein (TSPY) genes. Gene *302*, 11–19. https://doi.org/10.1016/s0378-1119(02)01104-6.

Kulaeva, O.I., Gaykalova, D.A., Pestov, N.A., Golovastov, V.V., Vassylyev, D.G., Artsimovitch, I., and Studitsky, V.M. (2009). Mechanism of chromatin remodeling and recovery during passage of RNA polymerase II. Nat Struct Mol Biol *16*, 1272–1278. https://doi.org/10.1038/nsmb.1689.

Laemmli, U.K. (1970). Cleavage of Structural Proteins during the Assembly of the Head of Bacteriophage T4. Nature *227*, 680–685. https://doi.org/10.1038/227680a0.

Lando, D., Endesfelder, U., Berger, H., Subramanian, L., Dunne, P.D., McColl, J., Klenerman, D., Carr, A.M., Sauer, M., Allshire, R.C., et al. (2012). Quantitative single-molecule microscopy reveals that CENP-ACnp1 deposition occurs during G2 in fission yeast. Open Biol *2*, 120078. https://doi.org/10.1098/rsob.120078.

Lankenau, S., Barnickel, T., Marhold, J., Lyko, F., Mechler, B.M., and Lankenau, D.-H. (2003). Knockout targeting of the Drosophila nap1 gene and examination of DNA repair tracts in the recombination products. Genetics *163*, 611–623. https://doi.org/10.1093/genetics/163.2.611.

Laskey, R.A., Mills, A.D., and Morris, N.R. (1977). Assembly of SV40 chromatin in a cell-free system from Xenopus eggs. Cell *10*, 237–243. https://doi.org/10.1016/0092-8674(77)90217-3.

Laskey, R.A., Honda, B.M., Mills, A.D., and Finch, J.T. (1978). Nucleosomes are assembled by an acidic protein which binds histones and transfers them to DNA. Nature *275*, 416–420. https://doi.org/10.1038/275416a0.

Latrick, C.M., Marek, M., Ouararhni, K., Papin, C., Stoll, I., Ignatyeva, M., Obri, A., Ennifar, E., Dimitrov, S., Romier, C., et al. (2016). Molecular basis and specificity of H2A.Z-H2B recognition and deposition by the histone chaperone YL1. Nat Struct Mol Biol *23*, 309–316. https://doi.org/10.1038/nsmb.3189.

Lechner, M.S., Schultz, D.C., Negorev, D., Maul, G.G., and Rauscher, F.J. (2005). The mammalian heterochromatin protein 1 binds diverse nuclear proteins through a common motif that targets the chromoshadow domain. Biochem Biophys Res Commun *331*, 929–937. https://doi.org/10.1016/j.bbrc.2005.04.016.

Levchenko, V., and Jackson, V. (2004). Histone release during transcription: NAP1 forms a complex with H2A and H2B and facilitates a topologically dependent release of H3 and H4 from the nucleosome. Biochemistry *43*, 2359–2372. https://doi.org/10.1021/bi035737q.

Li, J., and Stern, D.F. (2005). DNA damage regulates Chk2 association with chromatin. J Biol Chem *280*, 37948–37956. https://doi.org/10.1074/jbc.M509299200.

Li, M., Guo, H., and Damuni, Z. (1995). Purification and characterization of two potent heat-stable protein inhibitors of protein phosphatase 2A from bovine kidney. Biochemistry *34*, 1988–1996. https://doi.org/10.1021/bi00006a020.

Li, M., Strand, D., Krehan, A., Pyerin, W., Heid, H., Neumann, B., and Mechler, B.M. (1999). Casein kinase 2 binds and phosphorylates the nucleosome assembly protein-1

(NAP1) in Drosophila melanogaster. J Mol Biol *293*, 1067–1084. https://doi.org/10.1006/jmbi.1999.3207.

Li, Q., Zhou, H., Wurtele, H., Davies, B., Horazdovsky, B., Verreault, A., and Zhang, Z. (2008). Acetylation of histone H3 lysine 56 regulates replication-coupled nucleosome assembly. Cell *134*, 244–255. https://doi.org/10.1016/j.cell.2008.06.018.

Li, Z., Pearlman, A.H., and Hsieh, P. (2016). DNA mismatch repair and the DNA damage response. DNA Repair (Amst) *38*, 94–101. https://doi.org/10.1016/j.dnarep.2015.11.019.

Li, J., Wang, R., Jin, J., Han, M., Chen, Z., Gao, Y., Hu, X., Zhu, H., Gao, H., Lu, K., et al. (2020). USP7 negatively controls global DNA methylation by attenuating ubiquitinated histone-dependent DNMT1 recruitment. Cell Discov *6*, 58. https://doi.org/10.1038/s41421-020-00188-4.

Liang, X., Shan, S., Pan, L., Zhao, J., Ranjan, A., Wang, F., Zhang, Z., Huang, Y., Feng, H., Wei, D., et al. (2016). Structural basis of H2A.Z recognition by SRCAP chromatin-remodeling subunit YL1. Nat Struct Mol Biol *23*, 317–323. https://doi.org/10.1038/nsmb.3190.

Liang, Y., Zhang, R., Zhang, S., Ji, G., Shi, P., Yang, T., Liu, F., Feng, J., Li, C., Guo, D., et al. (2017). Association of ACYP2 and TSPYL6 Genetic Polymorphisms with Risk of Ischemic Stroke in Han Chinese Population. Mol Neurobiol *54*, 5988–5995. https://doi.org/10.1007/s12035-016-0086-x.

von Lindern, M., van Baal, S., Wiegant, J., Raap, A., Hagemeijer, A., and Grosveld, G. (1992). Can, a putative oncogene associated with myeloid leukemogenesis, may be activated by fusion of its 3' half to different genes: characterization of the set gene. Mol Cell Biol *12*, 3346–3355. https://doi.org/10.1128/mcb.12.8.3346-3355.1992.

Linger, J.G., and Tyler, J.K. (2007). Chromatin disassembly and reassembly during DNA repair. Mutat Res *618*, 52–64. https://doi.org/10.1016/j.mrfmmm.2006.05.039.

Liu, Z., Zhu, Y., Gao, J., Yu, F., Dong, A., and Shen, W.-H. (2009). Molecular and reverse genetic characterization of NUCLEOSOME ASSEMBLY PROTEIN1 (NAP1) genes unravels their function in transcription and nucleotide excision repair in Arabidopsis thaliana. Plant J *59*, 27–38. https://doi.org/10.1111/j.1365-313X.2009.03844.x.

Liu, Y., Huang, H., Zhou, B.O., Wang, S.-S., Hu, Y., Li, X., Liu, J., Zang, J., Niu, L., Wu, J., et al. (2010). Structural analysis of Rtt106p reveals a DNA binding role required

for heterochromatin silencing. J Biol Chem *285*, 4251–4262. https://doi.org/10.1074/jbc.M109.055996.

Liu, W.H., Roemer, S.C., Port, A.M., and Churchill, M.E.A. (2012). CAF-1-induced oligomerization of histones H3/H4 and mutually exclusive interactions with Asf1 guide H3/H4 transitions among histone chaperones and DNA. Nucleic Acids Res *40*, 11229–11239. https://doi.org/10.1093/nar/gks906.

Liu, M., Ingle, J.N., Fridley, B.L., Buzdar, A.U., Robson, M.E., Kubo, M., Wang, L., Batzler, A., Jenkins, G.D., Pietrzak, T.L., et al. (2013). TSPYL5 SNPs: Association with Plasma Estradiol Concentrations and Aromatase Expression. Mol Endocrinol *27*, 657–670. https://doi.org/10.1210/me.2012-1397.

Lorch, Y., Maier-Davis, B., and Kornberg, R.D. (2006a). Chromatin remodeling by nucleosome disassembly in vitro. Proc Natl Acad Sci U S A *103*, 3090–3093. https://doi.org/10.1073/pnas.0511050103.

Lorch, Y., Maier-Davis, B., and Kornberg, R.D. (2006b). Chromatin remodeling by nucleosome disassembly *in vitro*. Proc. Natl. Acad. Sci. U.S.A. *103*, 3090–3093. https://doi.org/10.1073/pnas.0511050103.

Loyola, A., Bonaldi, T., Roche, D., Imhof, A., and Almouzni, G. (2006). PTMs on H3 variants before chromatin assembly potentiate their final epigenetic state. Mol Cell *24*, 309–316. https://doi.org/10.1016/j.molcel.2006.08.019.

Luger, K., Rechsteiner, T.J., and Richmond, T.J. (1999a). Expression and purification of recombinant histones and nucleosome reconstitution. Methods Mol Biol *119*, 1–16. https://doi.org/10.1385/1-59259-681-9:1.

Luger, K., Rechsteiner, T.J., and Richmond, T.J. (1999b). Preparation of nucleosome core particle from recombinant histones. Methods Enzymol *304*, 3–19. https://doi.org/10.1016/s0076-6879(99)04003-3.

Luger, K., Dechassa, M.L., and Tremethick, D.J. (2012). New insights into nucleosome and chromatin structure: an ordered state or a disordered affair? Nat Rev Mol Cell Biol *13*, 436–447. https://doi.org/10.1038/nrm3382.

Luk, E., Vu, N.-D., Patteson, K., Mizuguchi, G., Wu, W.-H., Ranjan, A., Backus, J., Sen, S., Lewis, M., Bai, Y., et al. (2007). Chz1, a nuclear chaperone for histone H2AZ. Mol Cell *25*, 357–368. https://doi.org/10.1016/j.molcel.2006.12.015.

Lyu, J.H., Park, D.-W., Huang, B., Kang, S.H., Lee, S.J., Lee, C., Bae, Y.-S., Lee, J.-G., and Baek, S.-H. (2015). RGS2 suppresses breast cancer cell growth via a MCPIP1-dependent pathway. J Cell Biochem *116*, 260–267. https://doi.org/10.1002/jcb.24964.

Magni, M., Ruscica, V., Restelli, M., Fontanella, E., Buscemi, G., and Zannini, L. (2015). CCAR2/DBC1 is required for Chk2-dependent KAP1 phosphorylation and repair of DNA damage. Oncotarget *6*, 17817–17831. https://doi.org/10.18632/oncotarget.4417.

Malay, A.D., Umehara, T., Matsubara-Malay, K., Padmanabhan, B., and Yokoyama, S. (2008). Crystal Structures of Fission Yeast Histone Chaperone Asf1 Complexed with the Hip1 B-domain or the Cac2 C Terminus. Journal of Biological Chemistry *283*, 14022–14031. https://doi.org/10.1074/jbc.M800594200.

Mao, Z., Pan, L., Wang, W., Sun, J., Shan, S., Dong, Q., Liang, X., Dai, L., Ding, X., Chen, S., et al. (2014). Anp32e, a higher eukaryotic histone chaperone directs preferential recognition for H2A.Z. Cell Res *24*, 389–399. https://doi.org/10.1038/cr.2014.30.

Margueron, R., and Reinberg, D. (2010). Chromatin structure and the inheritance of epigenetic information. Nat Rev Genet *11*, 285–296. https://doi.org/10.1038/nrg2752.

Martire, S., and Banaszynski, L.A. (2020). The roles of histone variants in fine-tuning chromatin organization and function. Nat Rev Mol Cell Biol *21*, 522–541. https://doi.org/10.1038/s41580-020-0262-8.

Matsumoto, K., Nagata, K., Ui, M., and Hanaoka, F. (1993). Template activating factor I, a novel host factor required to stimulate the adenovirus core DNA replication. J Biol Chem *268*, 10582–10587. .

Matsumoto, K., Nagata, K., Miyaji-Yamaguchi, M., Kikuchi, A., and Tsujimoto, M. (1999). Sperm chromatin decondensation by template activating factor I through direct interaction with basic proteins. Mol Cell Biol *19*, 6940–6952. https://doi.org/10.1128/MCB.19.10.6940.

Mattiroli, F., Gu, Y., Yadav, T., Balsbaugh, J.L., Harris, M.R., Findlay, E.S., Liu, Y., Radebaugh, C.A., Stargell, L.A., Ahn, N.G., et al. DNA-mediated association of two histone-bound complexes of yeast Chromatin Assembly Factor-1 (CAF-1) drives tetrasome assembly in the wake of DNA replication. ELife *6*, e22799. https://doi.org/10.7554/eLife.22799.

Mazurkiewicz, J., Kepert, J.F., and Rippe, K. (2006). On the mechanism of nucleosome assembly by histone chaperone NAP1. J Biol Chem *281*, 16462–16472. https://doi.org/10.1074/jbc.M511619200.

McBryant, S.J., and Peersen, O.B. (2004). Self-association of the yeast nucleosome assembly protein 1. Biochemistry *43*, 10592–10599. https://doi.org/10.1021/bi035881b.

McBryant, S.J., Park, Y.-J., Abernathy, S.M., Laybourn, P.J., Nyborg, J.K., and Luger, K. (2003). Preferential binding of the histone (H3-H4)2 tetramer by NAP1 is mediated by the amino-terminal histone tails. J Biol Chem *278*, 44574–44583. https://doi.org/10.1074/jbc.M305636200.

Miyaji-Yamaguchi, M., Okuwaki, M., and Nagata, K. (1999). Coiled-coil structure-mediated dimerization of template activating factor-I is critical for its chromatin remodeling activity1 1Edited by T. Richmond. Journal of Molecular Biology *290*, 547–557. https://doi.org/10.1006/jmbi.1999.2898.

Miyaji-Yamaguchi, M., Kato, K., Nakano, R., Akashi, T., Kikuchi, A., and Nagata, K. (2003). Involvement of Nucleocytoplasmic Shuttling of Yeast Nap1 in Mitotic Progression. Mol Cell Biol *23*, 6672–6684. https://doi.org/10.1128/MCB.23.18.6672-6684.2003.

Mizuguchi, G., Shen, X., Landry, J., Wu, W.-H., Sen, S., and Wu, C. (2004). ATP-driven exchange of histone H2AZ variant catalyzed by SWR1 chromatin remodeling complex. Science *303*, 343–348. https://doi.org/10.1126/science.1090701.

Mizuguchi, G., Xiao, H., Wisniewski, J., Smith, M.M., and Wu, C. (2007). Nonhistone Scm3 and histones CenH3-H4 assemble the core of centromere-specific nucleosomes. Cell *129*, 1153–1164. https://doi.org/10.1016/j.cell.2007.04.026.

Moggs, J.G., Grandi, P., Quivy, J.P., Jónsson, Z.O., Hübscher, U., Becker, P.B., and Almouzni, G. (2000). A CAF-1-PCNA-mediated chromatin assembly pathway triggered by sensing DNA damage. Mol Cell Biol *20*, 1206–1218. https://doi.org/10.1128/MCB.20.4.1206-1218.2000.

Mosammaparast, N., Jackson, K.R., Guo, Y., Brame, C.J., Shabanowitz, J., Hunt, D.F., and Pemberton, L.F. (2001). Nuclear import of histone H2A and H2B is mediated by a network of karyopherins. J Cell Biol *153*, 251–262. https://doi.org/10.1083/jcb.153.2.251.

Mosammaparast, N., Ewart, C.S., and Pemberton, L.F. (2002). A role for nucleosome assembly protein 1 in the nuclear transport of histones H2A and H2B. EMBO J *21*, 6527–6538. https://doi.org/10.1093/emboj/cdf647.

Mousson, F., Lautrette, A., Thuret, J.-Y., Agez, M., Courbeyrette, R., Amigues, B., Becker, E., Neumann, J.-M., Guerois, R., Mann, C., et al. (2005). Structural basis for the interaction of Asf1 with histone H3 and its functional implications. Proc. Natl. Acad. Sci. U.S.A. *102*, 5975–5980. https://doi.org/10.1073/pnas.0500149102.

Müller, S., Montes de Oca, R., Lacoste, N., Dingli, F., Loew, D., and Almouzni, G. (2014). Phosphorylation and DNA Binding of HJURP Determine Its Centromeric Recruitment and Function in CenH3CENP-A Loading. Cell Reports *8*, 190–203. https://doi.org/10.1016/j.celrep.2014.06.002.

Munakata, T., Adachi, N., Yokoyama, N., Kuzuhara, T., and Horikoshi, M. (2000). A human homologue of yeast anti-silencing factor has histone chaperone activity. Genes Cells *5*, 221–233. https://doi.org/10.1046/j.1365-2443.2000.00319.x.

Murzina, N.V., Pei, X.-Y., Zhang, W., Sparkes, M., Vicente-Garcia, J., Pratap, J.V., McLaughlin, S.H., Ben-Shahar, T.R., Verreault, A., Luisi, B.F., et al. (2008). Structural basis for the recognition of histone H4 by the histone-chaperone RbAp46. Structure *16*, 1077–1085. https://doi.org/10.1016/j.str.2008.05.006.

Muto, S., Senda, M., Akai, Y., Sato, L., Suzuki, T., Nagai, R., Senda, T., and Horikoshi, M. (2007). Relationship between the structure of SET/TAF-Iβ/INHAT and its histone chaperone activity. Proceedings of the National Academy of Sciences *104*, 4285–4290. https://doi.org/10.1073/pnas.0603762104.

Mylonas, C., and Tessarz, P. (2018). Transcriptional repression by FACT is linked to regulation of chromatin accessibility at the promoter of ES cells. Life Sci Alliance *1*, e201800085. https://doi.org/10.26508/lsa.201800085.

Nabatiyan, A., and Krude, T. (2004). Silencing of chromatin assembly factor 1 in human cells leads to cell death and loss of chromatin assembly during DNA synthesis. Mol Cell Biol *24*, 2853–2862. https://doi.org/10.1128/MCB.24.7.2853-2862.2004.

Nagase, T., Kikuno, R., Hattori, A., Kondo, Y., Okumura, K., and Ohara, O. (2000). Prediction of the coding sequences of unidentified human genes. XIX. The complete sequences of 100 new cDNA clones from brain which code for large proteins in vitro. DNA Res *7*, 347–355. https://doi.org/10.1093/dnares/7.6.347.

Nakagawa, T., Bulger, M., Muramatsu, M., and Ito, T. (2001). Multistep chromatin assembly on supercoiled plasmid DNA by nucleosome assembly protein-1 and ATP-utilizing chromatin assembly and remodeling factor. J Biol Chem *276*, 27384–27391. https://doi.org/10.1074/jbc.M101331200.

Natsume, R., Eitoku, M., Akai, Y., Sano, N., Horikoshi, M., and Senda, T. (2007). Structure and function of the histone chaperone CIA/ASF1 complexed with histones H3 and H4. Nature *446*, 338–341. https://doi.org/10.1038/nature05613.

Newman, E.R., Kneale, G.G., Ravelli, R.B.G., Karuppasamy, M., Karimi Nejadasl, F., Taylor, I.A., and McGeehan, J.E. (2012). Large multimeric assemblies of nucleosome assembly protein and histones revealed by small-angle X-ray scattering and electron microscopy. J Biol Chem *287*, 26657–26665. https://doi.org/10.1074/jbc.M112.340422.

Nie, X., Wang, H., Li, J., Holec, S., and Berger, F. (2014). The HIRA complex that deposits the histone H3.3 is conserved in *Arabidopsis* and facilitates transcriptional dynamics. Biology Open *3*, 794–802. https://doi.org/10.1242/bio.20148680.

Nishiyama, A., Yamaguchi, L., Sharif, J., Johmura, Y., Kawamura, T., Nakanishi, K., Shimamura, S., Arita, K., Kodama, T., Ishikawa, F., et al. (2013). Uhrf1-dependent H3K23 ubiquitylation couples maintenance DNA methylation and replication. Nature *502*, 249–253. https://doi.org/10.1038/nature12488.

Obri, A., Ouararhni, K., Papin, C., Diebold, M.-L., Padmanabhan, K., Marek, M., Stoll, I., Roy, L., Reilly, P.T., Mak, T.W., et al. (2014). ANP32E is a histone chaperone that removes H2A.Z from chromatin. Nature *505*, 648–653. https://doi.org/10.1038/nature12922.

O'Donnell, A.F. (2004). Domain organization of the yeast histone chaperone FACT: the conserved N-terminal domain of FACT subunit Spt16 mediates recovery from replication stress. Nucleic Acids Research *32*, 5894–5906. https://doi.org/10.1093/nar/gkh922.

Ohkuni, K., Shirahige, K., and Kikuchi, A. (2003). Genome-wide expression analysis of NAP1 in Saccharomyces cerevisiae. Biochem Biophys Res Commun *306*, 5–9. https://doi.org/10.1016/s0006-291x(03)00907-0.

Oka, D., Yamashita, S., Tomioka, T., Nakanishi, Y., Kato, H., Kaminishi, M., and Ushijima, T. (2009). The presence of aberrant DNA methylation in noncancerous esophageal mucosae in association with smoking history: a target for risk diagnosis and prevention of esophageal cancers. Cancer *115*, 3412–3426. https://doi.org/10.1002/cncr.24394.

Okuwaki, M., and Nagata, K. (1998). Template Activating Factor-I Remodels the Chromatin Structure and Stimulates Transcription from the Chromatin Template *. Journal of Biological Chemistry *273*, 34511–34518. https://doi.org/10.1074/jbc.273.51.34511.

Okuwaki, M., Matsumoto, K., Tsujimoto, M., and Nagata, K. (2001). Function of nucleophosmin/B23, a nucleolar acidic protein, as a histone chaperone. FEBS Lett *506*, 272–276. https://doi.org/10.1016/s0014-5793(01)02939-8.

Okuwaki, M., Kato, K., Shimahara, H., Tate, S., and Nagata, K. (2005). Assembly and disassembly of nucleosome core particles containing histone variants by human nucleosome assembly protein I. Mol Cell Biol *25*, 10639–10651. https://doi.org/10.1128/MCB.25.23.10639-10651.2005.

Orphanides, G., Wu, W.H., Lane, W.S., Hampsey, M., and Reinberg, D. (1999). The chromatin-specific transcription elongation factor FACT comprises human SPT16 and SSRP1 proteins. Nature *400*, 284–288. https://doi.org/10.1038/22350.

Owen-Hughes, T., Utley, R.T., Côté, J., Peterson, C.L., and Workman, J.L. (1996). Persistent site-specific remodeling of a nucleosome array by transient action of the SWI/SNF complex. Science *273*, 513–516. https://doi.org/10.1126/science.273.5274.513.

Ozbun, L.L., You, L., Kiang, S., Angdisen, J., Martinez, A., and Jakowlew, S.B. (2001). Identification of differentially expressed nucleolar TGF-beta1 target (DENTT) in human lung cancer cells that is a new member of the TSPY/SET/NAP-1 superfamily. Genomics *73*, 179–193. https://doi.org/10.1006/geno.2001.6505.

Pardal, A.J., Fernandes-Duarte, F., and Bowman, A.J. (2019). The histone chaperoning pathway: from ribosome to nucleosome. Essays Biochem *63*, 29–43. https://doi.org/10.1042/EBC20180055.

Park, Y.-J., and Luger, K. (2006a). The structure of nucleosome assembly protein 1. Proceedings of the National Academy of Sciences *103*, 1248–1253. https://doi.org/10.1073/pnas.0508002103.

Park, Y.-J., and Luger, K. (2006b). Structure and function of nucleosome assembly proteins. Biochem Cell Biol *84*, 549–558. https://doi.org/10.1139/o06-088.

Park, Y.-J., Chodaparambil, J.V., Bao, Y., McBryant, S.J., and Luger, K. (2005). Nucleosome assembly protein 1 exchanges histone H2A-H2B dimers and assists

nucleosome sliding. J Biol Chem *280*, 1817–1825. https://doi.org/10.1074/jbc.M411347200.

Park, S., Hanekamp, T., Thorsness, M.K., and Thorsness, P.E. (2006). Yme2p is a mediator of nucleoid structure and number in mitochondria of the yeast Saccharomyces cerevisiae. Curr Genet *50*, 173–182. https://doi.org/10.1007/s00294-006-0087-9.

Park, Y.-J., Sudhoff, K.B., Andrews, A.J., Stargell, L.A., and Luger, K. (2008). Histone chaperone specificity in Rtt109 activation. Nat Struct Mol Biol *15*, 957–964. https://doi.org/10.1038/nsmb.1480.

Park, J., Lee, H., Han, N., Kwak, S., Lee, H.-T., Kim, J.-H., Kang, K., Youn, B.H., Yang, J.-H., Jeong, H.-J., et al. (2018). Long non-coding RNA ChRO1 facilitates ATRX/DAXX-dependent H3.3 deposition for transcription-associated heterochromatin reorganization. Nucleic Acids Res *46*, 11759–11775. https://doi.org/10.1093/nar/gky923.

Pchelintsev, N.A., McBryan, T., Rai, T.S., van Tuyn, J., Ray-Gallet, D., Almouzni, G., and Adams, P.D. (2013). Placing the HIRA histone chaperone complex in the chromatin landscape. Cell Rep *3*, 1012–1019. https://doi.org/10.1016/j.celrep.2013.03.026.

Peterson, C.L., Zhao, Y., and Chait, B.T. (1998). Subunits of the Yeast SWI/SNF Complex Are Members of the Actin-related Protein (ARP) Family*. Journal of Biological Chemistry *273*, 23641–23644. https://doi.org/10.1074/jbc.273.37.23641.

Pidoux, A.L., Choi, E.S., Abbott, J.K.R., Liu, X., Kagansky, A., Castillo, A.G., Hamilton, G.L., Richardson, W., Rappsilber, J., He, X., et al. (2009). Fission yeast Scm3: A CENP-A receptor required for integrity of subkinetochore chromatin. Mol Cell *33*, 299–311. https://doi.org/10.1016/j.molcel.2009.01.019.

Piwko, W., Buser, R., and Peter, M. (2011). Rescuing stalled replication forks: MMS22L-TONSL, a novel complex for DNA replication fork repair in human cells. Cell Cycle *10*, 1703–1705. https://doi.org/10.4161/cc.10.11.15557.

Polo, S.E., Roche, D., and Almouzni, G. (2006). New histone incorporation marks sites of UV repair in human cells. Cell *127*, 481–493. https://doi.org/10.1016/j.cell.2006.08.049.

Probst, A.V., Dunleavy, E., and Almouzni, G. (2009). Epigenetic inheritance during the cell cycle. Nat Rev Mol Cell Biol *10*, 192–206. https://doi.org/10.1038/nrm2640.

Puffenberger, E.G., Hu-Lince, D., Parod, J.M., Craig, D.W., Dobrin, S.E., Conway, A.R., Donarum, E.A., Strauss, K.A., Dunckley, T., Cardenas, J.F., et al. (2004). Mapping of

sudden infant death with dysgenesis of the testes syndrome (SIDDT) by a SNP genome scan and identification of TSPYL loss of function. Proc Natl Acad Sci U S A *101*, 11689–11694. https://doi.org/10.1073/pnas.0401194101.

Qiao, H., Li, Y., Feng, C., Duo, S., Ji, F., and Jiao, J. (2018). Nap1l1 Controls Embryonic Neural Progenitor Cell Proliferation and Differentiation in the Developing Brain. Cell Reports *22*, 2279–2293. https://doi.org/10.1016/j.celrep.2018.02.019.

Qiu, X., Cheng, J.-C., Klausen, C., Chang, H.-M., Fan, Q., and Leung, P.C.K. (2016a). EGF-Induced Connexin43 Negatively Regulates Cell Proliferation in Human Ovarian Cancer. J Cell Physiol *231*, 111–119. https://doi.org/10.1002/jcp.25058.

Qiu, Z., Zou, K., Zhuang, L., Qin, J., Li, H., Li, C., Zhang, Z., Chen, X., Cen, J., Meng, Z., et al. (2016b). Hepatocellular carcinoma cell lines retain the genomic and transcriptomic landscapes of primary human cancers. Sci Rep *6*, 27411. https://doi.org/10.1038/srep27411.

Quivy, J.P., Grandi, P., and Almouzni, G. (2001). Dimerization of the largest subunit of chromatin assembly factor 1: importance in vitro and during Xenopus early development. EMBO J *20*, 2015–2027. https://doi.org/10.1093/emboj/20.8.2015.

Ramos, I., Martín-Benito, J., Finn, R., Bretaña, L., Aloria, K., Arizmendi, J.M., Ausió, J., Muga, A., Valpuesta, J.M., and Prado, A. (2010). Nucleoplasmin binds histone H2A-H2B dimers through its distal face. J Biol Chem *285*, 33771–33778. https://doi.org/10.1074/jbc.M110.150664.

Ratti, A., Stuppia, L., Gatta, V., Fogh, I., Calabrese, G., Pizzuti, A., and Palka, G. (2000). Characterization of a new TSPY gene family member in Yq (TSPYq1). Cytogenet Cell Genet *88*, 159–162. https://doi.org/10.1159/000015510.

Ray-Gallet, D., Quivy, J.-P., Scamps, C., Martini, E.M.-D., Lipinski, M., and Almouzni, G. (2002). HIRA is critical for a nucleosome assembly pathway independent of DNA synthesis. Mol Cell *9*, 1091–1100. https://doi.org/10.1016/s1097-2765(02)00526-9.

Ray-Gallet, D., Woolfe, A., Vassias, I., Pellentz, C., Lacoste, N., Puri, A., Schultz, D.C., Pchelintsev, N.A., Adams, P.D., Jansen, L.E.T., et al. (2011). Dynamics of Histone H3 Deposition In Vivo Reveal a Nucleosome Gap-Filling Mechanism for H3.3 to Maintain Chromatin Integrity. Molecular Cell *44*, 928–941. https://doi.org/10.1016/j.molcel.2011.12.006.

Ray-Gallet, D., Ricketts, M.D., Sato, Y., Gupta, K., Boyarchuk, E., Senda, T., Marmorstein, R., and Almouzni, G. (2018). Functional activity of the H3.3 histone

chaperone complex HIRA requires trimerization of the HIRA subunit. Nat Commun *9*, 3103. https://doi.org/10.1038/s41467-018-05581-y.

Recht, J., Tsubota, T., Tanny, J.C., Diaz, R.L., Berger, J.M., Zhang, X., Garcia, B.A., Shabanowitz, J., Burlingame, A.L., Hunt, D.F., et al. (2006). Histone chaperone Asf1 is required for histone H3 lysine 56 acetylation, a modification associated with S phase in mitosis and meiosis. Proc Natl Acad Sci U S A *103*, 6988–6993. https://doi.org/10.1073/pnas.0601676103.

Rehtanz, M., Schmidt, H.-M., Warthorst, U., and Steger, G. (2004). Direct interaction between nucleosome assembly protein 1 and the papillomavirus E2 proteins involved in activation of transcription. Mol Cell Biol *24*, 2153–2168. https://doi.org/10.1128/MCB.24.5.2153-2168.2004.

Robbins, J., Dilwortht, S.M., Laskey, R.A., and Dingwall, C. (1991). Two interdependent basic domains in nucleoplasmin nuclear targeting sequence: Identification of a class of bipartite nuclear targeting sequence. Cell *64*, 615–623. https://doi.org/10.1016/0092-8674(91)90245-T.

Rodriguez, P., Munroe, D., Prawitt, D., Chu, L.L., Bric, E., Kim, J., Reid, L.H., Davies, C., Nakagama, H., Loebbert, R., et al. (1997). Functional characterization of human nucleosome assembly protein-2 (NAP1L4) suggests a role as a histone chaperone. Genomics *44*, 253–265. https://doi.org/10.1006/geno.1997.4868.

Rodriguez, P., Pelletier, J., Price, G.B., and Zannis-Hadjopoulos, M. (2000). NAP-2: histone chaperone function and phosphorylation state through the cell cycle. J Mol Biol *298*, 225–238. https://doi.org/10.1006/jmbi.2000.3674.

Rogner, U.C., Spyropoulos, D.D., Le Novère, N., Changeux, J.P., and Avner, P. (2000). Control of neurulation by the nucleosome assembly protein-1-like 2. Nat Genet *25*, 431–435. https://doi.org/10.1038/78124.

Rougeulle, C., and Avner, P. (1996). Cloning and characterization of a murine brain specific gene Bpx and its human homologue lying within the Xic candidate region. Hum Mol Genet *5*, 41–49. https://doi.org/10.1093/hmg/5.1.41.

Russell, J.H., and Ley, T.J. (2002). Lymphocyte-mediated cytotoxicity. Annu Rev Immunol *20*, 323–370. https://doi.org/10.1146/annurev.immunol.20.100201.131730.

Saredi, G., Huang, H., Hammond, C.M., Alabert, C., Bekker-Jensen, S., Forne, I., Reverón-Gómez, N., Foster, B.M., Mlejnkova, L., Bartke, T., et al. (2016). H4K20me0

marks post-replicative chromatin and recruits the TONSL–MMS22L DNA repair complex. Nature *534*, 714–718. https://doi.org/10.1038/nature18312.

Saridakis, V., Sheng, Y., Sarkari, F., Holowaty, M.N., Shire, K., Nguyen, T., Zhang, R.G., Liao, J., Lee, W., Edwards, A.M., et al. (2005). Structure of the p53 Binding Domain of HAUSP/USP7 Bound to Epstein-Barr Nuclear Antigen 1: Implications for EBV-Mediated Immortalization. Molecular Cell *18*, 25–36. https://doi.org/10.1016/j.molcel.2005.02.029.

Sauer, P.V., Timm, J., Liu, D., Sitbon, D., Boeri-Erba, E., Velours, C., Mücke, N., Langowski, J., Ochsenbein, F., Almouzni, G., et al. Insights into the molecular architecture and histone H3-H4 deposition mechanism of yeast Chromatin assembly factor 1. ELife *6*, e23474. https://doi.org/10.7554/eLife.23474.

Saunders, A., Werner, J., Andrulis, E.D., Nakayama, T., Hirose, S., Reinberg, D., and Lis, J.T. (2003). Tracking FACT and the RNA polymerase II elongation complex through chromatin in vivo. Science *301*, 1094–1096. https://doi.org/10.1126/science.1085712.

Schneiderman, J.I., Orsi, G.A., Hughes, K.T., Loppin, B., and Ahmad, K. (2012). Nucleosome-depleted chromatin gaps recruit assembly factors for the H3.3 histone variant. Proc Natl Acad Sci U S A *109*, 19721–19726. https://doi.org/10.1073/pnas.1206629109.

Schnieders, F., Dörk, T., Arnemann, J., Vogel, T., Werner, M., and Schmidtke, J. (1996). Testis-specific protein, Y-encoded (TSPY) expression in testicular tissues. Hum Mol Genet *5*, 1801–1807. https://doi.org/10.1093/hmg/5.11.1801.

Selth, L., and Svejstrup, J.Q. (2007). Vps75, a new yeast member of the NAP histone chaperone family. J Biol Chem *282*, 12358–12362. https://doi.org/10.1074/jbc.C700012200.

Selth, L.A., Lorch, Y., Ocampo-Hafalla, M.T., Mitter, R., Shales, M., Krogan, N.J., Kornberg, R.D., and Svejstrup, J.Q. (2009). An Rtt109-Independent Role for Vps75 in Transcription-Associated Nucleosome Dynamics. Molecular and Cellular Biology *29*, 4220–4234. https://doi.org/10.1128/MCB.01882-08.

Seo, S.B., McNamara, P., Heo, S., Turner, A., Lane, W.S., and Chakravarti, D. (2001). Regulation of histone acetylation and transcription by INHAT, a human cellular complex containing the set oncoprotein. Cell *104*, 119–130. https://doi.org/10.1016/s0092-8674(01)00196-9.

Shao, L., Shen, Z., Qian, H., Zhou, S., and Chen, Y. (2017). Knockdown of miR-629 Inhibits Ovarian Cancer Malignant Behaviors by Targeting Testis-Specific Y-Like Protein 5. DNA Cell Biol *36*, 1108–1116. https://doi.org/10.1089/dna.2017.3904.

Sharma, N., and Nyborg, J.K. (2008). The coactivators CBP/p300 and the histone chaperone NAP1 promote transcription-independent nucleosome eviction at the HTLV-1 promoter. Proc Natl Acad Sci U S A *105*, 7959–7963. https://doi.org/10.1073/pnas.0800534105.

Shen, H.H., Huang, A.M., Hoheisel, J., and Tsai, S.F. (2001). Identification and characterization of a SET/NAP protein encoded by a brain-specific gene, MB20. Genomics *71*, 21–33. https://doi.org/10.1006/geno.2000.6397.

Shen, X., Ranallo, R., Choi, E., and Wu, C. (2003). Involvement of actin-related proteins in ATP-dependent chromatin remodeling. Mol Cell *12*, 147–155. https://doi.org/10.1016/s1097-2765(03)00264-8.

Shen, Y., Yan, Y., Liu, Y., Zhang, S., Yang, D., Zhang, P., Li, L., Wang, Y., Ma, Y., Tao, D., et al. (2013). A significant effect of the TSPY1 copy number on spermatogenesis efficiency and the phenotypic expression of the gr/gr deletion. Hum Mol Genet *22*, 1679–1695. https://doi.org/10.1093/hmg/ddt004.

Shen, Y., Tu, W., Liu, Y., Yang, X., Dong, Q., Yang, B., Xu, J., Yan, Y., Pei, X., Liu, M., et al. (2018). TSPY1 suppresses USP7-mediated p53 function and promotes spermatogonial proliferation. Cell Death Dis *9*, 542. https://doi.org/10.1038/s41419-018-0589-7.

Skaletsky, H., Kuroda-Kawaguchi, T., Minx, P.J., Cordum, H.S., Hillier, L., Brown, L.G., Repping, S., Pyntikova, T., Ali, J., Bieri, T., et al. (2003). The male-specific region of the human Y chromosome is a mosaic of discrete sequence classes. Nature *423*, 825–837. https://doi.org/10.1038/nature01722.

Smerdon, M.J. (1991). DNA repair and the role of chromatin structure. Current Opinion in Cell Biology *3*, 422–428. https://doi.org/10.1016/0955-0674(91)90069-B.

Smith, S., and Stillman, B. (1991). Stepwise assembly of chromatin during DNA replication in vitro. EMBO J *10*, 971–980. https://doi.org/10.1002/j.1460-2075.1991.tb08031.x.

Smith, R.J., Dean, W., Konfortova, G., and Kelsey, G. (2003). Identification of novel imprinted genes in a genome-wide screen for maternal methylation. Genome Res *13*, 558–569. https://doi.org/10.1101/gr.781503.

Song, Y., He, F., Xie, G., Guo, X., Xu, Y., Chen, Y., Liang, X., Stagljar, I., Egli, D., Ma, J., et al. (2007). CAF-1 is essential for Drosophila development and involved in the maintenance of epigenetic memory. Developmental Biology *311*, 213–222. https://doi.org/10.1016/j.ydbio.2007.08.039.

Song, J.-J., Garlick, J.D., and Kingston, R.E. (2008). Structural basis of histone H4 recognition by p55. Genes Dev *22*, 1313–1318. https://doi.org/10.1101/gad.1653308.

Steer, W.M., Abu-Daya, A., Brickwood, S.J., Mumford, K.L., Jordanaires, N., Mitchell, J., Robinson, C., Thorne, A.W., and Guille, M.J. (2003). Xenopus nucleosome assembly protein becomes tissue-restricted during development and can alter the expression of specific genes. Mech Dev *120*, 1045–1057. https://doi.org/10.1016/s0925-4773(03)00176-x.

Steinmetz, E. (2011). Expresso® Cloning and Expression Systems: Expressioneering™ Technology streamlines recombinant protein expression. Nat Methods *8*, iii–iv. https://doi.org/10.1038/nmeth.f.344.

Stoler, S., Rogers, K., Weitze, S., Morey, L., Fitzgerald-Hayes, M., and Baker, R.E. (2007). Scm3, an essential Saccharomyces cerevisiae centromere protein required for G2/M progression and Cse4 localization. Proc Natl Acad Sci U S A *104*, 10571–10576. https://doi.org/10.1073/pnas.0703178104.

Stuwe, T., Hothorn, M., Lejeune, E., Rybin, V., Bortfeld, M., Scheffzek, K., and Ladurner, A.G. (2008). The FACT Spt16 "peptidase" domain is a histone H3–H4 binding module. Proc Natl Acad Sci U S A *105*, 8884–8889. https://doi.org/10.1073/pnas.0712293105.

Su, D., Hu, Q., Zhou, H., Thompson, J.R., Xu, R.-M., Zhang, Z., and Mer, G. (2011). Structure and histone binding properties of the Vps75-Rtt109 chaperone-lysine acetyltransferase complex. J Biol Chem *286*, 15625–15629. https://doi.org/10.1074/jbc.C111.220715.

Swaminathan, V., Kishore, A.H., Febitha, K.K., and Kundu, T.K. (2005). Human histone chaperone nucleophosmin enhances acetylation-dependent chromatin transcription. Mol Cell Biol *25*, 7534–7545. https://doi.org/10.1128/MCB.25.17.7534-7545.2005.

Tagami, H., Ray-Gallet, D., Almouzni, G., and Nakatani, Y. (2004). Histone H3.1 and H3.3 complexes mediate nucleosome assembly pathways dependent or independent of DNA synthesis. Cell *116*, 51–61. https://doi.org/10.1016/s0092-8674(03)01064-x.

Tan, B.C.-M., Chien, C.-T., Hirose, S., and Lee, S.-C. (2006). Functional cooperation between FACT and MCM helicase facilitates initiation of chromatin DNA replication. EMBO J *25*, 3975–3985. https://doi.org/10.1038/sj.emboj.7601271.

Tang, Y., Poustovoitov, M.V., Zhao, K., Garfinkel, M., Canutescu, A., Dunbrack, R., Adams, P.D., and Marmorstein, R. (2006). Structure of a human ASF1a-HIRA complex and insights into specificity of histone chaperone complex assembly. Nat Struct Mol Biol *13*, 921–929. https://doi.org/10.1038/nsmb1147.

Tang, Y., Meeth, K., Jiang, E., Luo, C., and Marmorstein, R. (2008). Structure of Vps75 and implications for histone chaperone function. Proc Natl Acad Sci U S A *105*, 12206–12211. https://doi.org/10.1073/pnas.0802393105.

Telese, F., Bruni, P., Donizetti, A., Gianni, D., D'Ambrosio, C., Scaloni, A., Zambrano, N., Rosenfeld, M.G., and Russo, T. (2005). Transcription regulation by the adaptor protein Fe65 and the nucleosome assembly factor SET. EMBO Rep *6*, 77–82. https://doi.org/10.1038/sj.embor.7400309.

Theunissen, T.W., Powell, B.E., Wang, H., Mitalipova, M., Faddah, D.A., Reddy, J., Fan, Z.P., Maetzel, D., Ganz, K., Shi, L., et al. (2014). Systematic identification of culture conditions for induction and maintenance of naive human pluripotency. Cell Stem Cell *15*, 471–487. https://doi.org/10.1016/j.stem.2014.07.002.

Thoma, F., Koller, T., and Klug, A. (1979). Involvement of histone H1 in the organization of the nucleosome and of the salt-dependent superstructures of chromatin. J Cell Biol *83*, 403–427. https://doi.org/10.1083/jcb.83.2.403.

Tie, F., Furuyama, T., Prasad-Sinha, J., Jane, E., and Harte, P.J. (2001). The Drosophila Polycomb Group proteins ESC and E(Z) are present in a complex containing the histone-binding protein p55 and the histone deacetylase RPD3. Development *128*, 275–286. https://doi.org/10.1242/dev.128.2.275.

Tóth, K.F., Mazurkiewicz, J., and Rippe, K. (2005). Association states of nucleosome assembly protein 1 and its complexes with histones. J Biol Chem *280*, 15690–15699. https://doi.org/10.1074/jbc.M413329200.

Tyler, J.K., Adams, C.R., Chen, S.-R., Kobayashi, R., Kamakaka, R.T., and Kadonaga, J.T. (1999). The RCAF complex mediates chromatin assembly during DNA replication and repair. Nature *402*, 555–560. https://doi.org/10.1038/990147.

Umehara, T., Chimura, T., Ichikawa, N., and Horikoshi, M. (2002). Polyanionic stretch-deleted histone chaperone cia1/Asf1p is functional both in vivo and in vitro. Genes Cells *7*, 59–73. https://doi.org/10.1046/j.1356-9597.2001.00493.x.

Umehara, T., and Horikoshi, M. (2003). Transcription initiation factor IID-interactive histone chaperone CIA-II implicated in mammalian spermatogenesis. J Biol Chem *278*, 35660–35667. https://doi.org/10.1074/jbc.M303549200.

Vachani, A., Nebozhyn, M., Singhal, S., Alila, L., Wakeam, E., Muschel, R., Powell, C.A., Gaffney, P., Singh, B., Brose, M.S., et al. (2007). A 10-gene classifier for distinguishing head and neck squamous cell carcinoma and lung squamous cell carcinoma. Clin Cancer Res *13*, 2905–2915. https://doi.org/10.1158/1078-0432.CCR-06-1670.

VanDemark, A.P., Blanksma, M., Ferris, E., Heroux, A., Hill, C.P., and Formosa, T. (2006). The structure of the yFACT Pob3-M domain, its interaction with the DNA replication factor RPA, and a potential role in nucleosome deposition. Mol Cell *22*, 363–374. https://doi.org/10.1016/j.molcel.2006.03.025.

VanDemark, A.P., Xin, H., McCullough, L., Rawlins, R., Bentley, S., Heroux, A., Stillman, D.J., Hill, C.P., and Formosa, T. (2008). Structural and functional analysis of the Spt16p N-terminal domain reveals overlapping roles of yFACT subunits. J Biol Chem *283*, 5058–5068. https://doi.org/10.1074/jbc.M708682200.

Verreault, A., Kaufman, P.D., Kobayashi, R., and Stillman, B. (1998). Nucleosomal DNA regulates the core-histone-binding subunit of the human Hat1 acetyltransferase. Current Biology *8*, 96–108. https://doi.org/10.1016/S0960-9822(98)70040-5.

Vogel, T., Dittrich, O., Mehraein, Y., Dechend, F., Schnieders, F., and Schmidtke, J. (1998). Murine and human TSPYL genes: novel members of the TSPY-SET-NAP1L1 family. Cytogenet Cell Genet *81*, 265–270. https://doi.org/10.1159/000015042.

Voon, H.P.J., Hughes, J.R., Rode, C., De La Rosa-Velázquez, I.A., Jenuwein, T., Feil, R., Higgs, D.R., and Gibbons, R.J. (2015a). ATRX Plays a Key Role in Maintaining Silencing at Interstitial Heterochromatic Loci and Imprinted Genes. Cell Reports *11*, 405–418. https://doi.org/10.1016/j.celrep.2015.03.036.

Walter, M.F., Jang, C., Kasravi, B., Donath, J., Mechler, B.M., Mason, J.M., and Biessmann, H. (1995). DNA organization and polymorphism of a wild-type Drosophila telomere region. Chromosoma *104*, 229–241. https://doi.org/10.1007/BF00352254.

Wang, G.-S., Hong, C.-J., Yen, T.-Y., Huang, H.-Y., Ou, Y., Huang, T.-N., Jung, W.-G., Kuo, T.-Y., Sheng, M., Wang, T.-F., et al. (2004). Transcriptional modification by a CASK-interacting nucleosome assembly protein. Neuron *42*, 113–128. https://doi.org/10.1016/s0896-6273(04)00139-4.

Wang, A.Y., Schulze, J.M., Skordalakes, E., Gin, J.W., Berger, J.M., Rine, J., and Kobor, M.S. (2009). Asf1-like structure of the conserved Yaf9 YEATS domain and role in H2A.Z deposition and acetylation. Proc Natl Acad Sci U S A *106*, 21573–21578. https://doi.org/10.1073/pnas.0906539106.

Wang, H., Wang, M., Yang, N., and Xu, R.-M. (2015). Structure of the quaternary complex of histone H3-H4 heterodimer with chaperone ASF1 and the replicative helicase subunit MCM2. Protein Cell *6*, 693–697. https://doi.org/10.1007/s13238-015-0190-0.

Weissbein, U., Plotnik, O., Vershkov, D., and Benvenisty, N. (2017). Culture-induced recurrent epigenetic aberrations in human pluripotent stem cells. PLoS Genet *13*, e1006979. https://doi.org/10.1371/journal.pgen.1006979.

Westhorpe, F.G., Fuller, C.J., and Straight, A.F. (2015). A cell-free CENP-A assembly system defines the chromatin requirements for centromere maintenance. J Cell Biol *209*, 789–801. https://doi.org/10.1083/jcb.201503132.

Wilhelm, F.X., Wilhelm, M.L., Erard, M., and Duane, M.P. (1978). Reconstitution of chromatin: assembly of the nucleosome. Nucleic Acids Res *5*, 505–521. https://doi.org/10.1093/nar/5.2.505.

Williams, S.K., and Tyler, J.K. (2007). Transcriptional regulation by chromatin disassembly and reassembly. Curr Opin Genet Dev *17*, 88–93. https://doi.org/10.1016/j.gde.2007.02.001.

Winkler, D.D., Muthurajan, U.M., Hieb, A.R., and Luger, K. (2011). Histone chaperone FACT coordinates nucleosome interaction through multiple synergistic binding events. J Biol Chem *286*, 41883–41892. https://doi.org/10.1074/jbc.M111.301465.

Wisniewski, J., Hajj, B., Chen, J., Mizuguchi, G., Xiao, H., Wei, D., Dahan, M., and Wu, C. (2014). Imaging the fate of histone Cse4 reveals de novo replacement in S phase and subsequent stable residence at centromeres. ELife *3*, e02203. https://doi.org/10.7554/eLife.02203.

Witek, Ł., Janikowski, T., Bodzek, P., Olejek, A., and Mazurek, U. (2016). Expression of tumor suppressor genes related to the cell cycle in endometrial cancer patients. Adv Med Sci *61*, 317–324. https://doi.org/10.1016/j.advms.2016.04.001.

Wongwisansri, S., and Laybourn, P.J. (2004). Reconstitution of yeast chromatin using yNap1p. Methods Enzymol *375*, 103–117. https://doi.org/10.1016/s0076-6879(03)75007-1.

Wysocka, J. (2006). Identifying novel proteins recognizing histone modifications using peptide pull-down assay. Methods *40*, 339–343. https://doi.org/10.1016/j.ymeth.2006.05.028.

Xiao, H., Mizuguchi, G., Wisniewski, J., Huang, Y., Wei, D., and Wu, C. (2011). Nonhistone Scm3 Binds to AT-Rich DNA to Organize Atypical Centromeric Nucleosome of Budding Yeast. Molecular Cell *43*, 369–380. https://doi.org/10.1016/j.molcel.2011.07.009.

Xu, M., Long, C., Chen, X., Huang, C., Chen, S., and Zhu, B. (2010). Partitioning of histone H3-H4 tetramers during DNA replication-dependent chromatin assembly. Science *328*, 94–98. https://doi.org/10.1126/science.1178994.

Xue, Y.-M., Kowalska, A.K., Grabowska, K., Przybyt, K., Cichewicz, M.A., Del Rosario, B.C., and Pemberton, L.F. (2013). Histone chaperones Nap1 and Vps75 regulate histone acetylation during transcription elongation. Mol Cell Biol *33*, 1645–1656. https://doi.org/10.1128/MCB.01121-12.

Yamaguchi, S., Isejima, H., Matsuo, T., Okura, R., Yagita, K., Kobayashi, M., and Okamura, H. (2003). Synchronization of cellular clocks in the suprachiasmatic nucleus. Science *302*, 1408–1412. https://doi.org/10.1126/science.1089287.

Yamaguchi, L., Nishiyama, A., Misaki, T., Johmura, Y., Ueda, J., Arita, K., Nagao, K., Obuse, C., and Nakanishi, M. (2017). Usp7-dependent histone H3 deubiquitylation regulates maintenance of DNA methylation. Sci Rep *7*, 55. https://doi.org/10.1038/s41598-017-00136-5.

Yang, J., Zhang, X., Feng, J., Leng, H., Li, S., Xiao, J., Liu, S., Xu, Z., Xu, J., Li, D., et al. (2016). The Histone Chaperone FACT Contributes to DNA Replication-Coupled Nucleosome Assembly. Cell Rep *14*, 1128–1141. https://doi.org/10.1016/j.celrep.2015.12.096.

Yarmush, M.L., Golberg, A., Serša, G., Kotnik, T., and Miklavčič, D. (2014). Electroporation-based technologies for medicine: principles, applications, and

challenges. Annu Rev Biomed Eng *16*, 295–320. https://doi.org/10.1146/annurev-bioeng-071813-104622.

Zhang, Z.-M., Rothbart, S.B., Allison, D.F., Cai, Q., Harrison, J.S., Li, L., Wang, Y., Strahl, B.D., Wang, G.G., and Song, J. (2015). An Allosteric Interaction Links USP7 to Deubiquitination and Chromatin Targeting of UHRF1. Cell Rep *12*, 1400–1406. https://doi.org/10.1016/j.celrep.2015.07.046.

Zhang, H., Gan, H., Wang, Z., Lee, J.-H., Zhou, H., Ordog, T., Wold, M.S., Ljungman, M., and Zhang, Z. (2017). RPA Interacts with HIRA and Regulates H3.3 Deposition at Gene Regulatory Elements in Mammalian Cells. Mol Cell *65*, 272–284. https://doi.org/10.1016/j.molcel.2016.11.030.

Zhou, Z., Feng, H., Hansen, D.F., Kato, H., Luk, E., Freedberg, D.I., Kay, L.E., Wu, C., and Bai, Y. (2008). NMR structure of chaperone Chz1 complexed with histones H2A.Z-H2B. Nat Struct Mol Biol *15*, 868–869. https://doi.org/10.1038/nsmb.1465.

Zhou, Z., Feng, H., Zhou, B.-R., Ghirlando, R., Hu, K., Zwolak, A., Miller Jenkins, L.M., Xiao, H., Tjandra, N., Wu, C., et al. (2011). Structural basis for recognition of centromere histone variant CenH3 by the chaperone Scm3. Nature *472*, 234–237. https://doi.org/10.1038/nature09854.

Zhu, Y., Dong, A., Meyer, D., Pichon, O., Renou, J.-P., Cao, K., and Shen, W.-H. (2006). Arabidopsis NRP1 and NRP2 encode histone chaperones and are required for maintaining postembryonic root growth. Plant Cell *18*, 2879–2892. https://doi.org/10.1105/tpc.106.046490.

Zhu, X., Zhang, Y., Bjornsdottir, G., Liu, Z., Quan, A., Costanzo, M., Dávila López, M., Westholm, J.O., Ronne, H., Boone, C., et al. (2011). Histone modifications influence mediator interactions with chromatin. Nucleic Acids Research *39*, 8342–8354. https://doi.org/10.1093/nar/gkr551.

Zimmerman, Z.A., and Kellogg, D.R. (2001). The Sda1 protein is required for passage through start. Mol Biol Cell *12*, 201–219. https://doi.org/10.1091/mbc.12.1.201.

Zlatanova, J., Seebart, C., and Tomschik, M. (2007). Nap1: taking a closer look at a juggler protein of extraordinary skills. The FASEB Journal *21*, 1294–1310. https://doi.org/10.1096/fj.06-7199rev.

PROCEEDINGS AND WORKSHOPS

1. Participated in Kolkata Chapter of the **Society of Biological Chemists (India) Annual Meeting for 2020** in Shankarpur, Digha, West Bengal during March 19 - 21, 2021.

2. Participated and Presented poster on **"Biophysical and Biochemical characterisation of Testis-specific Y encoded-like protein 5: new participants of the NAP Histone chaperone family"** at 1st **"EMBO Workshop on Histone Chaperones: Structure, Function and Role in Development and Disease**, Crete, Greece (October 6 - 10, 2019).

3. Participated and Presented poster on **"Biophysical and Biochemical characterization of Testis-specific Y-encoded-like protein 5: new participants in an old enigma"** in **SINP International Cancer Meeting**, organized by Dr. Chandrima Das at Saha Institute of Nuclear Physics (SINP), Kolkata (September 27 - 28, 2018).

4. Participated in **SINP School on Epigenetics**, organized by Dr. Chandrima Das at Saha Institute of Nuclear Physics (SINP), Kolkata (September 26, 2018).

5. Attended a 2-day Workshop on **"Molecular Docking, Virtual Screening and Biologics Discovery"** organized by Schrodinger LLC. and Bose Institute, Kolkata (December 5 – 6, 2016).

LIST OF PUBLICATIONS

1. **<u>Dalui S</u>**, Dasgupta A, Adhikari S, Das C, Roy S, Human testis-specific Yencoded protein-like protein 5 is a histone H3/H4-specific chaperone that facilitates histone deposition in vitro, Journal of Biological Chemistry (2022), doi: https://doi.org/10.1016/j.jbc.2022.102200.

2. Dasgupta A, Mondal P, **<u>Dalui S</u>**, Das C, Roy S. Molecular characterization of substrate-induced ubiquitin transfer by UBR7-PHD finger, a newly identified histone H2BK120 ubiquitin ligase. FEBS J. 2021 Nov 5. (DOI: 10.1111/febs.16262. Epub ahead of print. PMID: 34739193.

Certificates

Certificate of Participation

This is to certify that

Sambit Dalui

has successfully participated in

SINP International Cancer Meeting 2018
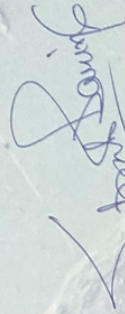
Cancer Biology – Still A Challenge in 21st Century

&

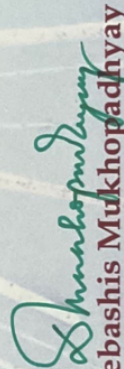### SINP School on Epigenetics

September 26-28, 2018

Saha Institute of Nuclear Physics

Kolkata, India

Chandrima Das
Chandrima Das
Joint Secretary

Debashis Mukhopadhyay
Debashis Mukhopadhyay
Joint Convener

Subrata Banerjee
Chairman
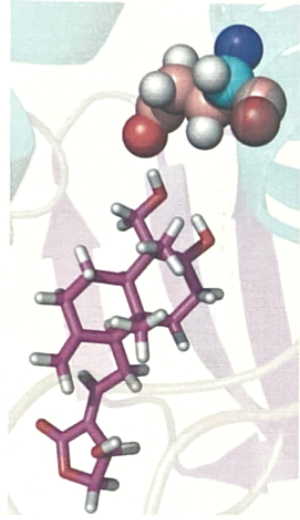
SCHRÖDINGER

Bose Institute

This is to certify that ...Saankit Dalui............ from...... IICB............has participated in a 2-day workshop on "Molecular Docking, Virtual Screening & Biologics Discovery" conducted by Schrödinger LLC. And Bose Institute on 5th and 6th December, 2016 at Department of Biophysics, Bose Institute, Kolkata, India.

Subhrangsu Chatterjee
Dr. Subhrangsu Chatterjee
Department of Biophysics, Bose Institute

Dr. Ravikumar. M
Sr. Applications Scientist, Schrödinger, India

CERTIFICATE
OF PARTICIPATION

This is to confirm that

Sambit Dalui

attended the EMBO Workshop

Histone chaperones: Structure, function and role in development and disease

from 06 – 10 October 2019 in Crete, Greece

Gerlind Wallon, PhD
EMBO Deputy Director

Date and location: 15 October 2019, Heidelberg

EMBO
excellence in life sciences

SOCIETY OF BIOLOGICAL CHEMISTS (I), KOLKATA CHAPTER

Organizes Symposium on

"Current Trends in Biology for Human Diseases and Medicine"

From 19-21st March 2021

&

Present this Certificate to

Sambit Dalui

in appreciation of Oral presentation/Co-Chair/Participation
in the conference at **Hotel "NEST" Shankarpur, Digha**

President	**Secretary**

Certificate

Presented to

SAMBIT DALUI

for participation in the

Training Programme On Laboratory Safety : Biosafety, Chemical Safety, Radiation Safety & Fire Safety.

Organized by

CSIR-Indian Institute of Chemical Biology, Kolkata
1st February 2016

Dr. D. Bhattacharyya
Chairman

Dr. R. K. Bhadra
Chairman

Dr. A. Bandyopadhyay
Chairman

Dr. M. C. Debnath
Organizing Secretary

Prof. Samit Chattopadhyay
Director

CSIR - Indian Institute of Chemical Biology

Enrolment No. : PhD CW / **2016/50**

(An autonomous body, under the Ministry of Science & Technology, Government of India)

Certificate

(Courses offered as per UGC guidelines, July 2009)

This is to certify that Mr./Ms. .... **Sambit Dalui** ....

has successfully completed the Ph.D Course Work conducted by CSIR-IICB for the session

2016

....

Uday Bandyopadhyay

Uday Bandyopadhyay
Chairperson, Academic Affairs Committee

Samit Chattopadhyay

Samit Chattopadhyay
Director

No. Sc. 0214

Jadavpur University

Registration Certificate

Shri/Sm _Sambit Dalui_

has been registered as a student of Ph.D. programme of this

university

His/her Registration Number is .....SLSBTl203517.....

Kolkata ...12.05.2017......   Registrar

Molecular characterization of substrate-induced ubiquitin transfer by UBR7-PHD finger, a newly identified histone H2BK120 ubiquitin ligase

Anirban Dasgupta[1], Payel Mondal[2,3], Sambit Dalui[1], Chandrima Das[2,3] (iD) and Siddhartha Roy[1] (iD)

1 Structural Biology and Bioinformatics Division, Council of Scientific and Industrial Research (CSIR) – Indian Institute of Chemical Biology, Kolkata, India
2 Biophysics and Structural Genomics Division, Saha Institute of Nuclear Physics, Kolkata, India
3 Homi Bhaba National Institute, Mumbai, India

Monoubiquitination of histone H2B at lysine 120 plays a vital role in active transcription and DNA damage response pathways. Ubiquitin protein ligase E3 component N-recognin 7 (UBR7) has been recently identified as an H2BK120 monoubiquitin ligase. However, the molecular details of its ubiquitin transfer mechanism are not well understood. Here, we report that the plant homeodomain (PHD) finger of UBR7 is essential for its association with E2 UbcH6 and consequent ubiquitin transfer to its substrate histone H2B. We also identified the critical region of UbcH6 involved in this function and shown that the residues stretching from 114 to 125 of histone H2B C-terminal tail are sufficient for UBR7/UbcH6-mediated ubiquitin transfer. We also employed antibody-independent mass spectrometry to confirm UBR7-mediated ubiquitination of the H2B C-terminal tail. We demonstrated that the PHD finger of UBR7 forms a dimer and this dimerization is essential for ubiquitination of histone H2B. We mapped the critical residues involved in the dimerization and mutation of these residues that abrogate E3 ligase activity and are associated with cancer. Furthermore, we compared the mode of ubiquitin discharge from UbcH6 mediated by UBR7 and RING finger protein 20 (RNF20) through a thioester hydrolysis assay. Interestingly, binding of substrate H2B to UBR7 induces a conformational change in the PHD finger, which triggers ubiquitin transfer from UbcH6. However, the RNF20 RING finger alone is sufficient to promote the release of ubiquitin from UbcH6. Overall, the mechanism of ubiquitin transfer by the newly identified E3 ubiquitin ligase UBR7 is markedly different from that of RNF20.

Introduction

The complex and elaborately packed state of DNA and histone proteins, folded into a 30-nm fibre within the eukaryotic nucleus, is referred to as chromatin. Structural studies of the chromatin fibre have revealed multiple tandem arrays of constituent units called nucleosomes [1], which are composed of 146-bp long DNA wrapped 1.65 times around two copies of H2A-H2B dimer and a single copy of H3–H4 tetramer

Journal Pre-proof

Human testis-specific Y-encoded protein-like protein 5 is a histone H3/H4-specific chaperone that facilitates histone deposition *in vitro*

Sambit Dalui, Anirban Dasgupta, Swagata Adhikari, Chandrima Das, Siddhartha Roy
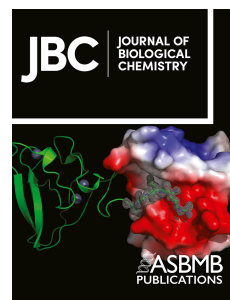
This is a PDF file of an article that has undergone enhancements after acceptance, such as the addition of a cover page and metadata, and formatting for readability, but it is not yet the definitive version of record. This version will undergo additional copyediting, typesetting and review before it is published in its final form, but we are providing this version to give early visibility of the article. Please note that, during the production process, errors may be discovered which could affect the content, and all legal disclaimers that apply to the journal pertain.

Sambit Dalui: Conceptualization, Methodology, Data curation, Investigation, Writing- Original draft preparation. Anirban Dasgupta: Investigation, Writing- Original draft preparation. Swagata Adhikari: Investigation, Chandrima Das: Conceptualization, Writing- Original draft preparation, Writing- Reviewing and Editing, Siddhartha Roy: Conceptualization, Methodology, Data curation, Supervision, Writing- Original draft preparation, Writing- Reviewing and Editing.

Human testis-specific Y-encoded protein-like protein 5 is a histone H3/H4-specific chaperone that facilitates histone deposition *in vitro*

Sambit Dalui[1], Anirban Dasgupta[1], Swagata Adhikari[2,3], Chandrima Das[2,3], Siddhartha Roy[1*]

[1]Structural Biology and Bioinformatics Division, Council of Scientific and Industrial Research (CSIR)-Indian Institute of Chemical Biology, Kolkata, India

[2]Biophysics and Structural Genomics Division, Saha Institute of Nuclear Physics, 1/AF Bidhannagar, Kolkata, India

[3]Homi Bhaba National Institute, Mumbai, India

* Corresponding author: Siddhartha Roy
Tel: +91-3324995733
E-mail: roysiddhartha@iicb.res.in

Running Title: TSPYL5 is an H3/H4-specific histone chaperone.

Keywords: Chromatin, Histone H3/H4, Histone Chaperone, NAP1, TSPYL5, Histone Deposition

Abstract

DNA and core histones are hierarchically packaged into a complex organization called chromatin. The nucleosome assembly protein (NAP) family of histone chaperones is involved in the deposition of histone complexes H2A/H2B and H3/H4 onto DNA and prevents non-specific aggregation of histones. Testis specific Y-encoded protein (TSPY)-like protein 5 (TSPYL5) is a member of the TSPY-like protein family, which has been previously reported to interact with ubiquitin-specific protease USP7 and regulate cell proliferation, and is thus implicated in various cancers, but its interaction with chromatin has not been investigated. In this study, we characterized the chromatin association of TSPYL5 and found that it preferentially binds histone H3/H4 via its C-terminal NAP-like domain both *in vitro* and *ex vivo*. We identified the critical residues involved in the TSPYL5-H3/H4 interaction and further quantified the binding affinity of TSPYL5 towards H3/H4 using bio-layer interferometry. We then determined the binding stoichiometry of the TSPYL5-H3/H4 complex *in vitro* using a chemical cross-linking assay and size exclusion chromatography-multi-angle laser light scattering (SEC-MALS). Our results indicate that a TSPYL5 dimer binds to either two histone H3/H4 dimers or a single tetramer. We further demonstrated that TSPYL5 has a specific affinity toward longer DNA fragments and that the same histone binding residues are also critically involved in its DNA binding. Finally, employing histone deposition and supercoiling assays, we confirmed that TSPYL5 is a histone chaperone responsible for histone H3/H4 deposition and nucleosome assembly. We conclude that TSPYL5 is likely a new member of the NAP histone chaperone family.

Introduction

Within the eukaryotic nucleus, chromatin exists as a highly compacted dynamic DNA-protein complex which regulates several critical cellular processes. Chromatin is constituted of functional units called Nucleosomes which in turn are comprised of core histone proteins wrapped around with a 146 base pair DNA in a left-handed superhelix. Each core histone octamer consists of two copies of each H2A, H2B, H3, and H4 (1). DNA-dependent cellular events like replication, transcription, and damage repair machinery require access to the free DNA which is regulated by the disassembly and reassembly of nucleosomes (2–5). Histones in their free state are prone to form non-nucleosomal aggregates. Hence, newly synthesized histones need constant governance during their import into the nucleus and subsequent repositioning onto DNA. Histone chaperones, which are a diverse group of proteins, bind to histones at the surfaces required for nucleosome formation (6–9) and shield them from non-nucleosomal interaction with the DNA (10). They are a multi-faceted group of proteins with distinct structural and functional properties which sometimes exhibit low or no sequence similarity with each other. However, with their involvement in histone folding and import, they are further implicated in histone de novo deposition, recycling, and exchange to maintain chromatin plasticity (8, 11). Some of the prominent histone chaperones that have been well studied and characterized include Nucleoplasmin (12), Chromatin assembly factor 1 (CAF-1), Ant silencing factor 1 (Asf1) (13–16), Facilitates chromatin transcription (FACT)(17, 18), Spt2 (19, 20), Regulator of Ty1 transposition 106 (Rtt106) (21–23) and Nucleosome assembly protein 1 (NAP1). NAP family of histone chaperones remains conserved from yeast to humans and are involved in cell-cycle regulation, transcription, replication, gene silencing, and apoptosis (24, 25). Structures of the yeast NAP1 (24), along with Vps75 (26–28) and human SET/TAF-1 (29) reveal that they have an N-terminal long helix and a globular domain at the C-terminus. In a dimeric state, the long helices interact with each other and form the dimerization interface while the two globular domains positioned at each end form the earmuff like structure. *In vivo* studies have previously shown that yeast NAP1 bind to histone H2A/H2B (24, 25, 30), but can also bind to H3/H4 *in vitro* (31). Most of the previous evidence suggested that the NAP1 dimer binds to a single H3/H4 dimer (31, 32). However, recent reports indicate that two H3/H4 dimers may also bind a single NAP1 dimer (30, 33, 34).

TSPYL5 belongs to the Testis-specific Y-encoded-like (TSPYL) protein family in humans and is found to be variably expressed in different tissues. Previous studies have shown that the TSPYL5 gene remains hypermethylated in nearly all of the primary gliomas and is a marker of the suppressor of cell growth. TSPYL5 also undergoes aberrant hypermethylation-mediated silencing in melanoma and increased methylation is correlated with disease progressions like gastric cancer and hepatocellular carcinoma (35, 36). Further, TSPYL5 was shown to modulate the growth of adenocarcinoma by regulating the cellular levels of p21(WAF1/Cip1) and the PTEN/AKT pathway in tern helps to grow resistance to cytotoxic agents such as γ-radiation (37). Recent reports suggests that TSPYL5 prevents USP7-dependent poly-ubiquitination of POT1 and its subsequent proteasomal degradation in ALT+ cells (38). TSPYL5 has also been reported to interact with USP7 to reduce the tumor suppressor activity of p53 and prevent oncogene-induced senescence (39, 40). TSPYL5 mediated activation of endoplasmic reticulum stress-induced apoptosis suppresses cell proliferation, migration, and invasion of tumor cells in colorectal cancer (41). Although tumor suppressor activity of TSPYL5 has also been reported in several cancers (42), no significant information is available regarding the role of TSPYL5 in chromatin-mediated processes. In this study, we identified human TSPYL5 as a novel member of the NAP histone chaperone family. Our data indicate that TSPYL5 preferentially binds to histones H3/H4 both *in vitro* and *ex vivo*. We have employed a biochemical and biophysical approaches to study the basis of TSPYL5 binding to histone H3/H4. In addition, we characterized TSPYL5-H3/H4 complex and their binding stoichiometry through size exclusion chromatography coupled with multi-angle light scattering (SEC-MALS) and chemical cross-linking assays. Further, we established the role of TSPYL5 as an H3/H4 specific histone chaperone using histone deposition and plasmid supercoiling assays.

Results

TSPYL5 exhibits homology with the NAP histone chaperone family

Nucleosome assembly proteins (NAP), that are characterized by the conserved α/β-earmuff motif across different species, facilitate *in vitro* assembly of nucleosomes (24). To find out possible proteins with sequence and structural similarity with TSPYL5, we employed multiple sequence alignment using NAP family proteins across different species. The alignment result suggests that TSPYL5 is a homolog of NAP family proteins that remains conserved among eukaryotes. (Fig 1a). The C-terminal stretch of TSPYL5 (198-398) shows significant sequence similarity with the SET/TAF1B and other NAP family proteins harboring the signature NAP fold, indicating the presence of NAP like domain (NLD) in TSPYL5. However, TSPYL5-NLD significantly lacks the extended NAP1 Accessory region present in most of the NAP family proteins across different species. The majority of the NAP family proteins share a common Acidic Region (AR) comprising mostly of Aspartate and Glutamate residues in their C-terminal stretch. Unlike other NAP family proteins, the Acidic Region (AR) of TSPYL5 is present at the N-terminus of the NLD (Fig 1b). Interestingly, compared to other eukaryotes, the NAP proteins in the human genome exist as multiple diverse sub-families. To understand the similarity between the different NAP family proteins in humans, we generated a phylogenetic tree using a maximum likelihood approach. Tree data shows the divergence of human NAP proteins into three distinguished sub-families- NAP1-Like proteins (NAP1L), TSPY proteins, and TSPY-Like proteins, while human SET/TAF1b diverged and remained distinct from the above sub-families (Fig. 1c). To obtain a detailed understanding of the structure of TSPYL5-NLD, we took recourse to molecular modelling using the AlphaFold software package. From the AlphaFold prediction, TSPYL5 was found to form a ''headphone'' structure consisting of 2 distinct regions. Region-I contained an extended helix (α-1) spanning 50 amino acid residues which form the ''head'' segment of the headphone structure. Region-II consists of the globular α/β ''earmuff'' segment of the headphone. This globular domain contains 4 antiparallel β-strands (β1–β4) and with 4 short α-helices (2, 3, 4, 5). β-strands forms a β-sheet and the short α-helices are arranged back side of the β-sheet headphone (Fig. 1d). We also generated the molecular model of TSPYL5 using the RoseTTAFold

server which is similar to the AlphaFold model (RMSD of the C_α atom is 2 Å). To check whether TSPYL5 showed structural similarity with the previously reported crystal structure of human SET/TAF-1B (PDB ID: 2E50), we superimposed them which revealed that TSPYL5 shared a similar structural fold with SET/TAF1B (RMSD is 2.2 Å) (Fig 1e).

TSPYL5 interacts specifically with Histone H3/H4 dimer

NAP family member proteins have been reported to be involved in multiple pathways including nucleocytoplasmic shuttling, chromatin assembly, remodeling, replication, transcription, gene silencing, and apoptosis (24, 25, 43–47) which requires cytoplasmic or nuclear localisation or both. To look into the localization of TSPYL5, we performed a cell fractionation assay using FLAG-TSPYL5 transfected HEK293T cell line. TSPYL5 was found to be present in both cytosolic and nuclear fractions (Fig 2a). Nuclear localization of TSPYL5 however raises the possibility of it having a role in a chromatin context, which has not yet been studied. Previously, NAP family histone chaperones have been widely reported to interact with both histones H2A/H2B and H3/H4 (25, 31). To identify histone interacting partners of TSPYL5, we performed a FLAG Immuno pulldown assay using overexpressed FLAG-TSPYL5 in HEK293T cells followed by immunoblotting with different histone antibodies. Results showed that TSPYL5 specifically interacts with histones H3 and H4 but not with histones H2A and H2B (Fig 2b). Next, we wanted to look into the histone interaction of endogenous TSPYL5. Since endogenous expression of TSPYL5 is significantly higher in the SH-SY5Y cell line compared to HEK293T, we performed an immunopulldown assay involving endogenous TSPYL5 in SH-SY5Y cells. Pulled samples using anti-TSPYL5 antibodies were immunoblotted with different histone antibodies, whereby TSPYL5 was found to interact specifically with H3 and H4 (Fig 2c). We further confirmed the interaction of TSPYL5 with histone H3/H4 by performing a reverse IP with an anti-H3 antibody (Fig. 2d). To check if TSPYL5 directly interacts with histones H3/H4, we further performed a GST pulldown assay using recombinant TSPYL5 and histones. *In vitro* pulldown assay indicates that TSPYL5 directly interacts with histone H3/H4 but not with histone H2A/H2B (Fig 2e). Next, to identify the region of TSPYL5 involved in H3/H4 interaction, we expressed and purified different deletion constructs of TSPYL5 and checked for their

H3/H4 binding ability through a GST pulldown assay. TSPYL5-NLD binds with histone H3/H4 with an intensity comparable to that of TSPYL5-FL, while TSPYL5-ΔNLD fails to interact (Fig. 2f). Thus, TSPYL5-NLD is essential for its interaction with histone H3/H4.

Mapping of TSPYL5 and histone H3/H4 interacting surface

We next attempted to fine-map the regions involved in histone H3/H4-TSPYL5 interaction. To identify the TSPYL5 binding surface of histone H3, we generated different biotinylated H3 peptide fragments encompassing full length histone H3. We performed an *in vitro* peptide-pulldown assay to score the interaction between H3 peptides and TSPYL5-NLD and observed that histone peptides involving the C-terminal H3 tail, encompassing 105-120 and 120-136 region, both showed significant interaction with TSPYL5-NLD (Fig. 3a). To quantify the affinity of TSPYL5-NLD towards histone H3 C-terminal region, we employed Bio-Layer Interferometry (BLI) and confirmed that TSPYL5-NLD binds to histone H3 C-terminal tail (120-136) with a significantly higher affinity (K_d = 4.19 ± 2.78 μM) compared to other histone H3 peptides (Fig. 3b). To further investigate if the C-terminal tail of H3 was sufficient for TSPYL5 interaction, we generated and purified histone H3 C-terminal tail deleted protein (H3ΔC) which lacks the last 21 residues. We then employed a GST pulldown assay using histone H3-WT and H3ΔC. The assay indicates a significant loss of interaction of histone H3ΔC with TSPYL5 compared to H3-WT (Fig. 3c). To check whether H3 C-terminal tail deletion had any effect on its conformation, we performed CD spectroscopy with histone H3-WT and H3ΔC-term mutants and did not observe any significant structural change upon the deletion (Fig. 3d). To map the residues of TSPYL5 that are involved in histone H3/H4 binding, we constructed three different histone binding deficient mutants (HBM), namely HBM1 (S268A/E270A), HBM2 (S340A/N343A/E345A) and HBM (1+2) (S268A/E270AS340A/N343A/E345A). These mutations have been highlighted in the TSPYL5-NLD model (cartoon representation) (Fig. 3e). Next, we performed GST pulldown assay, where HBM (1+2) exhibited a significant reduction in H3/H4 binding concerning WT (Fig. 3f). Subsequently, in order to confirm that the structural conformation of TSPYL5 remains unaltered upon mutations, we performed CD spectroscopy and found no significant conformational changes between WT and HBM mutants (Fig. 3g). We further quantified

the binding affinity of TSPYL5 towards histone H3/H4 using BLI. TSPYL5-FL and NLD showed significant affinity towards histone H3/H4 with K_d = 2.58 ± 0.33 and 2.16 ± 0.40 µM respectively. However, HBM (1+2) showed no detectable binding to H3/H4. The affinity of TSPYL5 and other mutants towards histone H3/H4 was also investigated using BLI kinetics and K_d values were summarised (Fig. 3h-i).

Determination of molecular stoichiometry of TSPYL5-H3/H4 complex

To gain further insights into the molecular stoichiometry of the TSPYL5-H3/H4 co-complex in solution, we used size-exclusion chromatography coupled with multiple-angle light scattering (SEC-MALS) to measure the molecular mass of the individual proteins as well as the complex. The measured mass of TSPYL5 was obtained at 34.39 (4% error) and 73.92 kDa (2.6% error) respectively. The corresponding expected monomer and dimer mass of TSPYL5 was 36 kDa and 72 kDa. This indicated that TSPYL5 in high salt conditions exists predominantly as a monomer to a lesser extent as a dimer. In a similar high salt condition, H3/H4 molecular mass was measured at 54.83 kDa (error 2%, expected histone H3/H4 tetramer mass was 56 kDa). Interestingly, in the case of the TSPYL5-H3/H4 complex, we obtained a molecular mass of 128.31 kDa, suggesting the molar stoichiometry of the complex to be TSPYL5:H3:H4(2:2:2). (Fig. 4a & 4b). We further performed DSS mediated protein crosslinking experiments to confirm the presence of the TSPYL5-H3/H4 complex in solution. Upon crosslinking, TSPYL5 and H3H4 together yielded a higher molecular weight species between 150 and 100kDa which was significantly absent when TSPYL5-NLD and H3/H4 were crosslinked individually. Western blot results using anti-H3 and anti-TSPYL5 antibodies confirmed the presence of the TSPYL5-H3/H4 complex (Fig. 4c). SEC-MALS and solution crosslinking studies indicate that the TSPYL5 dimer forms a complex with two H3/H4 dimers or one tetramer. To find out if TSPYL5 differentiates between H3/H4 dimer and tetramer, we generated a tetramerization disruptive mutant (H3M/H4) with C110E/L126R/I130E mutation and performed a GST pulldown assay. TSPYL5 was found to bind equally with H3/H4 dimer (involving H3M/H4) and H3/H4 tetramer indicating that TSPYL5 does not differentiate between histone H3/H4 dimer and

tetramer (Fig. 4d). Collectively, these results indicate that one TSPYL5 dimer can bind with two histone H3/H4 dimers or a single H3/H4 tetramer (Fig. 4e).

TSPYL5 binds to DNA *in vitro*

Histone chaperones, apart from their ability to interact with histones, also have been reported to bind DNA to regulate DNA mediated processes (48, 49). To check if TSPYL5 has DNA binding ability, we used an electrophoretic mobility shift assay (EMSA) using different DNA fragments ranging from 10 to 330 base pair (bp) as a substrate, where TSPYL5-NLD was found to bind to DNA above 80 bp length but had no binding with the shorter fragments of DNA (Fig 5a). To further investigate if the specific length of DNA fragment was a prerequisite for TSPYL5 binding, we performed EMSA with 20, 40, 80, and 146 bp dsDNA substrates individually and analysed the binding affinity of TSPYL5 towards them. We found that TSPYL5 shows no significant binding towards 20 bp and 40 bp DNA. On the other hand, it showed a high affinity toward 80 bp and 146 bp DNA (Fig 5b). Interestingly, while a minimum of 80 bp DNA is required to dock H3/H4 tetramer, 146 bp DNA is required to assemble a complete nucleosome. Thus, TSPYL5 binding to these longer DNA fragments indicates that it may have a role in DNA mediated histone deposition process. To further quantify the DNA binding affinity of TSPYL5, we measured the substrate DNA depletion in EMSA assays and the binding curve was plotted against increasing concentration of TSPYL5. From the binding data, TSPYL5 shows strong binding toward 80 and 146 bp of DNA with dissociation constant (K_d) values of 0.5 and 0.38 μM respectively (Fig 5c). To find out if NLD is sufficient for the DNA binding of TSPYL5, we used TSPYL5-ΔNLD and found no detectable DNA binding. This indicates that NLD is essential and sufficient for the DNA binding activity of TSPYL5 (Fig. 5d). To explore if the histone binding residues of TSPYL5 were also involved in its DNA binding, we performed EMSA using histone binding deficient mutant TSPYL5-HBM (1+2). We observed no significant DNA binding which suggests that the DNA binding surface of TSPYL5 may overlap with its histone binding surface (Fig. 5e).

TSPYL5-H3/H4 complex facilitates histone deposition and plasmid supercoiling *in vitro*

To determine if TSPYL5 acts as a bonafide histone H3/H4 chaperone, we performed an *in vitro* histone deposition assay. Upon incubation, TSPYL5-NLD in increasing concentration was able to deposit H3/H4 on to linear DNA substrate (Fig. 6a). On the other hand, histone binding deficient mutant TSPYL5-HBM (1+2), having impaired association towards histone H3/H4 *in vitro*, was unable to deposit histones (Fig. 6b). To investigate if TSPYL5 could facilitate DNA supercoiling upon histone deposition, we performed a plasmid supercoiling assay using Topoisomerase-I treated relaxed plasmid DNA. Increasing concentrations of TSPYL5-NLD resulted in efficient supercoiling of plasmid DNA, suggesting that TSPYL5 may have a role in promoting DNA supercoiling upon histone deposition. However, the TSPYL5-HBM (1+2), failed to facilitate plasmid supercoiling *in vitro* (Fig. 6c). Together, these results suggest that histone binding residues of TSPYL5 are critical for its histone deposition and plasmid supercoiling activity.

Discussion

Chromatin assembly involves a two-step process in which a histone H3/H4 dimer is deposited first onto the DNA followed by two H2A/H2B dimers, assisted by different histone chaperones (50, 51). NAP family of histone chaperones are conserved from yeast to higher eukaryotes. In humans, NAP family proteins have diverged into different sub-families – including NAP1-like (NAP1L1–5)(52), Testis-specific protein Y-encoded (TSPY1-10)(40), TSPY-like (1-6) and SET/TAF-1B (53). Despite sharing little sequence similarity, members of the NAP family (24) exhibit high structural conservation among each other. Yeast NAP1, the first reported member of the NAP protein family, has been majorly described as an H2A/H2B specific histone chaperone (10, 24, 25, 31, 33, 47, 54). Crystal structure of yNAP1 bound to H2A–H2B (55) together with *in vitro* and *in vivo* functional studies provides molecular evidence of NAP1 binding to H2A/H2B. In contrast, we found that TSPYL5 specifically interacts with histone H3/H4 and not with H2A/H2B in both overexpressed and endogenous conditions. Using recombinant proteins, we further confirmed the direct interaction of TSPYL5 with histone H3/H4. Interestingly, Vps75, which is a yeast homolog of NAP1, and human

SET/TAF-1B also show binding preference towards histone H3/H4 over H2A/H2B (7, 27, 28). To identify the histone interacting region of TSPYL5, we next generated a construct encompassing the C terminal NAP-like domain (NLD) of TSPYL5 and another construct with the TSPYL5 N-terminal stretch including its acidic region (AR). NLD was found sufficient for H3/H4 binding thus indicating that TSPYL5 interacts with H3/H4 via its NLD and not through its N-terminal region.

Although multiple NAP family members in humans have been reported to interact with histones, their binding surfaces have not been well studied. Our results revealed that TSPYL5 utilizes the loops, connecting the small helices located at the globular C-terminal NAP-like domain, for its histone binding. The involved loops were found to be present on the surface of the earmuff domain. On the other hand, it was intriguing to explore the specific region of histone H3 involved in TSPYL5 binding. We found that the H3 C-terminal tail exhibited strong interaction with TSPYL5. This was further validated using an H3 C-terminal tail deletion which abolished the TSPYL5 interaction. In contrast, yNAP1 has been found to interact with the N-terminal tail of histone H3 *in vitro* (31). This indicates that the binding modes of histones to different NAP family proteins may involve different binding regions.

We determined the binding stoichiometric ratio of the TSPYL5-H3/H4 complex to be 2:2:2 based on the obtained molecular mass of the complex in solution which suggests that a TSPYL5 dimer can bind with either two H3/H4 dimers or a single H3/H4 tetramer. Using an H3/H4 tetramer disruptive mutant, we found that TSPYL5 didn't differentiate between H3/H4 dimer and tetramer binding. The formation of a stable TSPYL5-H3/H4 complex of 128 kDa was further confirmed by cross-linking assay. Histone H3/H4 binding preference as exhibited by TSPYL5 is similar to Vps75, which interacts with both dimeric and tetrameric forms of histone H3/H4. Thus, it seems likely that TSPYL5 engages with histones H3/H4 in a similar way as Vps75 (7, 28), which assembles two H3/H4 dimers during nucleosome assembly or is involved in capturing the H3/H4 tetramer evicted during chromatin disassembly in replication-independent and replication-dependent processes.

Histone chaperones, which are directly involved in the DNA mediated histone deposition process, display DNA binding properties alongside their histone interacting ability. Yeast CAF1, which is involved in nucleosome assembly during replication shows DNA binding properties through the

coiled-coil and WHD regions of the Cac1 sub-unit (48, 49). Moreover, Rtt106 and HIRA, which are involved in the direct deposition of different histone H3 variants, bind DNA directly (56–58). Our findings denote that TSPYL5 has similar DNA binding property with a specific affinity towards 80 bp and higher length DNA fragments, but not with its shorter counterparts. It is noteworthy that yCAF1 also shows a similar mode of DNA binding. Moreover, our biochemical assays demonstrate that TSPYL5 promotes histone H3/H4 deposition and plasmid supercoiling *in vitro*, thereby confirming its histone chaperone activity. This suggests that TSPYL5 may have a direct role in DNA mediated nucleosome assembly process. Additionally, TSPYL5 has been previously shown to interact with USP7 (38,39). Interestingly, USP7 has been shown to negatively regulate UHRF1 mediated histone H3 ubiquitination (59, 60). In this context, it may be worthwhile to study the role of TSPYL5 in modulating USP7 mediated histone deubiquitination by its histone H3/H4 chaperone activity. In summary, our results established TSPYL5 as a new member of the human NAP histone chaperone family and confirm it as a histone H3/H4 specific chaperone.

Experimental procedures

Cloning and site-directed mutagenesis

TSPYL5 Full length, NLD (198-388), and ΔNLD (1-203) were cloned in the pGEX-6p-1 vector (GE Healthcare, GE28-9546-48) with N-Terminal GST tag for bacterial expression. TSPYL5-NLD was also cloned in the pETite N-His-SUMO expression vector (Lucigen, 49003-2) using the Expresso® T7 cloning system and modified by adding a PreScission protease recognition site for removal of the tags. All the point mutations were generated using QuickChange Site-directed mutagenesis kit (Stratagene, #200524). Histones H3 and H4 were PCR-amplified from cDNA isolated from HEK293T cells and cloned sequentially in both the multiple cloning site of the pETDuet-1 vector. Histone H3 has an N-terminal His-tag while H4 was untagged. Histone H3/H4 tetramer disruptive mutant (H3M) was also generated in the H3-H4 pETduet1 vector using site-directed mutagenesis according to previously described methods (61, 62). H3 C-terminal tail deleted construct (H3ΔC-term, 1-114), was also prepared in pETite N-His vector using the T7-His cloning system (Lucigen). All the clones were confirmed by sequencing.

In-Vitro Protein expression and purification

Chemically competent Rosetta™(DE3) pLysS cells (Novagen, 70956) were transformed with different TSPYL5 constructs. Cells were grown in a 37°C shaker incubator till OD600 reached 0.8 and then induced using 1mM IPTG (Gold BioI-2481C100) at 18°C for 16 hours. GST tagged proteins were purified in the GST affinity column, and subsequently eluted using reduced Glutathione. For biophysical assays, GST proteins were then cleaved by PreScission protease. His-SUMO tagged TSPYL5-NLD was expressed similarly as mentioned above. Protein was trapped with Ni-NTA bead (BIORAD, 780-0800), eluted, and purified on Superdex 200 Increase 16/600 GL gel filtration column in HBS Buffer (20mM HEPES pH 7.5, 500mM NaCl, 1mM TCEP, 5% Glycerol, 1mM PMSF). Histone H3/H-WT and H3M/H4 pETDuet-1 constructs were expressed in BL21(DE3) pLysS cells (Thermo Fisher Scientific, C606010) and induced with IPTG at 37°C for 4 hours. Recombinant His-tagged human histones H3, H3ΔC-term, and H4 were expressed in BL21(DE3) pLysS cells followed by purification and refolding following standard procedures (63). Eluted His tagged H3/H4 was further purified on gel filtration column using high salt HBS Buffer (20mM HEPES pH 7.5, 2M NaCl, 1mM TCEP, 5% Glycerol, 1mM PMSF). All purified proteins were concentrated, flash-frozen, and stored at -80ºC until further use.

Antibody generation

Polyclonal anti-TSPYL5 antibody was raised using purified recombinant TSPYL5-NLD protein. An amount of 200 mg of purified recombinant TSPYL5-NLD was injected subcutaneously into NZ white rabbit using Freund complete adjuvant in a 1: 1 ratio. This was followed by five booster doses at every 2-week interval after the first injection. The booster doses were given using Freund's incomplete adjuvant. Serum was obtained from blood collected from the sixth bleed and finally, purified TSPYL5 antibody was obtained by affinity chromatography. The specificity of the generated anti-TSPYL5 antibody was checked by assessing their binding to various concentrations of recombinant TSPYL5 protein by western blot.

Cell culture and cell fractionation

HEK293T and SHSY5Y cells were grown and maintained in Dulbecco's modified Eagle's medium (DMEM) (Gibco) at a 37 °C incubator supplied with 5% CO2. DMEM was supplemented with 10%

FBS (Gibco), 1% antibiotic-antimycotic (Gibco), and 1% essential amino acids (Gibco). Untransfected and FLAG-TSPYL5 transfected HEK293T cell pellets were resuspended in Hypotonic Buffer (10 mM HEPES, pH 7.4, 10 mM NaCl, 6 mM $MgCl_2$, 2 mM DTT, 0.05% NP40, 2 mM PMSF, 1X PIC), incubated on ice for 1hour and centrifuged at 3000 rpm for 5 mins. The supernatant fraction was collected as a cytosolic fraction. The pellet fraction was treated with DNase I in Nuclear extraction buffer (20 mM HEPES pH 7.4, 420 mM NaCl, 1.5 mM $MgCl_2$, 0.2 mM EDTA, 1 mM DTT, 20% Glycerol, 0.5% NP40) and incubated at 37°C for 30 mins followed by centrifugation at 13000 rpm for 10 mins at 4°C. The supernatant fraction thereafter collected was marked as a nuclear fraction and the pellet was discarded. Fractionation was analyzed by western blotting using anti-TSPYL5, anti-Tubulin (BIORAD, MCA78G) as a cytosolic marker, and anti-histone H3 (Abcam, ab10799) as a Nuclear marker.

Western blot analysis

For preparing whole cell lysates, cells were re-suspended in Laemmli Buffer (4% SDS, 20% Glycerol, and 120 mM Tris-HCl pH 6.8) (64) and sonicated before analysing by Western blot. Samples were run on 11% or 15% SDS-PAGE and transferred on PVDF membrane followed by blocking with 5% BSA in 1x TBS-T (Tris-Buffer Saline with 0.1% Tween-20) and probed with specific antibodies.

Immunoprecipitation (IP)

Cells were cross-linked with 4% paraformaldehyde in PBS for 15 mins at room temperature, lysed with IP buffer (50 mM HEPES pH7.5, 150 mM NaCl, 1.5 mM $MgCl_2$, 1 mM EDTA, 1% Triton X-100, 5% Glycerol, 1 mM DTT, 2 mM Protease inhibitor cocktail) and incubated on ice for 1 hour followed by sonication. Lysates were then centrifuged, collected supernatant was pre-cleared with IgG antibody, and IP was performed with FLAG (Sigma, F1804), H3 (Abcam, ab10799), and TSPYL5 antibodies. After washing thoroughly with the same buffer, IP samples were analysed by western blotting.

In-vitro Protein-Protein interaction studies

GST pulldown was performed where GST-fusion proteins along with histones were incubated in an equal molar ratio in GST-IP buffer (50 mM HEPES pH 7.5, 150 mM NaCl, 0.05% NP40, 1 mM DTT, 5% Glycerol, 1 mM PMSF). Pre-blocked Glutathione Sepharose (GST) beads (GE Healthcare, 17-

0756-01) were used for pulldown, and beads were washed in the same buffer and analysed by western blotting.

Bio-layer Interferometry (BLI) study for kinetic assay

BLI was used to study protein-protein binding kinetics (65) using the Octet-RED system (Forte´ Bio). For various assays, recombinant His tagged histones H3/H4 or H2A/H2B were immobilised on Ni-NTA Biosensors (Forte´ Bio NTA, 18-5102) in Binding buffer (50 mM HEPES pH 7.5, 150 mM NaCl, 0.05% NP40, 1 mM DTT, 5% Glycerol, 0.5 mg/ml BSA) and TSPYL5 WT and histone binding deficient mutants were used as analyte with increasing concentration. All the data were recorded in triplicates. Reference subtraction, Savitsky-Golay filtering, and local fitting of kinetic rates association and dissociation of the collected data were analysed using Forte´ Bio's software (version 11x).

Peptide pull-down assay

Biotinylated Histone H3 Peptides were purchased from GL-Biochem: H3 (1-21), H3 (21-44), H3 (44-69), H3 (69-89), H3 (105-120), H3 (120-135). Biotinylated Histone H3 peptides were incubated with GST (Control) and GST-TSPYL5 in peptide IP Buffer (50 mM Tris-HCl pH 7.5, 200 mM NaCl, 0.05% NP40, 1 mM DTT) at 4°C overnight. The next day pre-blocked streptavidin beads (GE Healthcare, 17-5113-01) were added to the samples to bind for 2 hours at 4°C. Bead-bound samples were washed in IP Buffer and analysed by western blot.

TSPYL5-H3/H4 complex purification

His-tagged H3/H4 in pETDuet-1 and His-SUMO tagged TSPYL5-NLD were co-expressed in Rosetta™(DE3) pLysS cells and were purified by His tagged affinity chromatography using Ni-NTA beads. Proteins were eluted using 500 mM imidazole in high salt HBS buffer. Eluted samples were loaded on Enrich SEC70 column using Next-Gen FPLC system (BIORAD) in high salt HBS buffer (20 mM HEPES pH 7.5, 2 M NaCl, 1 mM TCEP, 5% Glycerol) for purification. Fractions containing the complex were pooled and concentrated up to 10 mg/ml using Amicon centrifuge filter units (Millipore, ACS510012) and maintained at 4°C or flash frozen and stored at −80°C for further use.

DSS cross-linking experiments

DSS cross-linking experiments were performed using previously described methods (62). Briefly, TSPYL5-NLD, H3/H4, and TSPYL5-NLD-H3/H4 complex were incubated with a 1.5 mM DSS crosslinker (Thermo Scientific, 21655) for 30 mins at 25°C in Cross-linking buffer (20 mM HEPES pH 7.5, 150 mM or 300 mM NaCl, 1 mM TCEP). Reactions were quenched by the addition of 50 mM Tris-HCl pH 8.0, for 15 mins at 25°C, and samples were analysed in 12% SDS-PAGE and transferred to PVDF membranes, and incubated against H3, H4, and TSPYL5 antibodies. To perform this experiment, we incubated His-SUMO tagged TSPYL5-NLD and H3/H4 alone or with DSS and resolved crosslinked complexes by SDS-PAGE followed by western blot.

SEC-MALS of protein complexes

Purified TSPYL5-NLD-H3/H4 complex was analysed using SEC with Multi-angle Laser-light Scattering (SEC-MALS) connected with Enrich SEC 70 column equilibrated in high salt HBS buffer. The light scattering (LS) intensity, and differential refractive index (dRI) of the column eluate were recorded using a DAWN HELEOS8+laser photometer, Optilab T-rEX differential refractometer (Wyatt Technology) respectively. The weight average molecular mass of the sample peaks in the eluate was determined as a measure of the combined data from both detectors using ASTRA software Version 7.3.2 using 0.186 ml/g value of dn/dc.

Electrophoretic mobility shift assays

TSPYL5-NLD, HBM(1+2) and ΔNLD were used in increasing concentration (0.06, 0.125, 0.25, 0.5, 1, 2, 4, 8, 16 or 32 uM) and incubated with 20, 40, 80 bp and 146 bp dsDNA or 10bp ladder (Invitrogen, Cat. No. 10821-015) respectively in EMSA buffer (10 mM HEPES pH 7.5, 200 mM NaCl, 1 mM TCEP, 5% glycerol, 0.5 mM EDTA). The samples were maintained on ice for 30 min and then shifted at 25°C for 20 min before analysis. The binding reactions were analysed on a 6% native 1x TRIS-Glycine pH 8.3 PAGE using 1x TRIS-Glycine running buffer. The gel was stained with GelGreen™ (GoldBio, G745). Band intensities were quantified by Image-J software and the data were analysed in Prism 5.0 software using a Hill equation binding model.

Histone deposition assays

TSPYL5-NLD WT and HBM (1+2) mutant along with histones H3/H4 were incubated with 146 bp Widom 601 sequence DNA (Widom et al. 1998) in Tetrasome assembly buffer (10 mM HEPES pH 7.5, 200 mM NaCl, 1 mM TCEP, 5% glycerol, 0.5 mM EDTA). The samples were incubated at 25°C for 30 mins before analysis on a 6% native gel using 1x TAE as running buffer and stained in GelGreen™.

Plasmid supercoiling assay

Histone H3/H4 were incubated with increasing concentrations of TSPYL5-NLD in Supercoiling assay buffer (10 mM HEPES pH 7.5, 150 mM NaCl, 0.5 mM EDTA, 10% glycerol, and 10 mg/mL BSA) at 37°C for 30 mins. pBlueScript supercoiled plasmid DNA (66) were also treated with Topoisomerase I (Thermo Scientific, 38042024) for 30 mins separately. Topoisomerase treated relaxed plasmid DNA was added to the TSPYL5-NLD-H3/H4 mix and incubated for an additional 1 hr. at 25°C. Reactions were quenched by adding an equal volume of Stop buffer (25% Glycerol, 60 mM Tris-HCl, pH 8.0, 30 mM EDTA, 2% SDS) and incubated for another 30 mins. Samples were resolved by electrophoresis in 1.0% agarose gel followed by GelGreen™ staining.

Protein structural modelling

Structural modelling of the TSPYL5-NLD was done by the AlphaFold package which utilised the machine-based deep learning algorithm to design the model (67, 68). Similar model building software RoseTTA Fold (69) was also used for structural modeling of the TSPYL5-NLD. The crystal structure of SET/TAF1B (PDB ID: 2E50) obtained from the RCSB Protein Data Bank was used for superimposition analysis. The structural figures were created using PYMOL (Schr¨odinger, LLC, New York, NY, USA).

Phylogenetic tree analysis

Amino acid sequences of human NAP family proteins (NAP1-Like, SET/TAF1β, TSPY, TSPY-Like family proteins) were retrieved from the Uniprot database in FASTA format. Multiple sequence alignments using the MUSCLE program in MEGAX (70) software package were performed and these aligned sequences were used to generate the phylogenetic tree. The tree depicting evolutionary history was generated by the Maximum Likelihood method and JTT matrix-based model (71) by applying a total of 250 bootstrap iterations. The generated tree was exported and the figure for the phylogenetic

tree was prepared using Fig-Tree software. Structure based sequence alignment of human TSPYL5 with SET/TAF1-β and NAP1 proteins (from different organisms representing different phyla) using Espript3 (72) where the structure of SET/TAF1-β (PDB: 2E50) used a template.

Acknowledgments

Author Contributions

SD, AD, CD, and SR conceived the study, designed experiments, analysed data, and wrote the manuscript. SD, AD, and SA performed experiments and analysed the data. All authors reviewed the results and approved the final version of the manuscript.

Funding

Conflict of interest

The authors declare no conflict of interest.

Data availability

All relevant data are included in this manuscript.

References

1. Luger, K., Mäder, A. W., Richmond, R. K., Sargent, D. F., and Richmond, T. J. (1997) Crystal structure of the nucleosome core particle at 2.8 Å resolution. *Nature.* **389**, 251–260

2. Allis, C. D., and Jenuwein, T. (2016) The molecular hallmarks of epigenetic control. *Nat. Rev. Genet.* **17**, 487–500

3. Lai, W. K. M., and Pugh, B. F. (2017) Understanding nucleosome dynamics and their links to gene expression and DNA replication. *Nat. Rev. Mol. Cell Biol.* **18**, 548–562

4. Nicetto, D., Donahue, G., Jain, T., Peng, T., Sidoli, S., Sheng, L., Becker, J. S., Grindheim, J. M., Blahnik, K., Garcia, B. A., Tan, K., Bonasio, R., Jenuwein, T., and Zaret, K. S. (2019) Supplementary Materials for developmental lineage specification. *Science.* **363**, 294–297

5. Yadav, T., Quivy, J. P., and Almouzni, G. (2018) Chromatin plasticity: A versatile landscape that underlies cell fate and identity. *Science (80-.).* **361**, 1332–1336

6. Mattiroli, F., D'Arcy, S., and Luger, K. (2015) The right place at the right time: chaperoning core histone variants. *EMBO Rep.* **16**, 1454–1466

7. Hammond, C. M., Sundaramoorthy, R., Larance, M., Lamond, A., Stevens, M. A., El-Mkami, H., Norman, D. G., and Owen-Hughes, T. (2016) The histone chaperone Vps75 forms multiple oligomeric assemblies capable of mediating exchange between histone H3-H4 tetramers and Asf1-H3-H4 complexes. *Nucleic Acids Res.* **44**, 6157–6172

8. Hammond, C. M., Strømme, C. B., Huang, H., Patel, D. J., and Groth, A. (2017) Histone chaperone networks shaping chromatin function. *Nat. Rev. Mol. Cell Biol.* **18**, 141–158

9. Pardal, A. J., Fernandes-Duarte, F., and Bowman, A. J. (2019) The histone chaperoning pathway: from ribosome to nucleosome. *Essays Biochem.* **63**, 29–43

10. Andrews, A. J., Chen, X., Zevin, A., Stargell, L. A., and Luger, K. (2010) The Histone Chaperone Nap1 Promotes Nucleosome Assembly by Eliminating Nonnucleosomal Histone DNA Interactions. *Mol. Cell.* **37**, 834–842

11. Gurard-Levin, Z. A., Quivy, J. P., and Almouzni, G. (2014) Histone chaperones: Assisting histone traffic and nucleosome dynamics. *Annu. Rev. Biochem.* **83**, 487–517

12. Dutta, S., Akey, I. V., Dingwall, C., Hartman, K. L., Laue, T., Nolte, R. T., Head, J. F., and Akey, C. W. (2001) The crystal structure of nucleoplasmin-core: Implications for histone binding and nucleosome assembly. *Mol. Cell*. **8**, 841–853

13. Daganzo, S. M., Erzberger, J. P., Lam, W. M., Skordalakes, E., Zhang, R., Franco, A. A., Brill, S. J., Adams, P. D., Berger, J. M., and Kaufman, P. D. (2003) Structure and Function of the Conserved Core of Histone Deposition Protein Asf1. *Curr. Biol.* **13**, 2148–2158

14. Mousson, F., Lautrette, A., Thuret, J. Y., Agez, M., Courbeyrette, R., Amigues, B., Becker, E., Neumann, J. M., Guerois, R., Mann, C., and Ochsenbein, F. (2005) Structural basis for the interaction of Asf1 with histone H3 and its functional implications. *Proc. Natl. Acad. Sci. U. S. A.* **102**, 5975–5980

15. English, C. M., Maluf, N. K., Tripet, B., Churchill, M. E. A., and Tyler, J. K. (2005) ASF1 binds to a heterodimer of histones H3 and H4: A two-step mechanism for the assembly of the H3-H4 heterotetramer on DNA. *Biochemistry*. **44**, 13673–13682

16. English, C. M., Adkins, M. W., Carson, J. J., Churchill, M. E. A., and Tyler, J. K. (2006) Structural Basis for the Histone Chaperone Activity of Asf1. *Cell*. **127**, 495–508

17. Reinberg, D., Orphanides, G., Wu, W.-H., Lane, W. S., and Hampsey, M. (1999) The chromatin-specific transcription elongation factor FACT comprises human SPT16 and SSRP1 proteins : Article : Nature. *Nature*. **400**, 284–288

18. Jamai, A., Puglisi, A., and Strubin, M. (2009) Histone Chaperone Spt16 Promotes Redeposition of the Original H3-H4 Histones Evicted by Elongating RNA Polymerase. *Mol. Cell*. **35**, 377–383

19. Chen, S., Rufiange, A., Huang, H., Rajashankar, K. R., Nourani, A., and Patel, D. J. (2015) Structure–function studies of histone H3/H4 tetramer maintenance during transcription by chaperone Spt2. *Genes Dev.* **29**, 1326–1340

20. Osakabe, A., Tachiwana, H., Takaku, M., Hori, T., Obuse, C., Kimura, H., Fukagawa, T., and Kurumizaka, H. (2013) Vertebrate Spt2 is a novel nucleolar histone chaperone that assists in ribosomal DNA transcription. *J. Cell Sci.* **126**, 1323–1332

21. Berndsen, C. E., Tsubota, T., Lindner, S. E., Lee, S., Holton, J. M., Kaufman, P. D., Keck, J. L., and Denu, J. M. (2008) Molecular functions of the histone

acetyltransferase chaperone complex Rtt109-Vps75. *Nat. Struct. Mol. Biol.* **15**, 948–956

22. Tang, Y., Meeth, K., Jiang, E., Luo, C., and Marmorstein, R. (2008) Structure of Vps75 and implications for histone chaperone function. *Proc. Natl. Acad. Sci. U. S. A.* **105**, 12206–12211

23. Tang, Y., Holbert, M. A., Delgoshaie, N., Wurtele, H., Guillemette, B., Meeth, K., Yuan, H., Drogaris, P., Lee, E. H., Durette, C., Thibault, P., Verreault, A., Cole, P. A., and Marmorstein, R. (2011) Structure of the Rtt109-AcCoA/Vps75 complex and implications for chaperone-mediated histone acetylation. *Structure.* **19**, 221–231

24. Park, Y.-J. Y.-J., and Luger, K. (2006) The structure of nucleosome assembly protein 1. *Proc. Natl. Acad. Sci. U. S. A.* **103**, 1248–1253

25. Park, Y. J., and Luger, K. (2006) Structure and function of nucleosome assembly proteins. *Biochem. Cell Biol.* **84**, 549–558

26. Selth, L., and Svejstrup, J. Q. (2007) Vps75, a new yeast member of the NAP histone chaperone. *J. Biol. Chem.* **282**, 12358–12362

27. Bowman, A., Ward, R., Wiechens, N., Singh, V., El-Mkami, H., Norman, D. G., and Owen-Hughes, T. (2011) The Histone Chaperones Nap1 and Vps75 Bind Histones H3 and H4 in a Tetrameric Conformation. *Mol. Cell.* **41**, 398–408

28. Bowman, A., Hammond, C. M., Stirling, A., Ward, R., Shang, W., El-Mkami, H., Robinson, D. A., Svergun, D. I., Norman, D. G., and Owen-hughes, T. (2014) The histone chaperones Vps75 and Nap1 form ring-like, tetrameric structures in solution. *Nucleic Acids Res.* **42**, 6038–6051

29. Muto, S., Senda, M., Akai, Y., Sato, L., Suzuki, T., Nagai, R., Senda, T., and Horikoshi, M. (2007) Relationship between the structure of SET/TAF-Iβ/INHAT and its histone chaperone activity. *Proc. Natl. Acad. Sci. U. S. A.* **104**, 4285–4290

30. Park, Y. J., McBryant, S. J., and Luger, K. (2008) A β-Hairpin Comprising the Nuclear Localization Sequence Sustains the Self-associated States of Nucleosome Assembly Protein 1. *J. Mol. Biol.* **375**, 1076–1085

31. McBryant, S. J., Park, Y. J., Abernathy, S. M., Laybourn, P. J., Nyborg, J. K., and Luger, K. (2003) Preferential Binding of the Histone (H3-H4)2Tetramer by NAP1 Is Mediated by the Amino-terminal Histone Tails. *J. Biol. Chem.* **278**, 44574–44583

32. Tóth, K. F., Mazurkiewicz, J., and Rippe, K. (2005) Association states of nucleosome assembly protein 1 and its complexes with histones. *J. Biol. Chem.* **280**, 15690–15699

33. Andrews, A. J., Downing, G., Brown, K., Park, Y. J., and Luger, K. (2008) A thermodynamic model for Nap1-histone interactions. *J. Biol. Chem.* **283**, 32412–32418

34. Andrews, A. J., Chen, X., Zevin, A., Stargell, L. A., and Luger, K. (2010) 1Q2W7U8I9O0P-=\The Histone Chaperone Nap1 Promotes Nucleosome Assembly by Eliminating Nonnucleosomal Histone DNA Interactions. *Mol. Cell.* **37**, 834–842

35. Kim, T. Y., Zhong, S., Fields, C. R., Kim, J. H., and Robertson, K. D. (2006) Epigenomic profiling reveals novel and frequent targets of aberrant DNA methylation-mediated silencing in malignant glioma. *Cancer Res.* **66**, 7490–7501

36. Jung, Y., Park, J., Bang, Y. J., and Kim, T. Y. (2008) Gene silencing of TSPYL5 mediated by aberrant promoter methylation in gastric cancers. *Lab. Investig.* **88**, 153–160

37. Kim, E. J., Lee, S. Y., Kim, T. R., Choi, S. I., Cho, E. W., Kim, K. C., and Kim, I. G. (2010) TSPYL5 is involved in cell growth and the resistance to radiation in A549 cells via the regulation of p21WAF1/Cip1 and PTEN/AKT pathway. *Biochem. Biophys. Res. Commun.* **392**, 448–453

38. Episkopou, H., Diman, A., Claude, E., Viceconte, N., and Decottignies, A. (2019) TSPYL5 Depletion Induces Specific Death of ALT Cells through USP7-Dependent Proteasomal Degradation of POT1. *Mol. Cell.* **75**, 469-482.e6

39. Epping, M. T., Meijer, L. A. T., Krijgsman, O., Bos, J. L., Pandolfi, P. P., and Bernards, R. (2011) TSPYL5 suppresses p53 levels and function by physical interaction with USP7. *Nat. Cell Biol.* **13**, 102–108

40. Shen, Y., Tu, W., Liu, Y., Yang, X., Dong, Q., Yang, B., Xu, J., Yan, Y., Pei, X., Liu, M., Xu, W., and Yang, Y. (2018) TSPY1 suppresses USP7-mediated p53 function and promotes spermatogonial proliferation article. *Cell Death Dis.* 10.1038/s41419-018-0589-7

41. Huang, C., He, C., Ruan, P., and Zhou, R. (2020) TSPYL5 activates endoplasmic reticulum stress to inhibit cell proliferation, migration and invasion in colorectal cancer. *Oncol. Rep.* **44**, 449–456

42. Shao, L., Shen, Z., Qian, H., Zhou, S., and Chen, Y. (2017) Knockdown of miR-629 inhibits ovarian cancer malignant behaviors by targeting testis-specific Y-like protein 5. *DNA Cell Biol.* **36**, 1108–1116

43. Cervoni, N., Detich, N., Seo, S. B., Chakravarti, D., and Szyf, M. (2002) The oncoprotein set/TAF-1β, an inhibitor of histone acetyltransferase, inhibits active demethylation of DNA, integrating DNA methylation and transcriptional silencing. *J. Biol. Chem.* **277**, 25026–25031

44. Fan, Z., Beresford, P. J., Oh, D. Y., Zhang, D., and Lieberman, J. (2003) Tumor suppressor NM23-H1 is a granzyme A-activated DNase during CTL-mediated apoptosis, and the nucleosome assembly protein set is its inhibitor. *Cell*. **112**, 659–672

45. Fujii-Nakata, T., Ishimi, Y., Okuda, A., and Kikuchi, A. (1992) Functional analysis of nucleosome assembly protein, NAP-1. The negatively charged COOH-terminal region is not necessary for the intrinsic assembly activity. *J. Biol. Chem.* **267**, 20980–20986

46. Matsumoto, K., Nagata, K., Ui, M., and Hanaoka, F. (1993) Template activating factor I, a novel host factor required to stimulate the adenovirus core DNA replication. *J. Biol. Chem.* **268**, 10582–10587

47. Mosammaparast, N., Ewart, C. S., and Pemberton, L. F. (2002) A role for nucleosome assembly protein 1 in the nuclear transport of histones H2A and H2B. *EMBO J.* **21**, 6527–6538

48. Mattiroli, F., Gu, Y., Yadav, T., Balsbaugh, J. L., Harris, M. R., Findlay, E. S., Liu, Y., Radebaugh, C. A., Stargell, L. A., Ahn, N. G., Whitehouse, I., and Luger, K. (2017) DNA-mediated association of two histone-bound complexes of yeast chromatin assembly factor-1 (CAF-1) drives tetrasome assembly in the wake of DNA replication. *Elife*. **6**, 1–23

49. Sauer, P. V., Timm, J., Liu, D., Sitbon, D., Boeri-Erba, E., Velours, C., Mücke, N., Langowski, J., Ochsenbein, F., Almouzni, G., and Panne, D. (2017) Insights into the molecular architecture and histone H3-H4 deposition mechanism of yeast chromatin assembly factor 1. *Elife*. **6**, 1–18

50. Smith, S., and Stillman, B. (1991) Stepwise assembly of chromatin during DNA replication in vitro. *EMBO J.* **10**, 971–980

51. Das, C., Tyler, J. K., and Churchill, M. E. A. (2010) The histone shuffle: Histone

chaperones in an energetic dance. *Trends Biochem. Sci.* **35**, 476–489

52. Qiao, H., Li, Y., Feng, C., Duo, S., Ji, F., and Jiao, J. (2018) Nap1l1 Controls Embryonic Neural Progenitor Cell Proliferation and Differentiation in the Developing Brain. *Cell Rep.* **22**, 2279–2293

53. Muto, S., Senda, M., Akai, Y., Sato, L., Suzuki, T., Nagai, R., Senda, T., and Horikoshi, M. (2007) Relationship between the structure of SET/TAF-I /INHAT and its histone chaperone activity. *Proc. Natl. Acad. Sci.* **104**, 4285–4290

54. Mosammaparast, N., Jackson, K. R., Guo, Y., Brame, C. J., Shabanowitz, J., Hunt, D. F., and Pemberton, L. F. (2001) Nuclear import of histone H2A and H2B is mediated by a network of karyopherins. *J. Cell Biol.* **153**, 251–262

55. Aguilar-Gurrieri, C., Larabi, A., Vinayachandran, V., Patel, N. A., Yen, K., Reja, R., Ebong, I., Schoehn, G., Robinson, C. V, Pugh, B. F., and Panne, D. (2016) Structural evidence for Nap1-dependent H2A–H2B deposition and nucleosome assembly. *EMBO J.* **35**, 1465–1482

56. Pchelintsev, N. A., McBryan, T., Rai, T. S., VanTuyn, J., Ray-Gallet, D., Almouzni, G., and Adams, P. D. (2013) Placing the HIRA Histone Chaperone Complex in the Chromatin Landscape. *Cell Rep.* **3**, 1012–1019

57. Liu, Y., Huang, H., Zhou, B. O., Wang, S. S., Hu, Y., Li, X., Liu, J., Zang, J., Niu, L., Wu, J., Zhou, J. Q., Teng, M., and Shi, Y. (2010) Structural analysis of Rtt106p reveals a DNA binding role required for heterochromatin silencing. *J. Biol. Chem.* **285**, 4251–4262

58. Ray-Gallet, D., Woolfe, A., Vassias, I., Pellentz, C., Lacoste, N., Puri, A., Schultz, D. C., Pchelintsev, N. A., Adams, P. D., Jansen, L. E. T., and Almouzni, G. (2011) Dynamics of Histone H3 Deposition In Vivo Reveal a Nucleosome Gap-Filling Mechanism for H3.3 to Maintain Chromatin Integrity. *Mol. Cell*. **44**, 928–941

59. Yamaguchi, L., Nishiyama, A., Misaki, T., Johmura, Y., Ueda, J., Arita, K., Nagao, K., Obuse, C., and Nakanishi, M. (2017) Usp7-dependent histone H3 deubiquitylation regulates maintenance of DNA methylation. *Sci. Rep.* **7**, 55

60. Zhang, Z. M., Rothbart, S. B., Allison, D. F., Cai, Q., Harrison, J. S., Li, L., Wang, Y., Strahl, B. D., Wang, G. G., and Song, J. (2015) An Allosteric Interaction Links USP7 to Deubiquitination and Chromatin Targeting of UHRF1. *Cell Rep.* **12**, 1400–1406

61. Huang, H., Strømme, C. B., Saredi, G., Hödl, M., Strandsby, A., González-Aguilera, C., Chen, S., Groth, A., and Patel, D. J. (2015) A unique binding mode enables MCM2 to chaperone histones H3-H4 at replication forks. *Nat. Struct. Mol. Biol.* **22**, 618–626

62. Bellelli, R., Belan, O., Pye, V. E., Clement, C., Maslen, S. L., Skehel, J. M., Cherepanov, P., Almouzni, G., and Boulton, S. J. (2018) POLE3-POLE4 Is a Histone H3-H4 Chaperone that Maintains Chromatin Integrity during DNA Replication. *Mol. Cell*. **72**, 112-126.e5

63. Luger, K., Rechsteiner, T. J., and Richmond, T. J. (1999) Preparation of nucleosome core particle from recombinant histones. in *Nature*, pp. 3–19, **304**, 3–19

64. LAEMMLI, U. K. (1970) Cleavage of Structural Proteins during the Assembly of the Head of Bacteriophage T4. *Nature*. **227**, 680–685

65. Abdiche, Y., Malashock, D., Pinkerton, A., and Pons, J. (2008) Determining kinetics and affinities of protein interactions using a parallel real-time label-free biosensor, the Octet. *Anal. Biochem.* **377**, 209–217

66. Germond, J. E., Hirt, B., Oudet, P., Gross-Bellark, M., and Chambon, P. (1975) Folding of the DNA double helix in chromatin like structures from simian virus 40. *Proc. Natl. Acad. Sci. U. S. A.* **72**, 1843–1847

67. Jumper, J., Evans, R., Pritzel, A., Green, T., Figurnov, M., Ronneberger, O., Tunyasuvunakool, K., Bates, R., Žídek, A., Potapenko, A., Bridgland, A., Meyer, C., Kohl, S. A. A., Ballard, A. J., Cowie, A., Romera-Paredes, B., Nikolov, S., Jain, R., Adler, J., Back, T., Petersen, S., Reiman, D., Clancy, E., Zielinski, M., Steinegger, M., Pacholska, M., Berghammer, T., Bodenstein, S., Silver, D., Vinyals, O., Senior, A. W., Kavukcuoglu, K., Kohli, P., and Hassabis, D. (2021) Highly accurate protein structure prediction with AlphaFold. *Nature*. **596**, 583–589

68. Varadi, M., Anyango, S., Deshpande, M., Nair, S., Natassia, C., Yordanova, G., Yuan, D., Stroe, O., Wood, G., Laydon, A., Žídek, A., Green, T., Tunyasuvunakool, K., Petersen, S., Jumper, J., Clancy, E., Green, R., Vora, A., Lutfi, M., Figurnov, M., Cowie, A., Hobbs, N., Kohli, P., Kleywegt, G., Birney, E., Hassabis, D., and Velankar, S. (2022) AlphaFold Protein Structure Database: massively expanding the structural coverage of protein-sequence space with high-accuracy models. *Nucleic Acids Res.* **50**, D439–D444

69. Baek, M., DiMaio, F., Anishchenko, I., Dauparas, J., Ovchinnikov, S., Lee, G. R.,

Wang, J., Cong, Q., Kinch, L. N., Dustin Schaeffer, R., Millán, C., Park, H., Adams, C., Glassman, C. R., DeGiovanni, A., Pereira, J. H., Rodrigues, A. V., Van Dijk, A. A., Ebrecht, A. C., Opperman, D. J., Sagmeister, T., Buhlheller, C., Pavkov-Keller, T., Rathinaswamy, M. K., Dalwadi, U., Yip, C. K., Burke, J. E., Christopher Garcia, K., Grishin, N. V., Adams, P. D., Read, R. J., and Baker, D. (2021) Accurate prediction of protein structures and interactions using a three-track neural network. *Science (80-.).* **373**, 871–876

70. Kumar, S., Stecher, G., Li, M., Knyaz, C., and Tamura, K. (2018) MEGA X: Molecular evolutionary genetics analysis across computing platforms. *Mol. Biol. Evol.* **35**, 1547–1549

71. Jones, D. T., Taylor, W. R., and Thornton, J. M. (1992) The rapid generation of mutation data matrices from protein sequences. *Bioinformatics*. **8**, 275–282

72. Robert, X., and Gouet, P. (2014) Deciphering key features in protein structures with the new ENDscript server. *Nucleic Acids Res.* **42**, 320–324

Abbreviations:

NAP1(Nucleosome assembly protein 1), SET (Su(var)3-9, enhancer-of-zeste and trithorax), TAF1b (Template-activating factor 1b), NAP1L (NAP1-like proteins), TSPY (Testis-specific Y-encoded protein), TSPYL5 (Testis-specific Y-encoded like protein 5), USP7 (Ubiquitin specific protease 7), NLD (Nap like domain), HBM (Histone binding deficient mutant), RMSD (Root mean squre deviation).

Figure Legends

Figure 1. TSPYL5 shares significant sequence homology with NAP family proteins.

(a) Multiple Sequence alignment of human TSPYL5 (Q86VY4) with members of NAP protein family across different species. The different NAP family members (Uniprot accession ids within parenthesis) included in the analysis were, ScNAP1 (P25293), CeNAP1 (Q19007), DmNAP1 (Q9W1G7), DrNAP1 (Q803X7), XlNAP1 (Q4U0Y4), MmNAP1 (P28656), HsNAP1L1 (P55209), HsTSPY1 (Q01534), HsSET/TAF1B (Q01105). Identical residues are labelled in red. NAP1 accessory region is highlighted in blue. Secondary structure prediction of SET/TAF1B (PDB ID: 2E50) is shown above the multiple sequence alignment where alpha helix and beta-strand are indicated. (b) Domain architecture of human TSPYL5, SET/TAF1B, NAP1L1 and yeast NAP1. NAP domains are highlighted in cyan and Acidic region (AR) are highlighted in yellow. (c) Phylogenetic tree depicting different NAP like proteins in human. MEGA-X and Figtree Software packages were used for the analysis. Scale bar is indicated in figure. (d) Molecular model of TSPYL5 (198-398) in cartoon representation using Alpha Fold. Secondary structure is represented in colour codes- Helix (green), Beta sheet (pink), Loop (blue). (e) Superimposition of the C-alpha trace of earmuff domains of TSPYL5 (green), RoseTTAFold (blue) and SET/TAF-1B (red).

Figure 2. TSPYL5 interacts with Histone H3/H4.

(a-b) HEK293T cells were transfected with empty vector (EV; as a negative control) and FLAG–TSPYL5 and subsequently separated into cytosolic and nuclear fractions. The localization of TSYPL5 was detected using western blotting. Tubulin and H3 were used as cytosolic and nuclear markers (a). Immunoprecipitation of FLAG-TSPYL5 using anti- FLAG antibody was followed by immunoblotting with all four core histone αH2A, αH2B, αH3 and αH4 antibodies (b). (c-d) Endogenous association of TSYPL5 with core histones in SH-SY5Y cells. TSPYL5 was immunoprecipitated from SH-SY5Y cells using anti- TSPYL5 antibody and subsequently immunoblotted with αH2A, αH2B, αH3 and αH4 antibodies (c). Reciprocal immunoprecipitation with αH3 antibody was performed followed by immunoblotting with αTSPYL5 antibody (d). (e-f) *In vitro* interaction of GST-TSYPL5-FL or its different domains with histone H3/H4 or H2A/H2B dimer. GST pull-down assay was performed

followed by immunoblotting with αH2A, αH2B, αH3 and αH4 antibodies (e). Subsequently, GST-conjugated TSPYL5-FL, TSYPL5 NAP Like Domain (NLD) and ΔNLD proteins were pull down and probed with αH3 and αH4 antibodies (f). Domain architecture of different constructs used in the pulldown assay has been shown in the left panel.

Figure 3. Fine mapping of TSPYL5-H3/H4 interaction.

(a) Peptide pull-down assay of the recombinant TSPYL5-NLD with biotinylated histone H3 peptides. Streptavidin beads were used for histone peptide pull down assay and western blotting with αTSPYL5 antibody was performed. Peptide dot blot was performed to show equivalent amount of peptides were used in the assay. (b) Binding affinity of TSPYL5-NLD with Histone H3 C-terminal peptide (120-136 aa) using Bio-layer Interferometry (BLI). The analyte concentrations of TSPYL5 are shown in different colours. (c) *In vitro* GST pull-down assay of the TSPYL5-NLD with recombinant His tagged Histone H3/H4 or H3ΔC-term/H4 was performed and subsequently blotted with αHis and αGST antibodies. (d) Far-UV CD spectra of Histone His-H3/H4 or His-H3ΔC-term/H4 constructs. (e) Histone Binding-defective Mutants (HBM1 in pink and HBM2 in green) are highlighted in stick representation in the TSYPL5 cartoon diagram. (f) *In vitro* interaction of GST-TSYPL5-NLD, HBM1, HBM2 or HBM (1+2) with histone H3/H4. GST pull-down assay was performed followed by immunoblotting with αH3 and αH4 antibodies (g) Far-UV CD spectra of WT and HBM constructs of TSPYL5-NLD (h-i) Binding affinity of TSPYL5-NLD or HBM (1+2) with Histone H3/H4 using BLI. The analyte concentrations of TSYPL5-NLD or HBM (1+2) are shown in different colours (h). K_d values for the interaction between histone H3/H4 and TSYPL5-FL, TSYPL5-NLD or its different mutants are represented in Table (i).

Figure 4 : Molecular characterization of TSYPL5-H3/H4 complex.

(a) SEC-MALS analysis showing normalized Refractive Index (RI) trace of Histone H3/H4 (black), TSPYL5-NLD (blue) & TSPYL5-NLD-H3/H4 complex (red). (b) Molar mass measurements by SEC-MALS (marked in red) and the theoretical molecular weight predictions (marked in black) of each complex are represented in the Table. (c) DSS crosslinking performed with TSPYL5-NLD or H3/H4

alone or after incubation with TSPYL5-NLD and H3/H4 followed by western blot analysis. In each

case, Lane 1 shows control without DSS; lane 2 shows sample incubated with 2.5 mM DSS. Species

appearing upon cross-linking are marked. (d) *In vitro* GST pull-down assay of the TSPYL5-NLD with

recombinant Histone H3/H4 or H3M/H4 was performed and subsequently blotted with αH3, αH4 and

αGST antibodies. Tetramer disruptive Histone H3 construct (H3M) harbours C110E, L126R and

I130E mutations. (e) Schematic representation of binding modes for TSPYL5-H3/H4 complex.
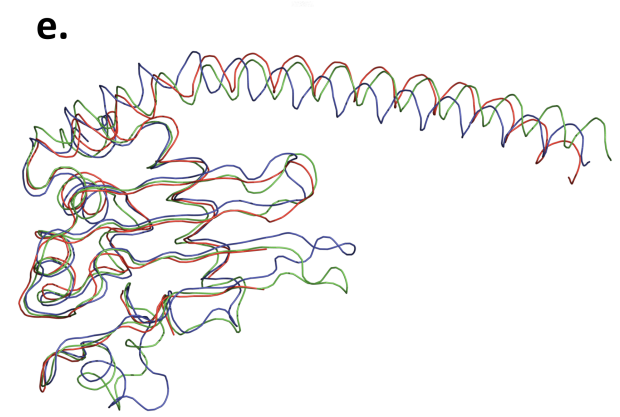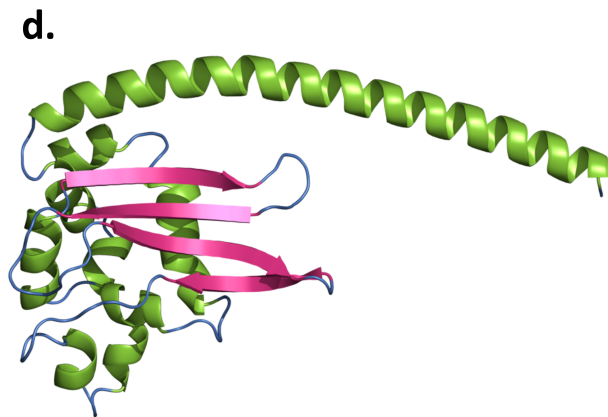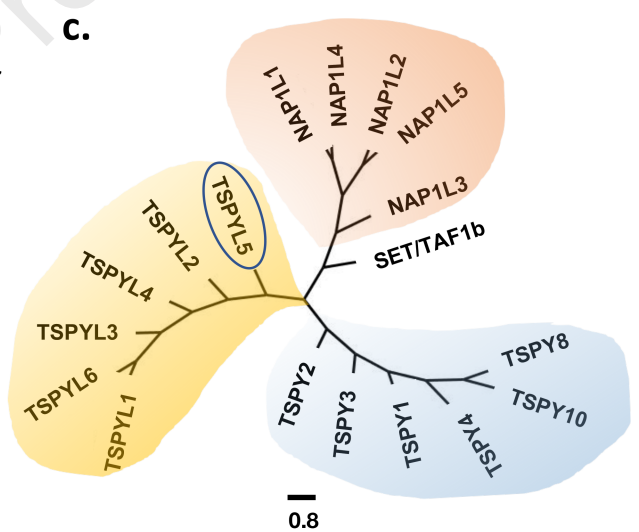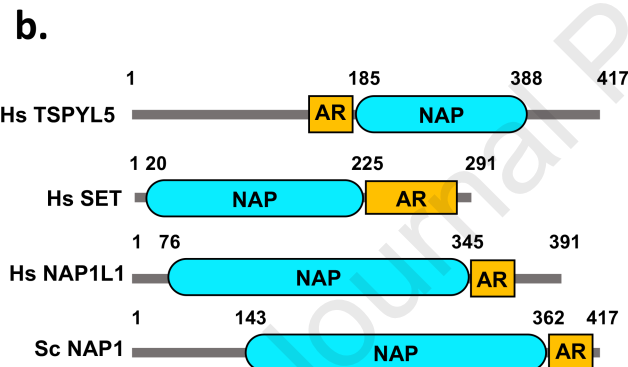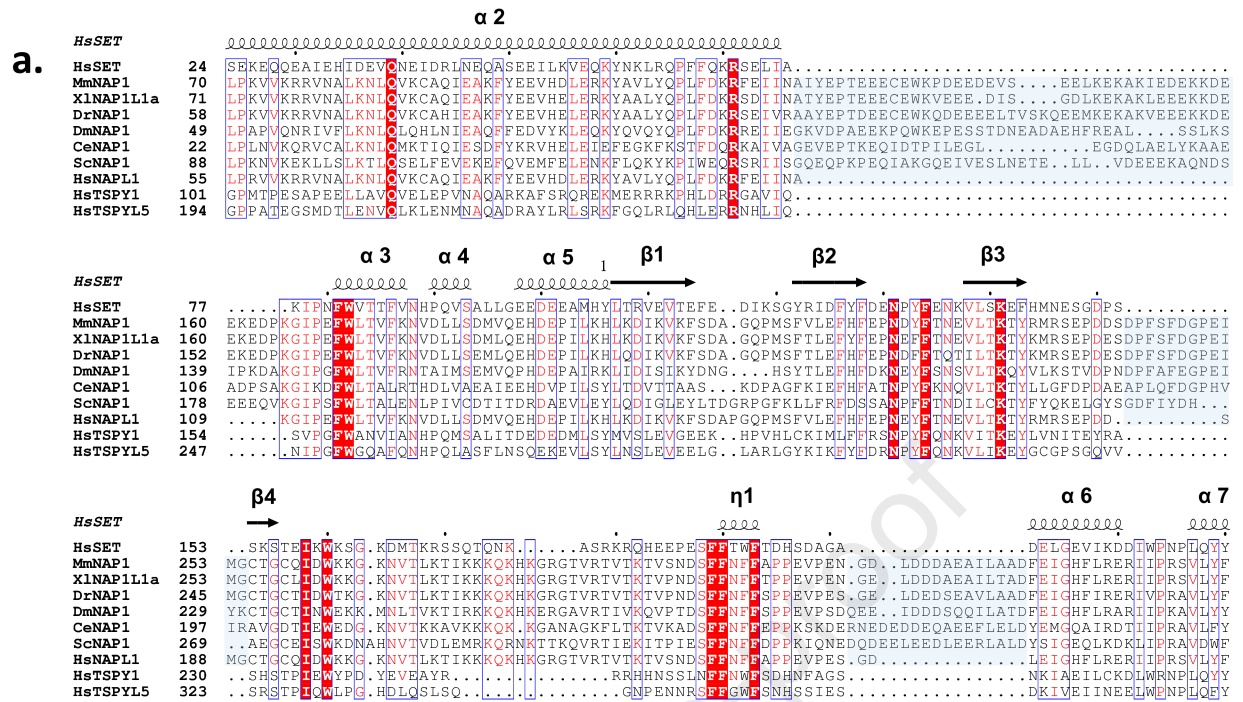

Figure 5. TSPYL5 binds to DNA.

(a) EMSA showing TSPYL5-NLD binding to free DNA fragments of varying lengths (10–330 bp).

(b) EMSA showing binding of TSPYL5-NLD using 20, 40, 80 and 146 bp DNA respectively.

Increasing amounts of TSPYL5 (0.06, 0.125, 0.25, 0.5, 1, 2, 4, 8, 16 or 32 uM) were mixed with 1 uM

DNA. (c) Corresponding binding curves of TSPYL5-NLD to 20 bp, 40 bp, 80 bp and 146bp DNA

interaction. The binding intensity is quantified by DNA depletion upon interaction with TSPYL5-

NLD. (d-e) EMSA showing binding of 146 bp DNA to increasing concentration of TSPYL5- ΔNLD

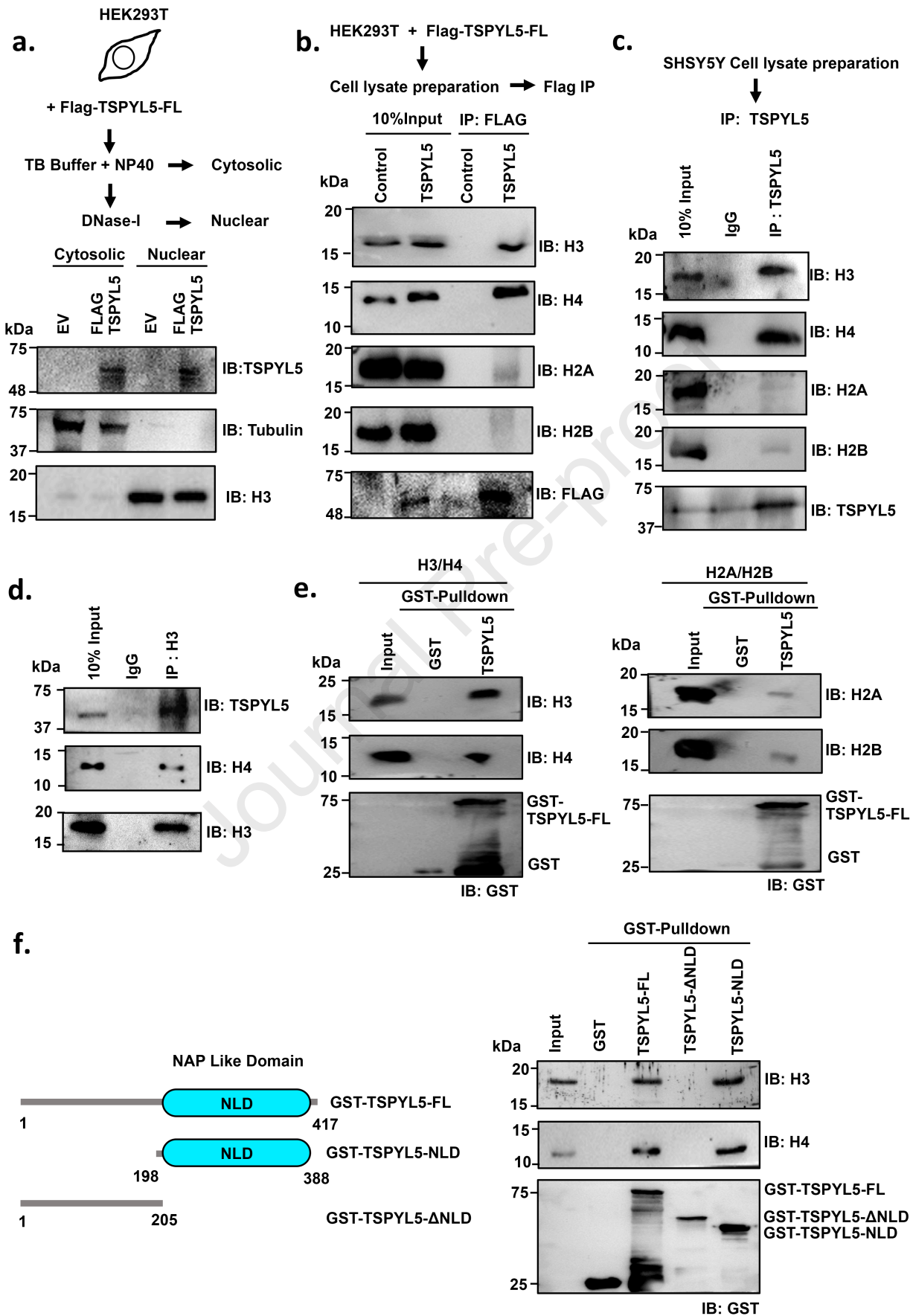(d) and HBM (1+2) (e). Free DNA and TSPYL5-bound DNA are indicated in all the above

experiments.

Figure 6. TSPYL5 promotes *in vitro* histone deposition and plasmid supercoiling.
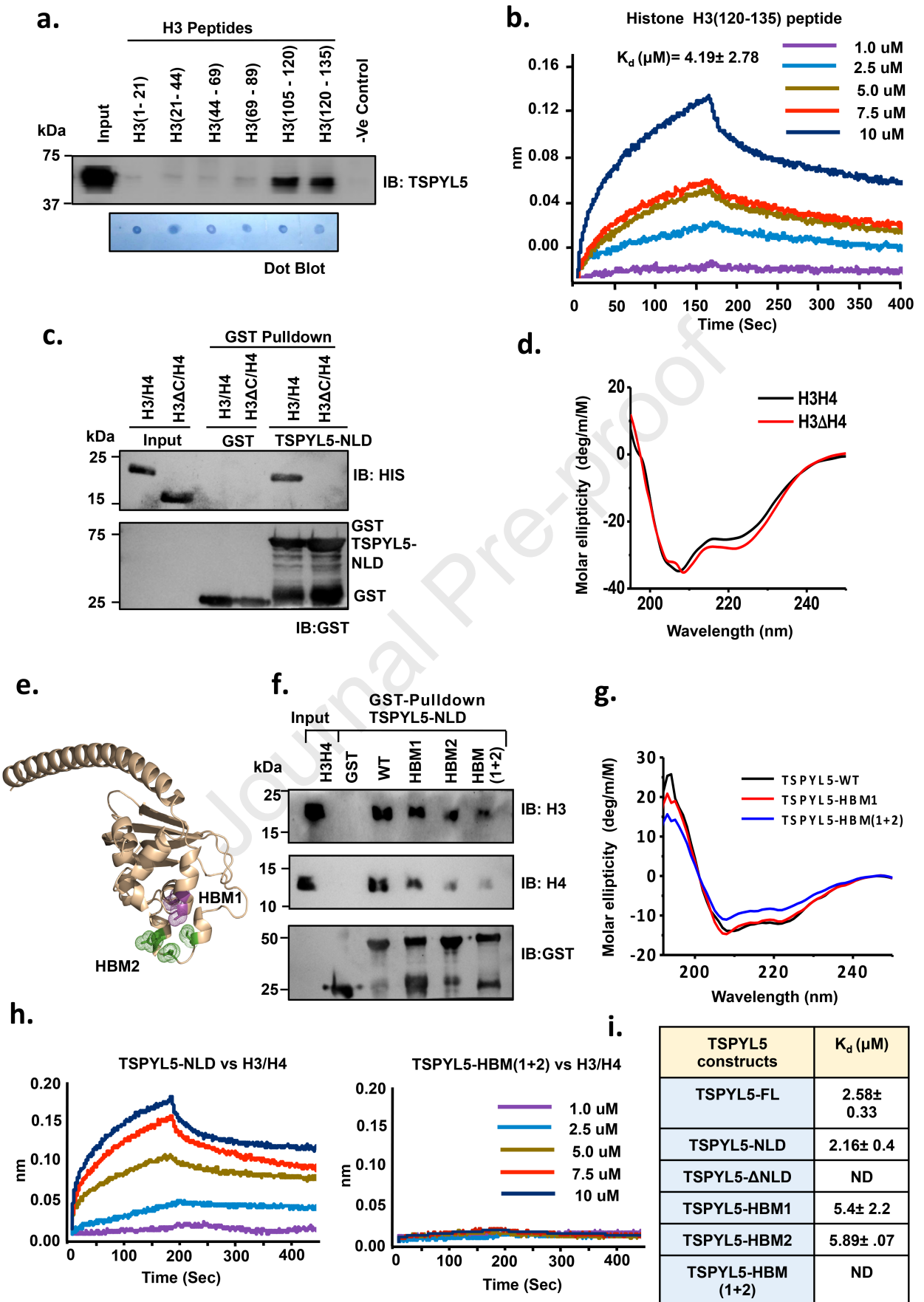
(a-b) Histone deposition assay performed with 146 bp linear DNA (Widom 601 sequence), H3/H4

and TSPYL5-NLD or TSPYL5-HBM (1+2). Samples run in 7% native PAGE and stained with Gel

green. Lane 1 and 2, shows free DNA input and tetrasome input respectively; Lane 3, shows

TSPYL5-NLD (a) or TSPYL5-HBM (1+2) (b) with free DNA. Lanes 4-6, shows free DNA incubated

with H3/H4 with increasing concentrations of TSPYL5-NLD (a) or TSPYL5-HBM (1+2) (b) as

indicated in the figure. (c-d) Plasmid supercoiling assay performed with plasmid DNA and

Topoisomerase-I, histone H3/H4 and TSPYL5-NLD or TSPYL5-HBM (1+2). Samples were resolved

with native agarose gel electrophoresis. Lane 1, shows supercoiled plasmid DNA input; Lane 2,

shows DNA relaxed by Topoisomerase-I; Lane 3, relaxed DNA incubated with histones only; and

Lanes 4–7, show pre-relaxed DNA with Topoisomerase-I, incubated with histone H3/H4 and increasing concentrations of TSPYL5-NLD (c) or TSPYL5-HBM (1+2) (d) as indicated in the figure.
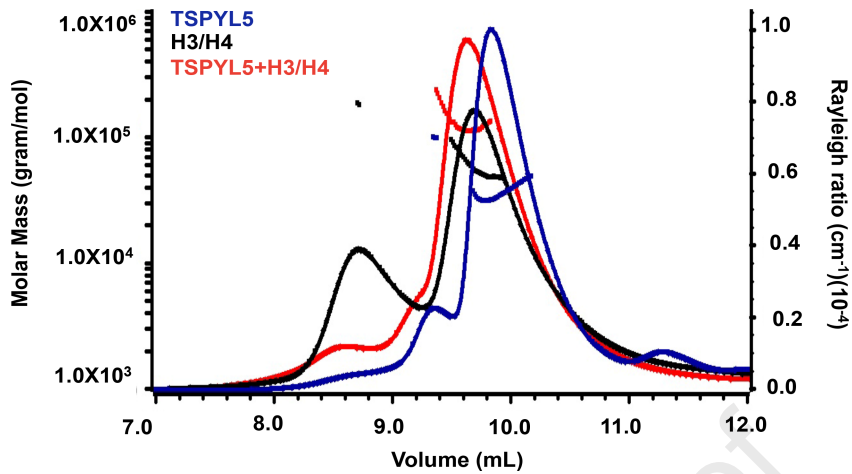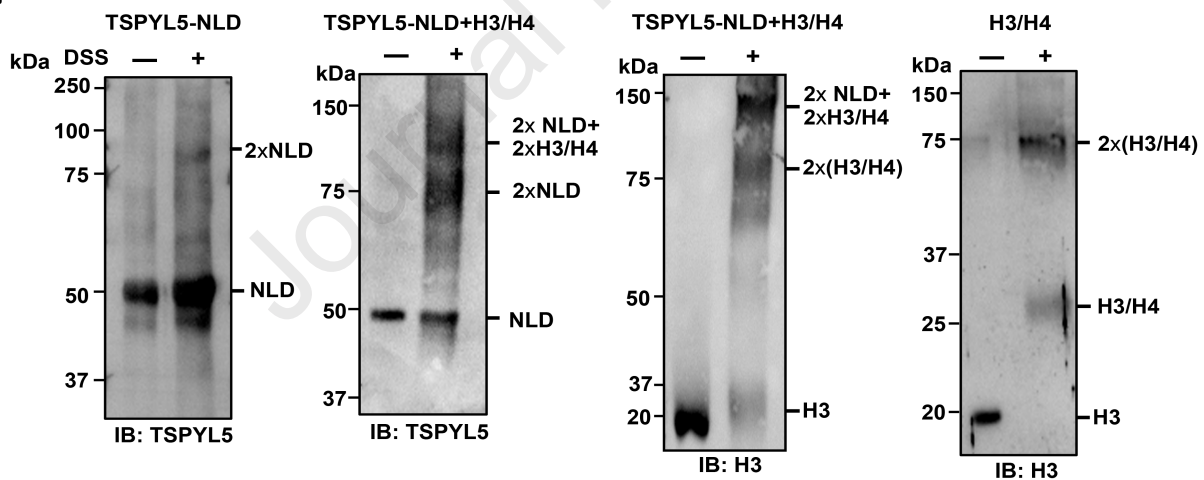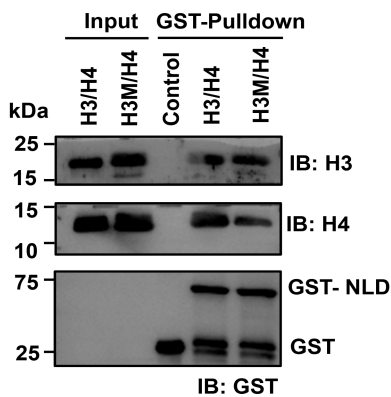
a.

b.

c.

d.

e.

a.

HEK293T

+ Flag-TSPYL5-FL

TB Buffer + NP40 → Cytosolic

DNase-I → Nuclear

	Cytosolic		Nuclear	
kDa	EV	FLAG TSPYL5	EV	FLAG TSPYL5

IB:TSPYL5

IB: Tubulin

IB: H3

b.

HEK293T + Flag-TSPYL5-FL

↓

Cell lysate preparation → Flag IP

10%Input | IP: FLAG

Control | TSPYL5 | Control | TSPYL5

IB: H3

IB: H4

IB: H2A

IB: H2B

IB: FLAG

c.

SHSY5Y Cell lysate preparation

↓

IP: TSPYL5

10% Input | IgG | IP : TSPYL5

IB: H3

IB: H4

IB: H2A

IB: H2B

IB: TSPYL5

d.

10% Input | IgG | IP : H3

IB: TSPYL5

IB: H4

IB: H3

e.

H3/H4
GST-Pulldown

Input | GST | TSPYL5

IB: H3

IB: H4

GST-TSPYL5-FL

GST

IB: GST

H2A/H2B
GST-Pulldown

Input | GST | TSPYL5

IB: H2A

IB: H2B

GST-TSPYL5-FL

GST

IB: GST

f.

NAP Like Domain

1 —— NLD —— 417   GST-TSPYL5-FL

198 —— NLD —— 388   GST-TSPYL5-NLD

1 —— 205   GST-TSPYL5-ΔNLD

GST-Pulldown

Input | GST | TSPYL5-FL | TSPYL5-ΔNLD | TSPYL5-NLD

IB: H3

IB: H4

GST-TSPYL5-FL
GST-TSPYL5-ΔNLD
GST-TSPYL5-NLD

IB: GST

a. H3 Peptides

b. Histone H3(120-135) peptide
$K_d (\mu M) = 4.19 \pm 2.78$

c. GST Pulldown

d.

e.

f. GST-Pulldown TSPYL5-NLD

g.

h. TSPYL5-NLD vs H3/H4 | TSPYL5-HBM(1+2) vs H3/H4

i.

TSPYL5 constructs	$K_d (\mu M)$
TSPYL5-FL	2.58± 0.33
TSPYL5-NLD	2.16± 0.4
TSPYL5-ΔNLD	ND
TSPYL5-HBM1	5.4± 2.2
TSPYL5-HBM2	5.89± .07
TSPYL5-HBM (1+2)	ND

a.

b.

Complex	Molecular Ratio 1	Expected Mass 1 (kDa)	Molecular Ratio 2	Expected Mass 2 (kDa)	Molecular Ratio 3	Expected Mass 3 (kDa)	Measured Mass(kDa)	(Error)
H3/H4	1:1	28	2:2	56	-	-	54.83	2.0%
TSPYL5-NLD	1	36	2	72	-	-	34.39	4.0%
TSPYL5-NLD+H3/H4	1:1:1	64	1:2:2	92	2:2:2	128	128.31	1.0%

c.

d.

e.

a.

TSPYL5-NLD

b.

TSPYL5-NLD

20 bp

TSPYL5-NLD

40 bp

TSPYL5-NLD

80 bp

TSPYL5-NLD

146 bp

c.

DNA length	K_d value (µM)
146 bp DNA	0.38±0.03
80 bp DNA	0.51±0.05
40 bp DNA	ND
20 bp DNA	ND

d. TSPYL5-ΔNLD

146 bp

e. TSPYL5-HBM(1+2)

146 bp

a.

TSPYL5-NLD	—	—	1.5	0.50	1.00	1.50 µM
H3/H4	—	0.30	—	0.15	0.15	0.15 µM
146 bp DNA	+	+	+	+	+	+

Disome / Tetrasome
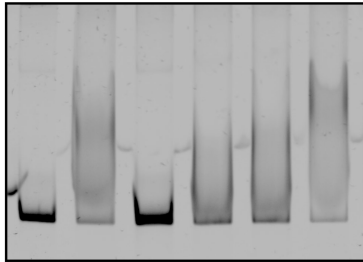
Free DNA

Lane: 1 2 3 4 5 6

b.

TSPYL5-HBM(1+2)	—	—	1.5	0.50	1.00	1.50 µM
H3/H4	—	0.30	—	0.15	0.15	0.15 µM
146 bp DNA	+	+	+	+	+	+

Lane: 1 2 3 4 5 6
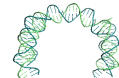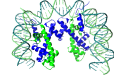
c.

TSPYL5-NLD	—	—	—	0.2	0.8	1.5	2.5 µM
H3/H4	—	—	1	1	1	1	1 µM
Topoisomerase	—	3	3	3	3	3	3 µM
PBS DNA	+	+	+	+	+	+	+

Relaxed DNA
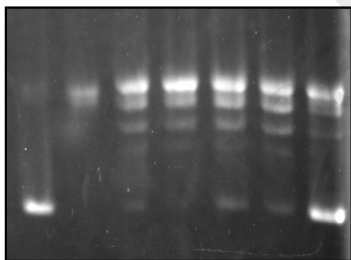
Supercoiled DNA

Lane : 1 2 3 4 5 6 7

d.

TSPYL5-HBM (1+2)	—	—	—	0.2	0.8	1.5	2.5 µM
H3/H4	—	—	1	1	1	1	1 µM
Topoisomerase	—	3	3	3	3	3	3 µM
PBS DNA	+	+	+	+	+	+	+

Relaxed DNA

Supercoiled DNA

Lane : 1 2 3 4 5 6 7